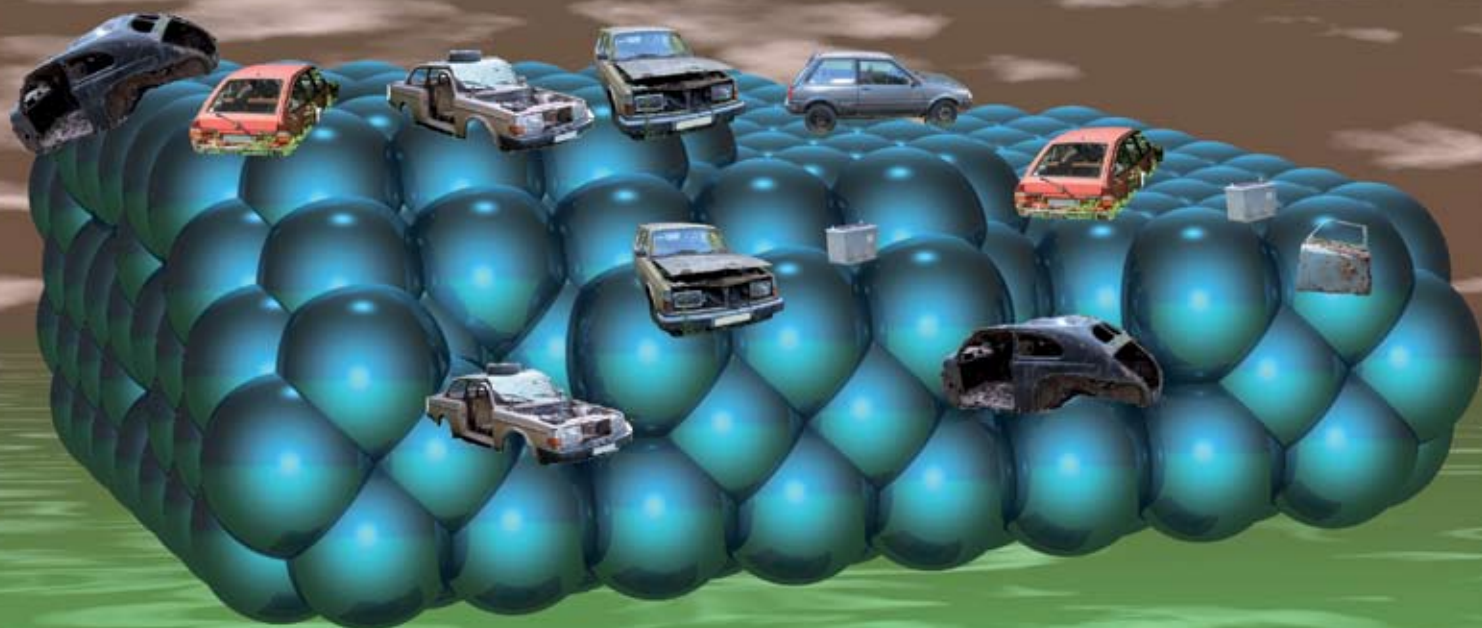


Green Chemistry

Cutting-edge research for a greener sustainable future

www.rsc.org/greenchem

Volume 10 | Number 8 | August 2008 | Pages 813–896



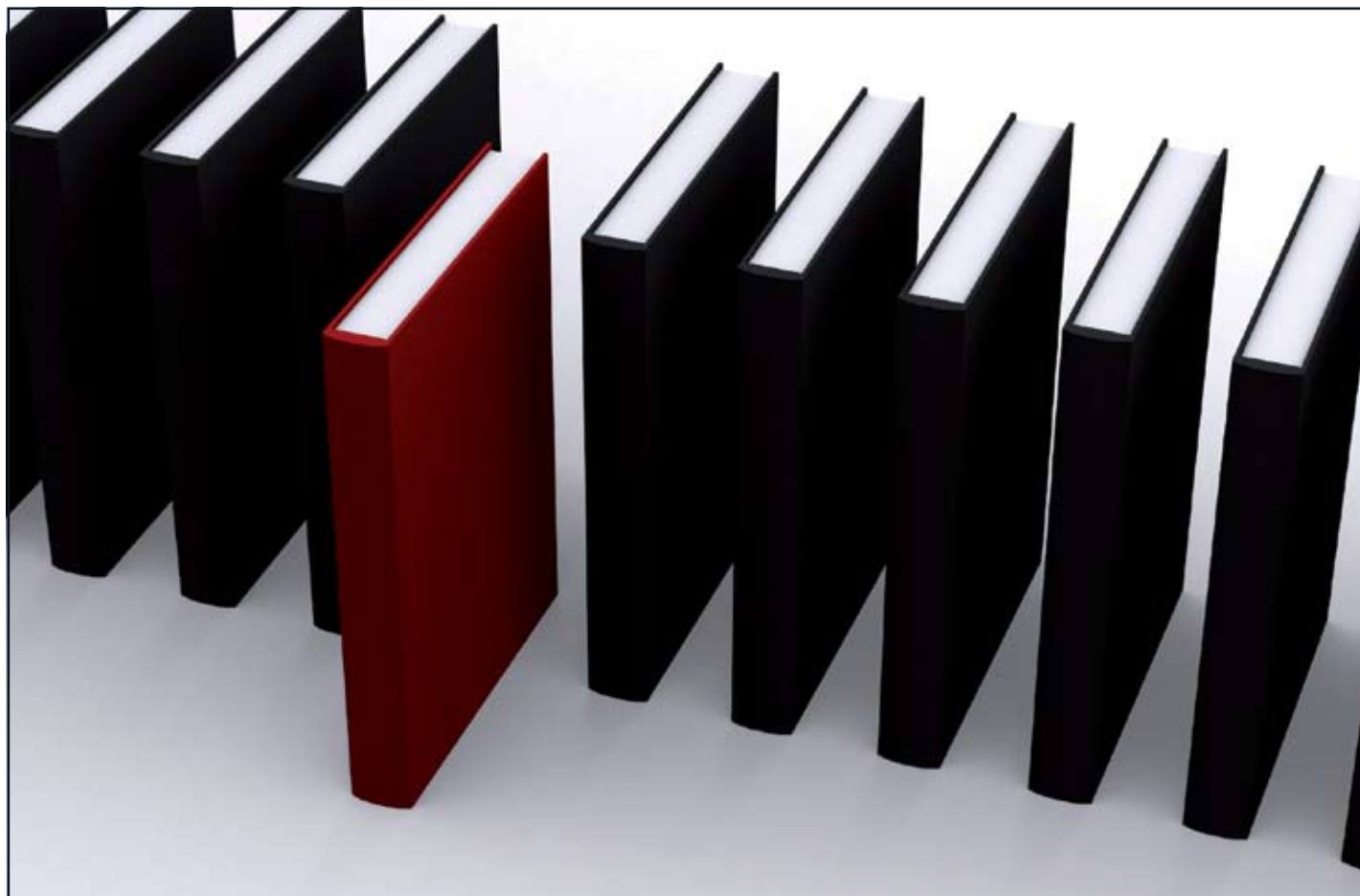
ISSN 1463-9262

RSC Publishing

Foreman *et al.*
Hydrogenation catalysts from used
batteries
Stephens *et al.*
Accumulation of ionic liquids in
E. Coli



1463-9262(2008)10:8;1-A



'Green Chemistry book of choice'



Why not take advantage of free book chapters from the RSC? Through our 'Green Chemistry book of choice' scheme *Green Chemistry* will regularly highlight a book from the RSC eBook Collection relevant to your research interests. Read the latest chapter today by visiting the *Green Chemistry* website.

The RSC eBook Collection offers:

- Over 900 new and existing books
- Fully searchable
- Unlimited access

Why not take a look today? Go online to find out more!

RSC Publishing

www.rsc.org/greenchem

Registered Charity Number 207890

Green Chemistry

Cutting-edge research for a greener sustainable future

www.rsc.org/greenchem

RSC Publishing is a not-for-profit publisher and a division of the Royal Society of Chemistry. Any surplus made is used to support charitable activities aimed at advancing the chemical sciences. Full details are available from www.rsc.org

IN THIS ISSUE

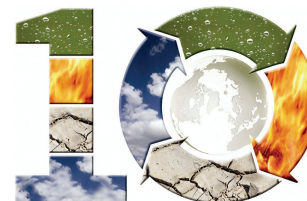
ISSN 1463-9262 CODEN GRCHFJ 10(8) 813–896 (2008)



Cover

See Foreman *et al.*, pp. 825–826. From scrap cars to useful synthetic tools. From used nickel hydride car electrical batteries it is possible to make mixed nickel/iron and nickel/cobalt hydrogenation catalysts.

Image reproduced with permission from Mark Foreman, from *Green Chem.*, 2008, **10**, 825.



CHEMICAL TECHNOLOGY

T57

Drawing together research highlights and news from all RSC publications, *Chemical Technology* provides a 'snapshot' of the latest applications and technological aspects of research across the chemical sciences, showcasing newsworthy articles and significant scientific advances.

Chemical Technology

August 2008/Volume 5/Issue 8

www.rsc.org/chemicaltechnology

NEWS

823

Workshop in green chemistry production of essential medicines in developing countries

O. O. Kunle,* Joseph M. Fortunak* and Robin D. Rogers*

Report on the Workshop in Green Chemistry Production of Essential Medicines in Developing Countries, held in Abuja, Nigeria from 18th–20th March, 2008. Left to right: Dr Tahir Amin, Dr Echezau Ogu, Prof. Stephen Byrn, Arc. Gabriel Yajubu Aduku, Prof. Joseph Fortunak, Prof. Robin D. Rogers, Sister Zita Ekochea.



EDITORIAL STAFF

Editor

Sarah Ruthven

Assistant editor

Sarah Dixon

Publishing assistant

Ruth Bircham

Team leader, serials production

Stephen Wilkes

Technical editor

Edward Morgan

Production administration coordinator

Sonya Spring

Administration assistantsClare Davies, Donna Fordham, Kirsty Lunnon,
Julie Thompson**Publisher**

Emma Wilson

Green Chemistry (print: ISSN 1463-9262; electronic: ISSN 1463-9270) is published 12 times a year by the Royal Society of Chemistry, Thomas Graham House, Science Park, Milton Road, Cambridge, UK CB4 0WF.

All orders, with cheques made payable to the Royal Society of Chemistry, should be sent to RSC Distribution Services, c/o Portland Customer Services, Commerce Way, Colchester, Essex, UK CO2 8HP. Tel +44 (0) 1206 226050; E-mail sales@rscdistribution.org

2008 Annual (print + electronic) subscription price: £947; US\$1799. 2008 Annual (electronic) subscription price: £852; US\$1695. Customers in Canada will be subject to a surcharge to cover GST. Customers in the EU subscribing to the electronic version only will be charged VAT.

If you take an institutional subscription to any RSC journal you are entitled to free, site-wide web access to that journal. You can arrange access via Internet Protocol (IP) address at www.rsc.org/ip. Customers should make payments by cheque in sterling payable on a UK clearing bank or in US dollars payable on a US clearing bank. Periodicals postage paid at Rahway, NJ, USA and at additional mailing offices. Airfreight and mailing in the USA by Mercury Airfreight International Ltd., 365 Blair Road, Avenel, NJ 07001, USA.

US Postmaster: send address changes to Green Chemistry, c/o Mercury Airfreight International Ltd., 365 Blair Road, Avenel, NJ 07001. All despatches outside the UK by Consolidated Airfreight.

PRINTED IN THE UK

Advertisement sales: Tel +44 (0) 1223 432246; Fax +44 (0) 1223 426017; E-mail advertising@rsc.org

Green Chemistry

Cutting-edge research for a greener sustainable future

www.rsc.org/greenchem

Green Chemistry focuses on cutting-edge research that attempts to reduce the environmental impact of the chemical enterprise by developing a technology base that is inherently non-toxic to living things and the environment.

EDITORIAL BOARD

Chair

Professor Martyn Poliakoff
Nottingham, UK

Scientific Editor

Professor Walter Leitner
RWTH-Aachen, Germany

Associate Editors

Professor C. J. Li
McGill University, Canada

Members

Professor Paul Anastas
Yale University, USA
Professor Joan Brennecke
University of Notre Dame, USA
Professor Mike Green
Sasol, South Africa
Professor Buxing Han
Chinese Academy of Sciences,
China

Dr Alexei Lapkin
Bath University, UK
Professor Steven Ley
Cambridge, UK
Dr Janet Scott
Unilever, UK
Professor Tom Welton
Imperial College, UK

ADVISORY BOARD

James Clark, York, UK
Avelino Corma, Universidad
Politécnica de Valencia, Spain
Mark Harmer, DuPont Central
R&D, USA
Herbert Hugl, Lanxess Fine
Chemicals, Germany
Roshan Jachuck,
Clarkson University, USA
Makato Misono, nite,
Japan

Colin Raston,
University of Western Australia,
Australia
Robin D. Rogers, Centre for Green
Manufacturing, USA
Kenneth Seddon, Queen's
University, Belfast, UK
Roger Sheldon, Delft University of
Technology, The Netherlands
Gary Sheldrake, Queen's
University, Belfast, UK

Pietro Tundo, Università ca
Foscari di Venezia, Italy

INFORMATION FOR AUTHORS

Full details of how to submit material for publication in Green Chemistry are given in the Instructions for Authors (available from <http://www.rsc.org/authors>). Submissions should be sent via ReSource: <http://www.rsc.org/resource>.

Authors may reproduce/republish portions of their published contribution without seeking permission from the RSC, provided that any such republication is accompanied by an acknowledgement in the form: (Original citation) – Reproduced by permission of the Royal Society of Chemistry.

© The Royal Society of Chemistry 2008. Apart from fair dealing for the purposes of research or private study for non-commercial purposes, or criticism or review, as permitted under the Copyright, Designs and Patents Act 1988 and the Copyright and Related Rights Regulations 2003, this publication may only be reproduced, stored or transmitted, in any form or by any means, with the prior permission in writing of the Publishers or in the case of reprographic reproduction in accordance with the terms of licences issued by the Copyright Licensing Agency in the UK. US copyright law is applicable to users in the USA.

The Royal Society of Chemistry takes reasonable care in the preparation of this publication but does not accept liability for the consequences of any errors or omissions.

The paper used in this publication meets the requirements of ANSI/NISO Z39.48-1992 (Permanence of Paper).

Royal Society of Chemistry: Registered Charity No. 207890

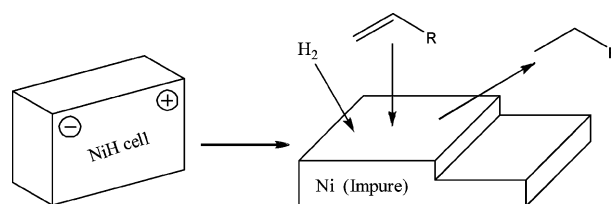
COMMUNICATIONS

825

Hydrogenation catalysts from used nickel metal hydride batteries

Mark R. St J. Foreman,* Christian Ekberg and Arvid Ödegaard Jensen

A synthesis of a safe and effective hydrogenation catalyst has been developed with used nickel metal hydride electrical cells as the starting material.

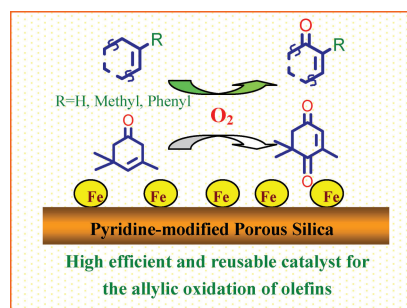


827

Iron chloride supported on pyridine-modified mesoporous silica: an efficient and reusable catalyst for the allylic oxidation of olefins with molecular oxygen

Jianyong Mao, Xingbang Hu, Haoran Li,* Yong Sun, Congmin Wang and Zhirong Chen

The novel heterogeneous catalyst with iron chloride immobilized on pyridine-modified mesoporous silica displayed excellent catalytic activity, selectivity and reusability for the allylic oxidation of olefins with molecular oxygen.

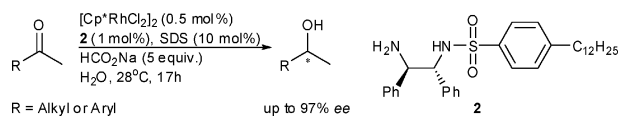


832

Rhodium-catalyzed asymmetric transfer hydrogenation of alkyl and aryl ketones in aqueous media

Katrin Ahlford, Jesper Lind, Lena Mäler and Hans Adolfsson*

Alkyl and aryl ketones are efficiently reduced under transfer hydrogenation conditions in water using a novel lipophilic rhodium catalyst based on ligand **2**.



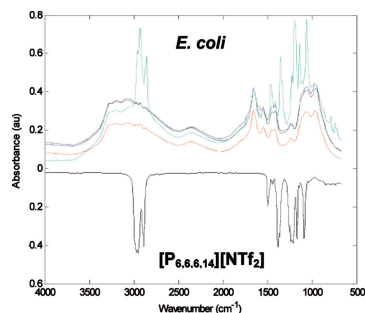
PAPERS

836

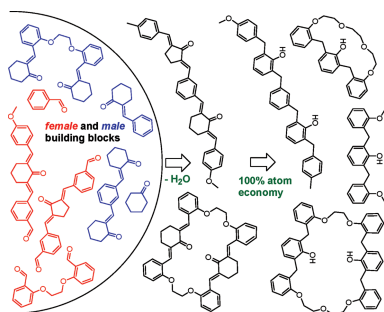
Accumulation of ionic liquids in *Escherichia coli* cells

Robert J. Cornmell, Catherine L. Winder, Gordon J. T. Tiddy, Royston Goodacre and Gill Stephens*

FT-IR spectroscopy can be used to detect accumulation of ionic liquids in *Escherichia coli* cells.



842

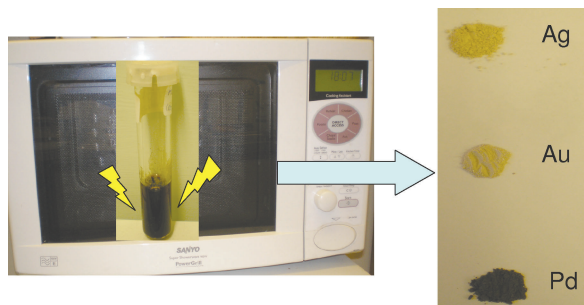


Platform technology for dienone and phenol–formaldehyde architectures

Marilena A. Giarrusso, Luke T. Higham, Ulf P. Kreher, Ram S. Mohan, Anthony E. Rosamilia, Janet L. Scott* and Christopher R. Strauss*

A simple, green chemistry strategy, utilising a building block approach, toward the development of an array of potentially useful families of compounds, including phenol–formaldehyde products and novel macrocycles is described.

853

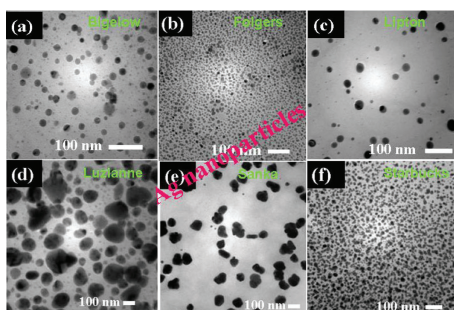


Microwave facile preparation of highly active and dispersed SBA-12 supported metal nanoparticles

Juan Manuel Campelo, Tomas David Conesa, Maria Jose Gracia, Maria Jose Jurado, Rafael Luque,* Jose Maria Marinas and Antonio Angel Romero

A simple and swift microwave protocol for the preparation of metal nanoparticles supported on a mesoporous structure has been developed. The supported materials were highly active and differently selective in the catalytic oxidations of styrene and benzyl alcohol.

859

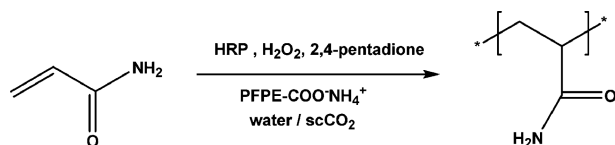


Green synthesis of silver and palladium nanoparticles at room temperature using coffee and tea extract

Mallikarjuna N. Nadagouda and Rajender S. Varma*

An extremely simple green approach that generates bulk quantities of nanocrystals of noble metals such as silver (Ag) and palladium (Pd) using coffee and tea extract at room temperature is described.

863



HRP-mediated inverse emulsion polymerisation of acrylamide in supercritical carbon dioxide

Silvia Villarroya,* Kristofer J. Thurecht and Steven M. Howdle*

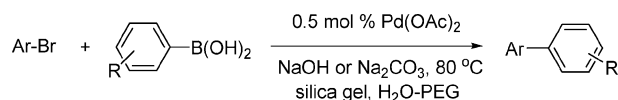
This article describes the horseradish peroxidase (HRP)-mediated inverse emulsion polymerisation of water-soluble acrylamide in supercritical carbon dioxide (scCO₂).

868

Silica-assisted Suzuki–Miyaura reactions of heteroaryl bromides in aqueous media

Shengyin Shi and Yuhong Zhang*

A new environmentally benign and recyclable catalytic system has been developed for the Suzuki–Miyaura cross-coupling of heteroaryl bromides and arylboronic acids in aqueous media.



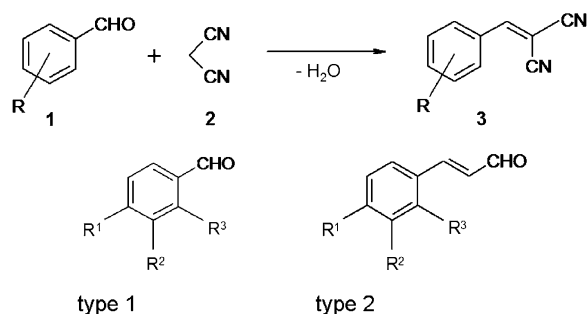
Ar = Heteroaryl, naphthalenyl, alkenyl

873

The Knoevenagel condensation at room temperature

Ronald Trotzki, Markus M. Hoffmann and Bernd Ondruschka*

The Knoevenagel condensation can proceed at room temperature to at times quantitative yields either solvent-free as a mixture of reactants or in a solution of ethanol.

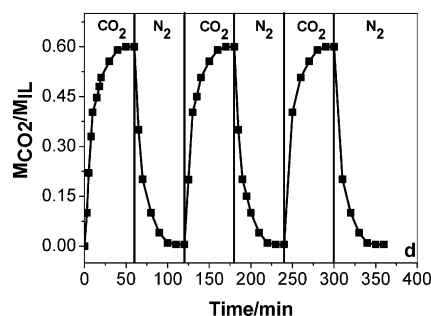


879

Absorption of CO₂ by ionic liquid/polyethylene glycol mixture and the thermodynamic parameters

Xiaoyong Li, Minqiang Hou, Zhaofu Zhang, Buxing Han,* Guanying Yang, Xiaoling Wang and Lizhuang Zou*

The ionic liquid [Choline][Pro] synthesized from renewable materials and [Choline][Pro]/polyethylene glycol 200 mixture can be used to absorb CO₂ effectively, and desorption of CO₂ can be easily achieved under vacuum or bubbling nitrogen through the solution.

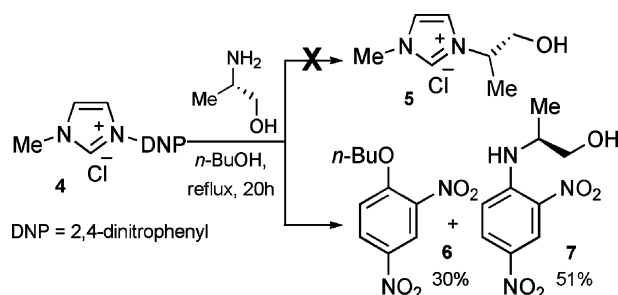


885

Non-occurrence of a Zincke-like process upon treatment of 1-(2,4-dinitrophenyl)-3-methylimidazolium chloride with a chiral primary amine

Julio Cezar Pastre, Carlos Roque D. Correia and Yves Génisson*

Huang's preparation of chiral imidazolium salts by means of a Zincke-like process was re-investigated.



AUTHOR INDEX

Adolfsson, Hans, 832
 Ahlford, Katrin, 832
 Campelo, Juan Manuel, 853
 Chen, Zhirong, 827
 Conesa, Tomas David, 853
 Cornmell, Robert J., 836
 Correia, Carlos Roque D., 885
 Ekberg, Christian, 825
 Foreman, Mark R. St J., 825
 Fortunak, Joseph M., 823
 Génisson, Yves, 885
 Giarrusso, Marilena A., 842
 Goodacre, Royston, 836
 Gracia, Maria Jose, 853


Han, Buxing, 879
 Higham, Luke T., 842
 Hoffmann, Markus M., 873
 Hou, Minqiang, 879
 Howdle, Steven M., 863
 Hu, Xingbang, 827
 Jurado, Maria Jose, 853
 Kreher, Ulf P., 842
 Kunle, O. O., 823
 Li, Haoran, 827
 Li, Xiaoyong, 879
 Lind, Jesper, 832
 Luque, Rafael, 853
 Mäler, Lena, 832

Mao, Jianyong, 827
 Marinas, Jose Maria, 853
 Mohan, Ram S., 842
 Nadagouda, Mallikarjuna N., 859
 Ödegaard Jensen, Arvid, 825
 Ondruschka, Bernd, 873
 Pastre, Julio Cezar, 885
 Rogers, Robin D., 823
 Romero, Antonio Angel, 853
 Rosamilia, Anthony E., 842
 Scott, Janet L., 842
 Shi, Shengyin, 868
 Stephens, Gill, 836
 Strauss, Christopher R., 842

Sun, Yong, 827
 Thurecht, Kristofer J., 863
 Tiddy, Gordon J. T., 836
 Trotzki, Ronald, 873
 Varma, Rajender S., 859
 Villarroya, Silvia, 863
 Wang, Congmin, 827
 Wang, Xiaoling, 879
 Winder, Catherine L., 836
 Yang, Guanying, 879
 Zhang, Yuhong, 868
 Zhang, Zhaofu, 879
 Zou, Lizhuang, 879

FREE E-MAIL ALERTS AND RSS FEEDS


Contents lists in advance of publication are available on the web *via* www.rsc.org/greenchem – or take advantage of our free e-mail alerting service (www.rsc.org/ej-alert) to receive notification each time a new list becomes available.

 Try our RSS feeds for up-to-the-minute news of the latest research. By setting up RSS feeds, preferably using feed reader software, you can be alerted to the latest Advance Articles published on the RSC web site. Visit www.rsc.org/publishing/technology/rss.asp for details.

ADVANCE ARTICLES AND ELECTRONIC JOURNAL

Free site-wide access to Advance Articles and the electronic form of this journal is provided with a full-rate institutional subscription. See www.rsc.org/ejs for more information.

* Indicates the author for correspondence: see article for details.

 Electronic supplementary information (ESI) is available *via* the online article (see <http://www.rsc.org/esi> for general information about ESI).

RSC online shop

Simple, secure, *fast!*

24/7 access: The RSC online shop gives you continuous access to class leading products and services, expertly tailored to cater for your training and educational needs.

Browse and buy: Visit our shop to browse over 750 book titles, subscribe or purchase an individual article in one of our journals, join or renew your RSC membership, or register to attend a conference or training event.

Gift ideas: If you're looking for gift ideas, look no further. In our online shop you'll find everything from popular science books like *The Age of the Molecule* and the inspirational *Elegant Solutions* from award winning writer, Philip Ball, to our stunning Visual Elements wall chart and jigsaw.

With secure online payment you can shop online with confidence.

The RSC has so much to offer... *why not go online today?*



RSC Publishing

www.rsc.org/shop

Registered Charity Number 207890

Chemical Technology

New forensic technology detects invisible fingerprints

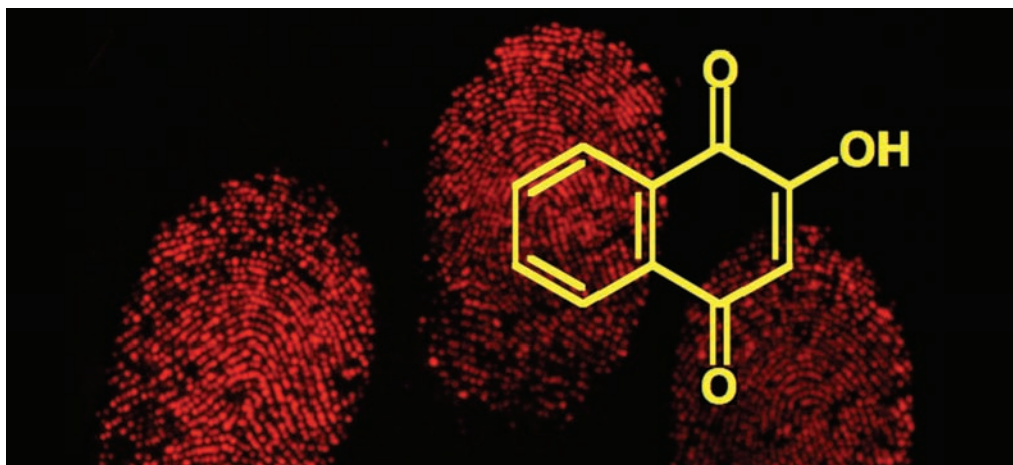
Could henna help catch criminals?

Scientists from Australia and Israel have discovered a new, safe way of detecting invisible fingerprints.

Fingerprints on porous surfaces such as paper are usually detected by a chemical called ninhydrin. Ninhydrin reacts with amino acids secreted by the fingers and turns invisible fingerprints dark purple. But ninhydrin is an irritant and so scientists are looking for safer alternatives.

Now, Simon Lewis at Curtin University of Technology, Perth, Australia and colleagues have found that a component of henna can work in a similar way to ninhydrin but without causing irritation. Henna is a traditional skin and hair dye, made from the leaves of the plant *Lawsonia inermis*. It has been used for more than a thousand years without ill effect.

Lawsonone is the compound thought to be responsible for the staining properties of henna. It is a naphthoquinone, a group of compounds already known to react with amino acids. Lewis' team



found that amino acids in invisible fingerprints turn a brown–purple colour when exposed to lawsonone and are strongly luminescent under a forensic light source.

'The discovery will no doubt generate lots of activity in the global forensic identification community,' says Della Wilkinson, a forensic expert from the Royal Canadian Mounted Police. 'Lawsonone has interesting spectroscopic

Amino acids in fingerprint residues react with lawsonone to give strongly luminescent fingerprints

Reference
R Jelly *et al*, *Chem. Commun.*, 2008, 3513 (DOI: 10.1039/b808424f)

characteristics that could prove to be very useful when examining surfaces that fluoresce under excitation wavelengths used for existing detection reagents.'

'This research opens the possibility of a whole suite of new analogues that may lead to further improvements in fingerprint detection,' says Lewis. His team are currently testing other closely related compounds. *Freya Mearns*

In this issue

Flow chemistry for the masses

Easy-to-use assembly blocks simplify microfluidic technology

Laying down a path to cheaper solar power

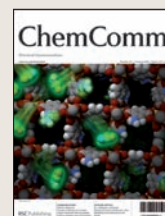
Electrodeposition yields semiconductor films at room temperature and pressure

Instant insight: Fuel cells get cooler

Dan Brett and colleagues discuss how advances in materials and engineering open up new opportunities for solid oxide fuel cells

Interview: Navy's sensing mission

Frances Ligler tells Kathleen Too about portable, automated biosensors for fast, on-site detection of toxins and explosives



The latest applications and technological aspects of research across the chemical sciences

Application highlights

Gel acts as scaffold for growing cylinders of living tissue

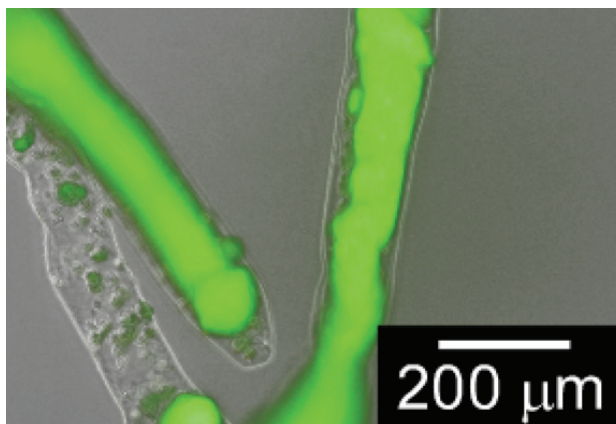
Tubular cells

Japanese researchers have developed a new method for growing cylinders of living cells.

Many tissues in the human body, such as muscle or nerve fibres, are cylinders, so growing cylindrical clumps of cells is a necessity for tissue engineering and cell transplantation.

Shinji Sugiura at the National Institute of Advanced Industrial Science and Technology, Tsukuba, and colleagues made micrometre-scale tubular gels by controlling the flow of two miscible fluids in a microchannel. The interaction between the two fluids led to the formation of droplets and gels. Sugiura showed that the gels can act as scaffolds for growing cylindrical tissues.

'In previous studies, immiscible two-phase flow in a microchannel has been successfully applied for the preparation of spherical materials,'



says Sugiura. 'We thought similar technology with miscible fluids could be applied to cylindrical and tubular tissues.'

Professor Teruo Fujii, an expert in microfluidics at the University of Tokyo, Japan, describes the work as 'interesting' but cautions: 'They

Cells use the gel microtubes as scaffolds for growth. Green fluorescence indicates viable cells

don't show any quantitative data on the activity or function of the cultivated cells. It is a bit difficult to draw a concrete conclusion from the photos of the cells shown in the figures.'

Sugiura acknowledges this: 'We have to investigate the cellular functions of the cylindrical tissue formed in detail. We hope it will have higher cellular activity than cells cultured conventionally in monolayers.'

'Another future challenge is fabricating tubular tissues. Unlike cylindrical tissues, tubular tissues, such as blood vessels or organ ducts, are hollow. We think the gel will be useful for making these types of tissue too,' Sugiura adds.

Colin Batchelor

Reference

S Sugiura *et al*, *Lab Chip*, 2008, **8**, 1255 (DOI: 10.1039/b803850c)

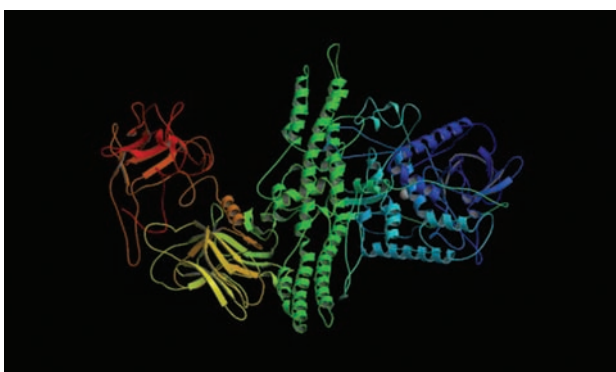
Scientists search for inhibitors of potential bioweapon

New test for deadly toxin

A new assay to measure the biological activity of a lethal neurotoxin could help scientists develop therapeutic inhibitors of the poison, say US chemists.

Botulinum neurotoxin A is the active ingredient in Botox, the cosmetic injection used to smooth out wrinkles. But if ingested or inhaled, the toxin's muscle-relaxing effect can be lethal, causing the muscle paralysis illness botulism. This has prompted fears that it could be used as a biological weapon. Current treatments are ineffective against the toxin once it has entered the cells, and only mechanical respirators can keep a patient alive once toxin stops them breathing. Such systems would be overwhelmed in the event of a bioterrorism attack, says Kim Janda and colleagues at the Scripps Research Institute in La Jolla, hence the need for better treatments.

In order to assess the effectiveness of potential inhibitors



of the toxin, reliable methods to measure their activity are needed. Current tests are not accurate enough for finer analysis, such as determining the mechanism of inhibition, says Janda. To improve sensitivity and reproducibility, Janda has developed a new assay based on LC-MS – liquid chromatography followed by mass spectrometry.

The new assay uses a peptide

A lethal poison: inhalation of less than a microgram of botulinum neurotoxin A can kill a human being

mimic of the substrate the neurotoxin targets in the body. The toxin slices the peptide into two pieces. The shorter section can be isolated from the reaction mixture by high performance LC and then quantified against an internal standard using a mass spectrometer. The team used this assay to confirm the potency of an inhibitor they had developed to block the toxin.

'Our aim is to identify a stable, potent and specific inhibitor which could eventually be used in clinical practice,' says Janda. 'The biggest challenge lies in the impossibility to conduct standard clinical trials.'

'This is a useful and robust approach,' says Linda Lawton, who studies naturally occurring toxins at the Robert Gordon University, Aberdeen, UK. 'It is great to see that they have not only developed the assay but clearly shown its value in their successful characterisation of a potent new inhibitor.'

James Mitchell Crow

Reference

K Čapková *et al*, *Chem. Commun.*, 2008, 3525 (DOI: 10.1039/b808305c)

Electrodeposition yields semiconductor films at room temperature and pressure

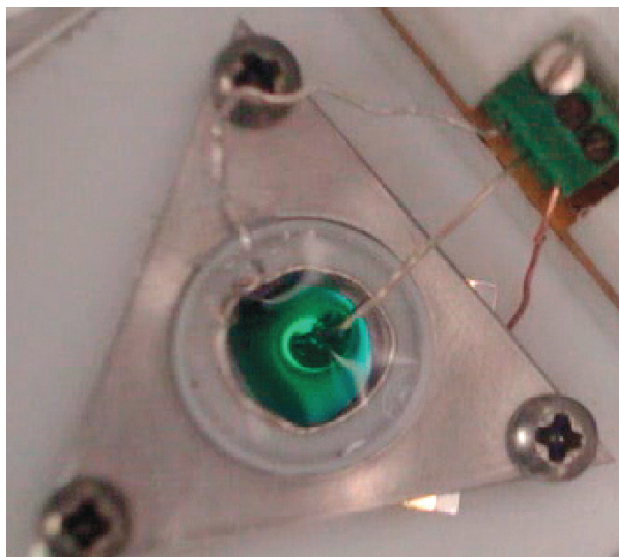
Laying down a path to cheaper solar power

A new way of making semiconductor films could lead to cheaper solar cells, claim scientists in Germany.

Frank Endres and colleagues at Clausthal University of Technology electrochemically deposited silicon-germanium films onto a gold electrode using an air- and water-stable ionic liquid as the solvent. This is the first time that high purity silicon-germanium films have been made in a controlled way at room temperature and pressure.

The method has a number of advantages over alternative deposition methods, which use ultra high vacuum and high temperatures. 'Electrodeposition is much cheaper and faster,' says Endres. 'Furthermore, if the electrodeposition bath is large enough, all sizes and shapes of substrate material can be coated.'

The electronic properties of silicon-germanium can be tuned to match its intended application by varying the germanium content



of the material, which can be anywhere in the spectrum from pure silicon to pure germanium. Endres showed that pure silicon, silicon-germanium alloys and pure

A film of silicon-germanium (green) is electrodeposited from the ionic liquid solvent

germanium can be deposited from the ionic liquid solution.

'Our results show for the first time that it is possible to electrodeposit semiconductors from ionic liquid solutions with a quality that is competitive with physical methods, such as molecular beam epitaxy,' comments Endres. 'This opens the door to many applications, from nanowires for lithium ion batteries to solar cells.'

Ingo Krossing, who studies the applications of ionic liquids in electrochemistry at the University of Freiburg, Germany, agrees with Endres. 'This is a remarkable step forward to achieving the goal of synthesising solar cells using electrochemistry rather than expensive and high energy melt procedures,' he says.

James Hodge

Reference

R Al-Salman, S Z El Abedin and F Endres, *Phys. Chem. Chem. Phys.*, 2008, DOI: 10.1039/b806996b

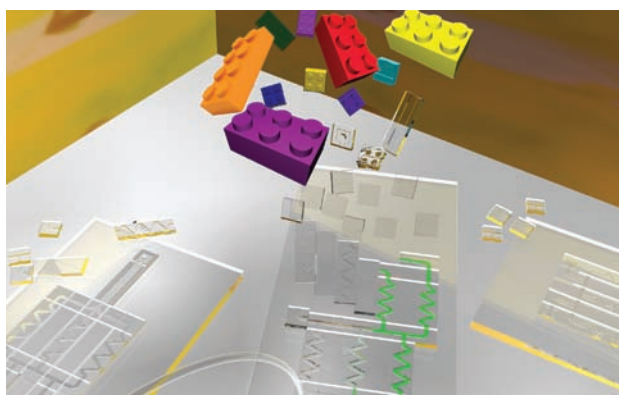
Easy-to-use assembly blocks simplify microfluidic technology

Flow chemistry for the masses

Two new build-your-own microfluidic systems promise to simplify the technology so the whole research community can use it, say scientists in the US.

Microfluidic systems offer chemists and biologists a host of advantages over conventional-scale experiments, including minimising the amount of expensive reagents required, and the ability to integrate multiple experiments into a single system. However, their complex set-up limits their use. Now, two groups in the US have developed sets of microfluidic components that can be simply connected together into a variety of reactor designs.

Mark Burns and Minsoung Rhee at the University of Michigan developed a selection of microfluidic assembly blocks, made by moulding polydimethylsiloxane, a cheap



silicon rubber. Burns showed that the blocks can be combined into a variety of systems – from mixers and separators to bioreactors – by connecting them together on a glass slide.

'I have one collaborator in the chemistry department using the blocks, but I'd like to set up a web

The microfluidic blocks connect together like Lego bricks

References

M Rhee and M A Burns, *Lab Chip*, 2008, **8**, 1365 (DOI: 10.1039/b805137b)
P K Yuen, *Lab Chip*, 2008, **8**, 1374 (DOI: 10.1039/b805086d)

page selling bags of them,' says Burns. And the system should be affordable, he adds: 'Each block should cost significantly under a US dollar.'

Meanwhile, Po Ki Yuen at US firm Corning has developed a series of microfluidic modules that clip together just like Lego bricks. The key development is a miniature luer fitting, which gives a leak-free seal between the components up to a pressure of at least 3.5 bar.

'My ultimate goal is to develop a complete 'plug-n-play' system that can be controlled by a computer,' says Yuen. 'The system has not been commercialised; a business decision has not yet been made to do so. My focus at this point in time is to work with university professors to see if the system can be a benefit for their microfluidics classes.'

James Mitchell Crow

Radionuclides used to piece together timescale of volcanic explosions

Understanding ancient eruptions

Scientists are a step nearer to understanding volcanic processes that occurred as far back as 8000 years ago.

Akio Makishima and colleagues at Okayama University at Misasa, Japan, have developed a method for measuring attogram (10^{-18} gram) amounts of radioactive elements in basalt rocks.

Basalt, one of the most common rock types on Earth, is formed when lava from volcanic eruptions cools. It contains small amounts of radium-226, a radionuclide that is formed over billions of years by the radioactive decay of uranium-238 via thorium-230. By measuring the quantities and ratios of these radionuclides in volcanic rocks, scientists can piece together the timescale of volcanic eruptions.

The team analysed basalts by multicollector inductively coupled plasma mass spectrometry. Makishima added a known amount of radium-228 to the samples to allow him to determine unknown amounts of radium-226. But radium-228 decays to form thorium-228 and because these



radionuclides have the same mass, the mass spectrometer cannot distinguish between them. This causes errors in the dating process.

Thorium-228 can be removed from the radium fraction by column chromatography but Makishima found this inefficient.

Radium in volcanic rocks reveals the timescale of the original eruption

Reference

A Makishima, T A Chekol and E Nakamura, *J. Anal. At. Spectrom.*, 2008, **23**, 1102 (DOI:10.1039/b807431c)

'If a delay occurred in analysing the sample, we had to do column chemistry again because more thorium-228 formed. To overcome this problem, in situ correction of thorium-228 was required,' he says.

Makishima found that thorium-228, but not radium-228, forms a positively charged oxide ion in the mass spectrometer. By measuring the intensity of the thorium oxide peak, Makishima calculated the amount of thorium-228 in the radium samples and used it to correct the radium measurements.

Marcel Regelous, an expert in the analysis of volcanic rocks at the Royal Holloway University, London, UK, says, 'Analysis of such small quantities of radium has applications in dating geological processes, in particular for investigating timescales involved in the crystallisation of volcanic rocks. This requires analysis of individual mineral fractions separated from the crushed rock sample, which often contain very little radium.'

Ziva Whitelock

Renewable fuel cell opens the door to electric vehicles

Driving power for electric cars

Scientists have made the first renewable fuel cell that can store more energy than petrol.

Electric vehicles are potentially more environmentally friendly than petrol vehicles because they do not emit greenhouse gases, but the cells they use for power can't store as much energy as fossil fuels. Now, Stuart Licht and colleagues at the University of Massachusetts, Boston, US, have developed a vanadium boride-air fuel cell with a much larger energy capacity than current vehicle batteries. 'The cell has ten times the energy capacity of lithium ion batteries and three times the energy density of zinc-air batteries,' says Licht, 'although all these devices work in the same way.'

In its electric car 'Volt', launching



Plug-in power: the future for transport?

Reference

S Licht *et al.*, *Chem. Commun.*, 2008, 3257 (DOI: 10.1039/b807929c)

in 2010, General Motors (GM) uses a lithium ion battery which can power the car for 40 miles before it needs to be recharged. To extend this range, GM added a standard combustion engine to recharge the battery when it runs low.

'Our renewable fuel cell opens the door to electric vehicles with viable driving ranges, without a separate combustion engine and frequent battery recharges,' says Licht. The vanadium boride-air fuel cell needs only air and fresh fuel to complete the recharge process. Using this system, a motorist would drive into a fuel station, receive fresh fuel and drive away.

Peter Bruce, an expert in new materials for energy storage devices at St Andrews University,

UK, comments: 'Finding ways to store more energy than is possible at present is a key challenge and imaginative solutions are necessary. Replacing the zinc in a zinc-air primary battery with a vanadium boride anode is certainly interesting. However, it does raise a number of challenges for practical devices, such as recharging the batteries, and more scientific questions to be answered.'

Licht acknowledges that there is a lot of work to do before the fuel cell can be commercialised. 'This is a first study demonstrating the very high capacity of the cell. Engineering details, systems optimisation and scale-up need to be developed,' he says.

Janet Crombie

Interview

Navy's sensing mission

Frances Ligler tells Kathleen Too about portable, automated biosensors for fast, on-site detection of pathogens, toxins, pollutants, drugs and explosives



Frances Ligler

Frances Ligler is a senior scientist at the US Naval Research Laboratory's Center for Bio/Molecular Science and Engineering. She has been the recipient of numerous medals and awards including the Women in Science and Engineering Outstanding Achievement in Science Award.

How did you come to work for the US Naval Research Laboratory?

Joel Schnur, the current director of the Center for Bio/Molecular Science and Engineering, was starting an interdisciplinary department studying the self-assembly of biomolecules. I thought this was an interesting vision and I wanted to work at the molecular level; I could see that this was where breakthroughs were happening. So I joined Joel and, after a year, started the programmes in biosensors, trying to make functional molecules on surfaces and using optical readout systems.

Tell us about the biodetection systems you designed. How long does it take to develop the technology, from having the idea to commercialising the device?

The 'Raptor' is a fibre optic biosensor that has four optical fibres with four different functions in a 12 pound box. The system is fully automated; all the user has to do is put in the sample and press run, and the result is given in ten minutes. Alternatively, it can be attached to an air sampler and left out in the field to send results at pre-programmed time intervals.

The 'Biohawk' has a sensor that is a third of the size of the 'Raptor'. It has eight fibres with eight different functions. The air sampler is integrated into a backpack, so collection of bacteria or toxins from the air, for example, can be done by someone wandering through the field operating the device from the backpack.

Both systems detect mostly biological warfare agents; they have been used in tests for anthrax at a post office. They have also been used for detecting bacteria and toxins in foods, and detecting *E. Coli* and other indicators of sewage contamination on beaches and in the Great Lakes.

We started working on these ideas in 1986; the very first fibre optics were available in 1997 and the first automated systems were available in 2000. But they didn't really become reliable systems until around 2003. That is a pretty typical path.

You put your biology expertise to excellent use by using on-chip and microarray technologies to detect multiple targets. How easy to use and stable are these devices?

If you immobilise proteins very carefully, their function is not jeopardised. If you dehydrate

them in the presence of a protective agent, that prevents denaturation, so you can keep them at room temperature for two years and continue to reuse them. They are pretty robust. There are other, even more robust molecules you can use as recognition molecules, such as the small molecules in low molecular weight antimicrobial reagents. Work being done by Ellen Goldman, George Anderson and others looks at small single-chain antibodies that are so robust, you can heat them to 90 degrees Celsius and they continue to work. You can put them in organic solvents to remove unbound material, and rehydrate them, and they will still work. Molecules like that will further extend the stability and reliability of the systems for long-term use by non-technical users.

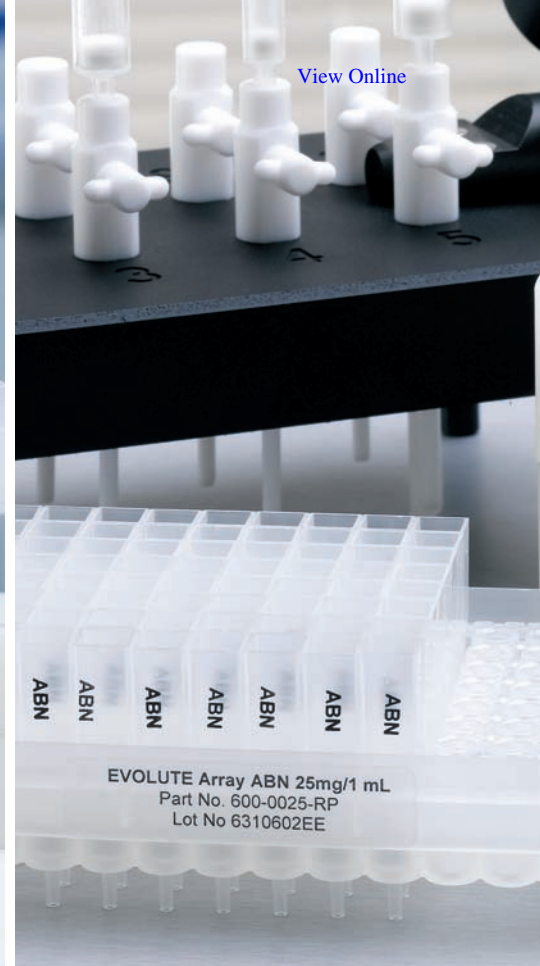
What is the ideal sensor for a non-expert to use?

The equivalent of a pregnancy test. The problem is that you can't usually get the sensitivity you want for multiple applications, and the amount of sample that you can actually test is limited. But these devices are ideal in that they are low cost, and you can see the results with your own eyes. So, the easier we can make a device to use in terms of limiting the complexities of the fluidics [the use of a fluid to perform analog or digital operations] and the read-out, the closer we get to something being broadly applicable.

What does the future hold for biosensor research?

I think biosensors will be a lot more user-friendly, and plastic optics will have an important part to play in making the optics cheaper and smaller. Right now, the optics are the most expensive part of the system, so if you can make those cheaper by integrating the optics and the fluidics, so much the better. I think plastic optics will be easier to integrate than trying to make the fluidics in silicon.

We are going to learn about disease markers such as cancer and other infection biomarkers. I think that will be a real breakthrough for casualty care or care of patients with infectious diseases or heart attacks, for example. I think that is going to be a pretty big market.



IST Sample Preparation • Bioanalysis • Clinical • Environmental • Forensic • Agrochemical • Food • Doping Control

EVOLUTE® CX **NEW!**

Mixed-mode selectivity, generic methodology and efficient extraction

EVOLUTE® CX mixed-mode resin-based SPE sorbent extracts a wide range of **basic drugs** from biological fluid samples. EVOLUTE CX removes matrix components such as proteins, salts, non-ionizable interferences and phospholipids, delivering cleaner extracts with reproducible recoveries for accurate quantitation.

EVOLUTE® ABN

Minimize matrix effects, reduce ion suppression and concentrate analytes of interest

EVOLUTE® ABN (Acid, Base, Neutral) is a water-wettable polymeric sorbent optimized for fast generic reversed phase SPE. Available in 30 μm columns and 96-well plates for bioanalysis and **NEW 50 μm columns** – ideally suited for environmental, food/agrochemical and industrial analysis as well as forensic and doping control applications.

Contact your local Biotage representative or visit www.biotage.com to request a **FREE** sample.

Instant insight

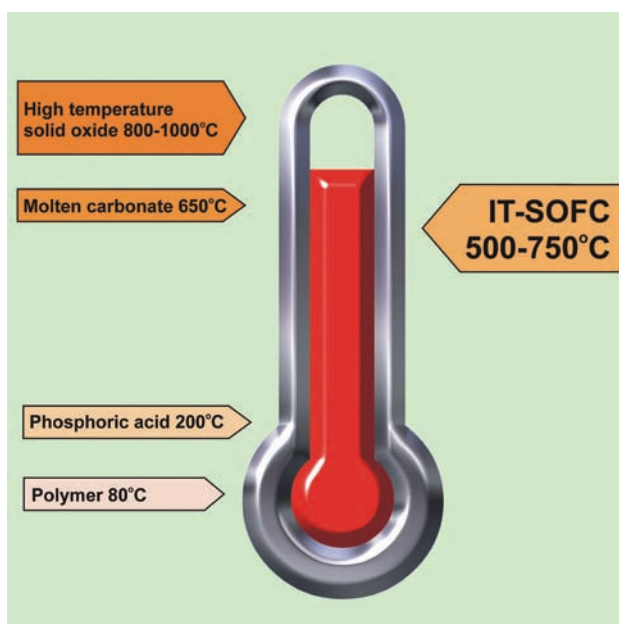
Fuel cells get cooler

Brett, Atkinson, Brandon and Skinner of the Imperial College Fuel Cell Network, London, UK, look at how advances in materials and engineering are presenting new opportunities for solid oxide fuel cells

Fuel cells are electrochemical energy conversion devices that convert the chemical energy in fuel directly into electricity and heat without combustion. Simplistically, a fuel cell can be viewed as a cross between a battery, which converts chemical energy directly into electrical energy, and a heat engine, a continuously fuelled, air breathing device. There is a range of different fuel cell technologies, each with its own materials set and operation temperature, ranging from room temperature to over 1000 degrees Celsius. However, they all share the characteristics of high efficiency, no moving parts, quiet operation and low or zero emissions.

There is no consensus as to the optimal operating temperature of fuel cells; the preferred temperature of operation depends to a large extent on the application. However, there is significant effort to raise the operating temperature of polymer electrolyte fuel cells (PEFCs) and reduce the operating temperature of solid oxide fuel cells (SOFCs). PEFCs currently operate at around 80 degrees Celsius and are used in automobiles, mobile phones and laptops. SOFCs operate at more than 800 degrees Celsius and use a ceramic oxide ion-conducting electrolyte to generate energy on a large scale.

Advances in the chemistry and processing of materials are allowing the operating temperature of SOFCs to be lowered into the so-called 'intermediate temperature' (IT) region of 500 to 750 degrees Celsius. The IT-SOFC opens up a new range of applications and opportunities for SOFCs in areas formally dominated by PEFCs,



while maintaining the ability to operate on hydrocarbon fuels and produce high quality heat.

Operation in the IT range expands the choice of materials and stack designs that can be used compared to conventional high temperature (HT) SOFCs. Lower temperature operation affords more rapid start-up, improved durability, reduced system cost and more robust construction through the use of compressive seals and metallic construction materials (as opposed to the all-ceramic HT-SOFCs).

There are two main routes by which SOFCs can be used at lower temperatures while still attaining comparable performance to the higher temperature technology. The first involves reducing the thickness of the electrolyte to the order of a few 10s of micrometres, so ions can travel more easily

through the fuel cell. Alternatively, the same result can be achieved by improving the electrolyte's ionic conductivity at lower temperatures and the electrodes' electrochemical performance.

The range of new applications for the IT-SOFC includes soldiers' personal power supplies, traction power for vehicles, remote telecommunications, power for isolated communities and back-up power units for trucks. However, it is the small-scale combined heat and power market where the IT-SOFC is particularly well suited. Operating on natural gas and with a heat-to-power ratio close to one, IT-SOFCs with an electrical power rating of about one kilowatt are expected to be popular as combined heat and power sources for use in the home. Indeed, IT-SOFCs have the potential to be the simplest fuel cell system and are a strong contender to be the first fuel cell technology to reach mass market.

As with all fuel cells, the cost of IT-SOFCs must be reduced for them to compete in the market with current technologies. Using less, and cheaper, material is necessary; moving to lower temperature operation represents a significant step in this direction. Scientists still need to develop IT-SOFCs with commercially meaningful levels of durability. Fundamental studies are improving our understanding of processes such as electrode sintering, anode-fuel interaction, electrocatalyst poisoning and the mechanical properties of electrolytes and support structures.

Intermediate temperature solid oxide fuel cells hold the middle ground in the temperature scale of fuel cell operation

Reference
D J L Brett *et al*, *Chem. Soc. Rev.*, 2008, **37**, 1568 (DOI: 10.1039/b612060c)

Read more in 'Intermediate temperature solid oxide fuel cells' in issue 8 of *Chemical Society Reviews*.

Essential elements

Even greater impact!

RSC authors, readers and publishing teams throughout the world are celebrating news of continued success for RSC journals, following the release of the 2007 Impact Factors, calculated by ISI®.

Titles from across the collection have again recorded impressive rises, while the latest immediacy indices confirm the relevance and topicality of research published by the RSC. According to Robert Parker, managing director of RSC Publishing, 'The number of citations to research published in RSC journals rose by an average of 36% in 2007, endorsement indeed to the efforts of our authors, referees and editorial teams.'

Flagship journal, *ChemComm* sees a 13% increase in impact factor to an all time high of 5.141, while *Chem Soc Rev* is ranked first for immediacy (3.406) in general chemistry review journals and third for impact factor (13.082).

Molecular BioSystems, now in its fourth year of publication, achieves a staggering increase of 68% to an impact factor of 4.121. *Soft Matter*, launched at the same time, retains its position as number one in the field for both impact and immediacy, at 4.703 and 0.784, respectively. Also in the materials field, *Journal of Materials Chemistry* has an impact factor of 4.339, representing an impressive 59% rise over three years.

Number one is a common theme across the RSC journal portfolio. *The Analyst* is first for immediacy in analytical chemistry at 1.032, and enjoys a rise in



impact factor of more than 10% for the second year running to 3.553. *JAAS (Journal of Analytical Atomic Spectrometry)* maintains its position as the number one journal in the field (impact factor 3.269) and, with an immediacy index of 0.614, *CrystEngComm* moves to the number one position for crystal engineering. *Dalton Transactions* maintains its position as the general inorganic chemistry journal with the highest immediacy index (0.758) and shows the biggest increase in impact factor (6.6% to 3.212) of any inorganic chemistry journal.

Green Chemistry extends its lead as the number one green chemistry journal with a 15% rise in impact factor to 4.836. *Journal of Environmental Monitoring* also sees a substantial increase with a 20% rise in impact factor to 1.833, while *Photochemical & Photobiological Sciences* maintains its position as the number one journal for photochemical and photobiological research (2.208).

Natural Product Reports is first for immediacy in the field of organic chemistry (1.672) and *Organic & Biomolecular Chemistry*

sees a 10% increase in impact factor to 3.167. *Lab on a Chip* remains one of the leading journals in micro- and nano-research with an impact factor of 5.068 and *PCCP (Physical Chemistry Chemical Physics)* clocks in with an impact factor of 3.343, representing an impressive 61% rise over three years.

RSC Publishing is committed to providing a world-class publishing service to its authors and from these results it is clear to see that journals from RSC Publishing are recognised by researchers throughout the world as a key resource to publish and read the very best research.

We would like to thank all our authors, referees and readers for their continued support.

Footnote:

The annual ISI® impact factors provide an indication of the average number of citations per paper. The impact factor for 2007 is calculated from the total number of citations given in 2007 to citeable articles published in 2005 and 2006, divided by the number of citeable articles published in 2005 and 2006. The immediacy index measures how topical and urgent the papers published in a journal are. The 2007 immediacy index is the total number of citations given in 2007 to citeable articles published in 2007 divided by the number of citeable articles published in 2007. Data based on 2007 impact factors, calculated by ISI®, released June 2008.

Apart from fair dealing for the purposes of research or private study for non-commercial purposes, or criticism or review, as permitted under the Copyright, Designs and Patents Act 1988 and the copyright and Related Rights Regulations 2003, this publication may only be reproduced, stored or transmitted, in any form or by any means, with the prior permission of the Publisher or in the case of reprographic reproduction in accordance with the terms of licences issued by the Copyright Licensing Agency in the UK. US copyright law is applicable to users in the USA.

And finally..

With the conference season in full swing, RSC Publishing staff are spread around the globe at a number of major conferences over the coming weeks.

Are you attending the ACS National Meeting & Exposition in Philadelphia? Make sure you visit the RSC Publishing stand where staff will be on hand to answer any questions you may have. You can pick up a copy of Issue 1 of *Energy & Environmental Science*, our newest journal, as it makes its print debut, and find out the latest journals news. Book authors John Emsley (*Molecules of Murder*) and Stephen Beckett (*The Science of Chocolate*) will be signing copies of their books.



PHOTO:DISC

In September, the focus is Turin, Italy, for the 2nd Annual EuCheMS meeting. The wide-ranging themes provide scope for showcasing RSC products – including the recently announced *Metallomics* and *Integrative Biology*, both launching January 2009.

If you're travelling to these or other conferences, look out for RSC Publishing staff – they will be happy to meet you.

Chemical Technology (ISSN:1744-1560) is published monthly by the Royal Society of Chemistry, Thomas Graham House, Science Park, Milton Road, Cambridge UK CB4 0WF. It is distributed free with *Chemical Communications*, *Journal of Materials Chemistry*, *The Analyst*, *Lab on a Chip*, *Journal of Atomic Absorption Spectrometry*, *Green Chemistry*, *CrystEngComm*, *Physical Chemistry Chemical Physics*, *Energy & Environmental Science* and *Analytical Abstracts*. *Chemical Technology* can also be purchased separately. 2008 annual subscription rate: £199; US \$396. All orders accompanied by payment should be sent to Sales and Customer Services, RSC (address above). Tel +44 (0) 1223 432360, Fax +44 (0) 1223 426017 Email: sales@rsc.org

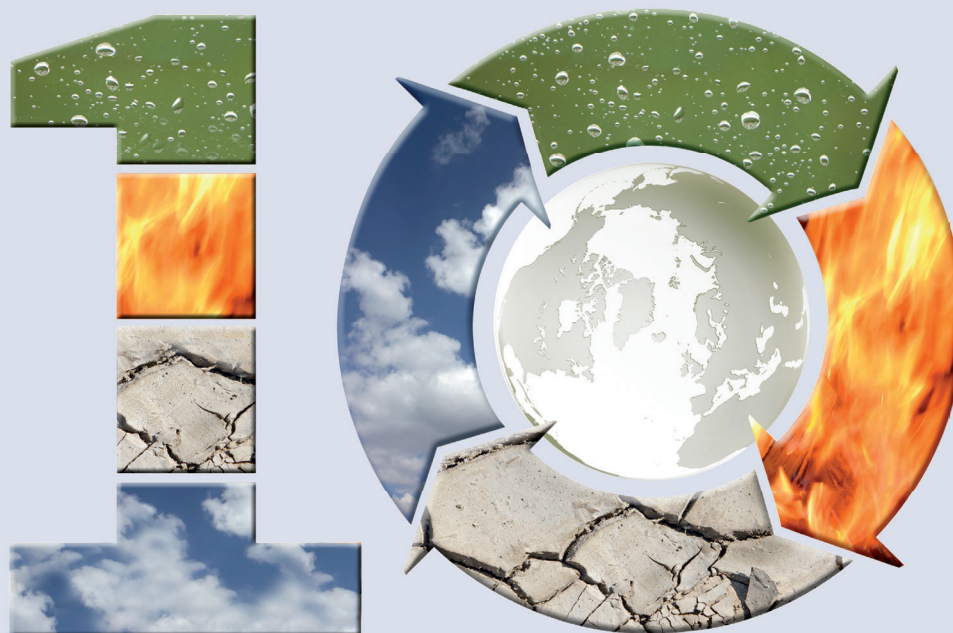
Editor: Joanne Thomson
Deputy editor: Michael Spence
Associate editors: Celia Gitterman, Nina Notman
Interviews editor: Elinor Richards
Web editors: Nicola Convine, Michael Townsend, Debora Giovannelli
Essential elements: Kathryn Lees and Valerie Simpson

Publishing assistant: Jackie Cockrill
Publisher: Graham McCann

The Royal Society of Chemistry takes reasonable care in the preparation of this publication but does not accept liability for the consequences of any errors or omissions.

Royal Society of Chemistry: Registered Charity No. 207890.

RSC Publishing



years of publishing!

Journal of Environmental Monitoring...



- Highly visible and cited in MEDLINE
- Accelerated publication rates, typically around 80 days
- Dedicated to the measurement of natural and anthropogenic sources of pollution with a view to assessing environmental and human health effects


Celebrating 10 years of publishing, *Journal of Environmental Monitoring* offers comprehensive and high quality coverage of multidisciplinary, international research relating to the measurement, pathways, impact and management of contaminants in all environments.

...for environmental processes and impacts!

RSC Publishing

www.rsc.org/jem

Registered Charity Number 207890



2ND EUCHEMS CHEMISTRY CONGRESS

2008 SEPTEMBER 16 - 20
TORINO, ITALY

CHEMISTRY: THE GLOBAL SCIENCE

PLENARY LECTURES BY

Peter AGRE (Baltimore, USA)
Avelino CORMA (Valencia, Spain)
Jean M.J. FRÉCHET (Berkeley, USA)
Robert H. GRUBBS (Pasadena, USA)
Kyriacos C. NICOLAOU (La Jolla, USA)
Martyn POLIAKOFF (Nottingham, UK)
K. Barry SHARPLESS (La Jolla, USA)

KEYNOTE LECTURES BY

Varinder AGGARWAL (Bristol, UK)
Lucia BIANCI (Florence, IT)
Matthias BELLER (Rostock, DE)
Richard CATLOW (London, UK)
Ken CAULTON (Bloomington, USA)
Fritz FRIMMEL (Karlsruhe, DE)
Dante GATTESCHI (Florence, IT)
Jana HAJŠLOVA (Prague, CZ)
Dino MORAS (Illkirch, FR)
Ulrich STIMMING (Munich, DE)
Philip TAYLOR (Geel, BE)
Jun-ichi YOSHIDA (Kyoto, JP)

SCIENTIFIC COMMITTEE

Chair **Hartmut MICHEL** (DE)
Co-chair **Igor TKATCHENKO** (FR)

ORGANISING COMMITTEE

Chair **Giovanni NATILE** (IT)
Co-chair **Francesco DE ANGELIS** (IT)

LOCAL ORGANISING COMMITTEE

Chair **Lorenza OPERTI** (IT)
Co-chair **Salvatore COLUCCIA** (IT)

Special topic symposia:

ADVANCES IN SYNTHESIS

- Organic Catalysis
- Radical Reactivity in Transition Metal Chemistry
- Reactions under Novel Conditions

ADVANCES IN UNDERSTANDING

- Chemical Measurement Quality: Societal Impact
- Cutting Edge Chemistry with Computers
- Food Analysis: Pushing Detection Limits down to Nothing

CHEMISTRY AND LIFE SCIENCES

- Biomolecular Interactions and Mechanisms
- Drug Targeting and Delivery
- Metal Homeostasis

ENERGY AND INDUSTRY

- Biorefineries and Biotechnologies
- Energy Production & Storage
- New Trends for Agrochemicals

ENVIRONMENT

- Greening Chemistry
- Greenhouse Gases
- Water Pollutants

MATERIALS AND DEVICES

- Branched Polymers - Smart Functional Materials
- Nanomaterials
- Porous Materials

 **ORGANISING SECRETARIAT**

Centro Congressi Internazionale s.r.l. - Corso Bramante 58/9 10126 Torino - I
tel +39 011.2446911 fax +39 011.2446900/44 - info@euchems-torino2008.it

www.euchems-torino2008.it

*EuCheMS, the European Association for Chemical and Molecular Sciences incorporates
50 member societies which in total represent some
150.000 individual chemists in academia, industry and government in over
35 countries across Europe.

Workshop in green chemistry production of essential medicines in developing countries

DOI: 10.1039/b806001k

Prof. O. O. Kunle, Prof. J. Fortunak and Prof. Robin D. Rogers report on the Workshop in green chemistry production of essential medicines in developing countries, held in Abuja, Nigeria from 18th–20th March, 2008.

Earlier this year, academics, industrialists, entrepreneurs, government and non-government organization representatives met in Abuja, Nigeria to discuss how to meet the needs of local chemical production in a paradigm of green chemistry. The workshop was a collaborative product of Howard University (Washington, DC, USA) and the National Institute for Pharmaceutical Research & Development (NIPRD; Abuja, Nigeria) with funding from the US National Science Foundation, the American Chemical Society's Green Chemistry International Developing Nation's Program, and the government of Nigeria.

The workshop was held to catalyze and encourage the production of high-value products from natural African biomass and the sustainable, regional production of high quality essential medicines. It was noted that the sustainability of long term efforts to promote economic development and reliable supply at affordable prices necessitates local production capacity within Africa. Manufacturing without the negative environmental consequences, that have been noted in India and China, is especially important to ensure the long-term sustainability of development efforts. Twin objectives were promoted, including encouraging education in green chemistry and its incorporation into the curricula of African universities, as well as the development of essential medicines.

The organizers, Prof. J. Fortunak (Howard), Prof. O. O. Kunle (NIPRD) and Dr. U. S. Inyang (NIPRD), put together a stimulating program of local and international experts. The meeting was opened with an address from the then Nigerian Minister of State for Health, Arc. Gabriel Yajubu Aduku. The Minister reiterated the importance of essential medicines in Nigeria and declared war on malaria; setting a goal of eliminating



Fig. 1 Left to right: Dr O. O. Kunle, Prof. Robin D. Rogers, Dr Uford S. Inyang, Prof. Stephen Byrn, Dr Eloan Pinheiro, Dr David Walwyn, Prof. Joseph Fortunak, Dr Tahir Amin, Dr David Ripin.

malaria by 2020 when Nigeria is expected to become one of the 'developed' countries.

NIPRD itself was established by the Nigerian government to provide national sources of raw materials to the country's manufacturing sector and to help promote development of the pharmaceutical industry. Its stated vision is "to build a centre of excellence for research and development of pharmaceuticals and biologicals for the service of mankind." NIPRD engages in basic and translational research and development of pharmaceutical products and raw materials from local sources.

A selection of major topics discussed included:

- Green chemistry for production of essential medicines (Fortunak)

- Green chemistry and transformational technology (Rogers)
- Drug discovery and development in Africa from indigenous knowledge: NIPRD's contribution to global health (Inyang)
 - Molecules to medicines (S. Byrn, Purdue University)
 - Overcoming patent barriers (T. Amin, Clinton Foundation)
 - Making cGMP pharmaceuticals in Africa (A. Graham, LaGray Chemicals)
- The challenges of introducing green chemistry practices in a developing country (J. Okogun, NIPRD)
 - Critical control elements for quality production in Africa (E. Ogu, Bon-Science)

- Making HIV/AIDS drugs (D. Walwyn, CEO Armir Corporation)
- The global framework for essential medicines (D. Ripin, Clinton Foundation)
- Antiretroviral quality assurance (E. Pinheiro, World Health Organization Consultant)
- The challenges of commercializing R & D results in Nigeria: The NICOSAN™ experience (I. Oniyide, Xechem Pharmaceutical Nigeria)

The discussions were lively and long, with serious debate centered around the needs of the local research and development and industrial communities. Often, the debate between the government officials and the local universities and research centers was quite heated. The sessions extended well into the evenings as the roughly 85 delegates took each issue seriously. The delegates approved a path forward, the “Abuja Declaration” (see below).

It was clear from the participation in the meeting, the vigorous discussions, and the program as a whole, that there is much to do to bring sustainable pharmaceutical manufacturing to Africa. It was also apparent that opportunities for collaboration and entrepreneurship are available. The goals of the workshop are achievable and participation by the World’s scientific, engineering, and business communities is encouraged.

Abuja Declaration

Communiqué

With the aim of instituting a sustainable model for increasing access to essential medicines within Africa, long after the International Donor Agencies have gone, the Howard University and the National Institute for Pharmaceutical Research and Development (NIPRD) considered it absolutely necessary to take

such steps as would actualize the aim. One of the steps considered most desirable is to build capabilities in terms of human resources/transfer of technology, and capacities in terms of manufacturing infrastructures/related facilities within the continent.

Consequently, participants – scientists and other professionals – from various institutions, public and private, within Nigeria, Ghana, South Africa, Zimbabwe and Tanzania, converged in Abuja for a workshop, from 18th–20th March, 2008. The theme was the production of essential medicines in developing countries. The core issue was green chemistry – the means for actualizing the aim. Resource persons, including world renowned professors, scientists, a lawyer and an economist, were drawn from Consultancies, Industries, Public Institutions and Universities in Brazil, Ghana, South Africa, Zimbabwe, Nigeria, Northern Ireland and the USA (Alabama, Howard, Purdue, Wisconsin, and the Clinton Health Access Initiative – CHAI).

The workshop was declared open by Arc. Gabriel Aduku, Honourable Minister of State for Health. The discussions/brain-storming sessions following each segment of the workshop led to the following five-point communiqué:

1. The participants expressed a strong need for local production of active pharmaceutical ingredients (API’s) and quality essential drugs, as had been recommended by the Minister in his opening address, and in consonance with the WHO Millennium Goals.
2. The participants drew particular attention to medicines for malaria, HIV/AIDS, TB, diabetes and cardiovascular drugs, stressing the conspiracy of these conditions in sustaining the vicious cycle of poverty and disease; and maintaining that the potentials of green

chemistry, properly harnessed, particularly in agrarian settings, would be vital to alleviating poverty.

3. The participants recognized and applauded the pioneering role of NIPRD in developing medicines from plants. These currently include antimalarials, antiretrovirals, antidiabetics, antifungals, and a score of others. The Institute’s ability to organize such a high profile workshop as this, drawing internationally recognized experts from the US, Brazil, Ireland, Ghana, Tanzania, South Africa and Nigeria, was particularly commended.

4. The workshop recommended the full implementation of its recommendations, stressing the need for stake holders, public and private, to have their hands on deck. The need for public institutions to summon the necessary political will, in terms of proactive policies and programmes, was stressed. Another area of emphasis was that sustainability for the long-term success of any efforts absolutely requires private sector initiative and participation.

5. The workshop recommended, above all, that public Institutions must not only set the pace but must blaze the trail, noting that the capital need of the enterprise is substantial, but not out of reach. The State must devise sustainable programmes, such as making infrastructures, especially power, available and affordable. The role of good legislations and environmental consciousness as drivers of green chemistry was well emphasized.

6. The role of the public sector is, largely, to enable, encourage, and nurture the development of private sector efforts in sustainability and access. The long term goal of any program is to build private sector capabilities for economic development, sustainability and access. This contributes to the security and stability of democratic governments as well as to the well-being of the general population.

Hydrogenation catalysts from used nickel metal hydride batteries†

Mark R. St J. Foreman,^{*a} Christian Ekberg^a and Arvid Ödegaard Jensen^b

Received 9th April 2008, Accepted 9th June 2008

First published as an Advance Article on the web 18th June 2008

DOI: 10.1039/b806034g

A synthesis of a safe and effective hydrogenation catalyst has been developed with used nickel metal hydride electrical cells as the starting material.

Introduction

It is reasonable to expect that within a decade a large number of nickel metal hydride electrical batteries will enter the car dismantling and scrap metal industries because of their use in hybrid vehicles.¹ In this paper the selective leaching to convert the batteries into a mixture of metals suitable for forming catalysts is considered as an alternative to refining these batteries to obtain the pure metals. Recently Raney nickel was reported as a green catalyst,² but it is pyrophoric and forms a carcinogenic smoke (nickel oxide). The Rocky Flats metal fires³ did clearly demonstrate the menace posed by pyrophoric solids which are able to form finely powdered carcinogenic oxidation products. The fact that our catalyst is of a less pyrophoric class than Raney nickel makes our catalyst greener in terms of worker safety. Also, the fact that this catalyst is formed from what would normally be regarded as scrap metal increases its greenness regarding the environment.

Results and discussion

The metal extract (**AL1**) formed by the initial treatment of the cell in acetic acid contained nickel, cobalt, iron, lanthanum and other metals (Table 1). It was found that on concentration of this solution by gentle heating that much of the iron was precipitated. By filtration of the mixture an iron depleted liquor (**AL2**) was obtained. The concentration and filtration process was repeated to form a new solution (**AL3**), from which a mixture of metal acetates (**RN1**) was obtained. By reacting solutions of **RN1** with alkaline sodium borohydride only slurry of a black solid could be obtained. It was hypothesized that the slurry was formed because the lanthanum present formed a colloidal hydroxide or borate⁴ during the reaction of the transition metals. When a mixture of nickel, cobalt and lanthanum salts was treated with sodium borohydride, a similar black slurry was obtained. An aqueous solution of **RN1** was treated with a large excess of

Table 1 The metal content of the acetate liquors (**ALx**), the chloride liquor (**CL**) and the recycled nickel solids (**RNx**)^a

Mixture	Metal concentration (% w/w)						
	Al	Mn	Fe	Co	Ni	Zn	La
AL1	0.9	5.7	7.9	8.7	58	2.7	16
AL2	1.2	6.2	1.6	8.6	62	3.3	17
AL3	1.4	6.1	0.4	8.9	63	3.4	17
RN1	0.2	2.2	0.6	9.4	76	0.7	11
AL4	0.0	2.2	0.2	9.8	87	0.7	0.0
CL	1.0	0.6	18	2.0	75	0.2	2.4
RN2	1.0	0.5	16	2.6	78	0.0	1.8

^a In calculating the table only the aluminium, manganese, iron, cobalt, nickel, zinc and lanthanum content as determined by ICPOES was considered.

potassium fluoride, before being filtered to provide a lanthanum free mixture of metal acetates (**AL4**). The lanthanum hypothesis was supported by the formation of a dense black solid by the treatment⁵ of **AL4** with sodium borohydride. Despite the fact that the formation of fluoride containing aqueous waste is undesirable,⁶ we decided to test the solid as a catalyst to discover if the impure nickel can be used to form a useful catalyst.

The metallic parts of the nickel metal hydride electrical cell which failed to react with the acetic acid were dissolved in concentrated hydrochloric acid to form a green solution of metal salts. This solution (**CL**) was concentrated to form a mixture of crystalline metal salts (**RN2**). By reacting **RN2** and sodium borohydride a black magnetic solid was formed, in common with the solid formed from pure nickel this solid is easy to separate from water and organic solvents because of its ferromagnetism. However the solid formed from **AL4** was weakly- or non-magnetic making the separation of the catalyst from liquids more difficult.

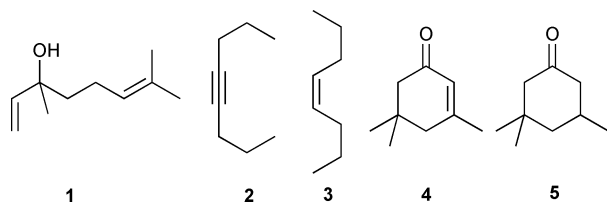
Linalool (**1**) was selected as a test compound because it contains two carbon-carbon double bonds with different reactivities to allow the selectivity of the catalysts to be tested by a volumetric method.^{†7} The chemoselectivities of the catalysts formed from **AL4** (37 : 1) and **RN2** (54 : 1) are better than that of the catalyst made from pure hydrated nickel chloride (33 : 1). The vinyl group was the first alkene in linalool to be hydrogenated, this was confirmed by NMR spectroscopy (¹H and ¹³C) when the **RN2** based catalyst was used. The catalysts made from the recycled metals were further tested for their ability to reduce a range of carbon-carbon multiple bond containing compounds (**2**, **3** and **4**) and a ketone (**5**), as shown in Scheme 1.

The partial hydrogenation of alkynes to form alkenes is a useful reaction. We found that with both new catalysts the ratio of the rate of alkene formation to the rate of alkane formation

^aIndustrial Recycling, Chalmers University of Technology, Chemical and Biological Engineering, 412 96, Göteborg, Sweden.
E-mail: Foreman@chalmers.se

^bNuclear Chemistry, Chalmers University of Technology, Chemical and Biological Engineering, 412 96, Göteborg, Sweden

† Electronic supplementary information (ESI) available: Details of the suppliers of the chemicals used, metal analysis, the equipment used for hydrogenation and the synthesis/testing of the catalysts and the experimental results. See DOI: 10.1039/b806034g



Scheme 1 The organic compounds used for the catalyst characterisation.

Table 2 The turnover rates for the catalysts made from the different nickel sources expressed in moles of hydrogen consumed per hour per mole of catalyst

Compound and functional group	Turnover rate/h ⁻¹		
	Nickel source		
	Pure	AL4	RN2
1 Linalool (Terminal alkene)	25.5	29.5	30.7
1 Linalool (Internal alkene)	0.78	0.79	0.56
2 Oct-4-yne (Internal alkyne)	6.6	50	25
3 Oct-4-ene (Internal alkene)	0.73	4.1	0.95
4 Isophorone (Internal alkene)	0.67	2.8	2.4

Table 3 The turnover rates of linalool chain and 3,3,5-trimethylcyclohexanone (**5**) using large samples of catalysts made from the different nickel sources

Compound and functional group	Turnover rate/h ⁻¹		
	Nickel source		
	Pure	AL4	RN2
1 (Internal alkene)	1.5	1.5	1.4
5 (Ketone)	0.081	0.40	0.50

was better (AL4 12 : 1 and RN2 27 : 1) than that obtained using pure nickel (9 : 1) as the catalyst starting material.⁸ The oct-4-ene (**3**) formed using RN2 was characterised by ¹H and ¹³C NMR without evaporation of the ethanol and was found to be exclusively the *cis* isomer. The hydrogenation of isophorone (**4**) was better catalysed by the solids made from recycled nickel than it was by the solid made from pure nickel chloride. As gas chromatography found only **5** as a product of the hydrogenation of **4** using the RN2 nickel catalyst (reaction stopped after the absorption of 0.96 equivalents of hydrogen), it is the case that the alkene was the first group to be reduced. In experiments where the hydrogenation of **4**, with either new catalyst, was allowed to continue for a long time, more than 110% of the theoretical hydrogen adsorption occurred. This suggested that some reduction of the carbonyl group occurred. This reduction of a ketone is quite reasonable as it is known that ketones may be reduced by a combination of finely divided nickel and hydrogen.⁹

The alkene to ketone selectivity was investigated using the trisubstituted alkene in linalool and 3,3,5-trimethylcyclohexanone (**5**) as the test compounds. The alkene/ketone selectivity for the pure nickel catalyst was higher than the recycled catalysts. This change in selectivity can be rationalised

by the fact that the addition of iron¹⁰ or cobalt¹¹ to a “nickel boride” catalyst promotes the reduction of the aldehyde groups.

Conclusions

We have easily prepared a pair of hydrogenation catalysts from a used nickel hydride electrical cell. While the chemoselectivity of these catalysts is different to the catalyst formed from pure nickel chloride, the new catalysts appear to have the potential to be useful synthetic tools. However, because of the use of potassium fluoride in production of the AL4 mixture, the catalyst made from AL4 is less green than the catalyst made from RN2. Further studies of these catalysts (and others formed from waste materials) are currently in progress.

Notes and references

‡ Synthesis and testing of catalysts (representative procedure). A 100 ml two necked round bottomed flask, containing a stir bar was charged with the nickel starting material and deionised water, to this was carefully added a solution of sodium borohydride in potassium hydroxide (0.1 M) using the method in ref. 5. After the reduction reaction has subsided, the supernatant was removed by pipette before the black solid was washed five times by the addition of water, brief stirring and then removal of the water. Then, after washing five times with ethanol in the same way, ethanol (3 ml) was added to the flask which was attached to the hydrogenation apparatus using the B19 neck and the other neck (B24) was sealed with a subaseal™. The air was removed using a vacuum pump before hydrogen gas (1 bar absolute) was admitted to the flask, before being removed again using the vacuum pump. After three such cycles, the hydrogen gas was allowed to remain in the flask with the catalyst, this was allowed to stand overnight before use. The next day when the volume of the system stabilised, an ethanol solution of the substrate was injected through the subaseal. The reaction was then monitored by observing the change in volume. At the end of the hydrogenation, the hydrogen gas was removed by vacuum pump before air was briefly admitted to the flask. The ethanol was removed from the flask with a pipette before the catalyst, stir bar and flask were rinsed with ethanol (3 ml). After the removal of this ethanol washing (by pipette), more ethanol (3 ml) was added to the reaction flask. The air in the flask was quickly replaced with hydrogen using the above method, and the catalyst was always stored wet with ethanol under a hydrogen atmosphere to prevent oxidation of the catalyst. For a typical catalytic run, sufficient amounts of the metal salt starting material to provide 16 mg of nickel/cobalt/iron was used, while for the hydrogenation of 3,3,5-trimethyl cyclohexanone three times as much catalyst was prepared and tested.

- O. Bitsche and G. Gutmann, *J. Power Sources*, 2004, **127**, 8.
- W. M. Czaplak, J.-M. Neudörfel and A. J. von Wangelin, *Green Chem.*, 2007, **9**, 1163.
- J. E. Till, A. S. Rood, P. G. Voilleque, P. D. McGavran, K. R. Meyer, H. A. Grogan, W. K. Sinclair, J. W. Aanenson, H. R. Meyer, H. J. Mohler, S. Rope and M. J. Case, *J. Exposure Anal. Environ. Epidemiol.*, 2002, **12**(5), 355.
- A. G. Ivanova, E. L. Belokoneva, O. V. Dimitrova and N. N. Mochanova, *Kristallografiya*, 2006, **51**, 1063.
- John A. Landgrebe, *J. Chem. Educ.*, 1995, **72**, A220.
- M. Lancaster, in *Green Chemistry An Introductory Text*, RSC, Cambridge, 2002, ch. 3, p 82.
- M. Casey, J. Leonard, B. Lygo, and G. Procter, in *Advanced Practical Organic Chemistry*, Blackie, Glasgow, 1990, ch. 14, p 219.
- C. A. Brown and V. K. Ahuja, *J. Org. Chem.*, 1973, **38**, 2226.
- P. Gallois, J.-J. Brunet and P. Caubere, *J. Org. Chem.*, 1980, **45**, 1946.
- H. Li, H. Luo, L. Zhuang, W. Dai and M. Qiao, *J. Mol. Catal. A: Chem.*, 2003, **203**, 267.
- Y.-Z. Chen, B.-J. Liaw and S.-J. Chiang, *Appl. Catal., A*, 2005, **284**, 97.

Iron chloride supported on pyridine-modified mesoporous silica: an efficient and reusable catalyst for the allylic oxidation of olefins with molecular oxygen†

Jianyong Mao,^a Xingbang Hu,^a Haoran Li,^{*a} Yong Sun,^a Congmin Wang^a and Zhirong Chen^b

Received 30th April 2008, Accepted 17th June 2008

First published as an Advance Article on the web 27th June 2008

DOI: 10.1039/b807234e

A novel heterogeneous catalyst with iron chloride immobilized on pyridine-modified mesoporous silica has been developed. The supported Fe(III)/SiO₂ catalyst displayed excellent catalytic properties for the allylic oxidation of 3,5,5-trimethylcyclohex-3-en-1-one (β -IP, **1**) to 3,5,5-trimethylcyclohex-2-ene-1,4-dione (KIP, **2**) with molecular oxygen as the oxidant under mild conditions. It can also catalyze the oxidation of other olefins, such as α -pinene and cyclohexene and its derivatives efficiently and selectively. In addition, the supported catalyst can be easily recycled without significant loss of activity and selectivity, which is a green alternative for practical applications.

Introduction

Allylic oxidation of olefins is an attractive process transforming cheap and readily available substrates to valuable intermediates for the fine chemical industry.¹ Until now, numerous reagents have been reported to accomplish this transformation effectively and selectively.² However, most of the oxidation reagents are toxic, hazardous, or required in large excess.³ Thus, despite the usefulness of the known procedures, the development of “greener” oxidation routes is essential for both organic synthesis and industrial applications. Molecular oxygen (O₂) as a terminal oxidant is an attractive option from an environmental and economical point of view.⁴ In recent years, it has become increasingly important in various oxidation reactions because it is cheap, readily available, and gives no co-product as pollutant.⁵ However, unlike traditional oxidants, molecular oxygen is not an active and selective oxidant. In this respect, the exploitation of efficient metal-containing catalysts has become the key point for most of aerobic oxidations.⁶

Iron-containing catalysts are among the most practical reagents for aerobic oxidations because iron as an active site can efficiently transfer an oxygen atom from molecular oxygen to organic substrates.⁷ Since the discovery of iron-containing enzymes⁸ (like cytochrome P-450s), much effort has been focused on the biomimetic catalysts such as iron-porphyrins,⁹ iron-phthalocyanines¹⁰ and iron-Schiff bases¹¹ for the past decade.

However, the difficulties in separation and the high cost of the bionic catalysts hindered commercialization of these procedures. The heterogenisation of the aforementioned catalysts is an attractive method from an environmental and economical point of view.¹² Unfortunately, both their activity and selectivity sharply decreased when they were immobilized on the support. Hence, there is a need to explore more simple, efficient, safe, and cost-effective iron-containing catalysts for practical applications.

Since iron acts as the key intermediate in Fe(III)-catalyzed oxidation procedures, the direct use of active Fe(III) for such reactions has been considered to be beneficial.¹³ Several strategies have been adopted to immobilize these iron-containing catalysts on various supports in an attempt to make them recyclable and to enhance their stability.¹⁴ Here, we describe a new protocol for the preparation of iron-containing heterogeneous catalyst with iron chloride immobilized onto pyridine-modified porous silica. The supported catalyst was tested in the allylic oxidation of cyclic olefins including 3,5,5-trimethylcyclohex-3-en-1-one (β -IP, **1**), α -pinene and cyclohexene and its derivatives. Meanwhile, special attention has been focused on its stability and reusability.

Experimental

Synthesis of Fe(III)/SiO₂ catalyst

2.0 g porous silica (SiO₂) was dispersed in a mixture of ethanol (100 ml) and pyridine (2 ml) under stirring (76 °C) for 12 h. Then the solid product was filtrated from the mixture, washed with ethanol and dried under vacuum at 150 °C overnight. The ethanol and pyridine mixture was reused to activate multiple batches of silica in the experiment (see ESI†).

The obtained pyridine-modified porous silica was dispersed in 100 ml ethanol. Then 0.54 g FeCl₃·6H₂O (2 mmol) in ethanol solution (5 ml) was added drop-wise under stirring at 76 °C for 12 h. The resulting precipitate was filtered and was washed with ethanol and acetone until no Fe³⁺ could be detected in the washing liquid. After a process of drying under vacuum at 150 °C for 8 h, a brown Fe(III)/SiO₂ power was obtained. The supported catalyst was analyzed by N₂ adsorption evaluation, atomic absorption spectrophotometry (AAS), FT-IR and SEM image analysis (see ESI†).

Allylic oxidation of **1** and other olefins

Allylic oxidation of **1** was carried out as described previously.¹⁵ In a typical oxidation, 13.8 g **1** (0.1 mol), 10 ml pyridine, 20 ml methyl ethyl ketone (MEK), and 0.55 g Fe(III)/SiO₂

^aDepartment of Chemistry, Zhejiang University, Hangzhou, 310027, P. R. China. E-mail: lihr@zju.edu.cn; Fax: +86-571-8795-1895

^bDepartment of Chemical Engineering, Zhejiang University, Hangzhou, 310027, P. R. China

† Electronic supplementary information (ESI) available: Additional experimental details and results. For ESI see DOI: 10.1039/b807234e

(catal./sub. = 4%) catalyst were added into a 50 ml four-neck round bottom reactor, which was fitted with an overhead stirrer and a reflux condenser. The reaction was performed at 66 °C in a water bath with fast stirring. High pressure air was flowing into the reactor at a constant flow rate (20 ml min⁻¹). The result was monitored by GC (with benzyl ethanoate as the internal standard). The products were analyzed by GC-MS. When the reaction was completed, the supported catalyst was filtrated from the products, washed with ethanol thoroughly, and dried under vacuum at 150 °C for reuse.

Fe(III)/SiO₂ catalyst was also applied in the oxidation of other olefins (α -pinene and cyclohexene and its derivatives). In a typical oxidation, 10 mmol olefin, 0.2 g catalyst and 10 ml acetonitrile were added in a 25 ml flask which fitted with an overhead stirrer and a reflux condenser. Pure oxygen was flowing into the reactor with a constant flow rate (20 ml min⁻¹). The reaction proceeded for 10 h under different temperatures (58 °C, 78 °C and 84 °C), and the products were analyzed by GC and GC-MS.

Results and discussion

Characterization of the material

As shown in Table 1, the supported materials exhibited decreased BET surface area and pore volume compared with porous silica. This indicated that iron complexes had been combined inside the channels of the porous silica. Compared with porous silica (3.3 cm³ g⁻¹, 199 m² g⁻¹), the supported catalyst without pyridine showed a BET surface area of 190 m² g⁻¹ and a total pore volume of 3.2 cm³ g⁻¹, while the values for the corresponding pyridine-modified catalyst were found to be 158 m² g⁻¹ and 2.8 cm³ g⁻¹. It was supposed that much more iron complex had been anchored onto the support in the presence of pyridine, thus its pore volume and surface area were clearly reduced. These results were consistent with a reasonable homogeneous building-up of the metal complex on the surface.¹⁶

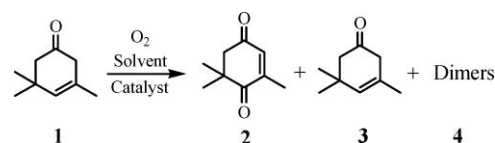
Atomic absorption spectrophotometry (AAS) analysis gave an iron loading of 0.49–0.85 mmol g⁻¹ on pyridine-modified porous silica, while there was only 0.051 mmol g⁻¹ of iron loading in the absence of pyridine. It was concluded that pyridine played an important role for immobilizing metal ions, which was consistent with N₂ adsorption analysis. SEM pictures¹⁷ recorded for porous silica and the immobilized catalysts showed that the porous structure has been maintained after immobilization. This

result was also confirmed by N₂ adsorption isotherms, where the isotherms for porous silica and the supported catalyst were of similar shape.

The FT-IR spectra of the silica support showed specific bands at around 1640, 1110, 803 and 467 cm⁻¹ assigned to characteristic vibrations of the mesoporous framework (Si–O–Si) and a broad peak around 3450 cm⁻¹ for the adsorbed H₂O molecules. Compared with porous silica, the new characteristic band of iron complexes at 1460 and 877 cm⁻¹ appeared in the spectrum, indicating that iron complexes were immobilized on the support. Besides, the brown color of the solid particles of the catalyst was indicative to the presence of an Fe(III) complex. Compared with the fresh catalyst, both the pore volume and surface area were sharply decreased in the recycled catalyst. However, there was still 0.44 mmol g⁻¹ of iron left on the recycled Fe(III)/SiO₂ catalyst. It was supposed that most of the iron was strongly anchored on the support and only a small amount was lost during the separation and recycling processes.

Allylic oxidation of 1 to 2

The supported Fe(III)/SiO₂ catalyst was firstly evaluated in the aerobic oxidation of **1** to **2** (Scheme 1). **2** is a valuable starting substance for flavors and fragrance in foodstuffs as well as an important intermediate for preparing vitamins, carotenoids and so on.¹⁸ As shown in Table 2, the homogeneous catalysts, especially metal porphyrins and Schiff bases, provided high activity and selectivity for **1** oxidation. However, most of them are difficult to separate from the products (entry 3, 5, 7 and 9). Some of them have been immobilized on the support, but the heterogeneous catalysts suffered from low activity and selectivity (entry 4, 6, 8 and 10). A new method for immobilizing iron chloride onto pyridine-modified silica was introduced in this study. The supported Fe(III)/SiO₂ catalyst displayed high selectivity (over 95%) for **1** oxidation (entry 1), which was much higher than general heterogeneous catalysts used before.



Scheme 1

For the further studies of its superior efficiency for **1** oxidation, the reaction was carried out with different catalysts under the same conditions. As shown in Fig. 1, **1** was slowly converted to **2** in the presence of molecular oxygen without any catalyst, along with plenty of by-products (mostly **3** through isomerization reaction) (A). The presence of porous silica promoted the oxidation of **1**. However, it still provided **2** in low selectivity due to the lack of an active metal site (B). Iron chloride was an efficient homogeneous catalyst. The oxidation of **1** could be completed in 10 h using iron chloride as catalyst, along with a small quantity of **3** (C). Nevertheless, it was not selective for β -IP oxidation. Much more high-boiling point by-products (like dimers and trimers of **1**) have been detected by GC-MS analysis

Table 1 Physical properties of SiO₂ supported FeCl₃ catalysts

Entry	Sample	Fe content ^a / mmol g ⁻¹	Pore vol. ^b /cm ³ g ⁻¹	Surf. area ^b /m ² g ⁻¹
1	SiO ₂	0.0030	3.3	199
2	FeCl ₃ + SiO ₂ ^c	0.051	3.2	190
3	I [#] Fe(III)/SiO ₂ ^d	0.49	2.9	179
4	II [#] Fe(III)/SiO ₂ ^d	0.53	2.8	158
5	III [#] Fe(III)/SiO ₂ ^d	0.85	2.6	144
6	I [#] Fe(III)/SiO ₂ ^e	0.44	1.6	50

^a By atomic absorption analysis. ^b Through gas adsorption method. ^c No pyridine was added. ^d With pyridine. ^e The supported catalyst has been recycled for more than four times.

Table 2 Allylic oxidation of **1** to **2** with different kinds of catalysts^a

Entry	Catalysts	Conv. (%)	Selec. (%)	Ref.
1	Fe(III)/SiO ₂	31.8	95.4	—
1 ^b	Fe(III)/SiO ₂	> 99	88	—
2	Transition metal salts (Cr, Mn, Co, Fe, Cu)	> 99	50	[21]
3	Manganese acetates	> 99	68–85	[22]
4	Manganese acetates on silica	90	28–41	[23]
5	Metal porphyrins or Schiff bases	> 99	67–93	[24]
6	Metal salen on silica	52	6–47	[25]
7	FePc ^c	> 99	55	[26]
8	FePc-SiO ₂	92	21–38	[26]
9	V(acac) ₃	> 99	91	[27]
10	Titania-silica	> 95	<10	[28]

^a The homogeneous and heterogeneous catalysts used previously and in this study. ^b The reaction was completed with the heterogeneous catalyst. ^c Pc = tetrasulfophthalocyanine.

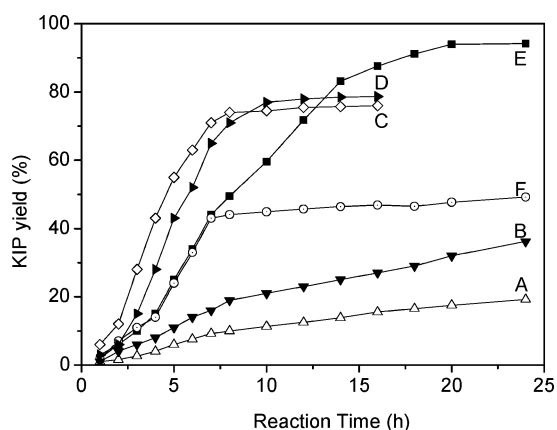


Fig. 1 Oxidation of **1** with different catalysts: (A) without catalyst; (B) silica as catalyst; (C) FeCl₃ as catalyst; (D) FeCl₃ + silica as catalyst; (E) I^a Fe(III)/SiO₂ as catalyst; (F) Fe(III)/SiO₂ was filtrated off after 7 h. Reaction conditions as Table 3.

during the reaction. It was supposed that the free iron(III) could also activate **1** directly, which may cause the coupling reactions.

Compared with using them separately, the highly active FeCl₃ played a dominant role for **1** oxidation in the supported Fe(III)/SiO₂ catalyst. Its activity has been highly improved when iron chloride was immobilized onto the silica support. On the other hand, as FeCl₃ coordinated with pyridine was firmly

anchored on the porous support, almost no free Fe³⁺ ion was present in the reaction system. It was hard to activate **1** directly and the conversion to dimers was also reduced. That is to say, the obtained Fe(III)/SiO₂ catalyst not only restricted the conversion to **3**, but also decreased the coupling reaction to dimers. Consequently, the heterogeneous catalyst provided **2** in a higher yield than using them separately (E). Silica and FeCl₃ have also been added simultaneously in the experiment (D). It was seen that FeCl₃ played a dominant role in the oxidation system, similar to using FeCl₃ alone. Adding SiO₂ had almost no effect on the reaction and the yield of **2** was not obviously improved.

The oxidation of **1** under different temperatures (46, 56, 66 and 76 °C) was investigated as well. As shown in Table 3, it was detected that a higher reaction temperature led to an acceleration of **1** oxidation (entry 1–4). However, the reaction at 56–66 °C provided **2** in higher yield because some **1** had been converted to **3** at 46 °C, and much more of **4** had been produced at higher temperature (76 °C). It is worth noting that the reaction at 56–66 °C was favorable for practical applications because it displayed excellent selectivity for **1** oxidation. Under this condition, the heterogeneous catalyst could be filtrated from the products for reuse and **2** could be separated in high yield (95.4%). On the other hand, the catalysts with different iron contents provided almost the same activity and selectivity for **1** oxidation (entry 6, 8 and 9). It was supposed that although

Table 3 Catalytic oxidation of **1** under different conditions^a

Entry	Catalysts	Catal./sub. (wt%)	1 Conv. (%)	2 Selec. (%)	3 Selec. (%)	4 Selec. (%)	TOF ^b /h ⁻¹
1	I(46 °C) ^c	4	9.6	90.5	8.2	0.3	19
2	I(56 °C) ^c	4	18.9	96.1	2.1	0.6	37
3	I(66 °C) ^c	4	31.8	95.4	2.9	0.7	63
4	I(76 °C) ^c	4	61.2	91.2	2.7	4.4	117
5	I ^d	2	78.6	89.3	3.0	3.2	75
6	I	4	> 99	88.5	4.8	2.8	63
7	I	8	> 99	87.1	4.1	4.3	51
8	II ^d	4	> 99	88.0	4.6	3.2	69
9	III ^d	4	> 99	86.8	6.2	4.8	61

^a Reaction conditions: **1** 13.8 g (0.1 mol), pyridine 10 ml, methyl ethyl ketone (MEK) 20 ml, *T* = 66 °C, reaction time 24 h; flowing air as oxidant. The reaction was monitored by GC (with benzyl ethanone as the internal standard). ^b TOF = (moles of **1** consumed)/[(moles of catalyst) × 1 h]. ^c Reaction time = 10 h. ^d catalyst I: [Fe] = 0.49 mmol g⁻¹, catalyst II: [Fe] = 0.53 mmol g⁻¹, catalyst III: [Fe] = 0.85 mmol g⁻¹.

Table 4 Catalyst reuse test for the oxidation of **1**^a

Run	1 Conv. ^b (%)	2 Selec. ^b (%)	3 Selec. ^b (%)	TOF ^c /h ⁻¹
1	98.7	86.5	6.5	61
2	98.3	85.2	7.2	57
3	97.4	84.7	7.7	56
4	95.5	84.1	8.5	53

^a Reaction conditions: **1** = 0.1 mol, pyridine = 10 ml, methyl ethyl ketone (MEK) = 20 ml, oxidant = air, temperature = 66 °C, reaction time = 24 h. ^b The reaction was monitored by GC (with benzyl ethanoate as the internal standard), the product and by-products were analysed by GC/MS. ^c TOF = (moles of **1** consumed)/[(moles of catalyst) × 1 h].

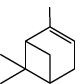
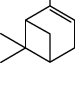
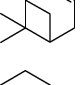
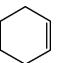
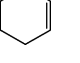
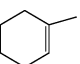
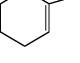
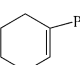
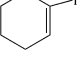
different amounts of the iron were immobilized on porous silica, the combination structure of the supported catalysts was almost the same, and so they displayed the same catalytic properties for the oxidation of **1**.

In order to test the true heterogeneity of the catalyst, following the method described by Sheldon *et al.*,¹⁹ the catalyst was filtered off after 7 h and the filtrate was allowed to react for further 10 h (F, as shown in Fig. 1). After 10 h, lower than 5% of **1** conversion was observed. The reaction containing Fe(III)/SiO₂ catalyst under the same conditions showed over 40% conversion of **1**. Catalyst reuse tests were also carried out to test its stability. The catalyst could be easily separated and recycled from the mixture. AAS analysis (Table 1) confirmed that the iron loading of the recycled catalyst was not obviously reduced after four cycles, although the pore volume and surface area had sharply decreased. As shown in Table 4, the catalyst was reused four times. However, its catalytic activity (TOF) was not decreased compared to the fresh ones. Moreover, the conversion to **3** and **4** was not increased in the reaction, thus it provided **2** still in high yield.

Allylic oxidation of other cyclic olefins

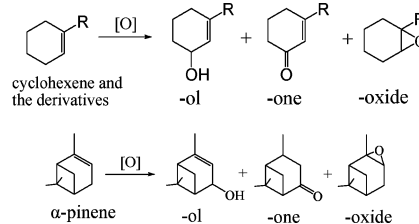
As shown in Scheme 2, α -pinene and cyclohexene and its derivatives were oxidized to the corresponding enones and/or enols

Table 5 Catalytic oxidation of other olefins with Fe(III)/SiO₂ catalyst^a

Entry	Olefin	Temp./°C	Conv. (%)	TOF ^b /h ⁻¹	Product yield (selectivity) (%)		
					-oxide ^c	-one ^c	-ol ^c
1		58	14.3	2.8	1.8 (13)	2.0 (14)	6.5 (45)
2		78	46.5	9.3	8.5 (18)	8.1 (17)	20 (43)
3		84	72.7	14.5	15.3 (21)	13 (18)	29 (40)
4		58	33.7	6.7	1.6 (4.7)	23.9 (71)	7.6 (22)
5		78	98.1	19.6	4.9 (5.0)	75.5 (77)	16.4 (17)
6		58	15.3	3.1	0.6 (3.9)	11.7 (76)	2.5 (16)
7		78	44.2	8.8	2.1 (4.8)	34.5 (80)	6.2 (13)
8		58	8.9	1.8	0.5 (5.6)	4.4 (49)	3.6 (40)
9		78	26.3	5.3	1.6 (6.1)	12.6 (48)	11.1 (42)

^a Reaction conditions: substrate = 10 mmol, solvent (CH₃CN) = 10 ml, Catalyst I (see Table 1) was used in the oxidation; Reaction time = 10 h, pure oxygen was flowing into the reactor at constant flow rate (about 20 ml/min), the reaction was monitored by GC and the products was analyzed by GC-MS. ^b TOF = (moles of olefins consumed)/[(moles of catalyst) × 1 h], ^c the products -oxide, -one, and -ol see Scheme 2.

smoothly under oxygen atmosphere. Similar to the oxidation of **1**, the Fe(III)/SiO₂ catalyst displayed good catalytic activity and selectivity for the oxidation of all the cyclic olefins (Table 5).

**Scheme 2**

In addition, it was found that increasing the reaction temperature accelerated the aerobic oxidation of olefins. For example, at the lowest temperature (58 °C), only 14.3% conversion of α -pinene could be observed at the end of 10 h (entry 1). On increasing the temperature to 84 °C, the conversion rose to 72.7% after 10 h (entry 3). The TOF (h⁻¹) values calculated at the end of 10 h were: 2.8, 9.3 and 14.5. This is in agreement with an earlier report where higher reaction temperatures led to a similar acceleration of α -pinene oxidation.²⁰ Furthermore, the supported Fe(III)/SiO₂ catalyst provided different catalytic activity for different substrates. It was found that 98% conversion of cyclohexene (entry 5) was observed at 78 °C while there was only 44% conversion of 1-methyl-cyclohexene (entry 7) and 26% conversion of 1-phenyl-cyclohexene (entry 9) under the same conditions.

Conclusions

In conclusion, the catalysts prepared by immobilizing iron chloride onto pyridine-modified mesoporous silica provided high activity and selectivity for the allylic oxidation of cyclic olefins. Though organic solvent has been used, the proposed catalytic method is a green alternative since it involves molecular oxygen as terminal oxidant and porous silica supported iron complex

as recyclable heterogeneous catalyst under mild conditions. In addition, the supported catalysts were obtained by a simple, facile and cheap synthesis methodology. All these facts allow us to view them as prospective heterogeneous catalysts for practical applications.

Acknowledgements

This work was supported by the National Natural Science Foundation of China (No. 20434020 and No. 20573093).

References

- 1 A. E. Shilov and G. B. Shul'pin, *Chem. Rev.*, 1997, **97**, 2879; M. S. Chen, N. Prabakaran, N. A. Labenz and M. C. White, *J. Am. Chem. Soc.*, 2005, **127**, 6970; J. Salvador and J. H. Clark, *Chem. Commun.*, 2001, 33; J. Salvador and J. H. Clark, *Green Chem.*, 2002, **4**, 352; N. V. Maksimchuk, M. S. Melgunov, J. Mrowiec-Bialon, A. B. Jarzebski and O. A. Kholdeeva, *J. Catal.*, 2005, **235**, 175.
- 2 M. A. Zolfigol, F. Shirini, A. G. Choghamarani and I. M. Baltork, *Green Chem.*, 2002, **4**, 562; H. Chu, L. Yang, Q. H. Zhang and Y. Wang, *J. Catal.*, 2006, **241**, 225; J. Y. Weng, C. M. Wang, H. R. Li and Y. Wang, *Green Chem.*, 2006, **8**, 96; C. M. Wang, L. P. Guo, H. R. Li, Y. Wang, J. Y. Weng and L. H. Wu, *Green Chem.*, 2006, **8**, 603.
- 3 T. M. Leu and E. Roduner, *J. Catal.*, 2004, **228**, 397; D. M. Boghaei and S. Mohebi, *J. Mol. Catal. A: Chem.*, 2002, **179**, 41; Q. H. Tang, Q. H. Zhang, H. L. Wu and Y. Wang, *J. Catal.*, 2005, **230**, 384; S. Sharma, B. Kerler, B. Subramaniam and A. S. Borovik, *Green Chem.*, 2006, **8**, 972; K. P. Ho, T. H. Chan and K. Y. Wong, *Green Chem.*, 2006, **8**, 900.
- 4 S. Casuscelli, E. Herrero, N. Crivello, C. Perez, M. G. Egusquiza, C. I. Cabello and I. L. Botto, *Catal. Today*, 2005, **107–08**, 230; O. V. Zalomaeva, O. A. Kholdeeva and A. B. Sorokin, *Green Chem.*, 2006, **8**, 883; A. J. Catino, R. E. Forslund and M. P. Doyle, *J. Am. Chem. Soc.*, 2004, **126**, 13622.
- 5 K. Ohkubo, K. Suga and S. Fukuzumi, *Chem. Commun.*, 2006, 2018; B. Guan, D. Xing, G. Cai, X. Wan, N. Yu, Z. Fang, L. Yang and Z. Shi, *J. Am. Chem. Soc.*, 2005, **127**, 18004; X. Baucherel, L. Gonsalvi, I. W. C. E. Arends, S. Ellwood and R. A. Sheldon, *Adv. Synth. Catal.*, 2004, **346**, 286; K. Mori, T. Hara, T. Mizugaki, K. Ebitani and K. Kaneda, *J. Am. Chem. Soc.*, 2004, **126**, 10657.
- 6 Q. H. Tang, Q. H. Zhang, H. L. Wu and Y. Wang, *J. Catal.*, 2005, **230**, 384; M. A. Zolfigol, F. Shirini, A. G. Choghamarani and I. Mohammadpoor-Baltork, *Green Chem.*, 2002, **4**, 562; S. Sharma, B. Kerler, B. Subramaniam and A. S. Borovik, *Green Chem.*, 2006, **8**, 972.
- 7 M. Nakanishi and C. Bolm, *Adv. Synth. Catal.*, 2007, **349**, 861; Q. X. Shi, R. W. Lu, K. Jin, Z. X. Zhang and D. F. Zhao, *Green Chem.*, 2006, **8**, 868.
- 8 *The Porphyrin Handbook*, ed. K. M. Kadish, K. M. Smith and R. Guilard, Academic Press, New York, 2000, vol. 4, ch. 28, p. 41.
- 9 W. D. Kerber, B. Ramdhanie and D. P. Goldberg, *Angew. Chem., Int. Ed.*, 2007, **46**, 3718; N. A. Stephenson and A. T. Bell, *J. Mol. Catal. A: Chem.*, 2007, **275**, 54.
- 10 N. Sehlotho and T. Nyokong, *J. Mol. Catal. A: Chem.*, 2004, **209**, 51; Y. Cimen and H. Turk, *J. Mol. Catal. A: Chem.*, 2007, **265**, 237.
- 11 K. C. Gupta and A. K. Sutar, *J. Mol. Catal. A: Chem.*, 2007, **44**, 1171.
- 12 O. V. Zalomaeva and A. B. Sorokin, *New J. Chem.*, 2006, **30**, 1768; M. S. M. Moreira, P. R. Martins, R. B. Curi, O. R. Nascimento and Y. Yamamoto, *J. Mol. Catal. A: Chem.*, 2005, **233**, 73; R. F. Parton, P. E. Neys, P. A. Jacobs, R. C. Sosa and P. G. Rouxhet, *J. Catal.*, 1996, **164**, 341; J. Ichihara, A. Kambara, K. Iteya, E. Sugimoto, T. Shinkawa, A. Takaoka, S. Yamaguchi and Y. Sasaki, *Green Chem.*, 2003, **5**, 491; H. G. Manyar, G. S. Chaure and A. Kumar, *Green Chem.*, 2006, **8**, 344.
- 13 F. G. Gelalcha, B. Bitterlich, G. Anilkumar, M. K. Tse and M. Beller, *Angew. Chem., Int. Ed.*, 2007, **46**, 7293; P. Nagaraju, N. Pasha, P. S. Sai Prasad and N. Lingaiah, *Green Chem.*, 2007, **9**, 126.
- 14 I. Megumu, M. Kazuhisa, S. Masahiro and T. Isao, *Green Chem.*, 2007, **9**, 638; X. X. Wang, Y. Wang, Q. H. Tang, Q. Guo, Q. H. Zhang and H. L. Wan, *J. Catal.*, 2003, **217**, 457; N. Perkas, Y. Q. Wang, Y. Kolytyn, A. Gedanken and S. Chandrasekaran, *Chem. Commun.*, 2001, 988.
- 15 J. Y. Mao, N. Li, H. R. Li and X. B. Hu, *J. Mol. Catal. A: Chem.*, 2006, **258**, 178.
- 16 R. L. Brutchey, I. J. Drake, A. T. Bell and T. D. Tilley, *Chem. Commun.*, 2005, 3736.
- 17 SEM images, FT-IR spectrum, and N₂ adsorption isotherms of these supported catalysts can be found in the ESI†.
- 18 J. J. Becker, W. Skorianetz, and U. P. Hochstrasser, *DE Patent*, 2459 148, 1976; M. J. Klatt, T. Mueller, and B. Bockstiegel, *DE Patent*, 19929 367, 2000; R. Hahn, U. Gora, K. Huthmacher, F. Huebner and S. Krill, *DE Patent*, 19 619 570, 1997.
- 19 H. E. B. Lempers and R. A. Sheldon, *J. Catal.*, 1998, **175**, 62.
- 20 R. Chakrabarty, B. K. Das and J. H. Clark, *Green Chem.*, 2007, **9**, 845.
- 21 E. F. Murphy, T. Mallat and A. Baiker, *Catal. Today*, 2000, **57**, 115.
- 22 H. Bellut, *DE Patent*, 3 842 547, 1990.
- 23 J. J. Becker, K. H. Schulte-Elte, H. Strickler, and G. Ohloff, *DE Patent*, 2 457 157, 1975.
- 24 I. Nobuhiko, E. Takeaki, H. Hisahiro and K. Michihara, *Synthesis*, 1997, 153; S. B. Halligudi, N. Raj, S. S. Deshpande and S. Gopinathan, *J. Mol. Catal. A: Chem.*, 2000, **157**, 9.
- 25 E. F. Murphy, T. Mallat, A. Baiker and M. Schneider, *Appl. Catal., A*, 2000, **197**, 295; E. F. Murphy and A. Baiker, *J. Mol. Catal. A: Chem.*, 2002, **179**, 233; T. Joseph, S. B. Halligudi, C. Satyanarayan, D. P. Sawant and S. Gopinathan, *J. Mol. Catal. A: Chem.*, 2001, **168**, 87.
- 26 M. Beyrhouty, A. B. Sorokin, S. Daniele and L. G. Hubert-Pfalzgraf, *New J. Chem.*, 2005, **29**, 1245.
- 27 W. Brenner, *CH Patent*, 605 536, 1978; W. Brenner, *DE Patent*, 2 515 304, 1975.
- 28 M. Costantini, A. Dromard, and M. Jouffret, *DE Patent*, 2 657 386, 1977.

Rhodium-catalyzed asymmetric transfer hydrogenation of alkyl and aryl ketones in aqueous media

Katrin Ahlford,^a Jesper Lind,^b Lena Mäler^b and Hans Adolfsson^{*a}

Received 11th April 2008, Accepted 30th June 2008

First published as an Advance Article on the web 14th July 2008

DOI: 10.1039/b806177g

A novel lipophilic rhodium catalyst was evaluated in the enantioselective transfer hydrogenation of ketones in water using sodium formate as the hydride donor, and in the presence of sodium dodecylsulfonate. Alkyl alkyl ketones were reduced in good yields and in moderate to good enantioselectivities, and the reduction of aryl alkyl ketones proceeded with excellent enantioselectivity (up to 97% ee).

Introduction

Traditionally most organic reactions are performed in organic solvents. However, more recently the use of water as a reaction medium has increased in popularity.¹ Water, being one of the essential compounds for life on earth, and a key component in all biological systems, is often considered as being far from the perfect solvent for performing organic chemistry. Obviously, the hydrophilic properties of water and aqueous media combines poorly with most typical properties connected with organic compounds. Nevertheless, the intrinsic hydrophilicity can actually be exploited in a positive manner, and novel or higher reactivities can be accomplished by performing classical organic reactions in water instead of in typical organic solvents. The Diels–Alder reaction is one example of a classical organic transformation which exhibits significantly higher reaction rates when performed in water as compared to when the corresponding reaction takes place in an organic solvent.² The reaction “on water” as described by Sharpless and co-workers is a recent example where high reactivity is achieved from insoluble reagents.³

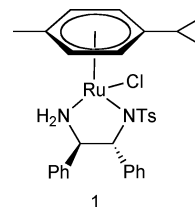
For organic reactions catalyzed by metal complexes, the solubility properties of reactants/reagents and the catalyst are often quite different. The nature of the metal complex can be either hydrophilic or hydrophobic depending on the ligands surrounding the metal. However, the organic reaction partners often exhibit poor solubility in the aqueous media. A classical approach to overcome this solubility problem is to add different surfactants (e.g. sodium dodecylsulfonate, SDS) to the reaction mixture.⁴ The interior lipophilicity of micelles created by the surfactants helps to solvate the reaction partners, and thereby facilitate a smooth reaction. Hence, increased reaction rates

are usually observed when organic reactions are performed in aqueous solutions in the presence of surfactants.

An additional factor to consider when developing synthetic methods with water as reaction medium is the selectivity of the reaction, in particular the stereoselectivity. Again, the classic method for metal catalyzed reactions is to develop chiral catalysts/ligands containing hydrophilic, often charged, functionalities.⁵ This concept takes care of the problem getting the selective catalyst soluble, however, it does not address the solubility issue of the organic substrates. To allow for good solubility of both catalyst and substrates in aqueous media, and at the same time generate a potentially more stereoselective protocol, we have investigated the possibility of using standard surfactants to facilitate both aspects. Herein, we present an approach for the stereoselective reduction of alkyl alkyl ketones under transfer hydrogenation conditions in water.

Results and discussion

The enantioselective reduction of ketones is a thoroughly investigated reaction, and there are several different stoichiometric and catalytic protocols developed for this particular transformation.^{6,7} Regarding catalytic methods, the ruthenium-based systems developed by Noyori and co-workers, using molecular hydrogen or formic acid as reducing agents are among the most successful for the stereoselective formation of secondary alcohols.^{8,9} The ruthenium-arene complex **1** containing a monosulfonated diamine (*i.e.* TsDPEN) is a particularly proficient precatalyst for asymmetric reduction of aryl alkyl ketones under transfer hydrogenation conditions, and the most advantageous hydride source used in combination with this catalyst system is either the formic acid-triethyl amine azeotrope or sodium formate.⁹ In the latter case the reactions are commonly performed in aqueous media, often in the presence of surfactants, which increase solubility of both reactants and catalysts.¹⁰



Recent modifications of the original Noyori complex **1**, have resulted in catalysts which show higher activities and selectivities when the reactions are performed in neat water using sodium formate as the hydride donor.¹¹ We have previously

^aDept of Organic Chemistry, Stockholm University, The Arrhenius Laboratory, SE-106 91, Stockholm, Sweden.

E-mail: hansa@organ.su.se; Fax: +46-8-154908; Tel: +46-8-162484

^bDept of Biochemistry and Biophysics, Stockholm University, The Arrhenius Laboratory, SE-106 91, Stockholm, Sweden

investigated the enantioselective reduction of aryl alkyl ketones using catalysts containing different amino acid based ligands.¹² The corresponding selective reduction of alkyl alkyl ketones is, however, considerably more difficult and remains as a problem.¹³ The high selectivity observed when ruthenium- or rhodium-arene catalysts are employed in the reduction of aryl alkyl ketones is believed to originate from stabilizing π -CH interactions between the substrate and the catalyst when the hydride transfer occurs.¹⁴ No such stabilizing effect can exist in the reduction of alkyl alkyl ketones, and therefore these reactions normally result in poor enantioselectivity. We have addressed this issue using an approach where proper catalyst modification would allow for selective reduction of long-chained alkyl ketones in water in the presence of SDS. The concept is presented in Fig. 1, which illustrates how a lipophilic mono-sulfonated diamine ligand will allow for the catalyst to be highly soluble in micelles created by SDS. The polar end (*i.e.* the transition metal site) is assumed to be close to the hydrophilic surface of the micelle. The poor solubility of long-chained alkyl alkyl ketones (*e.g.* 2-dodecanone) in water will force the substrate to enter the catalyst-containing SDS, with the polar carbonyl end of the molecule oriented towards the surface. Theoretically, this orientation of the ketone could result in a possible catalyst discrimination between the two enantiotopic faces of the substrate, which thereby would facilitate the reduction to proceed with higher stereochemical induction.

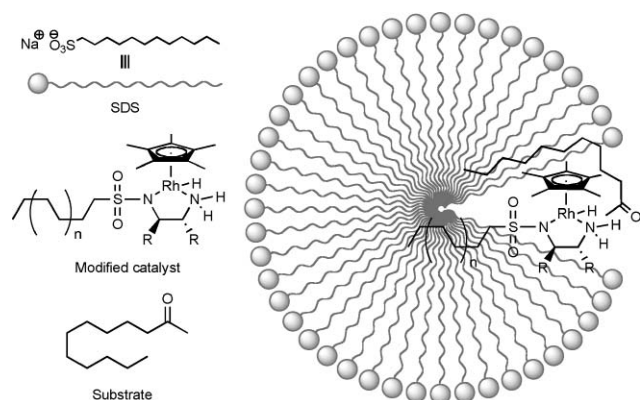
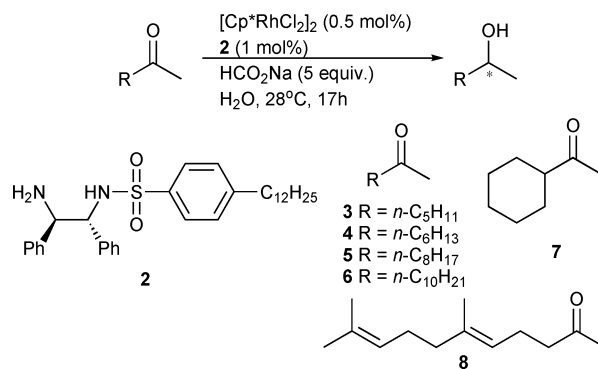


Fig. 1 Schematic drawing indicating possible catalyst and substrate interaction with micelles formed by SDS.

To test this hypothesis we prepared diamine ligand **2** starting from commercially available (*R,R*)-1,2-diphenyl-1,2-diaminoethane and 4-dodecylbenzenesulfonyl chloride (Scheme 1). Using ligand **2** in combination with $[\text{Cp}^*\text{RhCl}_2]_2$ ($\text{Cp}^*\text{Rh-2}$) for the asymmetric transfer hydrogenation of various alkyl methyl ketones without and in the presence of the SDS surfactant, resulted, in most cases, in good conversion to the corresponding secondary alcohol.[†] Interestingly, the reduction of 2-heptanone (**3**) and 2-octanone (**4**) proceeded smoothly regardless of whether SDS was present or not (Table 1, entries 1–4). The transfer hydrogenation of 2-decanone (**5**) resulted in better conversion when the surfactant was present (Table 1, entries 5 and 6). However, in the reduction of 2-dodecanone (**6**) a dramatic difference in the reaction outcome was observed and significantly higher conversion was obtained when SDS was present in the media (Table 1, entries 7 and 8). Furthermore,



Scheme 1

Table 1 Rhodium-catalyzed reduction of alkyl alkyl ketones in the presence of ligand **2**^a

Entry	Substrate	Surfactant ^b	Conversion (%) ^c	ee (%) ^d
1	3	—	99	42
2	3	SDS	98	42
3	4	—	97	39
4	4	SDS	99	45
5	5	—	85	44
6	5	SDS	96	47
7	6	—	46	43
8	6	SDS	99	47
9	7	—	83	84
10	7	SDS	97	84
11	8	—	69	37
12	8	SDS	74	38

^a For experimental conditions, see footnote. [†] 10 mol%. ^c Conversion was determined by GLC analysis using decane as internal standard. ^d Enantiomeric excess was determined on acetylated products using GLC (CP Chirasil DEX CB).

we investigated the reduction of cyclohexyl methyl ketone (**7**) and geranyl acetone (**8**), and found that these substrates behaved similar to 2-decanone (Table 1 entries 9–12). The reduction of sterically more demanding substrates such as adamantyl methyl ketone or *t*-butyl methyl ketone resulted in poor conversion. Not surprisingly, we can conclude that the reduction of substrates containing longer alkyl chains proceeded smoother when the reactions were performed with SDS present in the reaction mixture. We did not observe any dramatic effect on the enantioselectivity of the reaction from the combination of the modified catalyst and the surfactant. As can be seen in Table 1, an increase of enantioselectivity was obtained in some of the entries when the reactions were performed with SDS present, however, with the exception of compound **7**, only moderate ee's were measured.

In order to analyze the interaction between the catalyst $\text{Cp}^*\text{Rh-2}$ and SDS micelles, translational diffusion coefficients were determined by pulsed field gradient NMR for $\text{Cp}^*\text{Rh-2}$ in the presence of 38 mM and 80 mM SDS as well as for a pure 100 mM SDS sample.[‡] Spectral peaks for $\text{Cp}^*\text{Rh-2}$ could be distinguished from SDS methylene peaks and thus the diffusion constants for both the catalyst and the SDS could be determined. The detergent SDS is soluble in water and will appear also as monomers even above the critical micelle concentration, thus the observed diffusion will represent a weighted average between the participating states due to fast exchange. By assuming a two state

Table 2 Diffusion coefficients and hydrodynamic radii for SDS and Cp*Rh-2 at 25 °C

Sample	$D/10^{-11} \text{ m}^2 \text{ s}^{-1a}$		R_h/nm^b
	SDS	Cp*Rh-2	
SDS monomer	48 ^c	—	2.3
100 mM SDS	8.3	—	33.6
38 mM SDS + Cp*Rh-2 ^d	8.6	6.7	33.6
80 mM SDS + Cp*Rh-2 ^d	8.9	6.7	33.8

^a Diffusion constants in H₂O, normalized according to the diffusion of HDO to account for viscosity differences and compensated with a factor 1.23 due to the higher viscosity of D₂O. ^b Hydrodynamic radius. For the SDS micelle sample, the fraction of free monomer in solution was taken into account. For SDS/Cp*Rh-2 complex, the radius was calculated from the catalyst diffusion. A hydration layer with an estimated depth of 2.8 Å has been accounted for in the calculations. ^c Diffusion constant taken from ref. 15. ^d [Cp*Rh-2] = 4 mM.

model where SDS only appears either as a free monomer or as a part of a micelle, the measured diffusion constants (Table 2) for Cp*Rh-2 and SDS can be interpreted as the SDS/(Cp*Rh-2)-aggregate diffusion rate and the rate of the weighted average for the SDS states respectively. This relationship can be expressed as

$$D^{\text{obs}} = xD^{\text{micelle}} + (1 - x)D^{\text{monomer}}$$

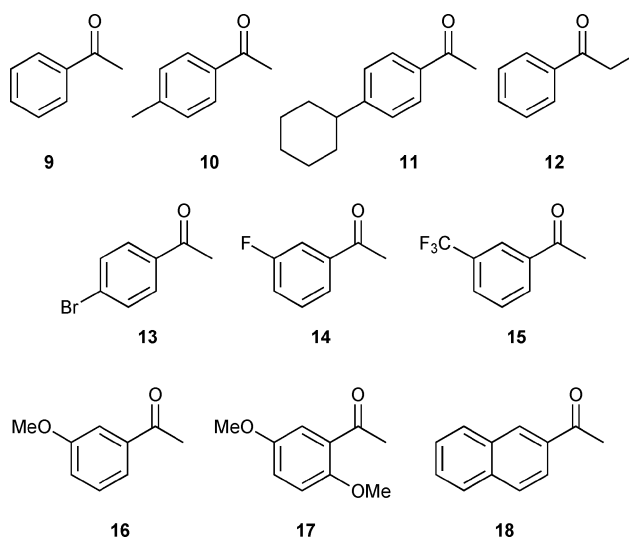
where D^{obs} is the observed diffusion constant, D^{micelle} is the diffusion rate for SDS micelles, D^{monomer} is the diffusion rate for monomers, and x is the fraction of SDS in the micelle state.¹⁵ Hence, the fraction of monomeric SDS could be estimated to be 5% in the Cp*Rh-2/SDS sample, and with this value a hydrodynamic radius of 33 Å was calculated for an SDS micelle, which is in agreement with previous results.¹⁶ In the calculations a diffusion constant for free monomeric SDS (48.0 m² s⁻¹) was taken from Jarvet *et al.*¹⁶ It should be noted that in the absence of SDS, Cp*Rh-2 did not dissolve well enough in D₂O to render any detectable signal in the NMR experiments. From the diffusion of Cp*Rh-2 in the Cp*Rh-2/SDS samples the catalyst obtains a diffusion constant fully comparable with the size of an SDS micelle which shows that stable isotropic aggregates between Cp*Rh-2 and the detergent are formed. Moreover, the data clearly shows that the size of the SDS-catalyst complex does not depend on the SDS concentration (Table 2). Hence, at the concentrations used in the catalytic experiments, the Cp*Rh-2 catalyst is fully incorporated in well defined micelles.

The observed catalytic activity of Cp*Rh-2, and the ability of the catalyst to fully interact with the surfactant, suggested that this catalyst-system would be useful for the reduction of other substrates in aqueous media. Thus, we examined aryl alkyl ketones **9–18** using the same reducing conditions as presented in Scheme 1 with SDS present (Table 3). As can be seen in Table 3, we obtained excellent conversion and enantioselectivity for all evaluated substrates, except for 2',5'-dimethoxyacetophenone (**17**, entry 9) and 2-acetonaphthone (**18**, entry 10). For comparison, we performed reductions without addition of SDS, and found that more water soluble substrates were readily reduced also under these conditions (*e.g.* acetophenone (**9**) gave 97% conversion and 96% ee). In contrast, the reduction of **11** resulted in merely 63% conversion (95% ee) when the surfactant was omitted.

Table 3 Rhodium-catalyzed reduction of aryl alkyl ketones in the presence of ligand **2**^a

Entry	Substrate	Conversion (%) ^b	ee (%) ^c
1	9	97	97 (<i>R</i>)
2	10	96	94 (<i>R</i>)
3	11	86	96 (<i>R</i>)
4	12	94	95 (<i>R</i>)
5	13	97	96 (<i>R</i>)
6	14	97	97 (<i>R</i>)
7	15	98	96 (<i>R</i>)
8	16	96	97 (<i>R</i>)
9	17	74	78 (<i>R</i>)
10	18	99	76 (<i>R</i>)

^a For experimental conditions, see footnote †. ^b Conversion was determined by GLC analysis. ^c Enantiomeric excess was determined by GLC (CP Chilasil DEX CB).



Concluding remarks

To summarize, we have investigated the possibility of gaining additional enantiocontrol in the aqueous asymmetric transfer hydrogenation of alkyl ketones using the combination of SDS as surfactant and a modified catalyst possessing low solubility in water. We found that employing a rhodium catalyst containing a mono-dodecylbenzenesulfonylated diamine ligand resulted in excellent conversion of long-chained alkyl ketones to their corresponding secondary alcohols using sodium formate as hydride donor in water and in the presence of SDS. An increase in enantioselectivity was observed in some cases when the surfactant was present. However, we cannot conclude that this is an effect of interactions between the catalyst and the substrate on the surface of the surfactant. The reduction of cyclohexyl methyl ketone resulted in excellent conversion and good enantioselectivity. In fact, this is the highest selectivity obtained under transfer hydrogenation conditions using sodium formate as hydride donor in aqueous media. Translational diffusion experiments showed that stable isotropic aggregates between Cp*Rh-2 and the SDS micelles are formed under the reaction conditions. In addition, we found that the reduction of aryl alkyl ketones using the modified catalyst system in

general resulted in high conversion and in high to excellent enantioselectivity.

Acknowledgements

We are grateful for financial support from the Swedish Research Council and the Carl Trygger Foundation.

Notes and references

† General procedure for the reduction of ketones using ligand **2**. The complex was initially prepared by mixing $[\text{Cp}^*\text{RhCl}_2]_2$ (0.005 mmol) and ligand **2** (0.01 mmol) in degassed dichloromethane (1.25 mL) and the resulting solution was stirred for 1 h at 40 °C. After evaporation of the solvent, SDS (0.1 mmol), sodium formate (5 mmol) and degassed water (2.5 mL) were added. The ketone substrate (1 mmol) was added and the reaction mixture was stirred at 28 °C for 17 h, quenched with EtOAc (2.5 mL) and after phase separation, aliquots from the organic layer were used for GLC analysis (CP Chirasil DEX CB). The alcohols obtained from alkyl alkyl ketones were acetylated with acetic anhydride and DMAP prior to analysis.

‡ Translational diffusion experiments were recorded at 25 °C on a Bruker Avance spectrometer equipped with a triple resonance probe head and operating at a ^1H frequency of 400 MHz. Diffusion constants were measured using a modified Stejskal–Tanner spin-echo experiment¹⁷ with a fixed diffusion time and a pulsed field gradient increasing linearly over 32 steps. The pulsed field gradients were calibrated using a 99.9% D_2O standard sample containing 1 mg ml^{-1} GdCl_3 . All measured samples were dissolved in D_2O . Viscosities of the samples were estimated by measuring the HDO diffusion rates and comparing it to standard values in D_2O and multiplied with a factor 1.23 to compensate for the higher viscosity in D_2O compared with H_2O .¹⁸ Viscosity-corrected diffusion constants could then be used to calculate hydrodynamic radii *via* the Stoke–Einstein relation, where a hydration layer with an estimated depth of 2.8 Å has been accounted for.

- (a) *Organic Reactions in Water*, ed. U. M. Lindström, Blackwell Publishing, Oxford, 2007; (b) U. M. Lindström, *Chem. Rev.*, 2002, **102**, 2751; (c) R. Breslow, *Acc. Chem. Res.*, 1991, **24**, 159.
- (a) S. Tiwari and A. Kumar, *Angew. Chem., Int. Ed.*, 2006, **45**, 4824; (b) S. Otto and J. B. F. N. Engberts, *Pure Appl. Chem.*, 2000, **72**, 1365.
- S. Narayan, J. Muldoon, M. G. Finn, V. V. Fokin, H. C. Kolb and K. B. Sharpless, *Angew. Chem., Int. Ed.*, 2006, **44**, 3275.
- (a) K. Holmberg, *Eur. J. Org. Chem.*, 2007, 731; (b) G. Oehme, I. Grassert, E. Paetzold, H. Fuhrmann, T. Dwars, U. Schmidt and I. Iovel, *Kinet. Katal.*, 2003, **44**, 766; (c) P. Scrimin, *Supramolecular Control of Structure and Reactivity*, ed. A. D. Hamilton, Wiley, Chichester, 1996, p. 101; (d) J. M. Brown, S. K. Baker, A. Colens, and J. R. Darwent, *Enzymatic and Nonenzymatic Catalysis*, ed. P. Dunhill, A. Wiseman and N. Blakebrough, Horwood, Chichester, 1980, p. 111.
- (a) D. Sinou, *Adv. Synth. Catal.*, 2002, **344**, 221; (b) *Aqueous-Phase Organometallic Chemistry: Concepts and Applications*, ed. B. Cornils, and W. A. Herrmann, VCH, Weinheim, 1998.
- (a) B. Carboni and L. Monnier, *Tetrahedron*, 1999, **55**, 1197; (b) S. Itsuno, *Org. React.*, 1998, **52**, 395; (c) E. J. Corey and C. J. Heral, *Angew. Chem., Int. Ed.*, 1998, **37**, 1986.
- (a) C. Hedberg, *Modern Reduction Methods*, ed. P. G. Andersson and I. J. Munslow, Wiley-VCH, Weinheim, 2008, p. 109; (b) S. Gladiali and E. Alberico, *Chem. Soc. Rev.*, 2006, **35**, 226.
- (a) T. Ohkuma, H. Ooka, T. Ikariya and R. Noyori, *J. Am. Chem. Soc.*, 1995, **117**, 10417; (b) R. Noyori, T. Ohkuma, M. Kitamura, H. Takaya, N. Sayo, H. Kombayashi and S. Akutagawa, *J. Am. Chem. Soc.*, 1987, **109**, 5856.
- (a) R. Noyori and S. Hashiguchi, *Acc. Chem. Res.*, 1997, **30**, 97; (b) S. Hashiguchi, A. Fujii, J. Takehara, T. Ikariya and R. Noyori, *J. Am. Chem. Soc.*, 1995, **117**, 7562.
- (a) X. Wu and J. Xiao, *Chem. Commun.*, 2007, 2449; (b) J. Xiao, X. Wu, A. Zanotti-Gerosa and F. Hancock, *Chim. Oggi*, 2005, **23**, 50.
- (a) Selected recent examples: Z. Xu, J. Mao, Y. Zhang, J. Guo and J. Zhu, *Catal. Commun.*, 2008, **9**, 618; (b) H.-F. Zhou, Q.-H. Fan, Y.-Y. Huang, L. Wu, Y.-M. He, W.-J. Tang, L.-Q. Gu and A. S. C. Chan, *J. Mol. Catal. A: Chem.*, 2007, **9**, 23; (c) N. A. Cortez, G. Aguirre, M. Parra-Hake and R. Somanathan, *Tetrahedron Lett.*, 2007, **48**, 4335; (d) J. Canivet and G. Süß-Fink, *Green Chem.*, 2007, **9**, 391; (e) L. Li, J. Wu, F. Wang, J. Liao, H. Zhang, C. Lian, J. Zhu and J. Deng, *Green Chem.*, 2007, **9**, 23; (f) D. S. Matharu, D. J. Morris, G. J. Clarkson and M. Wills, *Chem. Commun.*, 2006, 3232; (g) F. Wang, H. Liu, L. Cun, J. Zhu, J. Deng and Y. Jiang, *J. Org. Chem.*, 2005, **70**, 9424; (h) X. Wu, D. Vinci, T. Ikariya and J. Xiao, *Chem. Commun.*, 2005, 4447; (i) Y. Ma, H. Liu, L. Chen, X. Cui, J. Zhu and J. Deng, *Org. Lett.*, 2003, **5**, 2103.
- (a) J. Wettergren, A. B. Zaitsev and H. Adolfsson, *Adv. Synth. Catal.*, 2007, **349**, 2556; (b) K. Ahlford, A. B. Zaitsev, J. Ekström and H. Adolfsson, *Synlett*, 2007, 2541; (c) A. B. Zaitsev and H. Adolfsson, *Org. Lett.*, 2006, **8**, 5126; (d) P. Västilä, A. B. Zaitsev, J. Wettergren, T. Privalov and H. Adolfsson, *Chem.–Eur. J.*, 2006, **12**, 3218; (e) J. Wettergren, A. Bøgevig, M. Portier and H. Adolfsson, *Adv. Synth. Catal.*, 2006, **348**, 1277; (f) P. Västilä, J. Wettergren and H. Adolfsson, *Chem. Commun.*, 2005, 4039; (g) N. Dahlin, A. Bøgevig and H. Adolfsson, *Adv. Synth. Catal.*, 2004, **346**, 1101; (h) A. Bøgevig, I. M. Pastor and H. Adolfsson, *Chem.–Eur. J.*, 2004, **10**, 294; (i) I. M. Pastor, P. Västilä and H. Adolfsson, *Chem.–Eur. J.*, 2003, **9**, 4031; (j) I. M. Pastor, P. Västilä and H. Adolfsson, *Chem. Commun.*, 2002, 2046.
- (a) A. Schlatter and W.-D. Woggon, *Adv. Synth. Catal.*, 2008, **350**, 995; (b) M. T. Reetz and X. Li, *J. Am. Chem. Soc.*, 2006, **128**, 1044; (c) A. Schlatter, M. K. Kundu and W.-D. Woggon, *Angew. Chem., Int. Ed.*, 2004, **43**, 6731.
- (a) J. S. M. Samec, J.-E. Bäckvall, P. G. Andersson and P. Brandt, *Chem. Soc. Rev.*, 2006, **35**, 237; (b) P. Brandt, P. Roth and P. G. Andersson, *J. Org. Chem.*, 2004, **69**, 4885; (c) R. Noyori, M. Yamakawa and S. Hashiguchi, *J. Org. Chem.*, 2001, **66**, 7931; (d) M. Yamakawa, I. Yamada and R. Noyori, *Angew. Chem., Int. Ed.*, 2001, **40**, 2818; (e) M. Yamakawa, H. Ito and R. Noyori, *J. Am. Chem. Soc.*, 2000, **122**, 1466; (f) D. A. Alonzo, P. Brandt, S. J. M. Nordin and P. G. Andersson, *J. Am. Chem. Soc.*, 1999, **121**, 9580.
- B. Lindman, M. C. Puyal, N. Kamenka, R. Rymden and P. Stilbs, *J. Phys. Chem.*, 1984, **88**, 5048.
- J. Jarvet, J. Danielsson, P. Damberg, M. Oleszczuk and A. Gräslund, *J. Biomol. NMR*, 2007, **39**, 63.
- (a) E. O. Stejskal and J. E. Tanner, *J. Chem. Phys.*, 1965, **42**, 288; (b) P. T. Callaghan, M. E. Komlosh and M. Nyden, *J. Magn. Reson.*, 1998, **133**, 177; (c) E. von Meerwall and M. Kamat, *J. Magn. Reson.*, 1989, **83**, 309.
- L. G. Longworth, *J. Phys. Chem.*, 1960, **64**, 1914.

Accumulation of ionic liquids in *Escherichia coli* cells

Robert J. Cornmell,^a Catherine L. Winder,^b Gordon J. T. Tiddy,^a Royston Goodacre^b and Gill Stephens^{*a}

Received 28th April 2008, Accepted 11th June 2008

First published as an Advance Article on the web 4th July 2008

DOI: 10.1039/b807214k

Ionic liquids accumulate within *Escherichia coli* cells and can be detected by Fourier transform infrared (FT-IR) spectroscopy. Harvested cells were incubated with the biocompatible, water-immiscible ionic liquids, trihexyltetradecylphosphonium bis(trifluoromethylsulfonyl)imide ($[P_{6,6,6,14}][NTf_2]$) and methyltrioctylammonium bis(trifluoromethylsulfonyl)imide ($[N_{1,8,8,8}][NTf_2]$), and with the toxic chlorides, $[P_{6,6,6,14}][Cl]$ and $[N_{1,8,8,8}][Cl]$. The cells were harvested, washed and dried, and their FT-IR spectra were recorded. The ionic liquid spectra could be detected against the background spectra of the cells, demonstrating that they were accumulating within the cells. The toxic ionic liquids accumulated more rapidly than the biocompatible ionic liquids. Principal components analysis followed by discriminant function analysis showed that, compared to control cells, the toxic ionic liquids produced much bigger changes in the FT-IR fingerprint of the cellular chemicals than the biocompatible ionic liquids. Subcellular fractionation, followed by FT-IR analysis, demonstrated that $[P_{6,6,6,14}][NTf_2]$ accumulated specifically in the membrane fraction of the cells and not the cytoplasm.

Introduction

Ionic liquids are attracting an enormous amount of attention as clean, green alternatives to environmentally damaging conventional solvents in chemical and biocatalytic manufacturing processes.^{1–6} The most exciting feature is the unparalleled scope to tailor the solvent properties to match the requirements of the process, simply by selecting appropriate cation and anion combinations. However, this very diversity greatly complicates the task of understanding the safety and environmental impact of ionic liquids, which is crucial to obtain regulatory approval for ionic liquid-based processes and products. Fortunately, there has been remarkably rapid progress in developing structure–activity relationships for ionic liquid toxicity and environmental impact.^{7–9} However, we still know very little about the specific molecular interactions between these novel chemical entities and living organisms. For this reason, we used transmission Fourier transform infrared (FT-IR) spectroscopy to analyse the chemical composition of *Escherichia coli* cells after exposure to ionic liquids, to provide an insight into the mechanisms of toxicity.

The FT-IR spectra of cells provide metabolic fingerprints which are extremely useful for identification of microorganisms^{10–12} or to monitor their physiological state,¹³ but their use to identify naturally-occurring intracellular metabolites is generally difficult and needs complex chemometric processing.^{14–16} However, ionic liquids are xenobiotics which give

distinctive IR spectra that differ markedly from the spectra of cell components. This suggested that ionic liquids may be detectable if they accumulate inside the cells.

We tested this hypothesis by comparing the effects of toxic and biocompatible ionic liquids on the FT-IR spectra of *E. coli* cells. We chose trihexyltetradecylphosphonium bis(trifluoromethylsulfonyl)imide ($[P_{6,6,6,14}][NTf_2]$) and methyltrioctylammonium bis(trifluoromethylsulfonyl)imide ($[N_{1,8,8,8}][NTf_2]$) as examples of biocompatible ionic liquids, since they cause only modest inhibition of growth of *E. coli*.^{17,18} Furthermore, these two ionic liquids are extremely useful, since they are water-immiscible, and both can be used to provide dramatically improved product yields for redox biotransformations using bacterial cells.^{18,19} By contrast, changing the anion to chloride makes the ionic liquids so toxic that growth is inhibited completely even when the phase ratio of $[P_{6,6,6,14}][Cl]$ and $[N_{1,8,8,8}][Cl]$ is decreased to 0.0025.¹⁸ Therefore, these two ionic liquids were selected as examples of toxic, water-immiscible ionic liquids.

In this study, we show that ionic liquids are taken up into *E. coli* cells and can be readily detected against the background FT-IR spectrum of cellular chemicals. We also show that ionic liquids accumulate specifically within the membrane fraction of the cells.

Results and discussion

Effect of ionic liquids on cell viability

The first step was to produce *E. coli* cells that had been exposed to ionic liquids. *E. coli* can grow in the presence of $[P_{6,6,6,14}][NTf_2]$ and $[N_{1,8,8,8}][NTf_2]$ (although there is some inhibition) but the toxic ionic liquids, $[P_{6,6,6,14}][Cl]$ and $[N_{1,8,8,8}][Cl]$, do not allow any growth.¹⁸ Therefore, we studied the effects of the ionic liquids by first growing *E. coli* without the ionic liquids, harvesting the

^aSchool of Chemical Engineering and Analytical Science, Manchester Interdisciplinary Biocentre, University of Manchester, 131 Princess Street, Manchester, UK M1 7DN.

E-mail: gill.stephens@manchester.ac.uk; Fax: +44 161 3068918; Tel: +44 161 3064377

^bSchool of Chemistry, Manchester Interdisciplinary Biocentre, University of Manchester, 131 Princess Street, Manchester, UK M1 7DN

cells aseptically and resuspending them in fresh medium. The ionic liquids (phase ratio, 0.23; 23% v/v) were then added, and the cells were incubated for 24 h. We chose this solvent : water phase ratio because it is within the range that is suitable for two-liquid phase biotransformations²⁰ and because it allows direct comparison with our previous work on biotransformations using ionic liquids.¹⁸

Using culture medium meant that there was some growth in the control cell suspensions during the first 3 h, and in the suspensions exposed to $[N_{1,8,8,8}][NTf_2]$ and $[P_{6,6,6,14}][NTf_2]$ (Fig. 1). However, there was little growth thereafter. The optical (OD) and viable count were slightly lower in the cell suspensions exposed to these ionic liquids than in the control without ionic liquid.

By contrast, $[N_{1,8,8,8}][Cl]$ and $[P_{6,6,6,14}][Cl]$ both caused a dramatic decrease in OD when added to the cell suspensions, indicating that the cells were lysing. The cells began to recover after exposure to $[P_{6,6,6,14}][Cl]$ for 3 h, and there was a slight increase in the viable count and OD after 24 h. $[N_{1,8,8,8}][Cl]$ was completely bacteriocidal, since viable cells could not be detected. Thus, no colonies were formed even when the undiluted cell suspension was spread on agar plates. Similar behaviour was observed even when the phase ratio was decreased to 0.05. Nevertheless, sufficient residual cell material could be collected for FT-IR analysis by centrifugation. We assumed that this material consisted of dead cells and cell fragments.

FTIR spectroscopy of cells exposed to $[P_{6,6,6,14}]^+$ -containing ionic liquids

Next, we measured the FT-IR spectra of the cells after exposure to the ionic liquids, and compared them with the spectra of pure ionic liquids and with unexposed control cells. Exposure to $[P_{6,6,6,14}][NTf_2]$ had very little effect on the cell spectra after 30 min or 3 h (Fig. 2). However, the spectrum was dominated by the extremely distinctive fingerprint of $[P_{6,6,6,14}][NTf_2]$ after 24 h. This demonstrated that the ionic liquid was either being taken up by the cells or was so tightly bound to the cell surface that it could not be removed by our vigorous washing procedure. The fact that there was little accumulation during the first 3 h indicates either that the accumulation process was slow or that the cells were excluding the ionic liquid. Comparison of the spectra (Fig. 2) with the spectra of cells exposed to $[P_{6,6,6,14}][Cl]$ (Fig. 3) makes it possible to distinguish the peaks due to the cation and the anion, since, of course, the Cl^- anion does not give an FTIR signal. This comparison shows that the peaks were due to both the $P_{6,6,6,14}^+$ cation and the NTf_2^- anion, indicating that both were present in the cells.

The spectra of cells exposed to the toxic ionic liquid, $[P_{6,6,6,14}][Cl]$, contained small peaks due to the ionic liquid even after 30 min (Fig. 3). Therefore, accumulation of the toxic ionic liquid began more quickly than in the samples exposed to $[P_{6,6,6,14}][NTf_2]$. The intensity of the peaks increased relative to the cell fingerprint after 3 h, but decreased again after 24 h. This suggests that the ionic liquid was lost from the cells after prolonged incubation. Whether this was due to leakage or active exclusion associated with recovery of the cells (Fig. 1) remains to be determined.

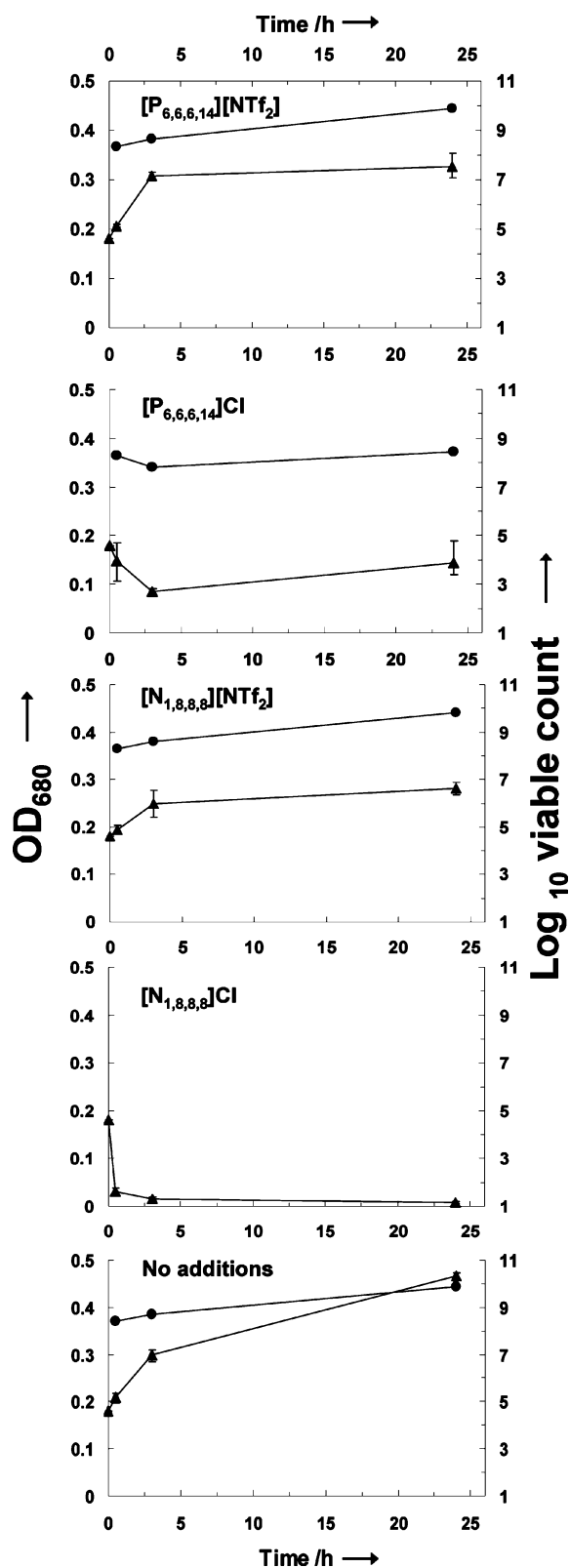


Fig. 1 Effect of ionic liquids on the optical density and viable count of *E. coli* after harvesting and resuspension in fresh culture medium. The cells were incubated with the ionic liquids shown and the OD (\blacktriangle) and viable counts (\bullet) were measured.

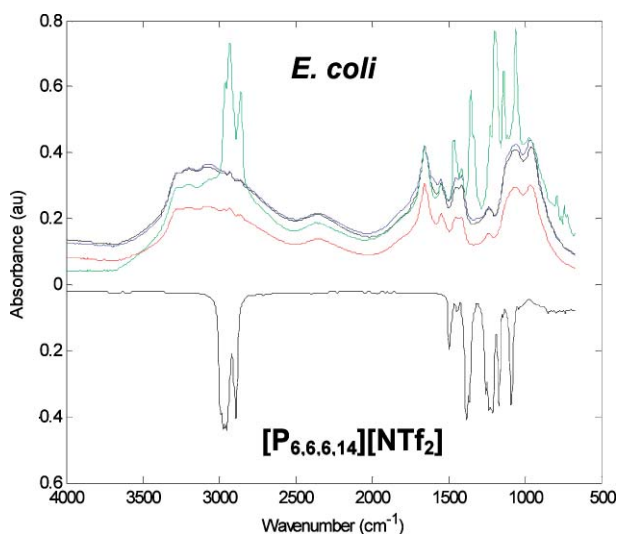


Fig. 2 FT-IR spectra of *E. coli* after exposure to $[P_{6,6,6,14}][NTf_2]$ after 30 min (green), 3 h (red) and 24 h (turquoise), or without ionic liquid (blue). The spectrum of authentic $[P_{6,6,6,14}][NTf_2]$ is plotted upside down for comparison.

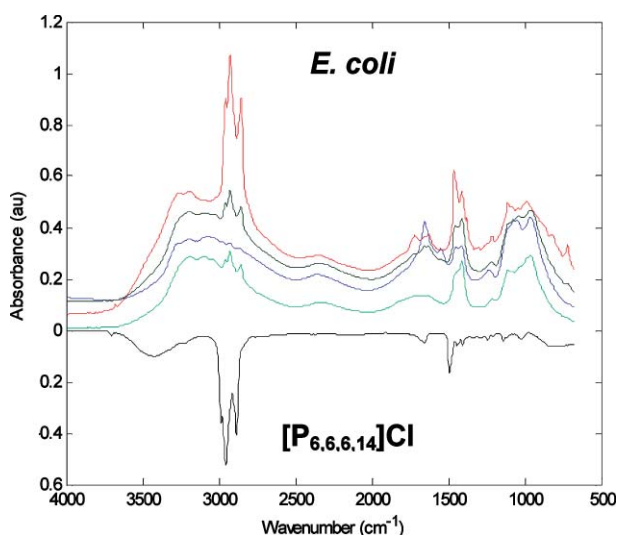


Fig. 3 FT-IR spectra of *E. coli* after exposure to $[P_{6,6,6,14}][Cl]$ after 30 min (green), 3 h (red) and 24 h (turquoise), or without ionic liquid (blue). The spectrum of authentic $[P_{6,6,6,14}][Cl]$ is plotted upside down for comparison.

FTIR spectroscopy of cells exposed to $[N_{1,8,8,8}]^+$ -containing ionic liquids

The FT-IR spectra of cells exposed to the biocompatible ionic liquid, $[N_{1,8,8,8}][NTf_2]$, contained small peaks due to the ionic liquid throughout the incubation period (Fig. 4). Comparison with spectra of cells exposed to $[N_{1,8,8,8}][Cl]$ (Fig. 5) shows that both the cation and the anion could be detected. However, it is difficult to interpret the kinetics of accumulation because the peak intensities were low, and the ratios of signal intensity between the cation and anion peaks cannot be judged accurately. Nevertheless, the fact that the ionic liquid accumulated rapidly is consistent with its increased growth inhibition compared with $[P_{6,6,6,14}][NTf_2]$.¹⁸

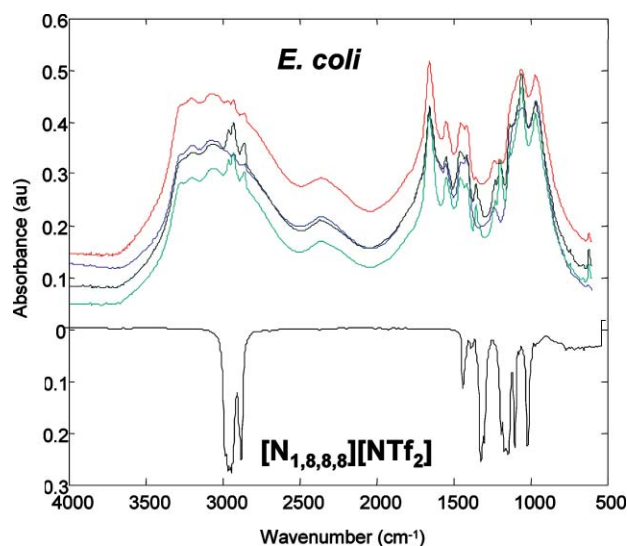


Fig. 4 FT-IR spectra of *E. coli* after exposure to $[N_{1,8,8,8}][NTf_2]$ after 30 min (green), 3 h (red) and 24 h (turquoise), or without ionic liquid (blue). The spectrum of authentic $[N_{1,8,8,8}][NTf_2]$ is plotted upside down for comparison.

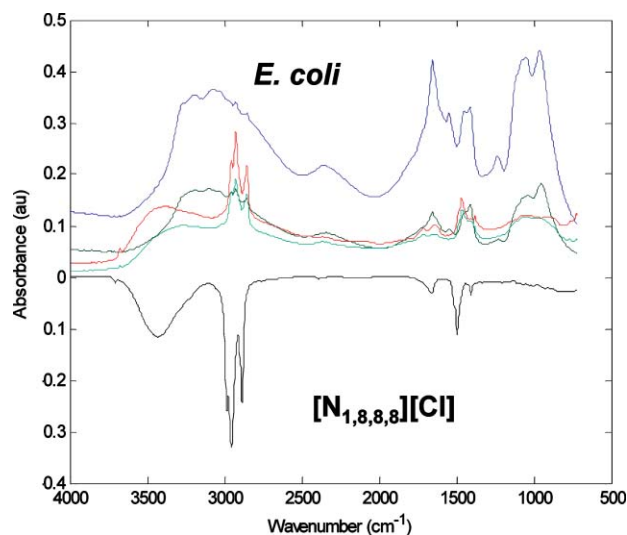


Fig. 5 FT-IR spectra of *E. coli* after exposure to $[N_{1,8,8,8}][Cl]$ after 30 min (green), 3 h (red) and 24 h (turquoise), or without ionic liquid (blue). The spectra of the cells exposed to the ionic liquid are much less intense than the control because there was extensive cell lysis, which caused loss of cell material. The spectrum of authentic $[N_{1,8,8,8}][Cl]$ is plotted upside down for comparison.

In cells exposed to $[N_{1,8,8,8}][Cl]$, the $N_{1,8,8,8}^+$ cation could be detected clearly after 3 h and 24 h, although it was not clear whether the ionic liquid was present or not after 30 min (Fig. 5). The background cell fingerprint was much weaker than in the control cells because very little cell material was available for analysis due to cell lysis (see Fig. 1). However, the peak intensities due to the ionic liquids were strong relative to the cell peaks, suggesting that the residual dead cell material had a very high capacity to bind the ionic liquid. As with $[P_{6,6,6,14}][Cl]$, $[N_{1,8,8,8}][Cl]$ accumulated in the cells relatively quickly, and this suggests that early accumulation of the ionic liquid is associated with

toxicity. However, methods for kinetic analysis would need to be developed to verify this hypothesis.

Analysis of FTIR data

Intracellular accumulation of the ionic liquids could be detected by simple visual inspection of the FT-IR spectra. However, FT-IR spectroscopy can also be used as a metabolic “fingerprinting” technique to detect changes in cell physiology.^{15,21,22} Therefore, we also wanted to find out if the spectra indicated any changes in the underlying cell chemistry. The complexity of cellular FT-IR spectra makes it essential to use multivariate statistical analysis methods to quantify the differences and identify differences between the spectra that may be attributable to the underlying biology and chemistry.^{23–25} Therefore, the multidimensional FT-IR data (1764 data points) were reduced by principal components analysis (PCA). Discriminant function analysis (DFA) was then used to discriminate between groups on the basis of the retained principal components and the *a priori* knowledge of which spectra were machine replicates.

Clustering patterns could be obtained from PC-DFA of the data with only 5 PCs selected (Fig. 6). The cell samples exposed to the biocompatible ionic liquid, [N_{1,8,8,8}][NTf₂], were located close to the tight cluster of the control cells, which had not been exposed to solvent. Therefore, [N_{1,8,8,8}][NTf₂] had relatively little effect on the metabolic fingerprint of the cells, suggesting that there was little perturbation of cellular chemistry.

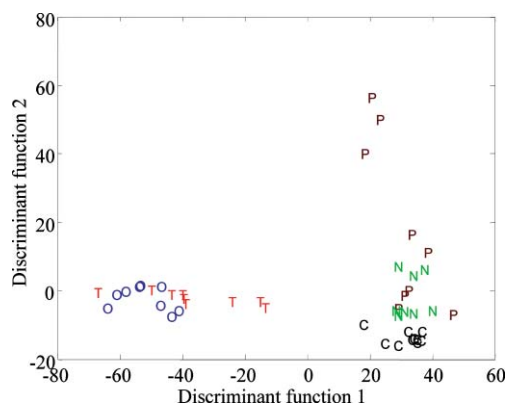


Fig. 6 PC-DFA scores plot based on the first 5 principal components from FT-IR spectra analysed by Matlab. The plot shows the relationship between FT-IR spectra of *E. coli* incubated without ionic liquids (C, black), or with [P_{6,6,6,14}][NTf₂] (P, brown), [N_{1,8,8,8}][NTf₂] (N, green), [P_{6,6,6,14}][Cl] (T, red) or [N_{1,8,8,8}][Cl] (O, blue) for 24 h.

The spectra of cells exposed to [P_{6,6,6,14}][NTf₂] clustered much less tightly with the controls, since one of the biological replicates clustered away from the controls in the second discriminant function (DF). However, it should be noted that the peaks due to [P_{6,6,6,14}][NTf₂] were very intense (see Fig. 2) and tended to dominate the underlying cell fingerprint, and this may have caused this change.

By contrast, the spectra of cells exposed to the toxic ionic liquids, [P_{6,6,6,14}][Cl] and [N_{1,8,8,8}][Cl] formed clusters that were completely distinct from the control cluster and were clearly separated from the controls and biocompatible ionic liquids in the first DF. This is highly significant because the first DF

is extracted to give the most variance with respect to group separation. The facts that the DFA algorithm was trained with machine replicates and not the toxicity (or otherwise) of the ionic liquid, and that the differentiation between toxic *versus* benign ionic liquids occurs in the first DF show that there are clear phenotypic differences between the *E. coli* cells when they are exposed to toxic ionic liquids compared to the controls and cells exposed to non-toxic solvents. Moreover, these ionic liquids should have a weaker influence on the overall spectrum than the bis-triflamide-containing ionic liquids, since we could see only the cation spectra superimposed on the underlying cell spectra. Therefore, the extent of the separation from the controls observed in Fig. 6 suggests further that the toxic ionic liquids really do have a marked effect on cellular biochemistry. Detailed metabolomic analysis will be needed in the future to identify the specific biochemical changes that were induced by the toxic ionic liquids.

FTIR spectroscopy of subcellular fractions

We were extremely curious to find out where the ionic liquids were accumulating in the cells. Therefore, we grew *E. coli* in the presence of [P_{6,6,6,14}][NTf₂], harvested the cells and fractionated them into cytoplasmic and membrane fractions. We also collected the residual buffer from the washing step, to check for leakage of the ionic liquids. We then measured the FT-IR spectra of the subcellular fractions and compared them with fractions from cells that had not been exposed to the ionic liquid (Fig. 7). Remarkably, the ionic liquid could only be detected in the cell membranes, and not in the cytoplasmic fraction or the extracellular wash fraction. Therefore, it seems that this hydrophobic ionic liquid is lipophilic enough to accumulate in the membranes, even though it causes relatively little growth inhibition.

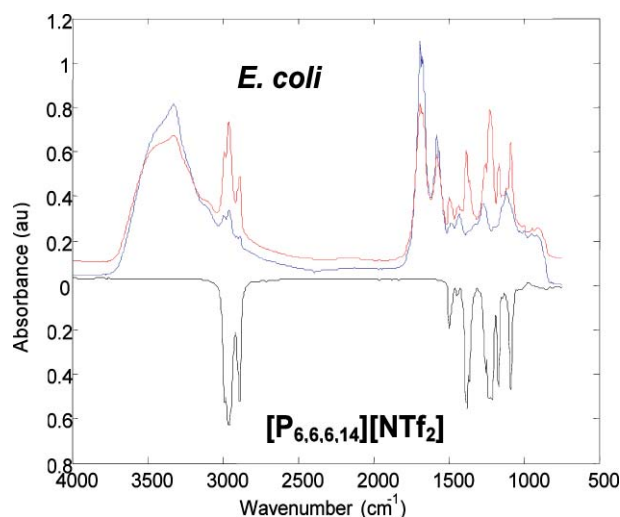


Fig. 7 FT-IR spectra of membrane fractions (red) of *E. coli* after growth in the presence of [P_{6,6,6,14}][NTf₂], compared with membrane fractions from unexposed cells (blue). For clarity, the spectra of cytoplasmic and wash fractions are not shown, since the ionic liquid could not be detected in either. The spectrum of authentic [P_{6,6,6,14}][NTf₂] is plotted upside down for comparison.

Conclusions

We have shown that FT-IR spectroscopy can be used to detect accumulation of ionic liquids inside microbial cells, and that there may be a connection between speed of accumulation and toxicity. FT-IR spectroscopy is especially convenient to use to study intracellular uptake because the ionic liquids can be detected without having to label them with heavy isotopes or radiolabels. Furthermore, FT-IR analysis can be applied to a wide range of cell types^{10,12,26,27} and can be done conveniently and rapidly in 96 well format.^{11,28} This makes FT-IR very attractive for high throughput screening for ionic liquid uptake.

The detection of ionic liquids inside cells provides an important advance in understanding the mechanisms of ionic liquid toxicity. The direct demonstration that ionic liquids really do partition into lipid membranes in cells is especially significant. There is a growing body of evidence that the toxicity of ionic liquids is strongly correlated with their lipophilicity,^{7,29–32} suggesting that toxicity is due to disruption of membrane structure. Our findings provide excellent mechanistic support for this correlation.

In conclusion, this is the first use of FT-IR spectroscopy to demonstrate the accumulation of ionic liquids within bacterial cells and their membranes, and provides a very sound basis for further, detailed investigation of toxicity mechanisms.

Experimental

Chemicals

[N_{1,8,8,8}][NTf₂], were purchased from Solvent Innovation, and [N_{1,8,8,8}][Cl], [P_{6,6,6,14}][Cl] and [P_{6,6,6,14}][NTf₂] were obtained from Sigma–Aldrich. All other reagents and media components were purchased from Sigma–Aldrich, unless otherwise stated.

Exposure of harvested cells to ionic liquids

Escherichia coli K12 MG1655³³ was maintained on LB agar. Inocula and experimental cultures were grown in MSX medium³⁴ at 37 °C with shaking at 200 rpm. Experimental cultures (150 ml; 1% inoculum) were grown for 24 h, divided into 15 separate aliquots (10 ml) and harvested by centrifugation at 4000 rpm for 10 min at 4 °C. The cell pellets were resuspended in 10 ml MSX medium as a control or 7.7 ml MSX medium plus 2.3 ml of ionic liquid, with 3 replicates for each condition. After incubation at 37 °C with shaking at 200 rpm, samples of the aqueous phases of the cultures were taken for measurement of OD₆₈₀, viable count measurements and FT-IR analysis. Viable counts were measured by serially diluting the samples in physiological saline (0.9% NaCl) and plating 100 µl aliquots on LB agar.

Sample preparation

Cells were prepared for FTIR analysis by taking samples of the aqueous phases of the cell suspensions during exposure to ionic liquids (2 ml). The cells were collected by centrifugation at 13 000 rpm for 3 min, washed 3 times by vortex mixing in physiological saline (1 ml) and resuspended in saline to give the same approximate cell concentration as the control sample. Thus, the control cells, and cells exposed to [P_{6,6,6,14}][NTf₂] and

[N_{1,8,8,8}][NTf₂] were resuspended in 125 µl saline, and samples exposed to [P_{6,6,6,14}][Cl] were resuspended in 62 µl saline. The cell concentration in samples exposed to [N_{1,8,8,8}][Cl] was extremely low, and so the samples were resuspended in 25 µl saline, the minimum possible volume suitable for analysis.

Subcellular fractionation

Cultures (50 ml) of *E. coli* were grown for 24 h at 37 °C in the presence of [P_{6,6,6,14}][NTf₂] (phase ratio 0.23) in MSX medium. The cells were harvested from the aqueous phase by centrifugation at 4000 rpm for 20 min at 4 °C. The resulting pellet was washed twice by resuspension in saline (5 ml), and harvested as before. The supernatants from both washing steps were pooled and stored for FT-IR analysis. The final cell pellet was resuspended in saline (2 ml) and disrupted using a homogeniser (Kinematica) for 10 min on ice. The homogenate was filtered through a 0.2 µm filter to remove any unbroken cells and cell wall debris, and then centrifuged at 13 000 rpm for 1 h at 4 °C. The pellet (cell membrane fraction) was resuspended in 200 µl saline. The membranes and the supernatant (cytoplasmic fraction) were then analysed immediately by FT-IR.

FT-IR spectroscopy

The cell samples were analysed in triplicate as detailed elsewhere.^{11,12,26} Aliquots (25 µl) of cell suspensions were applied evenly onto a zinc selenide (Bruker) plate for analysis by FT-IR. The samples were dried at 50 °C for 30 min. The plate was loaded onto a motorised microplate module HTS-XT™ attached to an Equinox 55 module (Bruker Optics Ltd., UK). A deuterated triglycine sulfate (DTGS) detector was employed for transmission measurements of the samples. Spectra were collected over the wavelength range of 4000 to 900 cm⁻¹ under the control of a computer programmed with Opus 4, operated under MS windows 2000. Spectra were acquired at a resolution of 4 cm⁻¹ and 64 spectra were co-added and averaged to improve the signal to noise ratio. The collection time for each spectrum was approximately 1 min, and the spectra were displayed in terms of absorbance. It should be noted that the FTIR spectra contain smaller peaks due to lipid and larger peaks due to polysaccharide than normally found in growing cells because the cells were not growing actively during the experiments. Authentic FT-IR spectra from [P_{6,6,6,14}][NTf₂], [P_{6,6,6,14}][Cl], [N_{1,8,8,8}][Cl] and [N_{1,8,8,8}][NTf₂] were acquired by loading 0.8 µl aliquots of each ionic liquid onto a calcium fluoride disc and collecting spectra from a mercury cadmium telluride (MCT) detector after initial measurement with a 15× objective lens.

Cluster analysis

Analysis of the FT-IR data was based on methods described previously.^{11,12,26} The multidimensional FT-IR data were reduced by principal components analysis (PCA).³⁵ PCA was performed according to the NIPALS algorithm.³⁶ In this manner the multivariate FT-IR spectra (containing 1764 data points) were reduced down to 5 PCs and discriminant function analysis (DFA) then discriminated between groups on the basis of the retained principal components and the *a priori* knowledge of which spectra were machine replicates (so for each of the

3 biological replicates which were analysed 3 times, 3 classes were used for each ionic liquid by the DFA algorithm). Thus, this process did not bias the analysis in any way.³⁷ These cluster analysis methods were implemented using Matlab version 7.1 (The Math Works, Inc., Natick, MA, USA), which runs under Microsoft Windows NT.

Acknowledgements

We are grateful to the Engineering and Biological Systems committee of the UK Biotechnology and Biological Sciences Research Council for financial support *via* grant number BB/C503346/1

References

- 1 M. Deetlefs and K. R. Seddon, *Chim. Oggi*, 2006, **24**, 16–23.
- 2 N. V. Plechkova and K. R. Seddon, *Chem. Soc. Rev.*, 2008, **37**, 123–150.
- 3 F. van Rantwijk, R. Madeira Lau and R. A. Sheldon, *Trends Biotechnol.*, 2003, **21**, 131–138.
- 4 S. Park and R. J. Kazlauskas, *Curr. Opin. Biotechnol.*, 2003, **14**, 432–437.
- 5 S. Cantone, U. Hanefeld and A. Basso, *Green Chem.*, 2007, **9**, 954–971.
- 6 F. Van Rantwijk and R. A. Sheldon, *Chem. Rev.*, 2007, **107**, 2757–2785.
- 7 J. Ranke, S. Stolte, R. Stoermann, J. Arning and B. Jastorff, *Chem. Rev.*, 2007, **107**, 2183–2206.
- 8 B. Jastorff, K. Moelter, P. Behrend, U. Bottin-Weber, J. Filser, A. Heimers, B. Ondruschka, J. Ranke, M. Schaefer, H. Schroeder, A. Stark, P. Stepnowski, F. Stock, R. Stoermann, S. Stolte, U. Welz-Biermann, S. Ziegert and J. Thoeming, *Green Chem.*, 2005, **7**, 362–372.
- 9 B. Jastorff, R. Stoermann, J. Ranke, K. Moelter, F. Stock, B. Oberheitmann, W. Hoffmann, J. Hoffmann, M. Nuechter, B. Ondruschka and J. Filser, *Green Chem.*, 2003, **5**, 136–142.
- 10 K. Maquelin, C. Kirschner, L. P. Choo-Smith, N. Van Den Braak, H. P. Endtz, D. Naumann and G. J. Puppels, *J. Microbiol. Methods*, 2002, **51**, 255–271.
- 11 C. L. Winder, S. V. Gordon, J. Dale, R. G. Hewinson and R. Goodacre, *Microbiology*, 2006, **152**, 2757–2765.
- 12 E. M. Timmins, S. A. Howell, B. K. Alsberg, W. C. Noble and R. Goodacre, *J. Clin. Microbiol.*, 1998, **36**, 367–374.
- 13 H. E. Johnson, D. Broadhurst, D. B. Kell, M. K. Theodorou, R. J. Merry and G. W. Griffith, *Appl. Environ. Microbiol.*, 2004, **70**, 1583–1592.
- 14 R. Goodacre, B. Shann, R. J. Gilbert, É. M. Timmins, A. C. McGovern, B. K. Alsberg, D. B. Kell and N. A. Logan, *Anal. Chem.*, 2000, **72**, 119–127.
- 15 W. B. Dunn, N. J. C. Bailey and H. E. Johnson, *Analyst*, 2005, **130**, 606–625.
- 16 A. C. McGovern, D. Broadhurst, J. Taylor, N. Kaderbhai, M. K. Winson, D. A. Small, J. J. Rowland, D. B. Kell and R. Goodacre, *Biotechnol. Bioeng.*, 2002, **78**, 527–538.
- 17 H. Pfruender, R. Jones and D. Weuster-Botz, *J. Biotechnol.*, 2006, **124**, 182–190.
- 18 R. J. Cornmell, C. L. Winder, S. Schuler, R. Goodacre and G. Stephens, *Green Chem.*, 2008, **10**, 685–691.
- 19 H. Pfruender, M. Midjojo, U. Kragl and D. Weuster-Botz, *Angew. Chem., Int. Ed.*, 2004, **43**, 4529–4531.
- 20 R. Leon, P. Fernandes, H. M. Pinheiro and J. M. S. Cabral, *Enzyme Microb. Technol.*, 1998, **23**, 483–500.
- 21 D. I. Ellis and R. Goodacre, *Analyst*, 2006, **131**, 875–885.
- 22 K. Hollywood, D. R. Brison and R. Goodacre, *Proteomics*, 2006, **6**, 4716–4723.
- 23 R. Goodacre, *J. Exp. Bot.*, 2005, **56**, 245–254.
- 24 R. Goodacre, S. Vaidyanathan, W. B. Dunn, G. G. Harrigan and D. B. Kell, *Trends Biotechnol.*, 2004, **22**, 245–252.
- 25 R. M. Jarvis and R. Goodacre, *Bioinformatics*, 2005, **21**, 860–868.
- 26 R. Goodacre, É. M. Timmins, R. Burton, N. Kaderbhai, A. M. Woodward, D. B. Kell and P. J. Rooney, *Microbiology*, 1998, **144**, 1157–1170.
- 27 D. Naumann, D. Helm and H. Labischinski, *Nature*, 1991, **351**, 81–82.
- 28 G. G. Harrigan, R. H. LaPlante, G. N. Cosma, G. Cockerell, R. Goodacre, J. F. Maddox, J. P. Luyendyk, P. E. Ganey and R. A. Roth, *Toxicol. Lett.*, 2004, **146**, 197–205.
- 29 J. Ranke, K. Molter, F. Stock, U. Bottin-Weber, J. Poczbott, J. Hoffmann, B. Ondruschka, J. Filser and B. Jastorff, *Ecotoxicol. Environ. Saf.*, 2004, **58**, 396–404.
- 30 S. Stolte, M. Matzke, J. Arning, A. Boeschen, W.-R. Pitner, U. Welz-Biermann, B. Jastorff and J. Ranke, *Green Chem.*, 2007, **9**, 1170–1179.
- 31 J. Ranke, A. Mueller, U. Bottin-Weber, F. Stock, S. Stolte, J. Arning, R. Stoermann and B. Jastorff, *Ecotoxicol. Environ. Saf.*, 2007, **67**, 430–438.
- 32 J. Ranke, K. Moelter, F. Stock, U. Bottin-Weber, J. Poczbott, J. Hoffmann, B. Ondruschka, J. Filser and B. Jastorff, *Ecotoxicol. Environ. Saf.*, 2004, **58**, 396–404.
- 33 F. R. Blattner, G. Plunkett, C. A. Bloch, N. T. Perna, V. Burland, M. Riley, J. ColladoVides, J. D. Glasner, C. K. Rode, G. F. Mayhew, J. Gregor, N. W. Davis, H. A. Kirkpatrick, M. A. Goeden, D. J. Rose, B. Mau and Y. Shao, *Science*, 1997, **277**, 1453–1462.
- 34 L. P. Wahbi, D. Gokhale, S. Minter and G. M. Stephens, *Enzyme Microb. Technol.*, 1996, **19**, 297–306.
- 35 I. T. Jolliffe, *Principal Component Analysis*, Springer-Verlag, New York, 1986.
- 36 H. Wold, in *Multivariate Analysis*, ed. K. R. Krishnaiah, Academic Press, New York, 1966, pp. 391–420.
- 37 B. F. J. Manly, *Multivariate Statistical Methods: A Primer*, Chapman & Hall, London, 1994.

Platform technology for dienone and phenol–formaldehyde architectures†

Marilena A. Giarrusso,^a Luke T. Higham,^a Ulf P. Kreher,^a Ram S. Mohan,^b Anthony E. Rosamilia,^a Janet L. Scott*‡^a and Christopher R. Strauss*^{c,d}

Received 18th February 2008, Accepted 20th May 2008

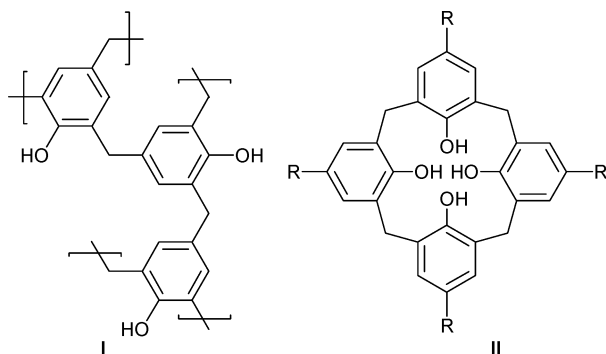
First published as an Advance Article on the web 20th June 2008

DOI: 10.1039/b802755b

Claisen–Schmidt condensations, yielding only water as a by-product, performed on building blocks serving as shape-selective male or female terminals and unions, enable the preparation of diverse molecular structures including novel linear rods and semi-elliptical, rectangular or trapezoidal macrocycles. Isoaromatization affords a corresponding range of phenol–formaldehyde derivatives, in atom economical reactions.

Introduction

Phenols and formaldehyde undergo coupling reactions to produce resins¹ **I** that have been used widely as bulk chemicals in the cookware, plywood, particleboard, abrasive papers and adhesives industries for a century. Calixarenes **II**, cyclic oligomeric by-products of phenol–formaldehyde reactions,² constitute a class of macrocycles on their own. They have applications as ligands,³ nanoparticle modifiers⁴ and supramolecular building blocks⁵ as well as in ion scavenging, chromatography,⁶ controlled release,⁷ enzyme mimicry⁸ and in the biomedical area.⁹



Perhaps owing to the traditional roots of phenol–formaldehyde chemistry, preparations have often depended upon empirical methods that provide limited scope for ready introduction of structural diversity. Although random coupling of the aldehyde through the aryl 2, 4 and 6-positions confers strength and rigidity to phenol–formaldehyde resins, it precludes the practical preparation of parent calixarenes from phenol directly. Instead, 4-substituted phenols, usually *p*-*t*-butylphenol, are employed to generate macrocyclic ring scaffolds. Parent calixarenes comprising repeating phenolic and methylene units are obtained by dealkylation at all *para*-positions (a step often employing the undesirable reagent AlCl₃). In the parent macrocycles, chemo and regioselective derivatization of specific phenolic rings, among other identical moieties located within the same molecule, is not trivial. It can be difficult to control and has the potential to afford complex mixtures requiring tedious and often wasteful separation and purification of the individual components.

Consequently, we decided to pursue the synthesis of an alternative array of somewhat related, novel molecules that could be more readily accessed and manipulated synthetically. The platform consisted of structurally diverse open-chain oligomers and macrocycles that we hoped would perhaps supplement, or in some cases even replace, those available through traditional phenol–formaldehyde chemistry. Starting materials were chosen from readily available and, where possible, renewably sourced chemicals. Direct pathways were employed to obviate the need for protection/deprotection or activation strategies. Also, priority was given to the control of spatial aspects and conformation of the target molecules.

Herein, we present this alternative, green platform technology that does not require phenol or formaldehyde as starting materials.^{10–14} The platform is based upon the connection of simple building blocks by Claisen–Schmidt condensations to generate dienone architectures.^{10,11,14} Subsequent isoaromatization affords phenolic derivatives.^{12,13} Claisen–Schmidt condensation and isoaromatization proceed catalytically and in high atom economy^{11,12} and the condensations also afford good chemo, regio and stereoselectivity to generate *trans*-selective olefinic bonds, with water as the major by-product.¹⁵

^aARC Special Research Centre for Green Chemistry, Monash University, Wellington Rd, Clayton, Victoria, 3800, Australia.

E-mail: janet.l.scott@sci.monash.edu.au

^bDepartment of Chemistry, Illinois Wesleyan University, Bloomington, IL, 61701, USA

^cQUILL Centre, The Queen's University of Belfast, Belfast, Northern Ireland BT9 5AG. E-mail: chris.strauss@qub.ac.uk

^dStrauss Consulting Ltd, Box 1065 Kunyung LPO, Mt Eliza, Victoria, 3930, Australia

† CCDC reference numbers 629937, 630660, 630661 and 630662. For crystallographic data in CIF or other electronic format see DOI: 10.1039/b802755b

‡ Current address: Unilever Home and Personal Care Research & Development, Quarry Road East, Bebington, Wirral, UK, CH63 3JW. Fax: +44 (0)151 641 1852; Tel: +44 (0)151 641 3726; E-mail: janet.l.scott@unilever.com

Results and discussion

The concept of a modular, “building block” approach to constructing complex molecules led us to define different sized and shaped “unions” and “terminals”, which were expected to be simple to access by the reactions mentioned above. These reactions and either commercially available, or simply synthesised, components provided access to a vast range of complex molecules with interesting architectures and a high degree of control over spatial aspects.

Building blocks, serving as terminals or as rigid or flexible unions, contained activated, nucleophilic methylene groups (herein termed *male*), or electrophilic, non-enolizable aldehydic functionalities (*female*). Terminals had only one aldehydic or activated methylene group (Fig. 1). Female–female and male–male unions had two aldehydic and two methylene groups, respectively (Figs. 1 and 2). Polyaryl rings (e.g. in **10**) and heteroatoms (e.g. in **15**, **17** and **26**) could be incorporated into all types of building blocks. Female–female flexible unions (e.g. **35**–**39**, Scheme 1) were formed from two phenolic aldehydes etherally linked to both ends of a flexible chain. A synthetic route utilising DIMCARB, a “distillable”, largely ionic reaction medium, which may serve as both solvent and catalyst, was established for male terminals such as **3**–**10**.¹⁰ This method provided a direct, green and convenient route to 2-arylidene-cycloalkanones that are otherwise difficult to prepare using traditional Claisen–Schmidt condensation conditions.^{10,15,16} We now report that in DIMCARB, compounds with two aldehydic groups on one or two aryl rings, afforded diketones as rigid (e.g. **29** and **30**, Fig. 1) or flexible (e.g. **40**–**42**, Scheme 1) male–male unions. Herein, female terminals (e.g. **16**–**20**) and rigid female–female unions (e.g. **34**) have been selectively produced in 80–98% yields and with high atom economies by employing (*n*Bu)₄NOH as base and by exploiting the low solubility of the products in aqueous EtOH at room temperature.

Dienone rods and macrocycles were prepared by combinations of tandem and cascade processes according to an established hierarchical order of reactivities and events.^{11,13} The geometry of connections was predetermined by the relative positions of aryl substituents. *meta*-Aryldialdehydes (rigid female–female unions, e.g. **31**–**34**) and salicylyl-linked dialdehydes (flexible female–female unions, e.g. **35**–**39**) afforded approximately linear and perpendicular connections, respectively, after condensation.

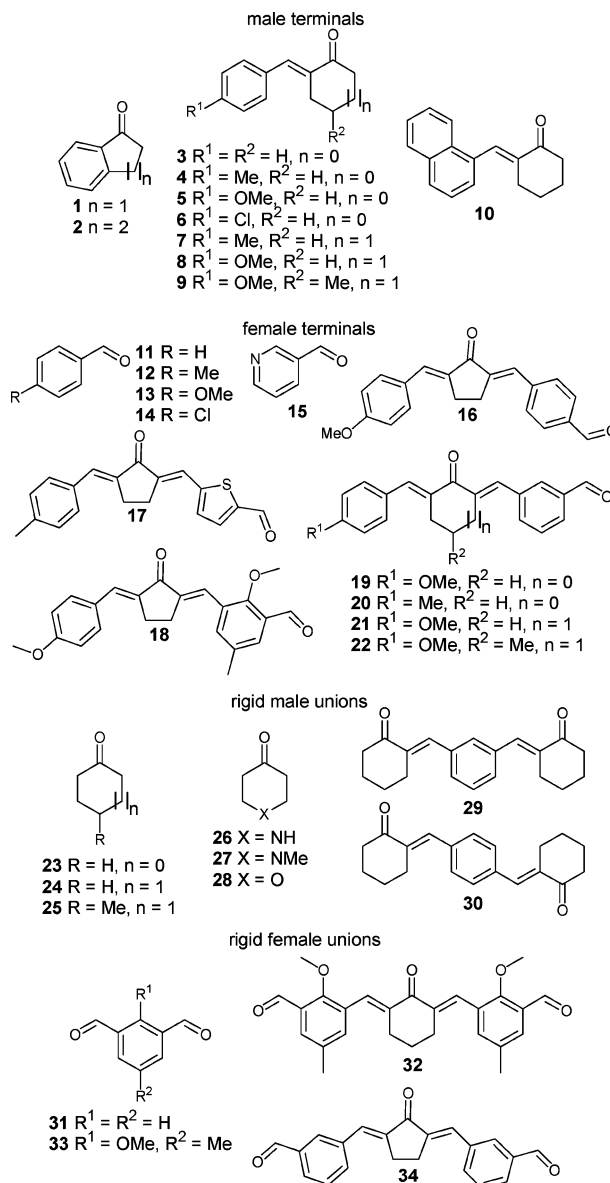


Fig. 1 Examples of male and female building blocks.

With cyclohexanone derivatives, if the flexible female–female unions had chains containing <7 atoms joined by single bonds

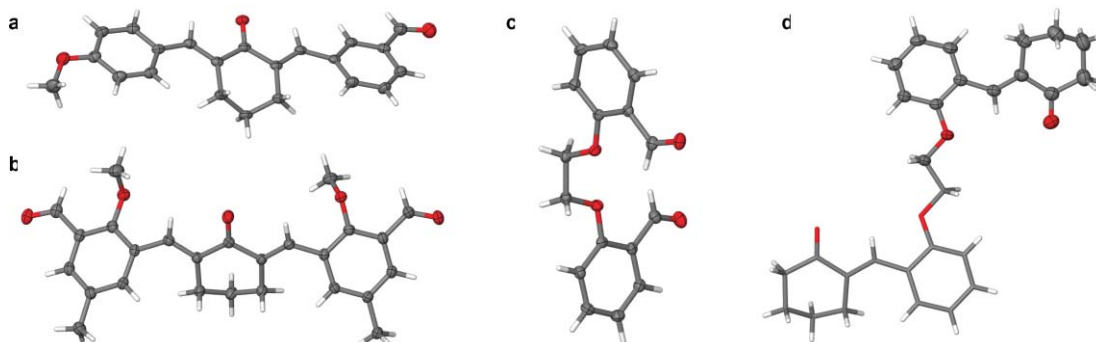
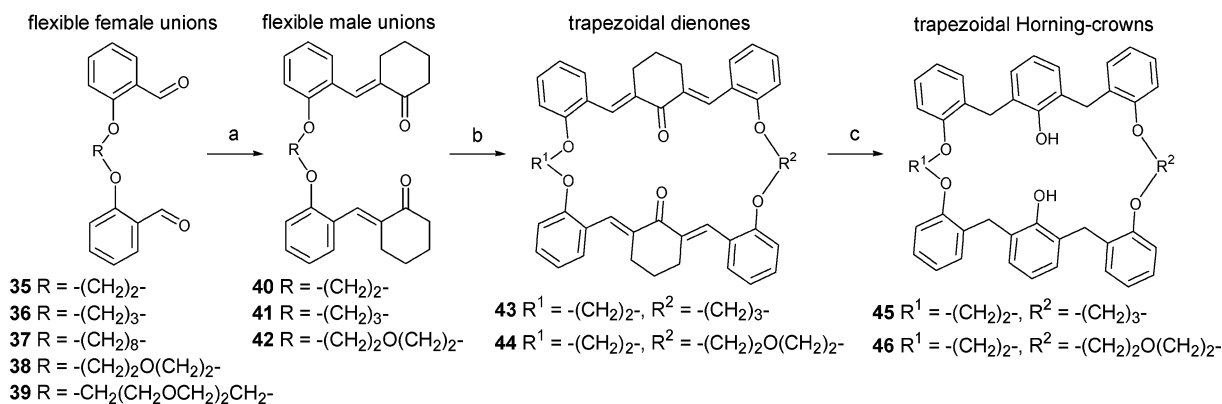


Fig. 2 Molecular diagrams of building blocks, derived from single crystal structures, with anisotropic atoms presented as ellipsoids at the 50% probability level and hydrogen atoms (or symmetry generated atoms) indicated in stick mode: (a) female terminal **21**; (b) rigid female union **32**; (c) flexible female union **35** (previously reported in ref 11); (d) flexible male union **40**.



Scheme 1 Syntheses of trapezoidal dienone and Horning-crown macrocycles: (a) 2 equiv. **24**, 15–25 equiv. DIMCARB, RT, 3–6 d, 47–66%; (b) 1 equiv. **35**, **36** or **38**, 15 equiv. NaOH, 96% EtOH, 25–50 °C, 1–4 d, 40–47%; (c) 0.7–1.0 equiv. Pd/C, N₂, *p*-xylene, reflux, 10–16 h, 20–26% (b and c).

(e.g. **35**, **36**, and **38**), ring closure with rigid male–male unions afforded macrocycles derived from two female–female and two male–male unions (e.g. **49** and **50**, Fig. 3).¹¹

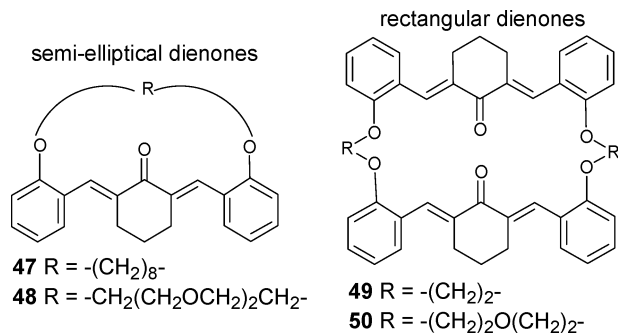


Fig. 3 Examples of dienone macrocycles.¹¹

For organic molecules, available bond angles tend to be restricted to approximately 109, 120 and 180°. Scope for square and rectangular shapes is limited. Even though a 90° angle can be obtained relatively readily through the use of metals

in organometallic systems,¹⁷ efficient formation of rectangular molecules still is challenging. Here, the original salicylyl moiety approached a 90° corner piece (but with the vertex not located at the centre of the aryl ring) and macrocycles obtained from two identical female–female and two identical male–male unions could be depicted two-dimensionally as rectangular, with the conjugated moieties making up one pair of parallel sides and the flexible chains, the other pair.¹¹

As the use of DIMCARB gives access to flexible male–male unions (e.g. **40–42**), the preparation of less symmetrical trapezoidally-shaped examples of these dienone macrocycles (e.g. **43** and **44**) is facilitated. Macrocycles produced from one flexible male–male and one flexible female–female union, having chains of differing lengths, appeared from above as trapezoidal (Scheme 1 and Fig. 4). In profile, many dienone macrocycles showed folding (e.g. Fig. 4b). Some symmetrical macrocycles had clefts, which allowed molecular stacking, as well as cavities that could be aligned.¹¹

We recently reported a direct, efficient synthesis of unsymmetrically substituted, short rod-like bis(arylidene)-alkanones.¹⁴ Here, rigid building blocks comprising female and male

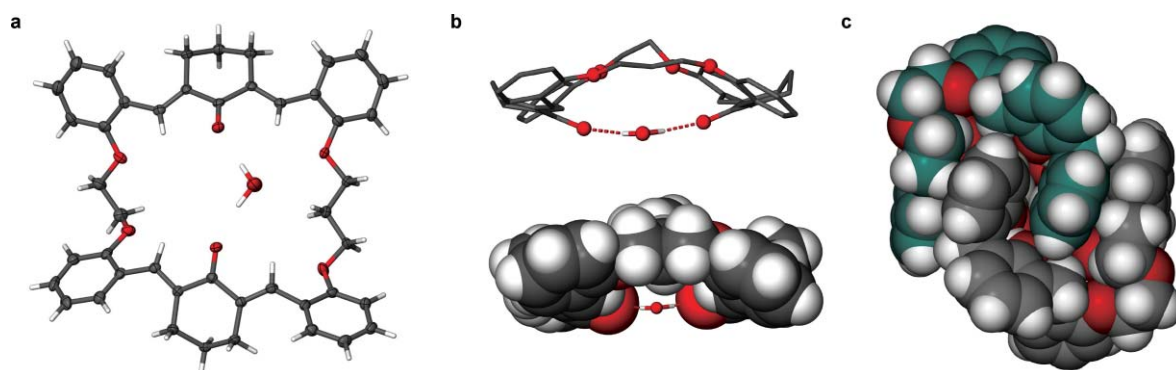


Fig. 4 Molecular diagrams of macrocycles derived from single crystal structures: (a) trapezoidal dienone macrocycle **43** (anisotropic atoms are presented as ellipsoids at the 50% probability level and hydrogen atoms indicated in stick mode). The macrocycle crystallized as a solvate hydrate with $\frac{1}{2}$ a CHCl₃ molecule (omitted for clarity) and one water molecule per **43**; (b) side view of **43** showing the folded shape of the macrocycle, stabilized by hydrogen bonding. Top: stick mode with hydrogen atoms, except those involved in H-bonding, excluded. Bottom: macrocycle shown in space-fill mode; (c) trapezoidal Horning-crown macrocycle **46** crystallized from CHCl₃ as nano-sized dimers (as a CHCl₃ solvate). Two molecules of **46** (presented in space-fill mode with carbon atoms of separate molecules colored cyan and grey) with similar but not identical conformation comprise the asymmetric unit along with two highly-disordered CHCl₃ molecules (omitted for clarity).

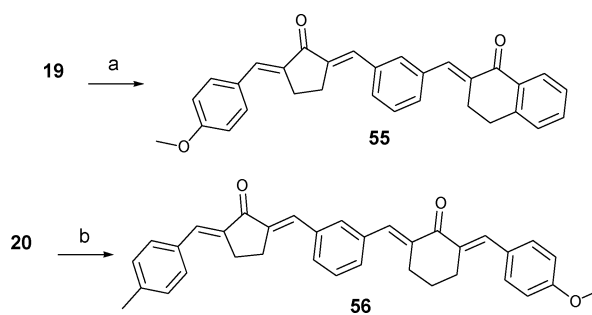
terminals and unions have been used to construct longer zig-zag rods.¹⁸ Rods are characterized by *trans* methine-interrupted alternating cyclic keto and cycloaryl moieties, any or all of which could incorporate heteroatoms. “Symmetrical” rod **51** (*i.e.* with the same moieties either side of the central Ar ring) was prepared by Claisen–Schmidt condensation of male terminal **8** with dialdehyde **31** (Scheme 2). “Unsymmetrical” rods (*e.g.* **52**, **55** and **56**) could be assembled from female terminals such as **16–22** and male terminals such as **1–10**. Hence, rods in which each ring system is unique, may be prepared, if desired (Scheme 3). The extent of curvature (*e.g.* as with **55** and **56**) could be altered through the use of rigid elbows (beyond the scope of the present report) or five-membered ring compounds (*e.g.* **1**, **16–20**, and **34**) as well as by the relative positions of aryl substituents. Such compounds have potential applications as spacers and in optical and electronic devices.

An attractive feature of dienone rods and macrocycles is their potential for facile transformation into new compounds that may have vastly different properties. The “parent” 2,6-dibenzylidencyclohexanone can undergo selective reduction,¹⁹ isomerization,²⁰ photoisomerization,^{20,21} Wittig olefination,²² oximation,²³ epoxidation,²⁴ dimerization²⁵ and Michael addition.²⁶ Of particular importance to the development of this phenol–formaldehyde platform technology is the Pd-catalyzed isoaromatization of 2,6-dibenzylidencyclohexanone to 2,6-dibenzylphenol, reported by Horning about 60 years ago.²⁷

Isoaromatization of dienone macrocycles afforded Horning-crowns,¹² the conformations of which sometimes were solvent-dependent and switchable.²⁸ Self-complementarity was observed, as was a range of inclusion compounds or solvates.^{12,28} These properties suggest potential applications in analysis, separation and detection.

The synthetic scope has been broadened here to include products with fewer axes of symmetry and differently configured cavities. Horning-crown macrocycles **45** and **46** were produced by isoaromatization of trapezoidal dienones **43** and **44**, respectively (Scheme 1). In the solid state and in solution, **45** was monomeric. Macrocycle **46**, however, crystallized as a dimer from CHCl₃ (Fig. 4c). These interesting aspects will be discussed elsewhere along with the host:guest chemistry of some of these compounds.

Recently, we disclosed lithium, sodium, potassium, strontium and barium phenolates and lanthanoid aryloxides of 2,6-dibenzylphenols, obtained using Horning’s approach.^{13,29,30} From the present report it can be seen that longer rods, containing more than one 2,6-bis(arylidene)cyclohexanone



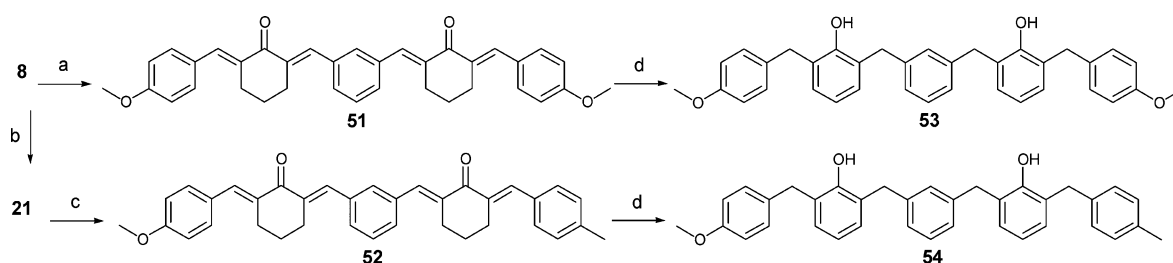
Scheme 3 Dienone rods with 4 to 5 different rings: (a) 1 equiv. **2**, 0.5 equiv. *p*-TsOH, toluene, reflux (Dean–Stark), 24 h, 74%; (b) 1 equiv. **8**, 1 equiv. KOH, CH₂Cl₂/96% EtOH, RT, 24 h, 56% yield.

motif, can also be isoaromatized, *e.g.* dienones **51** and **52**, to give phenols **53** and **54**, respectively (Scheme 2). This range of oligomeric phenols has potential in diverse applications in areas such as antioxidants, antimicrobials, metal scavenging, crystal engineering and copolymerization.

Conclusions

The main purpose of this paper is to outline a strategy toward the development of an array of potentially useful families of compounds, some of which include phenol–formaldehyde products, and that can be obtained simply, by employing the principles of green chemistry. Accordingly, green aspects have been discussed in a broad context and not all the syntheses reported herein have been optimised. Such examples have been presented primarily to demonstrate the scope and versatility of the methodology and, significantly, yields presented for several compounds were nearly quantitative.

To summarise some of the main points: atom economy is excellent where yields have been optimised; the co-product, water, is innocuous and does not hinder purification or recycling of the solvent (ethanol); and (once conversion of raw materials to products is maximised and by-products minimised) no further waste arises as is illustrated in a range of examples. This direct approach avoids the use of protection/deprotection or “derivatisation for activation” strategies and is highly flexible. In previous papers, we have compared various parts of the approach espoused here with alternative synthetic routes and have discussed sources of raw materials.^{10–12,14} While it would be most desirable if the raw materials were all derived from renewable resources, this is not yet possible, although many are produced in large volumes in optimised processes.



Scheme 2 Syntheses of dienone rods and their corresponding phenols: (a) 0.5 equiv. **31**, 1 equiv. NaOH, aq. EtOH, RT, 6 h, 96%; (b) 5 equiv. **31**, 0.4 equiv. (*n*Bu)₄NOH, 96% EtOH, RT, 77%; (c) 1 equiv. **7**, 0.4 equiv. (*n*Bu)₄NOH, 96% EtOH, RT, 27 h, 63%; (d) 0.1 equiv. Pd/C, N₂, 180–190 °C, 1–2 h, 70–80%.

The platform, which could be considered as open-ended in its scope, incorporates engineered macromolecules for applications including (but not limited to) synthetic building blocks, intermediates, linkers in polymer and peptide chemistry, chelating agents, ion or radical scavengers, ion-exchangers, spacers, molecular wires and switches for incorporation into devices and polymeric materials.

Experimental

All solvents, reagents and starting materials were of purity >98% and were used as purchased from the supplier. The syntheses of 2-arylidene-cycloalkanones **3**, **5**, **6**, **8–10**,¹⁰ and dienone macrocycles **47–50**¹¹ have been reported previously. Dialdehydes **33**³¹ and **35–39**^{32,33} were prepared according to methods previously reported in the literature.

Thin layer chromatography (TLC) was performed on silica gel 60 F-254 plates, which were visualized using UV light (254 nm) or reactive sprays/dips *p*-anisaldehyde and/or 2,4-DNP, as required.

The stationary phase for gravity and flash column chromatography was silica gel 60, 0.040–0.063 mm (230–400 mesh). Flash column chromatography was carried out using a Büchi C-601 dual pump system controlled by a Büchi C-615 pump manager at a flow rate of 13 mL min⁻¹ and a maximum pressure of 2.0 MPa. Eluent compositions are reported below.

Melting points were recorded on a Büchi Melting Point B-545 or a Stuart Scientific SMP3 apparatus and C, H, N analysis was carried out by the Campbell Microanalysis Laboratory, Department of Chemistry, University of Otago, Dunedin, New Zealand.

Infrared spectra of neat samples were obtained using a Bruker Equinox 55 fitted with a Specac Diamond ATR and MCT detector or, alternatively, as KBr pellets or nujol mulls using a Perkin–Elmer 1600 Series FT-IR spectrophotometer.

UV-visible spectra were recorded using a Varian CARY 100 Bio UV-Vis spectrophotometer in the solvent indicated.

¹H Nuclear magnetic resonance spectra were recorded on Bruker AV-200, DXP-300 or DRX-400 spectrometers at 200, 300 or 400 MHz, respectively, and ¹³C NMR spectra at 50, 75 or 100 MHz, respectively. Samples were dissolved in CDCl₃ (unless otherwise stated) and spectra measured at 30 °C, referenced to TMS (δ 0.00 ppm for ¹H spectra) or CDCl₃ (δ 77.23 ppm for ¹³C spectra). *J* values are given in Hz.

High resolution mass spectra were recorded on a Bruker BioApex 47e (4.7 Tesla magnet) spectrometer, fitted with an HP electrospray source and calibrated using NaI. Electro-spray ionisation mass spectra (ESI-MS) were recorded on a Micromass Platform II, with cone voltage 35, 40 or 50 V and a capillary voltage of 3.5 kV. Analyses were conducted in positive ESI mode.

Crystals suitable for single crystal X-ray diffraction experiments were grown by slow evaporation of solutions in suitable solvents. Data were collected on an Enraf-Nonius Kappa CCD or a Bruker Kappa Apex CCD diffractometer at 123K using graphite monochromated Mo-K α radiation (λ = 0.71073 Å, and ω scans in 1° or 0.5° steps as appropriate). Structures were solved by direct methods using the program SHELXS-97³⁴ and refined by full matrix least squares refinement on *F*² using the programs SHELXL-97³⁵ and X-Seed.³⁶ Non-hydrogen atoms were refined

anisotropically and hydrogen atoms (except those of the phenol OH groups) were inserted in geometrically determined positions with temperature factors fixed at 1.2 of the parent atom. Full details of insertion of OH hydrogen atoms and disorder models, where appropriate, are contained in the deposited cif files.

(*E*)-2-(4-Methylbenzylidene)cyclopentanone (4)

A mixture of 4-methylbenzaldehyde (**12**; 6.01 g, 50.0 mmol) and cyclopentanone (**23**; 6.31 g, 75.0 mmol) in DIMCARB (40 mL, 0.31 mol) was stirred at RT for 10 h. DIMCARB and other volatile components were then removed under reduced pressure at 60 °C to give an orange residue, which was dissolved in ether (100 mL) and stirred at RT with 1M HCl_(aq) (100 mL) for 1 h. The organic layer was separated and washed with satd. aq. NaCl (2 × 50 mL), dried with anhyd. MgSO₄, filtered and concentrated. The residue was recrystallized from ether by cooling the solution in a liquid N₂ bath to yield enone **4** (5.12 g, 55%) as a light brown solid, m.p. 60–61.5 °C (lit.,³⁷ 62–63 °C); δ_{H} (300 MHz; CDCl₃; TMS) 7.43 (2H, d, *J* 8.1, Ar), 7.37 (1H, t, *J* 2.8, CH), 7.21 (2H, d, *J* 8.1, Ar), 2.96 (2H, td, *J* 7.2 and 2.8, CH₂), 2.39 (2H, t, *J* 7.6, CH₂), 2.37 (3H, s, CH₃), 2.02 (2H, t, *J* 7.5, CH₂); δ_{C} (75 MHz; CDCl₃) 208.3, 139.9, 135.3, 132.9, 132.5, 130.7, 129.6, 38.0, 29.5, 21.6, 20.3.

(*E*)-2-(4-Methylbenzylidene)cyclohexanone (7)

(*E*)-2-(4-Methylbenzylidene)cyclohexanone (**7**) was prepared from cyclohexanone (**24**) and 4-methylbenzaldehyde (**12**) using a similar procedure to that used for enone **4**, and has the following physical data: m.p. 61–62 °C (lit.,³⁸ m.p. 61–62 °C); δ_{C} (100 MHz; CDCl₃) 201.9, 139.0, 136.0, 136.0, 133.0, 130.6, 130.6, 129.3, 129.3, 129.2, 40.4, 24.1, 23.5, 21.5; *m/z* (ESI) 201.1274 (M + H⁺. C₁₄H₁₇ O⁺ requires 201.1274).

(*E*)-2-(4-Methoxybenzylidene)-4-methylcyclohexanone (9)

A mixture of 4-methoxybenzaldehyde (**13**; 6.1 mL, 50 mmol) and 4-methylcyclohexanone (**25**; 6.4 mL, 50 mmol) in DIMCARB–ether (100 mL, 1 : 1 v/v) was heated at reflux with stirring for 106 h. DIMCARB and other volatile components were then removed under reduced pressure at 60 °C to give the enone **9** (10.1 g.) as a yellow solid. Recrystallization of the solid from hexane afforded enone **9** (4.86 g, 55%) as a yellow powder, m.p. 89–90 °C (lit.,³⁹ 91.5–93 °C); ν_{max} /cm⁻¹ (nujol) 1667 m, 1603 m, 1658 m, 1510 s, 1456 s, 1405 w, 1292 m, 1252 m, 1252 s, 1175 s, 1146 s, 1030 m, 940 w; δ_{H} (300 MHz; CDCl₃; TMS) 7.48 (1H, s, CH), 7.39 (2H, d, *J* 8.8, Ar), 6.92 (2H, d, *J* 8.8, Ar), 3.84 (3H, s, OCH₃), 3.07–3.01 (1H, m, CH₂), 2.67–2.60 (1H, m, CH₂), 2.48–2.29 (2H, m, CH₂), 1.99–1.82 (2H, m, CH and CH₂), 1.65–1.54 (1H, m, CH₂), 1.09 (3H, d, *J* 6.3, CH₃); δ_{C} (75 MHz; CDCl₃) 195.0, 160.0, 135.8, 132.2, 113.9, 55.3, 39.0, 37.3, 31.2, 30.2, 21.8; *m/z* (ESI) 231.2 (M + H⁺, 100%).

4-((*E*)-((*E*)-3-(4-methoxybenzylidene)-2-oxocyclopentylidene)methyl)benzaldehyde (16)

A mixture of terephthalaldehyde (0.166 g, 1.24 mmol) and 40% w/w aq. (*n*Bu)₄NOH (0.800 g, 1.23 mmol) in 96% EtOH (5 mL) was stirred at RT as an EtOH solution of enone **5** (0.250 g, 1.24 mmol, in 2.5 mL abs. EtOH) was added in

portions (0.250 mL every 5 min). After stirring at RT for 2 h, the precipitated solid was collected by vacuum filtration, washed with cold 96% EtOH (2 × 5 mL), and dried under vacuum to give aldehyde **16** (0.361 g, 91%) as a yellow solid, m.p. 193–194 °C; $\nu_{\max}/\text{cm}^{-1}$ (KBr) 2965 w, 2923 w, 2852 w, 1796 s, 1696 s, 1680 s, 1620 s, 1611 s, 1569 s, 1562 s, 1512 s, 1454 m, 1420 m, 1394 m, 1308 s, 1284 s, 1250 s, 1212 s, 1162 s, 1116 m, 1028 s, 986 m, 930 m; δ_{H} (400 MHz; CDCl₃; TMS) 10.05 (1H, s, CHO), 7.94 (2H, d, *J* 8.3, Ar), 7.74 (2H, d, *J* 8.3, Ar), 7.62–7.26 (4H, m, Ar and CH), 6.98 (2H, d, *J* 8.8, Ar), 3.87 (3H, s, OCH₃), 3.20–3.09 (4H, m, CH₂); δ_{C} (75 MHz; CDCl₃) 196.0, 191.7, 142.1, 140.9, 136.2, 135.0, 134.6, 133.0, 131.5, 131.1, 130.1, 128.7, 114.7, 55.6; 26.9; 26.6; *m/z* (ESI) 319.1 (M + H⁺, 100%), 341.1 (M + Na⁺, 63), 373.0 (M + Na⁺ + MeOH, 52).

5-((*E*)-((*E*)-3-(4-Methylbenzylidene)-2-oxocyclopentylidene)methyl)thiophene-2-carbaldehyde (**17**)

A mixture of thiophene-2,5-dicarbaldehyde (0.400 g, 2.85 mmol) and 40% w/w aq. (*n*Bu)₄NOH (1.85 g, 2.85 mmol) in 96% EtOH (7 mL) was stirred at RT as enone **4** (0.53 g, 2.85 mmol) was added in portions (53 mg) every 5 min. After stirring at RT for 3 h, the precipitated solid was collected by vacuum filtration, washed with cold 96% EtOH (2 mL), and dried under vacuum to give aldehyde **17** (0.710 g, 81%) as an orange solid, m.p. 225–228 °C; $\nu_{\max}/\text{cm}^{-1}$ (KBr) 3078 w, 3027 w, 2918 w, 2814 w, 1662 s, 1614 s, 1588 s, 1509 m, 1444 s, 1313 w, 1303 m, 1284 m, 1247 m, 1222 s, 1189 s, 1174 s, 1053 m, 975 m, 808 m; δ_{H} (300 MHz; CDCl₃; TMS) 9.96 (1H, s, CHO), 7.78 (1H, d, *J* 4.0, Ar), 7.76 (1H, t, *J* 2.9, CH), 7.60 (1H, t, *J* 2.6, CH), 7.52 (2H, d, *J* 8.2, Ar), 7.43 (1H, d, *J* 4.0, Ar), 7.27 (2H, d, *J* 7.9, Ar), 3.74–3.16 (2H, m, CH₂), 3.10–3.04 (2H, m, CH₂), 2.41 (3H, s, CH₃); δ_{C} (75 MHz; CDCl₃) 195.5, 183.1, 149.1, 146.1, 140.6, 140.5, 136.5, 136.4, 135.3, 133.0, 132.8, 131.3, 129.9, 125.0, 26.9, 26.5, 21.7; *m/z* (ESI) 309.1, (M + H⁺, 100%), 331.0 (M + Na⁺, 75).

3-((*E*)-((*E*)-3-(4-methoxybenzylidene)-2-oxocyclopentylidene)methyl)-5-methylbenzaldehyde (**18**)

A mixture of dialdehyde **33** (0.445 g, 2.50 mmol) and enone **5** (0.506 g, 2.50 mmol) in abs. EtOH (30 mL) was stirred at RT as 40% w/w aq. (*n*Bu)₄NOH (0.800 g, 1.23 mmol) was added in one portion. After stirring at RT for 3 h, the precipitated solid was collected by vacuum filtration, washed with cold 96% EtOH (2 × 5 mL), and dried under vacuum to give aldehyde **18** (0.779 g, 86%) as a yellow solid, m.p. 188–190 °C; found: C, 76.1; H, 6.1. C₂₃H₂₂O₄ requires C, 76.2; H, 6.1%; $\nu_{\max}/\text{cm}^{-1}$ (KBr) 2952 w, 2857 w, 1692 s, 1622 s, 1596 s, 1458 m, 1422 w, 1393 w, 1312 m, 1268 s, 1247 s, 1196 m, 1175 s, 1022 m, 986 m, 935 m, 828 m, 695 w; δ_{H} (300 MHz; CDCl₃; TMS) 10.41 (1H, s, CHO), 7.80 (1H, s, CH), 7.67 (1H, s, CH), 7.61 (2H, m, Ar), 7.58 (2H, d, *J* 8.8, Ar), 6.98 (2H, d, *J* 8.8, Ar), 3.89 (3H, s, OCH₃), 3.87 (3H, s, OCH₃), 3.09–3.01 (4H, m, CH₂), 2.41 (3H, s, ArCH₃), δ_{C} (75 MHz; CDCl₃) 196.0, 190.1, 161.5, 161.0, 140.0, 136.7, 134.9, 134.1, 132.9, 130.8, 129.6, 129.6, 129.6, 128.8, 126.2, 114.6, 65.1, 55.6, 26.8, 26.7, 21.2; *m/z* (ESI) 385.2 (M + Na⁺, 100%), 417.3 (M + Na⁺ + MeOH, 48), 363.3 (M + H⁺, 8).

3-((*E*)-((*E*)-3-(4-Methoxybenzylidene)-2-oxocyclopentylidene)methyl)benzaldehyde (**19**)

A mixture of isophthalaldehyde (**31**; 0.168 g, 1.25 mmol) and 40% w/w aq. (*n*Bu)₄NOH (0.800 g, 1.23 mmol) in 96% EtOH (5 mL) was stirred at RT as an EtOH solution of enone **5** (0.253 g, 1.25 mmol, in 2.5 mL abs. EtOH) was added in portions (0.25 mL every 5 min). After stirring at RT for 2 h, the precipitated solid was collected by vacuum filtration, washed with cold 96% EtOH (2 × 5 mL), and dried under vacuum to give aldehyde **19** (0.389 g, 98%) as a yellow solid, m.p. 190–192 °C; found: C, 79.2; H, 5.8. C₂₁H₁₈O₃ requires C, 79.2; H, 5.7%; $\nu_{\max}/\text{cm}^{-1}$ (KBr) 1688 m, 1620 s, 1588 s, 1511 m, 1422 w, 1254 s, 1170 s, 1032 w, 821 w; δ_{H} (300 MHz; CDCl₃; TMS) 10.07 (1H, s, CHO), 8.09 (1H, s, CH), 7.87 (1H, dt, *J* 7.6 and 1.4, Ar), 7.82 (1H, d, *J* 7.8, Ar), 7.63–7.53 (5H, m, Ar and CH), 6.98 (2H, d, *J* 8.9, Ar), 3.86 (3H, s, OCH₃), 3.20–3.07 (4H, m, CH₂); δ_{C} (75 MHz; CDCl₃) 196.1, 192.1, 161.1, 139.6, 137.2, 137.0, 136.0, 134.8, 134.7, 132.9, 131.5, 131.1, 130.2, 129.7, 128.7, 114.3, 55.6, 26.8, 26.6; *m/z* (ESI) 319.4 (M + H⁺, 100%).

3-((*E*)-((*E*)-3-(4-Methylbenzylidene)-2-oxocyclopentylidene)methyl)benzaldehyde (**20**)

A mixture of isophthalaldehyde (**31**; 0.288 g, 2.15 mmol) and 40% w/w aq. (*n*Bu)₄NOH (1.39 g, 2.15 mmol) in 96% EtOH (5 mL) was stirred at RT as enone **4** (0.400 g, 2.20 mmol) was added in portions (40 mg every 5 min). After stirring at RT for 2.5 h, the precipitated solid was collected by vacuum filtration, washed with cold 96% EtOH (2 × 5 mL), and dried under vacuum to give aldehyde **20** (0.611 g, 94%) as a yellow solid, m.p. 197–199 °C; $\nu_{\max}/\text{cm}^{-1}$ (KBr) 3027 w, 2920 w, 2832 w, 2799 w, 2731 w, 1698 s, 1082 s, 1628 s, 1596 s, 1511 m, 1427 w, 1385 w, 1286 m, 1266 s, 1196 m, 1181 s, 1170s; δ_{H} (300 MHz; CDCl₃; TMS) 10.09 (1H, s, CHO), 8.10 (1H, s, CH), 7.89 (1H, d, *J* 7.9, Ar), 7.84 (1H, d, *J* 7.9, Ar), 7.65–7.60 (3H, m, Ar and CH), 7.52 (2H, d, *J* 8.0, Ar), 7.27 (2H, d, *J* 8.0, Ar), 3.21–3.12 (4H, m, CH₂), 2.42 (3H, s, CH₃); δ_{C} (75 MHz; CDCl₃) 196.3, 192.0, 140.4, 139.5, 137.2, 137.1, 136.5, 136.5, 134.9, 133.2, 131.8, 131.2, 131.1, 130.3, 129.8, 129.7, 26.8, 26.7, 21.7; *m/z* (ESI) 325.1 (M + Na⁺, 100%), 357.2 (M + MeOH + Na⁺, 33).

3-((*E*)-((*E*)-3-(4-Methoxybenzylidene)-2-oxocyclohexylidene)methyl)benzaldehyde (**21**)

A mixture of isophthalaldehyde (**31**; 3.10 g, 23.1 mmol) and 40% w/w aq. (*n*Bu)₄NOH (1.19 g, 1.85 mmol) in 96% EtOH (35 mL) was stirred at RT as an EtOH solution of (*E*)-2-(4-methoxybenzylidene)cyclohexanone (**8**; 0.99 g, 4.6 mmol, in 4 mL 96% EtOH) was added in one portion. After stirring at RT for 10 h, the precipitated solid was filtered, washed with cold 96% EtOH (2 × 5 mL), and dried under vacuum to give aldehyde **21** (1.3 g, 77%) as a yellow solid, m.p. 116–118 °C; found: C, 79.2; H, 6.1. C₂₂H₂₀O₃ requires C, 79.5; H, 6.1%; λ_{\max} (EtOH)/nm 240 and 348 (ε/dm³ mol⁻¹ cm⁻¹ 20 300 and 23 200); $\nu_{\max}/\text{cm}^{-1}$ (KBr) 1687 m, 1657 m, 1598 s, 1560 s, 1508 s, 1459 s, 1316 w, 1296 m, 1276 m, 1253 s, 1206 w, 1180 w, 1158 s, 1141 s, 1062 w, 1028 m, 972 w; δ_{H} (300 MHz; CDCl₃; TMS) 10.05 (1H, s, CHO), 7.95 (1H, s, CH), 7.85 (1H, d, *J* 7.4, Ar), 7.80 (2H, t, *J* 2.0, CH),

7.69 (1H, d, *J* 7.9, Ar), 7.58 (1H, t, *J* 7.6, Ar), 7.47 (2H, d, *J* 8.9, Ar), 6.95 (2H, dd, *J* 6.8 and 2.1, Ar), 3.85 (3H, s, OCH₃), 2.97–2.91 (4H, m, CH₂), 1.82 (2H, p, *J* 6.2, CH₂); δ_{C} (100 MHz; CDCl₃) 192.1, 190.4, 190.1, 160.4, 138.1, 137.8, 137.4, 136.8, 136.3, 134.7, 134.0, 132.6, 131.1, 129.7, 129.4, 128.8, 114.2, 55.5, 28.7, 28.6, 23.1; *m/z* (ESI) 333.2 (M + H⁺, 100%); *m/z* (ESI) 355.1302 (M + Na⁺. C₂₂H₂₀NaO₃ requires 355.1310).

3-((*E*)-((*E*)-3-(4-Methoxybenzylidene)-5-methyl-2-oxocyclohexylidene)methyl)benzaldehyde (**22**)

A mixture of isophthalaldehyde (**31**; 0.76 g, 5.65 mmol) and 40% w/w aq. (*n*Bu)₄NOH (1.41 g, 2.18 mmol) in EtOH (30 mL) was stirred at RT as an EtOH solution of enone **9** (1.00 g, 4.34 mmol, in 25 mL EtOH) was added dropwise over 2 h. After stirring for a total of 2.5 h, the mixture was then concentrated to ca. 10 mL and cooled at 0 °C for 10 min. The precipitated solid was collected by vacuum filtration and washed with cold 96% EtOH (5 mL) to give a yellow solid (0.65 g). The filtrate was concentrated and the residue dissolved in CH₂Cl₂ (25 mL), washed with 0.5 M aq. H₂SO₄ (15 mL), satd. aq. NaHCO₃ (20 mL) and satd. aq. NaCl (20 mL), dried with anhyd. MgSO₄, and then concentrated to give viscous yellow oil (0.77 g). The yellow solid and viscous oil were combined and purified by flash chromatography on silica gel (CH₂Cl₂) to give aldehyde **22** (0.70 g, 47%) as a yellow solid, m.p. 134–135 °C; λ_{max} (EtOH)/nm 242 and 348 ($\epsilon/\text{dm}^3 \text{ mol}^{-1} \text{ cm}^{-1}$ 70 900 and 74 700); $\nu_{\text{max}}/\text{cm}^{-1}$ (KBr) 1694 m, 1662 w, 1602 s, 1563 m, 1510 s, 1420 w, 1379 w, 1313 w, 1297 w, 1255 s, 1202 w, 1177 s, 1145 s, 1027 m; δ_{H} (400 MHz; CDCl₃; TMS) 10.04 (1H, s, CHO), 7.92 (1H, br s), 7.85–7.82 (1H, m), 7.79–7.77 (2H, m), 7.68–7.66 (1H, m, Ar), 7.57 (1H, t, *J* 7.6, Ar), 7.47–7.43 (2H, m, Ar), 6.96–6.92 (2H, m, Ar), 3.84 (3H, s, OCH₃), 3.09–2.97 (2H, m, CH₂), 2.56–2.48 (2H, m, CH₂), 1.93–1.86 (1H, m, CH), 1.08 (3H, d, *J* 6.6, CH₃); δ_{C} (100 MHz; CDCl₃) 191.9, 189.5, 160.1, 137.7, 137.1, 136.9, 136.5, 135.9 ($\times 2$), 134.7 ($\times 2$), 132.9, 132.3, 130.9, 129.3, 129.1, 128.4, 55.3, 36.5, 36.2, 29.2, 21.5; *m/z* (ESI) 347.1646 (M + H⁺). C₂₃H₂₃O₃⁺ requires 347.1642.

(2*E*,2'*E*)-2,2'-(1,3-Phenylenebis(methan-1-yl-1-ylidene))dicyclohexanone (**29**)

A mixture of isophthalaldehyde (**31**; 1.00 g, 7.5 mmol), ZnCl₂ (1.02 g, 7.5 mmol) and cyclohexanone (**24**; 2.20 g, 22.4 mmol) in DIMCARB (10 mL, 78 mmol) was stirred at RT for 24 h. The DIMCARB and other volatile components were then removed under reduced pressure at 60 °C. The residue was dissolved in EtOAc (50 mL) and the solution was acidified with 2 M aq. HCl (50 mL) and stirred for 2 h. The organic layer was collected and washed with satd. aq. NaCl (40 mL), dried with anhyd. MgSO₄, filtered and then concentrated. Flash chromatography of the residue on silica gel (EtOAc : hexane = 10 : 90–20 : 80) afforded diketone **29** (0.542 g, 25%) as an off-white solid, m.p. 158–159 °C; found: C, 81.7; H, 7.6. C₂₀H₂₂O₂ requires: C, 81.6; H, 7.5%; $\nu_{\text{max}}/\text{cm}^{-1}$ (KBr) 2939 s, 2862 m, 1679 s, 1590 s, 1480 w, 1450 w, 1418 m, 1318 m, 1240 s, 1216 m, 1144 s, 1069 m, 970 w, 941 m; δ_{H} (300 MHz; CDCl₃; TMS) 7.48 (2H, t, *J* 2.1, CH), 7.43–7.39 (2H, m, Ar), 7.36–7.32 (2H, m, Ar), 2.83 (4H, td, *J* 6.4 and 2.1, CH₂), 2.55 (4H, t, *J* 6.6, CH₂), 1.98–1.90 (4H, m, CH₂), 1.82–1.74 (4H, m, CH₂); δ_{C} (75 MHz; CDCl₃) 201.8,

137.5, 136.0, 135.1, 132.1, 130.4, 128.6, 40.6, 29.2, 24.1, 23.6; *m/z* (ESI) 317.1 (M + Na⁺, 100%), 349.1 (M + MeOH + Na⁺, 71), 295.0 (M + H⁺, 5); *m/z* (EI) 294 (M⁺, 100%), 265 (55), 237 (34), 223 (114), 198 (46), 185 (58), 165 (17), 152 (16), 141 (14), 129 (17), 128 (17), 115 (13).

(2*E*,2'*E*)-2,2'-(1,4-Phenylenebis(methan-1-yl-1-ylidene))dicyclohexanone (**30**)

A mixture of terephthalaldehyde (1.00 g, 7.46 mmol) and cyclohexanone (**24**; 1.55 g, 15.8 mmol) in DIMCARB (10 mL, 78 mmol) was stirred at RT for 7 d. The DIMCARB was removed under reduced pressure at 60 °C to give an orange/brown residue. To this residue, water (10 mL) and 1.0 M aq. H₂SO₄ (4 mL) was added and then the suspension was extracted with CH₂Cl₂, dried with anhyd. MgSO₄, and concentrated to give diketone **30**⁴⁰ (1.915 g) as a sticky brown solid. Analysis of ¹H NMR spectra and GC-MS data indicated >90% purity: δ_{H} (300 MHz; CDCl₃; TMS) 7.64 (2H, t, *J* 2.2, CH), 7.41 (4H, m, Ar), 2.84 (4H, m, CH₂), 2.52 (4H, m, CH₂), 1.92 (4H, m, CH₂), 1.77 (4H, m, CH₂); δ_{C} (75 MHz; CDCl₃) 202.2, 137.6, 136.2, 135.1, 130.6, 39.9, 28.6, 23.4, 22.8; *m/z* (EI) 294 (M⁺, 100%), 265 (80), 237 (75), 207 (66), 185 (48), 165 (25), 152 (32), 141 (25), 129 (42), 128 (42), 115 (33), 91 (25).

3,3'-(1*E*,1'*E*)-(2-Oxocyclohexane-1,3-diylidene)bis(methan-1-yl-1-ylidene)bis(2-methoxy-5-methylbenzaldehyde) (**32**)

A mixture of dialdehyde **33** (0.915 g, 5.14 mmol) and 20% w/v aq. NaOH solution (2 mL, 10 mmol) in EtOH (10 mL) was stirred at RT as cyclohexanone (**24**; 0.25 g, 2.6 mmol) was added dropwise over 40 min. The solution was stirred overnight (approx. 15 h) and then neutralized with gaseous CO₂. The solution was extracted with CH₂Cl₂, the organic phase dried over anhyd. MgSO₄, and then concentrated to give a yellow solid (0.808 g). A portion of the solid (0.518 g) was stirred in refluxing EtOH for 5 min and then filtered in order to separate larger polymeric by-products. After cooling to RT, an initial orange precipitate (0.029 g), of which the heptamer (*n* = 2) was identified as a constituent (by MS: *m/z* (ESI) 899 (M + H⁺)), was filtered. The filtrate was concentrated to give an orange solid (0.29 g). A portion of this solid (0.24 g) was purified by flash column chromatography on silica-gel (EtOAc : CH₂Cl₂ = 1 : 99) to afford dienone **32** (0.098 g, 17%) as yellow crystals, suitable for single crystal X-ray diffractometry, m.p. 158–159.5 °C; δ_{H} (200 MHz; CDCl₃; TMS) 10.40 (2H, s, CHO), 7.91 (2H, s, CH), 7.65 (2H, d, *J* 2.2, Ar), 7.38 (2H, d, *J* 2.2, Ar), 3.85 (6H, s, CH₃), 2.81 (2H, m, CH₂), 2.38 (6H, s, CH₃), 1.79 (4H, m, CH₂); δ_{C} (125 MHz; CDCl₃) 189.9, 189.3, 137.9, 137.1, 133.7, 131.5, 130.2, 129.0, 64.2, 28.7, 23.0, 20.8; *m/z* 441 (M + Na⁺).

The flash column chromatographic separation also afforded a sample of pentamer (*n* = 1, 0.055 g, 6%) that has the following spectral data: δ_{H} (200 MHz; CDCl₃; TMS) 10.39 (2H, s, CHO), 7.93–7.88 (4H, s, CH), 7.62 (2H, d, *J* 2.2, Ar), 7.37 (2H, d, *J* 2.2, Ar), 7.14 (2H, s, Ar), 3.84 (6H, s, OCH₃), 3.70 (3H, s, OCH₃), 2.82 (8H, m, CH₂), 2.36 (9H, m, CH₃), 1.77 (4H, m, CH₂); δ_{C} (125 MHz; CDCl₃) 189.9, 189.6, 160.5, 156.6, 138.2, 137.2, 133.6, 132.9, 132.4, 131.5, 131.1, 130.3, 129.4, 129.0, 128.8, 64.1, 62.3, 28.7, 23.1, 21.0, 20.7; *m/z* (ESI) 659 (M + H⁺).

3,3'-(1*E*,1'*E*)-(2-Oxocyclopentane-1,3-diylidene)bis(methan-1-yl-1-ylidene)dibenzaldehyde (34)

A mixture of isophthalaldehyde (**31**; 1.00 g, 7.46 mmol) and 40% w/w aq. (*n*Bu)₄NOH (2.40 g, 3.70 mmol) in 96% EtOH (10 mL) was stirred at RT as an EtOH solution of cyclopentanone (**23**; 0.314 g, 3.73 mmol in 2 mL 96% EtOH) was added in portions (0.25 mL every 5 min). After stirring at RT for 3.5 h, the precipitated solid was collected by vacuum filtration, washed with cold 96% EtOH (2 × 5 mL), and dried under vacuum to give dialdehyde **34** (1.12 g, 95%) as a yellow solid, m.p. 184–186 °C; found: C, 79.7; H, 5.3. C₂₁H₁₆O₃ requires C, 79.7; H, 5.1%; ν_{max}/cm⁻¹ (KBr) 3036 w, 2919 w, 2828 w, 2791 w, 2728 w, 1706 s, 1676 s, 1628 s, 1586 s, 1484 w, 1429 m, 1396 m, 1363 w, 1304 m, 1287 s, 1265 s, 1211 s, 1173 s, 1154 s, 951 s, 906s; δ_H(300 MHz; CDCl₃; TMS) 10.09 (2H, s, CHO), 8.10 (2H, s, CH), 7.90 (2H, dt, *J* 7.6 and 1.3, Ar), 7.84 (2H, d, *J* 7.8, Ar), 7.66–7.60 (4H, m, Ar), 3.20 (4H, s, CH₂); δ_C(75 MHz; CDCl₃) 196.0, 191.9, 138.8, 137.1, 136.9, 136.6, 132.8, 131.2, 130.6, 129.8, 26.7; *m/z* (ESI) 317.1 (M + H⁺, 100%).

(2*E*,2'*E*)-2,2'-(2,2'-(Ethane-1,2-diylbis(oxy))bis(2,1-phenylene))bis(methan-1-yl-1-ylidene)dicyclohexanone (40)

A mixture of dialdehyde **35** (0.207 g, 0.770 mmol) and cyclohexanone (**24**; 0.151 g, 1.54 mmol) in DIMCARB (2.5 mL, 20 mmol) was stirred at RT for 6 d. The DIMCARB was removed under reduced pressure at 60 °C to give a brown residue that was partitioned between water (10 mL) and CH₂Cl₂ (10 mL). The organic phase was separated and extracted with water (2 × 10 mL), dried with anhyd. MgSO₄, and concentrated to give a brown residue (0.385 g). A sample (0.217 g) of the residue was purified by recrystallization from CH₂Cl₂–hexane to give diketone **40** (0.092 g, 47%) as a yellow solid, m.p. 134.5–136 °C; found: C, 78.0; H, 7.1. C₂₈H₃₀O₄ requires C, 78.1; H, 7.0%; δ_H(300 MHz; CDCl₃; TMS) 7.60 (2H, m, CH), 7.33–7.21 (4H, m, Ar), 7.00–6.92 (4H, m, Ar), 4.36 (4H, s, OCH₂), 2.72 (4H, dt, *J* 6.6 and 2.1, CH₂), 2.51 (4H, t, *J* 6.6, CH₂), 1.89 (4H, m, CH₂), 1.71 (4H, m, CH₂); δ_C(75 MHz; CDCl₃) 201.9, 157.3, 137.1, 131.0, 130.4, 130.1, 125.0, 120.5, 112.3, 67.2, 40.5, 29.2, 24.0, 23.7; *m/z* (ESI) 883.4 (2M + Na⁺, 100%), 431.2 (M + H⁺, 72), 453.2 (M + Na⁺, 51).

(2*E*,2'*E*)-2,2'-(2,2'-(Propane-1,3-diylbis(oxy))bis(2,1-phenylene))bis(methan-1-yl-1-ylidene)dicyclohexanone (41)

A mixture of dialdehyde **36** (1.192 g, 4.178 mmol) and cyclohexanone (**24**; 0.883 g, 9.10 mmol) in DIMCARB (10 mL, 20 mmol) was stirred at RT for 3 d. The mixture was then heated at 40 °C for 3 h, after which the DIMCARB was removed under reduced pressure at 60 °C to give a brown residue that was partitioned between 0.2 M aq. H₂SO₄ (30 mL) and CH₂Cl₂ (30 mL). The organic phase was separated and extracted with water (2 × 10 mL), dried with anhyd. MgSO₄, and concentrated to give a brown residue (1.61 g). The residue was purified by recrystallization from CH₂Cl₂–heptane to give diketone **41** (1.11 g, 60%) as a yellow solid, m.p. 109–110 °C; found: C, 78.3; H, 7.4. C₂₉H₃₂O₄ requires C, 78.4; H, 7.3%; δ_H(300 MHz; CDCl₃; TMS) 7.63 (2H, m, CH), 7.32–7.18 (4H, m, Ar), 7.00–6.80 (4H, m, Ar), 4.16 (4H, t, *J* 6.0, OCH₂), 2.69 (4H, dt, *J* 4.9 and 1.8,

CH₂), 2.48 (4H, t, *J* 6.6, CH₂), 2.25 (2H, t, *J* 4.9, CH₂), 1.87 (4H, m, CH₂), 1.67 (4H, m, CH₂); δ_C(75 MHz; CDCl₃) 201.8, 157.6, 136.8, 131.0, 130.3, 130.1, 124.8, 120.0, 111.8, 64.7, 40.5, 29.2, 29.1, 24.0, 23.6; *m/z* (ESI) 467.4 (M + Na⁺, 100%), 445.4 (M + H⁺, 8), 911.8 (2M + Na⁺, 4).

(2*E*,2'*E*)-2,2'-(2,2'-(2,2'-Oxybis(ethane-2,1-diyl)bis(oxy))bis(2,1-phenylene))bis(methan-1-yl-1-ylidene)dicyclohexanone (42)

A mixture of dialdehyde **38** (1.24 g, 4.94 mmol) and cyclohexanone (**24**; 0.796 g, 8.12 mmol) in DIMCARB (10 mL, 20 mmol) was stirred at RT for 3 d. Then the mixture was heated at 40 °C for 3 h, after which the DIMCARB was removed under reduced pressure at 60 °C to give a brown residue that was partitioned between 0.2 M aq. H₂SO₄ (30 mL) and CH₂Cl₂ (20 mL). The organic phase was separated and extracted with water (2 × 10 mL), dried with anhyd. MgSO₄, and concentrated to give a brown residue (1.83 g). The residue was purified by recrystallization from CH₂Cl₂–heptane to give diketone **42** (1.02 g, 66%) as a yellow solid, m.p. 110–111 °C; found: C, 75.8; H, 7.2. C₃₀H₃₄O₅ requires C, 75.9; H, 7.2%; δ_H(300 MHz; CDCl₃; TMS) 7.65 (2H, m, CH), 7.31–7.20 (4H, m, Ar), 6.97–6.84 (4H, m, Ar), 4.16 (4H, t, *J* 5.1, OCH₂), 3.91 (4H, t, *J* 5.1, OCH₂), 2.73 (4H, dt, *J* 6.6 and 2.3, CH₂), 2.49 (4H, t, *J* 6.6, CH₂), 1.89 (4H, m, CH₂), 1.70 (4H, m, CH₂); δ_C(75 MHz; CDCl₃) 201.8, 157.7, 136.8, 131.1, 130.3, 130.0, 125.1, 120.2, 112.3, 70.0, 68.4, 40.5, 29.2, 24.0, 23.7; *m/z* (ESI) 497.4 (M + Na⁺, 100%), 475.5 (M + H⁺, 8), 971.6 (2M + Na⁺, 4).

(1*E*,11*E*,16*E*,27*E*)-3,4:9,10:18,19:25,26-Tetrabenzo-5,8,20,24-tetraoxa-tricyclo[26.3.1.1^{12,16}]tritiaconta-1,3,9,11,16,18,25,27-octaene-32,33-dione (43)

A suspension of dialdehyde **35** (0.650 g, 2.40 mmol) and diketone **41** (1.034 g, 2.33 mmol) in 96% EtOH (0.47 L) was stirred at RT as 20% w/v aq. NaOH (5.7 mL, 28.5 mmol) was added in one portion. After stirring at RT for 16 h, the precipitated solid was collected by vacuum filtration and washed with 1.0 M aq. HCl (2 × 5 mL), water (3 × 10 mL) and 96% EtOH (2 × 10 mL), and then dried under vacuum to constant weight (1.30 g). The solid was recrystallized from CH₂Cl₂ (25 mL) to give dienone **43** (0.630 g, 0.927 mmol, 40%) as a yellow solid, which was pure by NMR spectroscopy; m.p. 269–270 °C; δ_H(300 MHz; CDCl₃; TMS) 8.00 (2H, s, CH), 7.93 (2H, br s, CH), 7.39–7.26 (8H, m, Ar), 7.02–6.89 (8H, m, Ar), 4.46 (4H, s, OCH₂), 4.18 (4H, t, *J* 7.0, OCH₂), 2.85 (8H, m, CH₂), 2.39 (2H, p, *J* 7.0, OCH₂CH₂CH₂O), 1.78 (4H, m, CH₂); δ_C(100 MHz; CDCl₃) 190.7, 157.8, 157.7, 137.2, 137.1, 132.8, 132.4, 131.1, 130.8, 129.9, 129.9, 126.2, 120.9, 120.4, 113.0, 112.2, 68.3, 65.5, 29.4, 29.4, 29.2, 24.0; *m/z* (ESI) 679.4 (M + H⁺, 100%); *m/z* (ESI) 679.3045 (M + H⁺, 100%). C₄₄H₄₃O₆⁺ requires 679.3054).

(1*E*,11*E*,16*E*,29*E*)-3,4:9,10:18,19:27,28-Tetrabenzo-5,8,20,23,26-pentaoxa-tricyclo[28.3.1.1^{12,16}]pentatriaconta-1,3,9,11,16,18,27,29-octaene-34,35-dione (44)

A mixture of dialdehyde **38** (0.314 g, 0.999 mmol) and diketone **40** (0.445 g, 1.03 mmol) in 96% EtOH (75 mL) was stirred at 50 °C as 20% w/v aq. NaOH (3.0 mL, 15 mmol) was added

in one portion. After stirring at 50 °C for 4 d, the precipitated solid was collected by vacuum filtration and washed with water (3 × 5 mL) and 96% EtOH (3 × 5 mL), and then dried under vacuum to constant weight (0.550 g). Recrystallization of the solid from CH₂Cl₂ (15 mL) yielded dienone **44** (0.330 g, 0.46 mmol, 47%) as bright yellow crystals, m.p. 208–210 °C; δ_{H} (300 MHz; CDCl₃; TMS) 7.96 (2H, s, CH), 7.93 (2H, s, CH), 7.33–7.24 (8H, m, Ar), 7.01–6.89 (8H, m, Ar), 4.44 (4H, s, OCH₂), 4.17 (4H, m, OCH₂), 3.99 (4H, m, OCH₂), 2.79 (8H, m, CH₂), 1.72 (4H, m, CH₂); δ_{C} (75 MHz; CDCl₃) 190.4, 157.8, 157.5, 137.3, 137.1, 132.7, 132.4, 131.1, 130.7, 129.9, 126.5, 126.2, 120.9, 120.5, 113.0, 112.8, 70.5, 68.8, 67.8, 29.3, 29.2, 23.7; m/z (ESI) 731.2 (M + Na⁺, 100%), 709.3 (M + H⁺, 23); m/z (ESI) 709.3146 (M + H⁺, 100%. C₄₆H₄₅O₇⁺ requires 709.3160), 731.3 (M + Na⁺, 20).

3,4,9,10,18,19,25,26-Tetrabenzo-5,8,20,24-tetraoxatricyclo[26.3.1.1^{12,16}]trtriaconta-1(31),3,9,12,14,16(33),18,25,28(32),29-decaene-32,33-diol (45)

A mixture of unpurified dienone **43** (0.80 g) and 10% Pd/C (0.30 g, 0.28 mmol Pd) in *p*-xylene (20 mL) was heated to reflux under N₂ for 10 h. The catalyst was removed by filtration, and the *p*-xylene removed under vacuum to give a light yellow residue. The residue was recrystallized from acetone to give phenol **45** (0.23 g, 20%) as a white solid, m.p. 206–207 °C; found: C, 79.7; H, 6.1. C₄₅H₄₂O₆ requires C, 79.6; H, 6.2%. $\nu_{\text{max}}/\text{cm}^{-1}$ (neat) 3341b, 3068 w, 3025 w, 2936 w, 2878 w, 1589 w, 1491, 1467, 1449 s, 1393 w, 1352 w, 1292 w, 1268 w, 1229 s, 1162 w, 1106, 1046, 1000 w, 980 w, 933 w, 743s; δ_{H} (400 MHz; CDCl₃; TMS) 7.17–7.08 (8H, m, Ar), 7.06 (2H, s, OH), 6.91–6.81 (12H, m, Ar), 6.76 (2H, m, Ar), 6.65 (2H, t, *J* 7.4, Ar), 4.28 (4H, s, OCH₂), 3.98 (4H, t, *J* 6.5, OCH₂), 3.91 (4H, s, ArCH₂), 3.78 (4H, s, ArCH₂), 2.14 (2H, p, *J* 6.5, CH₂CH₂CH₂); δ_{C} (75 MHz; CDCl₃) 155.9, 155.7, 152.3, 131.0, 130.9, 130.0, 129.9, 129.1, 128.4, 128.3, 127.5, 127.5, 127.4, 121.7, 121.3, 119.9, 112.0, 111.8, 66.9, 65.1, 30.9, 30.2, 29.0; m/z (ESI) 701.4 (M + Na⁺, 19%).

3,4,9,10,18,19,27,28-Tetrabenzo-5,8,20,23,26-pentaoxatricyclo[28.3.1.1^{12,16}]pentatriaconta-1(34),3,9,12,14,16(35),18,27,30,32-decaene-34,35-diol (46)

A mixture of unpurified dienone **44** (0.30 g) and 10% Pd/C (0.10 g, 0.094 mmol Pd) in *p*-xylene (20 mL) was heated at reflux under N₂ for 16 h. The catalyst was removed by filtration and the *p*-xylene removed under vacuum to give a light yellow residue. The residue was recrystallized from acetone to give phenol **46** (0.125 g, 26%) as a white solid, m.p. 168–168.5 °C; found: C, 77.9; H 6.0. C₄₆H₄₄O₇ requires C, 77.9; H, 6.3%; $\nu_{\text{max}}/\text{cm}^{-1}$ (neat) 3529 w, 3373b, 3062 w, 3022 w, 2923 w, 2868 w, 1589 w, 1491, 1446 s, 1291, 1228 s, 1180 w, 1154 w, 1133 w, 1107, 1058 w, 1049 w, 940 w, 925 w, 750s; δ_{H} (400 MHz; CDCl₃; TMS) 7.16–7.09 (8H, m, Ar), 7.01 (2H, s, OH), 6.89–6.79 (12H, m, Ar), 6.67 (2H, t, *J* 7.5, Ar), 4.28 (4H, s, OCH₂), 3.98 (4H, t, *J* 4.7, OCH₂), 3.91 (4H, s, ArCH₂), 3.90 (4H, s, ArCH₂), 3.71 (4H, t, *J* 4.7, OCH₂); δ_{C} (100 MHz; CDCl₃) 156.1, 155.8, 152.3, 130.9, 130.9, 128.5, 128.3, 127.5, 127.5, 121.7, 121.4, 120.0, 111.9, 111.9, 69.8, 68.6, 67.1, 31.1, 30.8, 30.3; m/z (ESI) 731.5 (M + Na⁺, 100%).

(2E,2'E,6E,6'E)-6,6'-(1,3-Phenylenebis(methan-1-yl-1-ylidene))bis(2-(4-methoxybenzylidene)cyclohexanone) (51)

A mixture of enone **8** (2.59 g, 12 mmol), isophthalaldehyde (**31**; 0.81 g, 6 mmol), and 20% w/v aq. NaOH (1.2 mL, 6 mmol) in 96% EtOH (30 mL) was stirred at RT for 6 h. Then, the precipitated solid was collected by filtration, washed with 96% EtOH (3 mL), and dried under vacuum to give dienone **51** (0.51 g, 96%) as a yellow solid, m.p. 177–180 °C; λ_{max} (EtOH)/nm 243 and 348 ($\epsilon/\text{dm}^3 \text{ mol}^{-1} \text{ cm}^{-1}$ 17 600 and 26 300); $\nu_{\text{max}}/\text{cm}^{-1}$ (KBr) 1658 m, 1600 s, 1588 s, 1556 m, 1509 s, 1420 m, 1313 m, 1287 m, 1251 s, 1210 w, 1180 m, 1159 s, 1118 m, 1964 w, 1031 m, 985 w; δ_{H} (300 MHz; CDCl₃; TMS) 7.79 (4H, d, *J* 1.8, CH), 7.53–7.43 (8H, m, Ar), 6.95 (4H, d, *J* 8.8, Ar), 3.86 (6H, s, OCH₃), 2.93 (8H, m, CH₂), 1.82 (4H, p, *J* 6.1, CH₂); δ_{C} (100 MHz; CDCl₃) 190.5, 160.5, 137.6, 137.3, 136.6, 136.2, 134.4, 132.7, 132.7, 132.2, 130.6, 129.0, 128.8, 114.3, 55.7, 28.9, 28.8, 23.4; m/z (ESI) 553.2 (M + Na⁺, 100%); m/z (ESI) 531.2539 (M + H⁺. C₃₆H₃₄NO₄⁺ requires 531.2535).

(2E,6E)-2-(4-Methoxybenzylidene)-6-(3-((E)-((E)-3-(4-methylbenzylidene)-2-oxocyclohexylidene)methyl)benzylidene)cyclohexanone (52)

A mixture of aldehyde **21** (0.05 g, 0.15 mmol) and 40% w/w aq. (*n*Bu)₄NOH (0.16 g, 0.25 mmol) in MeCN/96% EtOH (5 mL, 3:2 v/v) stirring at RT was added a 96% EtOH solution of enone **7** (30 mg, 0.90 mmol in 1 mL of 96% EtOH) in small aliquots, over 25 min. After stirring at RT overnight, the precipitated solid was collected by vacuum filtration, washed with 96% EtOH (5 mL), and dried under vacuum to give dienone **52** (0.40 g, 53%) as a yellow solid, m.p. 160–162 °C; λ_{max} (EtOH)/nm 236 and 348 ($\epsilon/\text{dm}^3 \text{ mol}^{-1} \text{ cm}^{-1}$ 22 500 and 42 800); $\nu_{\text{max}}/\text{cm}^{-1}$ (nujol) 1658 m, 1603 m, 1588 m, 1560 m, 1508 m, 1287 m, 1250 m, 1159 m, 1032 m; δ_{H} (200 MHz; CDCl₃; TMS) 7.79 (4H, s, CH), 7.53–7.37 (8H, m, Ar), 7.22 (2H, m, Ar), 6.95 (2H, d, *J* 8.8, Ar), 3.85 (3H, s, OCH₃), 2.94–2.92 (8H, m, CH₂), 2.39 (3H, s, CH₃), 1.81 (4H, m, CH₂); δ_{C} (100 MHz; CDCl₃) 190.3, 190.2, 160.3, 139.1, 137.5, 137.4, 137.1, 137.0, 136.4, 136.4, 136.2, 136.0, 135.5, 134.2, 133.3, 132.5, 132.1, 130.7, 130.4, 130.4, 129.3, 128.8, 128.6, 114.1, 55.5, 28.7, 28.7, 28.7, 28.6, 23.2, 21.6; m/z (ESI) 515.2589 (M + H⁺. C₃₆H₃₅O₃⁺ requires 515.2586).

6,6'-(1,3-Phenylenebis(methylene))bis(2-(4-methoxybenzyl)phenol) (53)

An intimate mixture of dienone **51** (0.22 g, 0.42 mmol) and 10% Pd/C (0.05 g, 0.05 mmol) was placed in a Schlenk tube under N₂ and heated at 180–190 °C for 1 h. The mixture was cooled to RT, mixed with CH₂Cl₂ (5 mL), filtered to remove the catalyst, and concentrated to give phenol **53** (0.2 g, found to be ca. 90% pure by ¹H NMR spectroscopy, *i.e.* ca. 80% yield) as a yellow oil. A sample was purified by column chromatography on silica gel (CH₂Cl₂ : hexane = 70 : 30) to give phenol **53** as a colorless oil, δ_{H} (400 MHz; CDCl₃; TMS) 7.18 (1 H, t, *J* 7.6, Ar), 7.13–7.09 (4H, m, Ar), 7.07 (1H, s, Ar), 7.02–6.96 (6H, m, Ar), 6.84–6.80 (6H, m, Ar), 4.62 (2H, s, OH), 3.91–3.90 (8H, m, CH₂), 3.76 (6H, s, OCH₃); δ_{C} (75 MHz; CDCl₃) 158.5, 152.4, 140.4, 131.7, 129.8, 129.5, 129.4, 129.3, 129.2, 127.6, 127.4,

126.9, 120.8, 114.4, 55.5, 36.7, 36.1; m/z (ESI) 548.2799 ($M + NH_4^+$. $C_{36}H_{38}NO_4^+$ requires 548.2801).

2-(3-(2-Hydroxy-3-(4-methoxybenzyl)benzyl)benzyl)-6-(4-methylbenzyl)phenol (54)

An intimate mixture of dienone **52** (0.05 g, 0.1 mmol) and 10% Pd/C (0.01 g, 0.01 mmol) was placed in Schlenk tube under N_2 and heated at 180–190 °C for 2 h. The mixture was cooled to RT, mixed with CH_2Cl_2 (3 mL), filtered to remove the catalyst, and concentrated to give phenol **54** (0.043 g, found to be *ca.* 80% pure by 1H NMR spectroscopy estimated, *i.e.* *ca.* 70% yield) as a yellow-brown oil. A sample was purified by flash column chromatography on silica gel (CH_2Cl_2 : hexane = 60 : 40) to give phenol **54** as a pale yellow oil, δ_H (400 MHz; $CDCl_3$; TMS) 7.18 (1H, t, J 7.6, Ar), 7.12–7.10 (2H, m, Ar), 7.08–7.02 (5H, m, Ar), 7.00–6.97 (5H, m, Ar), 6.84–6.80 (5H, m, Ar), 4.61 (2H, d, J 3.8, OH), 3.92–3.92 (8H, m, CH_2), 3.77 (3H, s, OCH_3), 2.30 (3H, s, CH_3); δ_C (100 MHz; $CDCl_3$) 163.6, 52.4, 140.4, 131.7, 129.8, 129.7, 129.5, 129.4, 129.4, 129.2, 128.7, 127.8, 127.5, 127.6, 127.4, 127.0, 120.8, 114.4, 55.5, 36.6, 36.6, 36.1, 21.2; m/z (ESI) 532.2845 ($M + NH_4^+$. $C_{36}H_{38}NO_3^+$ requires 532.2852), 537.2406 ($M + Na^+$. $C_{36}H_{34}NaO_3^+$ requires 537.2406).

(E)-2-(3-((E)-((E)-3-(4-Methoxybenzylidene)-2-oxocyclopentylidene)methyl)benzylidene)-3,4-dihydronaphthalen-1(2H)-one (55)

A mixture of aldehyde **19** (120 mg, 0.380 mmol), 1-tetralone (**2**; 55 mg, 0.38 mmol) and p -TsOH· H_2O (29 mg, 0.19 mmol) in toluene (20 mL) was heated at reflux using a Dean–Stark apparatus for 24 h. After cooling to RT, the mixture was washed with satd. aq. $NaHCO_3$ (2×30 mL) and satd. aq. $NaCl$ (30 mL), dried with anhyd. $MgSO_4$, filtered, and concentrated to give a brown solid. Flash column chromatography of the solid on silica gel (EtOAc : hexane = 10 : 90) afforded dienone **55** (0.125 g, 74%) as a yellow solid, m.p. 203–204 °C; ν_{max}/cm^{-1} (KBr) 2936 w, 2836 w, 1692 m, 1664 m, 1588 s, 1509 s, 1458 m, 1420 m, 1301 m, 1284 s, 1193 m, 1168 s, 1137 m, 1031 m, 992 w; δ_H (200 MHz; $CDCl_3$; TMS) 8.16 (1 H, d, J 7.7, Ar), 7.90 (1H, s, Ar, CH), 7.67 (1H, s, CH), 7.62–7.58 (4H, m), 7.56–7.36 (5H, m), 7.29 (1H, d, J 6.6, Ar), 6.99 (2H, d, J 8.4, Ar), 3.88 (3H, s, OCH_3), 3.32–3.14 (6H, m, CH_2), 2.99 (2H, t, J 6.4, CH_2); δ_C (100 MHz; $CDCl_3$) 196.3, 187.9, 161.0, 143.4, 138.5, 136.6, 136.5, 136.4, 136.1, 135.0, 134.5, 134.4, 133.6, 132.9, 132.8, 131.9, 130.8, 130.7, 129.1, 128.8, 128.5, 127.3, 114.6, 55.6, 29.1, 27.5, 26.8, 26.7; m/z (ESI) 469 ($M + Na^+$, 100%), 501 ($M + MeOH + Na^+$, 92), 447 ($M + H^+$, 40).

(2E,6E)-2-(4-Methoxybenzylidene)-6-(3-((E)-((E)-3-(4-methylbenzylidene)-2-oxocyclopentylidene)methyl)benzylidene)cyclohexanone (56)

A mixture of aldehyde **20** (0.200 g, 0.660 mmol) and enone **8** (0.143 g, 0.660 mmol) in CH_2Cl_2 –96% EtOH (12 mL, 2 : 1 v/v) was stirred at RT as powdered KOH (37 mg, 66 mmol) was added in one portion. After stirring at RT for 24 h, the precipitated solid was collected by vacuum filtration, washed with water (3 mL) and 96% EtOH (2×3 mL), and dried under vacuum to give dienone **56** (0.185 g, 56%) as a yellow

solid, 182–184 °C; ν_{max}/cm^{-1} (KBr) 2936 w, 2911 w, 2844 w, 1692 m, 1663 w, 1622 m, 1601 s, 1570 m, 1512 s, 1418 m, 1284 m, 1210 s, 1193 m, 1178 m, 1184 s, 1144 s, 1034 m, 935 m, 811 m; δ_H (200 MHz; $CDCl_3$; TMS) 7.85–7.79 (2H, m, Ar and CH), 7.70–7.40 (10H, m, Ar and CH), 7.25 (2H, d, J 7.7, Ar), 6.95 (2H, d, J 8.8, Ar), 3.86 (3H, s, OMe), 3.13 (4H, s, CH_2CH_2), 3.00–2.90 (4H, m, CH_2), 2.41 (3H, s, $ArCH_3$), 1.83 (2H, p, J 6.3, CH_2); δ_C (50 MHz; $CDCl_3$) 196.5, 190.3, 160.3, 138.3, 137.3, 137.0, 136.8, 136.4, 136.3, 135.9, 134.5, 134.2, 133.3, 133.2, 132.6, 132.4, 131.2, 131.1, 130.8, 129.8, 129.5, 129.0, 128.8, 114.2, 55.6, 28.8, 28.7, 26.8, 23.2, 21.7; m/z (ESI) 501.1 ($M + H^+$, 100%), 523.1 ($M + Na^+$, 96), 555.0 ($M + MeOH + Na^+$, 62).

Crystallography

Crystal data for 21. CCDC deposition number 629937, $C_{22}H_{30}O_3$, $M_r = 332.38$, monoclinic, space group $P2_1/c$, $a = 16.0672(8)$, $b = 14.9408(8)$, $c = 7.1505(3)$ Å, $\beta = 96.855(2)^\circ$, $V = 1704.26(1)$ Å³, $Z = 4$, $D_{calc} = 1.295$ g cm⁻³, $\mu(MoK\alpha) = 0.085$ mm⁻¹. Of 3100 ($R_{int} = 0.0740$) unique reflections, 2222 had $I > 2\sigma(I)$, R indices [$I > 2\sigma(I)$] $R_1 = 0.0456$, $wR_2 = 0.0966$, GoF on $F^2 = 1.044$ for 227 refined parameters and 0 restraints.

Crystal data for 32. CCDC deposition number 630660, $C_{26}H_{26}O_5$, $M_r = 418.47$, monoclinic, space group $P2_1/n$, $a = 11.446(2)$, $b = 15.395(3)$, $c = 12.411(3)$ Å, $\beta = 92.07(3)^\circ$, $V = 2185.5(8)$ Å³, $Z = 4$, $D_{calc} = 1.272$ g cm⁻³, $\mu(MoK\alpha) = 0.087$ mm⁻¹. Of 5375 ($R_{int} = 0.039$) unique reflections, 3183 had $I > 2\sigma(I)$, R indices [$I > 2\sigma(I)$] $R_1 = 0.0469$, $wR_2 = 0.1243$, GoF on $F^2 = 0.951$ for 284 refined parameters and 0 restraints.

Crystal data for 40. CCDC deposition number 630661, $C_{28}H_{30}O_4$, $M_r = 430.52$, monoclinic, space group $P2_1/n$, $a = 14.1051(5)$, $b = 5.9840(2)$, $c = 14.3719(6)$ Å, $\beta = 114.297(2)^\circ$, $V = 105.61(7)$ Å³, $Z = 2$, $D_{calc} = 1.293$ g cm⁻³, $\mu(MoK\alpha) = 0.085$ mm⁻¹. Of 2677 ($R_{int} = 0.051$) unique reflections measured, 1336 had $I > 2\sigma(I)$, R indices [$I > 2\sigma(I)$] $R_1 = 0.0483$, $wR_2 = 0.1118$, GoF on $F^2 = 0.939$ for 145 refined parameters and 0 restraints.

Crystal data for 43·(CHCl₃)_{0.5}·H₂O. CCDC deposition number 630662, $C_{45}H_{42}O_6 \cdot (CHCl_3)_{0.5} \cdot H_2O$, $M_r = 756.49$, monoclinic, space group $P2_1/n$, $a = 15.1785(2)$, $b = 15.0780(2)$, $c = 16.5313(3)$ Å, $\beta = 97.645(1)^\circ$, $V = 3749.8(2)$, $Z = 4$, $D_{calc} = 1.340$ g cm⁻³, $\mu(MoK\alpha) = 0.192$ mm⁻¹. Of 9011 ($R_{int} = 0.0778$) unique reflections measured, 5312 had $I > 2\sigma(I)$, R indices [$I > 2\sigma(I)$] $R_1 = 0.0625$, $wR_2 = 0.1308$, GoF on $F^2 = 1.048$ for 508 refined parameters and 0 restraints.

Crystal data for 46·CHCl₃. CCDC deposition number 630663 ($C_{46}H_{44}O_7$)₂·(CHCl₃)₂, $M_r = 1656.36$, monoclinic, space group $P2_1/c$, $a = 12.1150(3)$, $b = 23.364(1)$, $c = 30.838(1)$ Å, $\beta = 92.377(1)^\circ$, $V = 8348.0(4)$, $Z = 4$, $D_{calc} = 1.138$ g cm⁻³, $\mu(MoK\alpha) = 0.271$ mm⁻¹. Of 19746 ($R_{int} = 0.1973$) unique reflections measured, 6972 had $I > 2\sigma(I)$, R indices [$I > 2\sigma(I)$] $R_1 = 0.0938$, $wR_2 = 0.1557$, GoF on $F^2 = 1.017$ for 1028 refined parameters and 12 restraints.

Acknowledgements

The Australian Research Council (ARC) is acknowledged for financial support and one of us (CRS) wishes to thank the RSC for a Journal Grant for International Authors for travel to QUB. RSM would like to acknowledge the American Chemical Society-Petroleum Research Fund for a type UFS (Undergraduate Faculty Sabbatical) grant (PRF# 42656-UFS).

Notes and references

- (a) For recent reviews, see: A. Gardziella, L. A. Pilato, A. Knop, *Phenolic Resins: Chemistry, Applications, Standardization, Safety, and Ecology*, Springer, New York, 2000; (b) D. H. Solomon, G. G. Qiao and M. J. Caulfield in *Chemistry of Phenols*, ed. Z. Rappoport, Chichester, England, 2003, pp. 1455-1506.
- For reviews, see: (a) V. Böhmer, *Angew. Chem.*, 1995, **107**, 785; V. Böhmer, *Angew. Chem., Int. Ed. Engl.*, 1995, **34**, 713; (b) A. Ikeda and S. Shinkai, *Chem. Rev.*, 1997, **97**, 1713; (c) C. D. Gutsche, *Calixarenes Revisited, Monographs in Supramolecular Chemistry*, ed. J. F. Stoddart, The Royal Society of Chemistry, Cambridge, England, 1998; (d) *Calixarenes in Action*, ed. L. Mandolini and R. Ungaro, Imperial College Press, London, 2000; (e) *Calixarenes 2001*, ed. Z. Asfari, V. Böhmer, J. M. Harrowfield, J. Vicens and M. Saadioui, Kluwer, Dordrecht, 2001.
- L. Baldini, A. Casnati, F. Sansone and R. Ungaro, *Chem. Soc. Rev.*, 2007, **36**, 254; A. J. Petrella and C. L. Raston, *J. Organomet. Chem.*, 2004, **689**, 4125.
- A. Wei, *Chem. Commun.*, 2006, 1581.
- S. J. Dalgarno, J. L. Atwood and C. L. Raston, *Chem. Commun.*, 2006, 4567.
- R. Meyer and T. Jira, *Curr. Anal. Chem.*, 2007, **3**, 161.
- E. da Silva, A. N. Lazar and A. W. Coleman, *J. Drug Delivery Sci. Technol.*, 2004, **14**, 3.
- C. D. Gutsche, *Acc. Chem. Res.*, 1983, **16**, 161.
- F. Perret, A. N. Lazar and A. W. Coleman, *Chem. Commun.*, 2006, 2425.
- U. P. Kreher, A. E. Rosamilia, C. L. Raston, J. L. Scott and C. R. Strauss, *Org. Lett.*, 2003, **5**, 3107.
- L. T. Higham, U. P. Kreher, C. L. Raston, J. L. Scott and C. R. Strauss, *Org. Lett.*, 2004, **6**, 3257.
- L. T. Higham, U. P. Kreher, C. L. Raston, J. L. Scott and C. R. Strauss, *Org. Lett.*, 2004, **6**, 3261.
- M. L. Cole, L. T. Higham, P. C. Junk, K. M. Proctor, J. L. Scott and C. R. Strauss, *Inorg. Chim. Acta*, 2005, **358**, 3159.
- A. E. Rosamilia, M. A. Giarrusso, J. L. Scott and C. R. Strauss, *Green Chem.*, 2006, **8**, 1042.
- (a) A. T. Nielson and W. J. Houlihan, *Org. React.*, 1968, **16**, 1; (b) C. H. Heathcock in *Comprehensive Organic Synthesis, Vol. 2*, series ed. B. M. Trost and I. Fleming, vol. ed. C. H. Heathcock, Pergamon, Oxford, 1991, pp. 133-179.
- C. E. Garland and E. E. Reid, *J. Am. Chem. Soc.*, 1925, **47**, 2333.
- M. Fujita, *Chem. Soc. Rev.*, 1998, **27**, 417.
- P. F. H. Schwab, J. R. Smith and J. Michl, *Chem. Rev.*, 2005, **105**, 1197.
- (a) R. S. Varma and G. W. Kabalka, *Synth. Commun.*, 1985, **15**, 985; (b) J. L. Irvine, I. H. Hall, G. L. Carlson and C. Piantadosi, *J. Org. Chem.*, 1972, **37**, 2033.
- Z. Aizenshtat, M. Hausmann, Y. Pickholtz, D. Tal and J. Blum, *J. Org. Chem.*, 1977, **42**, 2386.
- W. J. Guilford, K. J. Shaw, J. L. Dallas, S. Koovakkat, W. Lee, A. Liang, D. R. Light, M. A. McCarrick, M. Whitlow, B. Ye and M. M. Morrissey, *J. Med. Chem.*, 1999, **42**, 5415.
- H. Frey, *Synthesis*, 1992, 387.
- R. Dimmock, K. K. Sidhu, M. Chen, J. Li, J. W. Quail, T. M. Allen and G. Y. Kao, *J. Pharm. Sci.*, 1994, **83**, 852.
- A. E.-G. E. Amr, H. S. Sayed and M. M. Abdulla, *Arch. Pharm.*, 2005, **338**, 433.
- H. O. House and A. G. Hortmann, *J. Org. Chem.*, 1961, **26**, 2190.
- T.-S. Jin, L.-B. Liu, Y. Zhao and T.-S. Li, *Synth. Commun.*, 2005, **35**, 1859.
- E. C. Horning, *J. Org. Chem.*, 1945, **10**, 263.
- (a) L. T. Higham, U. P. Kreher, J. L. Scott and C. R. Strauss, *CrystEngComm*, 2004, 484; (b) L. T. Higham, U. P. Kreher, R. J. Mulder, C. R. Strauss and J. L. Scott, *Chem. Commun.*, 2004, 2264.
- M. L. Cole, G. B. Deacon, P. C. Junk, K. M. Proctor, J. L. Scott and C. R. Strauss, *Eur. J. Inorg. Chem.*, 2005, 4138.
- (a) M. L. Cole, P. C. Junk, K. M. Proctor, J. L. Scott and C. R. Strauss, *Dalton Trans.*, 2006, 3338; (b) M. L. Cole, G. B. Deacon, C. M. Forsyth, P. C. Junk, K. M. Proctor, J. L. Scott and C. R. Strauss, *Polyhedron*, 2007, **26**, 244.
- K. E. Koenig, G. M. Lein, P. Stuckler, T. Kaneda and D. J. Cram, *J. Am. Chem. Soc.*, 1979, **101**, 3553.
- C. Simion, A. Simion, Y. Mitoma, S. Nagashima, T. Kawaji, I. Hashimoto and M. Tashiro, *Heterocycles*, 2000, **53**, 2459.
- M. S. Brody, R. M. Williams and M. G. Finn, *J. Am. Chem. Soc.*, 1997, **119**, 3429.
- G. M. Sheldrick, *SHELXS-97, Program for solution of crystal structures*, University of Göttingen, Germany, 1997.
- G. M. Sheldrick, *SHELXL-97, Program for refinement of crystal structures*, University of Göttingen, Germany, 1997.
- L. J. Barbour, *J. Supramol. Chem.*, 2001, **1**, 189.
- A. Maccioni and E. Marongiu, *Anal. Chim. Acta*, 1958, **48**, 557; A. Maccioni and E. Marongiu, *Chem. Abstr.*, 1959, **52**, 29019.
- R. Poggi and S. Sacchi, *Gazz. Chim. Ital.*, 1940, **70**, 269; R. Poggi and S. Sacchi, *Chem. Abstr.*, 1941, **35**, 17920.
- R. Poggi and M. Gottlieb, *Gazz. Chim. Ital.*, 1934, **64**, 852; R. Poggi and M. Gottlieb, *Chem. Abstr.*, 1935, **29**, 16802.
- J. R. Dimmock, A. Jha, P. Kumar, G. A. Zello, J. W. Quail, E. O. Oloo, J. J. Oucharek, M. K. Pasha, D. Seitz, R. K. Sharma, T. M. Allen, C. L. Santos, E. K. Manavathu, E. De Clercq, J. Balzarini and J. P. Stables, *Eur. J. Med. Chem.*, 2002, **37**, 35.

Microwave facile preparation of highly active and dispersed SBA-12 supported metal nanoparticles

Juan Manuel Campelo,^a Tomas David Conesa,^a Maria Jose Gracia,^a Maria Jose Jurado,^a Rafael Luque,^{*b} Jose Maria Marinas^a and Antonio Angel Romero^a

Received 31st January 2008, Accepted 9th May 2008

First published as an Advance Article on the web 23rd June 2008

DOI: 10.1039/b801754a

The successful preparation of highly active and dispersed metal nanoparticles on a mesoporous material was accomplished in a conventional microwave oven using an environmentally friendly protocol in which ethanol and acetone–water were employed as both solvents and reducing agents. The materials exhibited different particle sizes depending on the metal and the time of microwave irradiation. The nanoparticles were very active and differently selective in the oxidation of styrene.

Introduction

The development of highly ordered mesoporous silica structures introduced a new degree of freedom in the concept of catalysts.¹ Such mesoporous silica materials, including the M41S and the SBA families opened up new and exciting opportunities in materials science and their catalytic applications have been extensively investigated.^{2,3} In particular, the members of the SBA family (including the hexagonal SBA-15 and SBA-12 structures), feature a unique porous distribution, highly structural orders, ease of tuneability and outstanding stability that made them very promising candidates as catalysts and/or supports.^{4,5}

Compared to SBA-15 (*p6mm*), SBA-12 (*P6₃/mmc*) has not received a great deal of attention despite its three-dimensional hexagonal structure.^{4,6} Only a few reports can be found regarding the modification and catalytic activity of SBA-12 materials.⁷

Metal nanoparticles (MNP) are nowadays a very hot topic and several reports for the preparation of highly dispersed and active noble MNP on different supports, including Au,⁸ Ag⁹ and Pd¹⁰ can be found over the last few years. However, the protocols employed in most of the reported studies involve the use of additional reductant (*e.g.* NaBH₄, H₂, hydrazine, *etc.*) and an improvement of the green credentials in the preparation of MNP is needed. We have recently developed an easy and efficient route to the preparation of MNP supported on polysaccharide derived mesoporous materials overcoming the main drawbacks associated with the use of such reducing agents.¹¹

Following a similar methodology, we report here the facile and quick preparation of highly active and dispersed SBA-12 supported MNP using a conventional microwave domestic oven without the need of additional reductant.

Experimental

The synthesis of the parent SBA-12 materials was performed following the procedure described by Stucky *et al.*⁶ with some variations. In a typical synthesis, 3.0 g of Brij 76 (C₁₈EO₁₀ polymer) were dissolved in 57.4 g of distilled water under vigorous magnetic stirring. 8.65 g of tetraethyl orthosilicate (TEOS) were then added giving a clear solution at room temperature. 17.7 g of concentrated HCl were quickly added to this reaction mixture. The final gel mixture was stirred for 1 day at room temperature and subsequently heated for 1 day at 100 °C. The solid product was recovered by filtration, dried in air at RT, and then calcined in air at 500 °C for 6 h.

A typical procedure for the straightforward preparation of the mesoporous supported MNP was as follows: 0.4 g SBA-12 and 2 mL of a solution of gold bromide (Aldrich, 99.9%) or palladium acetate (Sigma–Aldrich, 99.9+%) in ethanol : acetone or ethanol : water (when silver nitrate was employed for the preparation of Ag-SBA-12 materials) 1 : 1 v/v were microwaved (CEM-DISCOVER or domestic microwave) for the desired period of time (usually 2 min) at 300–450 W (maximum power output, 100–140 °C temperature reached). The mixture was filtered off and the recovered solid was thoroughly washed with ethanol and acetone and oven dried overnight at 100 °C prior its utilization in the oxidation reaction. Materials were prepared at three different times (2, 5, 10 and 20 min) and different metal loadings were obtained. The preparation of the supported MNP was generally carried out in a microwave reactor (CEM-DISCOVER) and in a domestic microwave oven (Sanyo Super showerwave 900 W powergrill), obtaining similar results. The obtained materials were highly reproducible from batch to batch and some catalytic results for materials obtained in different batches are summarised in Table 3.

Microwave reaction experiments were carried out in a CEM-DISCOVER model with PC control and monitored by sampling aliquots of reaction mixture that were subsequently analysed by GC/GC-MS using an Agilent 6890 N GC model equipped, with a 7683B series autosampler, fitted with a DB-5 capillary column and an FID detector. Experiments were conducted in

^aDepartamento de Química Orgánica, Campus de Rabanales, Edificio Marie Curie, Ctra Nnal IV, Km 396, Universidad de Córdoba, E-14014, Córdoba, Spain

^bGreen Chemistry Centre of Excellence, The University of York, Heslington, York, UK YO10 5DD.

E-mail: q62alsor@uco.es, rla3@york.ac.uk

a closed vessel (pressure controlled) under continuous stirring. The microwave method was generally temperature controlled where the samples were irradiated with the required power output (settings at maximum power) to achieve the desired temperature (90 °C).

Response factors of the reaction products (styrene oxide, benzaldehyde, phenylacetaldehyde, acetophenone and benzoic acid) were determined with respect to styrene from GC analysis using known compounds in calibration mixtures of specified compositions.

Powder X-ray diffraction patterns were carried out using a Siemens D-5000 diffractometer with $\text{CuK}\alpha$ ($\lambda = 1.518 \text{ \AA}$), a step size of 0.02° and counting time per step of 1.2 s, over a range from 1° to 10° .

Nitrogen physisorption was measured with a Micromeritics instrument model ASAP 2000 at -196°C . The samples were outgassed for 2 h at 100°C under vacuum ($p < 10^{-2} \text{ Pa}$) and subsequently analyzed. The linear part of the BET equation (relative pressure between 0.05 and 0.22) was used for the determination of the specific surface area. The pore size distribution was calculated from the adsorption branch of the N_2 physisorption isotherms and the Barret–Joyner–Halenda (BJH) formula. The cumulative mesopore volume V_{BJH} was obtained from the PSD curve.

Scanning electron micrographs (SEM) and elemental composition of the calcined samples were recorded using a JEOL JSM-6300 Scanning Microscope with energy-dispersive X-ray analysis (EDX) at 20 kV. Samples were Au/Pd coated on a high resolution sputter SC7640 at a sputtering rate of 1500 V per minute, up to 7 nm thickness.

Transmission electron microscopy (TEM) micrographs were recorded on a FEI Tecnai G^2 fitted with a CCD camera for ease and speed of use. The resolution is around 0.4 nm. Samples were suspended in ethanol and deposited straight away on a copper grid prior to analysis.

Temperature programmed reduction (TPR) was conducted on a Stanton-Redcroft STA750 thermal analyser under a 10 vol% H_2/He stream with a total flow rate of 20 mL min^{-1} and ramp rate of 12 K min^{-1} between room temperature and 800°C .

Results and discussion

Powder X-ray diffraction patterns (Fig. 1) obtained for the SBA-12 materials exhibited the typical diffraction lines at $1\text{--}2^\circ$ and two weak peaks in the $2\text{--}5^\circ$ 2θ range that can be indexed in the $\text{P6}_3/\text{mmc}$ group as initially reported by Zhao *et al.*⁴ The unit cell parameters of the SBA-12 ($a = 65 \text{ \AA}$, $c = 106 \text{ \AA}$, $c/a = 1.63$) were in good agreement with previously reported results.^{4,6} The incorporation of the different metals on the hexagonal three-dimensional mesoporous structure did not considerably alter the structural order in the materials after relatively long times of microwave irradiation (Fig. 1). Various diffraction lines, including the (111), (200), (220) and (311), were found for the various supported MNP, in good agreement with the corresponding JCPDS files.

N_2 physisorption experiments showed the type IV isotherm profile, typical of mesoporous materials (Fig. 2). Data regarding the pore size distribution, surface area and pore volume is included in Table 1. The textural properties of the material

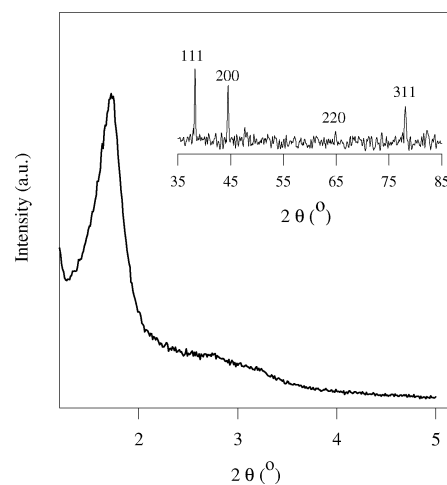


Fig. 1 XRD patterns of Pd-SBA-12 prepared after 20 min of mw irradiation. Inset corresponds to the various diffraction lines (111, 200, 220 and 311) of the metallic palladium (JCPDS file: 46-1043).

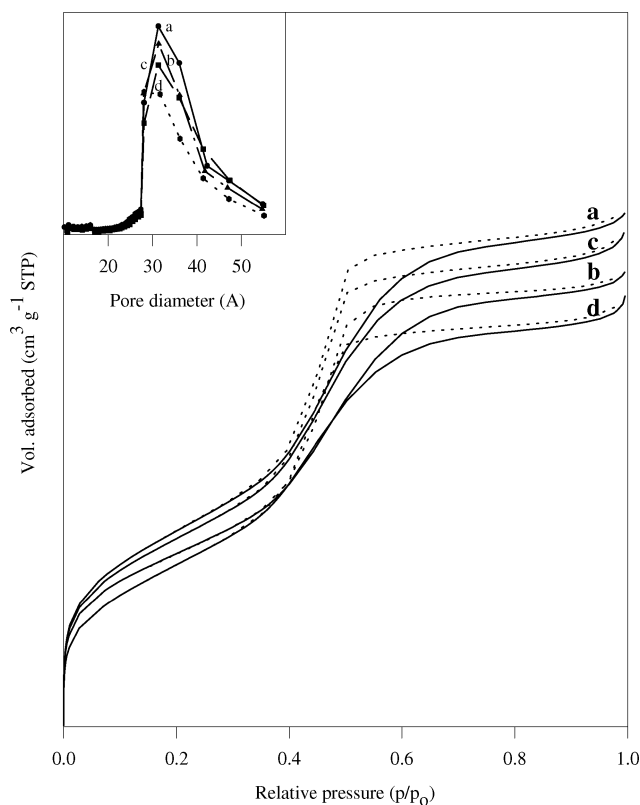


Fig. 2 Isotherm profile and pore size distribution of SBA-12 materials: (a) SBA-12; (b) Ag-SBA-2 (2 min mw); (c) Pd-SBA-12 (2 min mw); (d) Pd-SBA-12 (20 min mw).

supported MNPs were not significantly affected by the incorporation of the various metals. The pore size was around 3.2–3.4 nm and it was found to decrease with an increase of the metal loading.

Temperature-programmed reduction confirmed that only reduced metals (Au, Ag and Pd) were present in all samples, irrespective of the metal loading.

Table 1 Textural properties and metal loadings (determined by elemental analysis) of various NP supported SBA-12 mesoporous materials^a

Material	$S_{\text{BET}}/\text{m}^2 \text{g}^{-1}$	Pore size/nm	Pore volume/ $\text{cm}^3 \text{g}^{-1}$	Metal loading (%)
SBA-12	645	3.5	0.71	—
Au-SBA-12	608	3.2	0.56	1.2
Ag-SBA-12	563	3.4	0.63	1.1
Pd-SBA-12	621	3.4	0.65	1.5
Pd-SBA-12 ^b	552	3.3	0.59	5.6

^a Materials prepared after 2 min microwave irradiation. ^b 20 min mw irradiation.

SEM micrographs of the SBA-12 materials (Fig. 3) showed the mesoporous solids have sort-of spike-crystal morphology with a particle size of *ca.* 1–5 μm . The particle morphology did not change with the incorporation of the different metals onto the SBA-12.

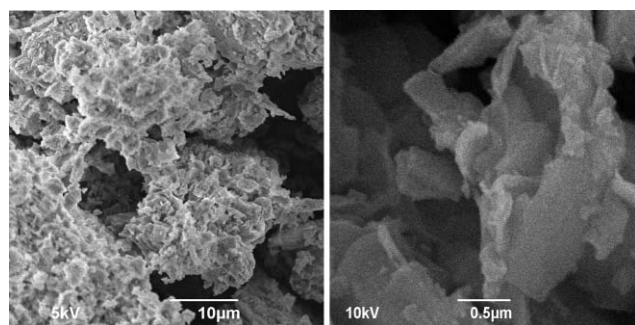


Fig. 3 SEM micrographs of SBA-12 materials at different magnifications ($\times 5000$, 10 μm , left and $\times 10000$, 0.5 μm , right).

TEM micrographs are shown in Fig. 4. The characteristic three-dimensional hexagonal array of mesopores can be observed (Fig. 4, top images), confirming the $P6_3/mmc$ space group symmetry of the mesoporous SBA-12.¹² The TEM micrographs

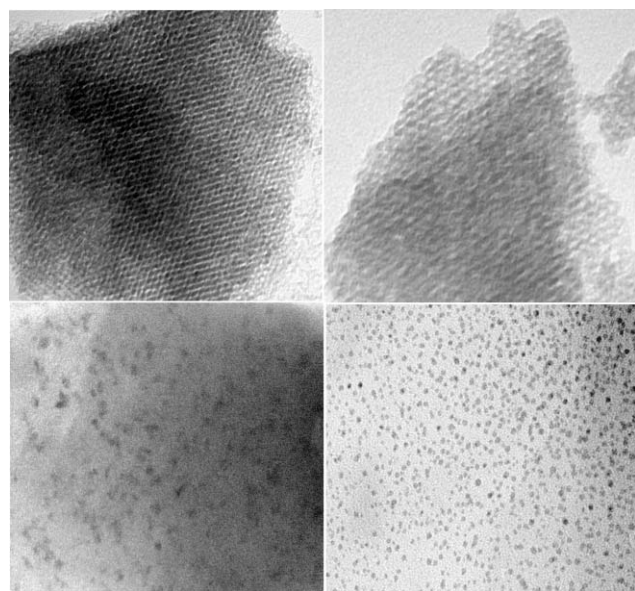


Fig. 4 TEM micrographs of the parent SBA-12 ($\times 160000$, top left) and $\times 300000$ (top right) and Ag (bottom left) and Au nanoparticles on SBA-12 (bottom right) at the same magnification ($\times 300000$, 50 nm scale bar) prepared in a domestic microwave oven.

of the SBA-12 supported MNP (Fig. 4 bottom images) proved the successful preparation of such Au-, Pd- and Ag-SBA-12 materials after 2 minutes of microwave irradiation regardless of the method of preparation. The loading of metal after 2 min was found to be around 1–1.5 wt%.

Microwave irradiation was found to be critical for the preparation of controllable sized, evenly distributed particles. Microwave synthesized supported MNP were compared to those obtained under conventional heating at the same conditions (temperature and time of heating) and the results have been included in Fig. 5. Conventional heating preparation gave an extremely low metal loading with a very poor dispersion of supported MNP (Fig. 5, left) and only higher nanoparticle formation was observed at relatively long times of reaction (over 1 h). An uneven distribution and dispersion of the MNP was also found. The effect of the microwave irradiation is clear. The rapid heating of the reaction mixtures, specially those containing polar solvents (*e.g.* ethanol, water), leads to a rapid and almost simultaneous precipitation of the metal solution of the precursor, which in turn renders materials with small particle sizes and narrow size distributions at very short reaction times (less than 3 min). In addition to that, the solvent (EtOH) reduces the solutions to elemental metal, offering a better control of particle size and morphology, as previously reported.¹³

The average nanoparticle size in the materials was found to be relatively different depending on the metal and the time of microwave irradiation. Au nanoparticles were found to be well dispersed and homogeneously distributed with very small size and reasonably narrow particle size distribution (*ca.* 1.9 nm). Interestingly, Ag- and Pd-SBA-12 materials exhibited less homogeneous nanoparticle dispersion with a bigger nanoparticle size (*ca.* 3.8 and 11.3 nm, respectively). A representative bar plot (inset) of the distribution of the various metal nanoparticle SBA-12 at different times of irradiation are depicted in Fig. 6 and 7.

The particle size distribution shows a very narrow MNP size for each one of the nanoparticles prepared. The particle size was found to increase considerably with an increase in the time of microwave irradiation (Fig. 6 and 7). Longer times of microwave irradiation promoted nanoparticle aggregation and formation of big metal clusters. Of note was the particular case of Pd-SBA-12 prepared after 20 min of mw irradiation (Fig. 7, right) compared to that of the 2 min Pd-SBA-12 (Fig. 7, left). The formation of big palladium clusters (60–70 nm) was exclusively observed in the Pd-SBA-12 after 20 min of microwave irradiation. Such palladium clusters were found to have a 3D structure comprising of smaller nanoparticle agglomerates that can be clearly seen in Fig. 7.

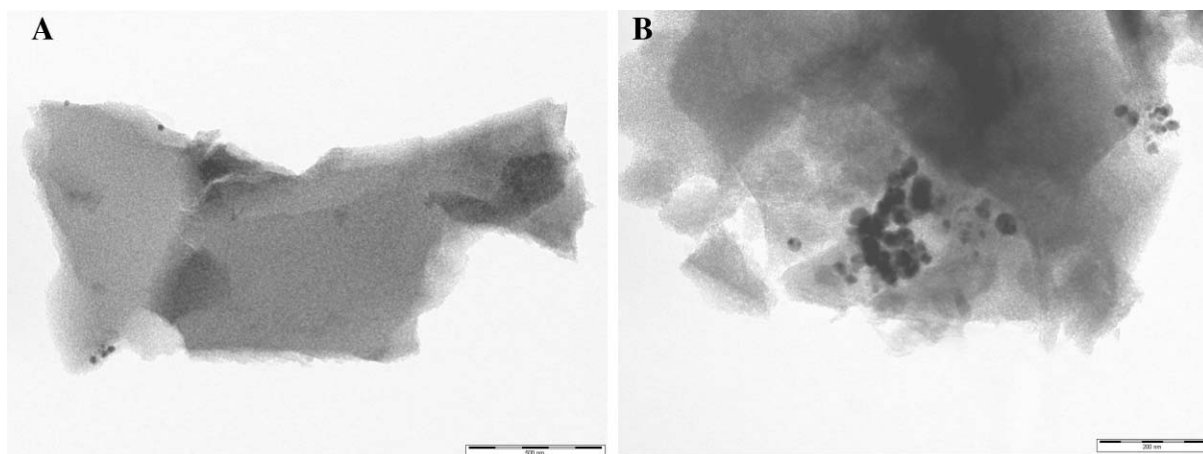


Fig. 5 Au-SBA-12 materials prepared under conventional heating after (A) 15 min (few Au particles can be observed on the top and bottom left of the TEM image) and (B) 1 h (uneven distribution of particles can be observed).

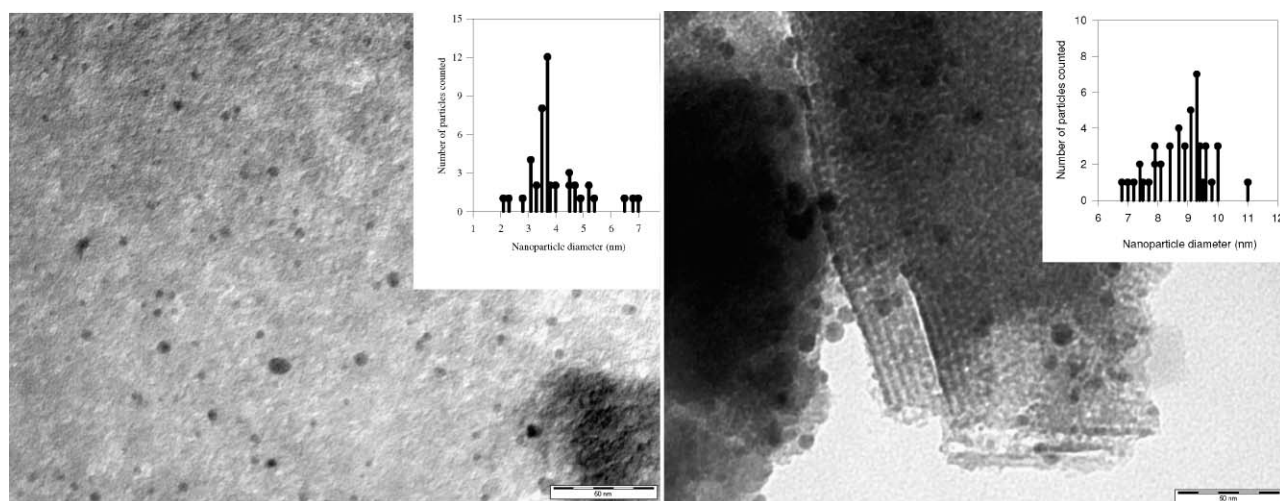


Fig. 6 TEM micrographs and nanoparticle size distribution (inset) of Ag-SBA-12 materials prepared in a domestic microwave oven: Ag-SBA-2 ($\times 300\,000$, 50 nm bar scale) after 2 min (top) and 20 min (bottom) microwave irradiation.

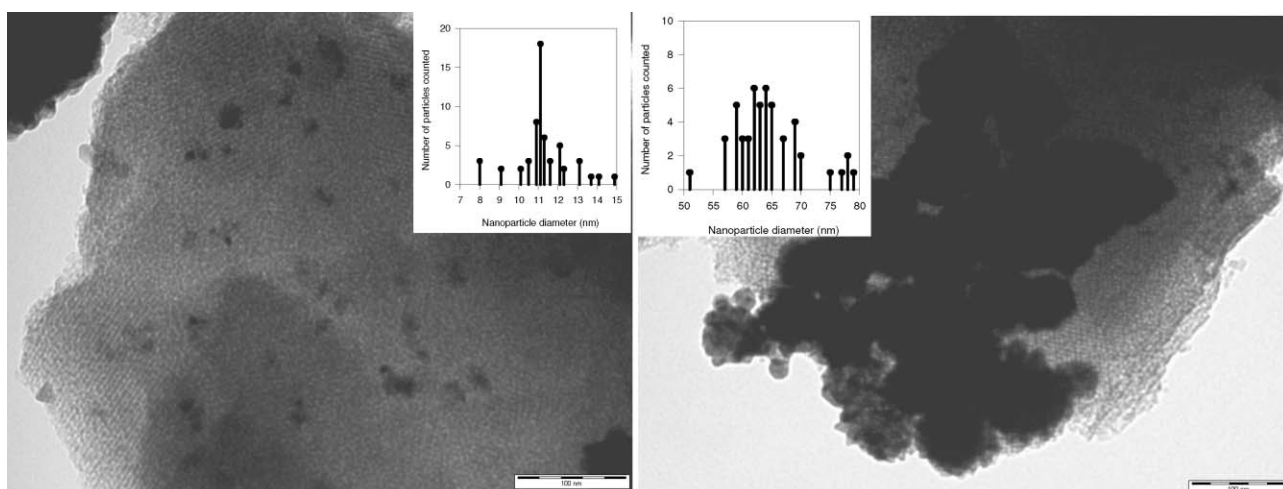


Fig. 7 TEM micrographs and nanoparticle size distribution (inset) of Pd-SBA-12 ($\times 160\,000$, 100 nm bar scale) prepared in a domestic microwave oven after 2 (top) and 20 min (bottom) of microwave irradiation.

Table 2 Catalytic activities [conversion (mol%) and selectivities to the epoxide (S_{epoxide} , mol%), benzaldehyde ($S_{\text{benzaldehyde}}$, mol%) and benzylbenzoate ($S_{\text{benzylbenzoate}}$, mol%)] of metal supported SBA-12 materials in the oxidations of styrene and benzyl alcohol with H_2O_2 under microwave irradiation^a

Material	Oxidation of styrene			Oxidation of benzyl alcohol		
	Conversion (mol%)	S_{epoxide} (mol%)	$S_{\text{benzaldehyde}}$ (mol%)	Conversion (mol%)	$S_{\text{benzaldehyde}}$ (mol%)	$S_{\text{benzylbenzoate}}$ (mol%)
SBA-12	<5	—	—	—	—	—
Au-SBA-12	75	>99	—	50	>95	—
Ag-SBA-12	90	85 ^b	—	<15	>99	—
Pd-SBA-12	>95	—	>95 ^c	68	>95	<5
Pd-SBA-12 ^d	85	—	>99	>99	90	>5

^a 5 mmol starting material, 15 mmol H_2O_2 , 0.1 g catalyst, 300 W (maximum power output), 100–50 °C, 30 min. ^b Phenylacetaldehyde was obtained as major byproduct. ^c Minor quantities of benzoic acid were obtained. ^d 20 min mw irradiation.

Table 3 Reproducibility of the activity of various metal supported SBA-12 materials in the oxidation of styrene with H_2O_2 under microwave irradiation^a

Material	Conversion (mol%)	Selectivity epoxide (mol%)	Selectivity benzaldehyde (mol%)
Au-SBA-12-batch 1	75	>99	—
Au-SBA-12-batch 2	82	>99	—
Au-SBA-12-batch 3	80	>99	—
Au-SBA-12-batch 4	79	>99	—
Ag-SBA-12-batch 1	90	85 ^b	—
Ag-SBA-12-batch 2	87	90 ^b	—
Ag-SBA-12-batch 3	95	83 ^b	—
Pd-SBA-12-batch 1	> 95	—	>95 ^c
Pd-SBA-12-batch 2	> 99	—	>95 ^c
Pd-SBA-12-batch 3	> 99	—	>95 ^c

^a 5 mmol styrene, 15 mmol H_2O_2 , 0.1 g catalyst, 300 W (maximum power output), 100–150 °C, 30 min. ^b Phenylacetaldehyde was obtained as major byproduct. ^c Minor quantities of benzoic acid were obtained.

Judging from the experimental data obtained, it seems that the formation of supported MNP with a narrow size distribution can be achieved under microwave irradiation in a very short period of time (<3 min) using a domestic microwave oven.

MNP with different shapes have different crystallographic faces. It is therefore of interest to study the effect of their shapes and sizes on their catalytic activity in various reactions. The catalytic activity of metal supported SBA-12 materials was investigated in the oxidations of styrene and benzyl alcohol with hydrogen peroxide under microwave irradiation. Results are summarized in Table 2. The oxidation of styrene has been reported to be sensitive to single crystal surfaces in silver.¹⁴

The supported MNP were found to be extremely active and differently selective in the oxidation of styrene. Au- and Ag-SBA-12 promoted the formation of the styrene oxide, and only minor quantities of phenylacetaldehyde were found. Compared to Au and Ag, Pd-SBA-12 materials exhibited great selectivities to benzaldehyde. Au-, Ag- and Pd-SBA-12 materials had different activities in the oxidation of benzyl alcohol. While Ag-SBA-12 was not active, Au- and Pd-SBA-12 exhibited a moderate activity in the oxidation. An increase in metal loading provided quantitative conversion of starting material (Table 2). Almost complete selectivities to benzaldehyde, with minor quantities (<5%) of various by-products, including benzoic acid and benzylbenzoate, were obtained.

The catalytic activity of the materials was also highly reproducible (Table 3). MNP obtained in four different batches exhibited very similar activities and selectivities under identical reaction conditions.

Conclusions

We report a facile and environmentally friendly protocol for the preparation of MNP on SBA-12 using a domestic microwave oven in a very short period of time. Samples were highly active and differently selective depending on the supported metal. The nanoparticle size can be easily controlled for an optimum performance in a particular application (e.g. catalysis) therefore making the supported materials of extreme interest.

References

- (a) C. T. Kresge, M. E. Leonowicz, W. J. Roth, J. C. Vartuli and J. S. Beck, *Nature*, 1992, **359**, 710–12; (b) J. S. Beck, J. C. Vartuli, W. J. Roth, M. E. Leonowicz, C. T. Kresge, K. D. Schmitt, C. T. W. Chu, D. H. Olson, E. W. Sheppard, S. B. McCullen, J. B. Higgins and J. L. Schlenker, *J. Am. Chem. Soc.*, 1992, **114**, 10834–10843; (c) A. Taguchi and F. Schüth, *Microporous Mesoporous Mater.*, 2005, **77**, 1–5; (d) G. E. Fryxell, *Inorg. Chem. Commun.*, 2006, **9**, 1141–1150.
- (a) D. Trong-On, D. Desplandier-Giscard, C. Danumah and S. Kaliaguine, *Appl. Catal., A*, 2003, **253**, 545–553; (b) G. Øye, W. R. Glomm, T. Vrålstad, S. Volden, H. Magnusson, M. Stöcker and J. Sjöblom, *Adv. Colloid Interface Sci.*, 2006, **123–126**, 17–32; (c) J. Y. Ying, C. P. Mehnert and M. S. Wong, *Angew. Chem., Int. Ed.*, 1999, **38**, 56–77.
- (a) J. M. Campelo, D. Luna, R. Luque, J. M. Marinas, A. A. Romero, J. J. Calvino and M. P. Rodriguez-Luque, *J. Catal.*, 2005, **230**, 327–338; (b) R. Luque, J. M. Campelo, D. Luna, J. M. Marinas and A. A. Romero, *Microporous Mesoporous Mater.*, 2005, **84**, 11–0.
- D. Zhao, Q. Huo, J. Feng, B. F. Chmelka and G. D. Stucky, *J. Am. Chem. Soc.*, 1998, **120**, 6024–6036.
- (a) D. Zhao, J. Feng, Q. Huo, N. Melosh, G. H. Fredrickson, B. F. Chmelka and G. D. Stucky, *Science*, 1998, **279**, 548–552; (b) D. Zhao, P. Yang, N. Melosh, J. Feng, B. F. Chmelka and G. D. Stucky, *Adv. Mater.*, 1998, **10**, 1380–1385; (c) B. Karimi, A. Biglari, J. H. Clark and V. Budarin, *Angew. Chem., Int. Ed.*, 2007, **46**, 1–5; (d) G. Du,

- S. Lin, M. Pinault, C. Wang, F. Fang, L. Pfefferle and G. L. Haller, *J. Catal.*, 2008, **253**, 74–90.
- 6 Y. Sakamoto, I. Diaz, O. Terasaki, D. Zhao, J. Perez-Pariente, J. M. Kim and G. D. Stucky, *J. Phys. Chem. B*, 2002, **106**, 3118–3123.
- 7 (a) I. Diaz, F. Mohino, J. Perez-Pariente and E. Sastre, *Stud. Surf. Sci. Catal.*, 2001, **135**, 1383–1390; (b) J. P. Gabaldon, M. Bore and A. K. Datye, *Top. Catal.*, 2007, **44**, 253–62.
- 8 (a) N. Lewis, *Chem. Rev.*, 1993, **93**, 2693–2730; (b) X. Wang, C. E. Egan, M. Zhou, K. Prince, D. R. G. David and R. A. Caruso, *Chem. Commun.*, 2007, 3060–3062; (c) J. K. Edwards, A. Thomas, A. F. Carley, A. A. Herzing, C. J. Kiely and G. J. Hutchings, *Green Chem.*, 2008, **10**, 388–394.
- 9 (a) R. J. Chimentao, I. Kirm, F. Medina, X. Rodriguez, Y. Cesteros, P. Salagre and J. E. Sueiras, *Chem. Commun.*, 2004, 846–847; (b) P. Raveendran, J. Fu and S. L. Wallen, *Green Chem.*, 2006, **8**, 34–38.
- 10 (a) B. Karimi, S. Abedi, J. H. Clark and V. Budarin, *Angew. Chem., Int. Ed.*, 2006, **45**, 4776–4779; (b) V. Budarin, J. H. Clark, R. Luque, D. J. Macquarrie and R. J. White, *Green Chem.*, 2008, **10**, 382–387.
- 11 (a) V. Budarin, J. H. Clark, R. Luque, D. J. Macquarrie, K. Milkowski and R. J. White, *PCT International Patent* WO 2007104798 A2 20070920, 2007; (b) V. Budarin, J. H. Clark, R. Luque, D. J. Macquarrie and R. J. White, *GB Patent Application*, 2007.
- 12 (a) Q. Huo, R. Leon, P. M. Petroff and G. D. Stucky, *Science*, 1995, **268**, 1324–327; (b) Q. Huo, D. I. Margolese and G. D. Stucky, *Chem. Mater.*, 1996, **8**, 1147–160.
- 13 I. Pastoriza-Santos and L. M. Liz-Marzan, *Langmuir*, 2002, **18**, 2888–2894.
- 14 X. Liu, A. Klust, R. J. Madix and C. M. Friend, *J. Phys. Chem. C*, 2007, **111**, 3675–3679.

Microwave facile preparation of highly active and dispersed SBA-12 supported metal nanoparticles

Juan Manuel Campelo,^a Tomas David Conesa,^a Maria Jose Gracia,^a Maria Jose Jurado,^a Rafael Luque,^{*b} Jose Maria Marinas^a and Antonio Angel Romero^a

Received 31st January 2008, Accepted 9th May 2008

First published as an Advance Article on the web 23rd June 2008

DOI: 10.1039/b801754a

The successful preparation of highly active and dispersed metal nanoparticles on a mesoporous material was accomplished in a conventional microwave oven using an environmentally friendly protocol in which ethanol and acetone–water were employed as both solvents and reducing agents. The materials exhibited different particle sizes depending on the metal and the time of microwave irradiation. The nanoparticles were very active and differently selective in the oxidation of styrene.

Introduction

The development of highly ordered mesoporous silica structures introduced a new degree of freedom in the concept of catalysts.¹ Such mesoporous silica materials, including the M41S and the SBA families opened up new and exciting opportunities in materials science and their catalytic applications have been extensively investigated.^{2,3} In particular, the members of the SBA family (including the hexagonal SBA-15 and SBA-12 structures), feature a unique porous distribution, highly structural orders, ease of tuneability and outstanding stability that made them very promising candidates as catalysts and/or supports.^{4,5}

Compared to SBA-15 (*p6mm*), SBA-12 (*P6₃/mmc*) has not received a great deal of attention despite its three-dimensional hexagonal structure.^{4,6} Only a few reports can be found regarding the modification and catalytic activity of SBA-12 materials.⁷

Metal nanoparticles (MNP) are nowadays a very hot topic and several reports for the preparation of highly dispersed and active noble MNP on different supports, including Au,⁸ Ag⁹ and Pd¹⁰ can be found over the last few years. However, the protocols employed in most of the reported studies involve the use of additional reductant (*e.g.* NaBH₄, H₂, hydrazine, *etc.*) and an improvement of the green credentials in the preparation of MNP is needed. We have recently developed an easy and efficient route to the preparation of MNP supported on polysaccharide derived mesoporous materials overcoming the main drawbacks associated with the use of such reducing agents.¹¹

Following a similar methodology, we report here the facile and quick preparation of highly active and dispersed SBA-12 supported MNP using a conventional microwave domestic oven without the need of additional reductant.

Experimental

The synthesis of the parent SBA-12 materials was performed following the procedure described by Stucky *et al.*⁶ with some variations. In a typical synthesis, 3.0 g of Brij 76 (C₁₈EO₁₀ polymer) were dissolved in 57.4 g of distilled water under vigorous magnetic stirring. 8.65 g of tetraethyl orthosilicate (TEOS) were then added giving a clear solution at room temperature. 17.7 g of concentrated HCl were quickly added to this reaction mixture. The final gel mixture was stirred for 1 day at room temperature and subsequently heated for 1 day at 100 °C. The solid product was recovered by filtration, dried in air at RT, and then calcined in air at 500 °C for 6 h.

A typical procedure for the straightforward preparation of the mesoporous supported MNP was as follows: 0.4 g SBA-12 and 2 mL of a solution of gold bromide (Aldrich, 99.9%) or palladium acetate (Sigma–Aldrich, 99.9+%) in ethanol : acetone or ethanol : water (when silver nitrate was employed for the preparation of Ag-SBA-12 materials) 1 : 1 v/v were microwaved (CEM-DISCOVER or domestic microwave) for the desired period of time (usually 2 min) at 300–450 W (maximum power output, 100–140 °C temperature reached). The mixture was filtered off and the recovered solid was thoroughly washed with ethanol and acetone and oven dried overnight at 100 °C prior its utilization in the oxidation reaction. Materials were prepared at three different times (2, 5, 10 and 20 min) and different metal loadings were obtained. The preparation of the supported MNP was generally carried out in a microwave reactor (CEM-DISCOVER) and in a domestic microwave oven (Sanyo Super showerwave 900 W powergrill), obtaining similar results. The obtained materials were highly reproducible from batch to batch and some catalytic results for materials obtained in different batches are summarised in Table 3.

Microwave reaction experiments were carried out in a CEM-DISCOVER model with PC control and monitored by sampling aliquots of reaction mixture that were subsequently analysed by GC/GC-MS using an Agilent 6890 N GC model equipped, with a 7683B series autosampler, fitted with a DB-5 capillary column and an FID detector. Experiments were conducted in

^aDepartamento de Química Orgánica, Campus de Rabanales, Edificio Marie Curie, Ctra Nnal IV, Km 396, Universidad de Córdoba, E-14014, Córdoba, Spain

^bGreen Chemistry Centre of Excellence, The University of York, Heslington, York, UK YO10 5DD.

E-mail: q62alsor@uco.es, rla3@york.ac.uk

a closed vessel (pressure controlled) under continuous stirring. The microwave method was generally temperature controlled where the samples were irradiated with the required power output (settings at maximum power) to achieve the desired temperature (90 °C).

Response factors of the reaction products (styrene oxide, benzaldehyde, phenylacetaldehyde, acetophenone and benzoic acid) were determined with respect to styrene from GC analysis using known compounds in calibration mixtures of specified compositions.

Powder X-ray diffraction patterns were carried out using a Siemens D-5000 diffractometer with $\text{CuK}\alpha$ ($\lambda = 1.518 \text{ \AA}$), a step size of 0.02° and counting time per step of 1.2 s, over a range from 1° to 10° .

Nitrogen physisorption was measured with a Micromeritics instrument model ASAP 2000 at -196°C . The samples were outgassed for 2 h at 100°C under vacuum ($p < 10^{-2} \text{ Pa}$) and subsequently analyzed. The linear part of the BET equation (relative pressure between 0.05 and 0.22) was used for the determination of the specific surface area. The pore size distribution was calculated from the adsorption branch of the N_2 physisorption isotherms and the Barret–Joyner–Halenda (BJH) formula. The cumulative mesopore volume V_{BJH} was obtained from the PSD curve.

Scanning electron micrographs (SEM) and elemental composition of the calcined samples were recorded using a JEOL JSM-6300 Scanning Microscope with energy-dispersive X-ray analysis (EDX) at 20 kV. Samples were Au/Pd coated on a high resolution sputter SC7640 at a sputtering rate of 1500 V per minute, up to 7 nm thickness.

Transmission electron microscopy (TEM) micrographs were recorded on a FEI Tecnai G^2 fitted with a CCD camera for ease and speed of use. The resolution is around 0.4 nm. Samples were suspended in ethanol and deposited straight away on a copper grid prior to analysis.

Temperature programmed reduction (TPR) was conducted on a Stanton-Redcroft STA750 thermal analyser under a 10 vol% H_2/He stream with a total flow rate of 20 mL min^{-1} and ramp rate of 12 K min^{-1} between room temperature and 800°C .

Results and discussion

Powder X-ray diffraction patterns (Fig. 1) obtained for the SBA-12 materials exhibited the typical diffraction lines at $1\text{--}2^\circ$ and two weak peaks in the $2\text{--}5^\circ$ 2θ range that can be indexed in the $\text{P6}_3/\text{mmc}$ group as initially reported by Zhao *et al.*⁴ The unit cell parameters of the SBA-12 ($a = 65 \text{ \AA}$, $c = 106 \text{ \AA}$, $c/a = 1.63$) were in good agreement with previously reported results.^{4,6} The incorporation of the different metals on the hexagonal three-dimensional mesoporous structure did not considerably alter the structural order in the materials after relatively long times of microwave irradiation (Fig. 1). Various diffraction lines, including the (111), (200), (220) and (311), were found for the various supported MNP, in good agreement with the corresponding JCPDS files.

N_2 physisorption experiments showed the type IV isotherm profile, typical of mesoporous materials (Fig. 2). Data regarding the pore size distribution, surface area and pore volume is included in Table 1. The textural properties of the material

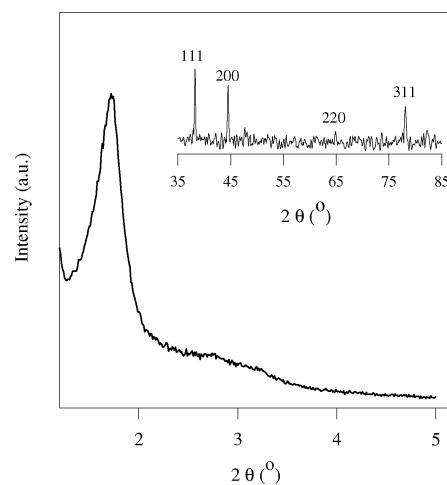


Fig. 1 XRD patterns of Pd-SBA-12 prepared after 20 min of mw irradiation. Inset corresponds to the various diffraction lines (111, 200, 220 and 311) of the metallic palladium (JCPDS file: 46-1043).

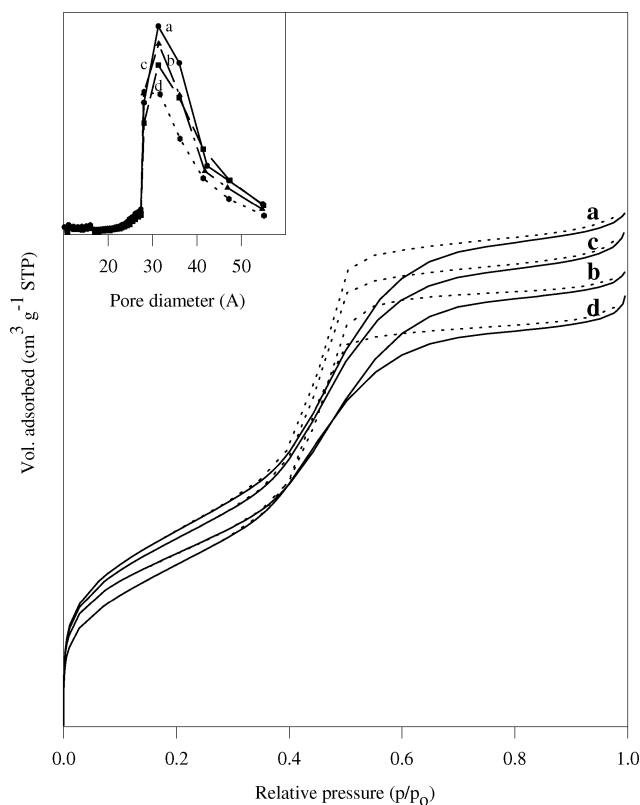


Fig. 2 Isotherm profile and pore size distribution of SBA-12 materials: (a) SBA-12; (b) Ag-SBA-2 (2 min mw); (c) Pd-SBA-12 (2 min mw); (d) Pd-SBA-12 (20 min mw).

supported MNPs were not significantly affected by the incorporation of the various metals. The pore size was around 3.2–3.4 nm and it was found to decrease with an increase of the metal loading.

Temperature-programmed reduction confirmed that only reduced metals (Au, Ag and Pd) were present in all samples, irrespective of the metal loading.

Table 1 Textural properties and metal loadings (determined by elemental analysis) of various NP supported SBA-12 mesoporous materials^a

Material	$S_{\text{BET}}/\text{m}^2 \text{g}^{-1}$	Pore size/nm	Pore volume/ $\text{cm}^3 \text{g}^{-1}$	Metal loading (%)
SBA-12	645	3.5	0.71	—
Au-SBA-12	608	3.2	0.56	1.2
Ag-SBA-12	563	3.4	0.63	1.1
Pd-SBA-12	621	3.4	0.65	1.5
Pd-SBA-12 ^b	552	3.3	0.59	5.6

^a Materials prepared after 2 min microwave irradiation. ^b 20 min mw irradiation.

SEM micrographs of the SBA-12 materials (Fig. 3) showed the mesoporous solids have sort-of spike-crystal morphology with a particle size of *ca.* 1–5 μm . The particle morphology did not change with the incorporation of the different metals onto the SBA-12.

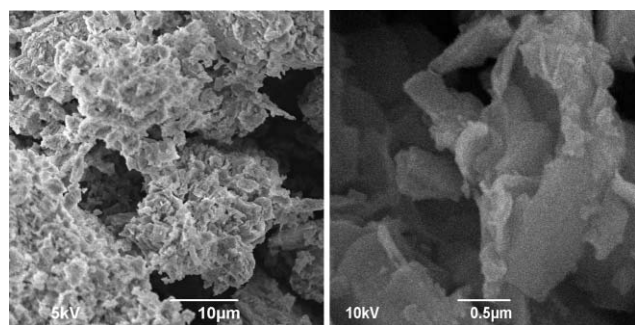


Fig. 3 SEM micrographs of SBA-12 materials at different magnifications ($\times 5000$, 10 μm , left and $\times 10000$, 0.5 μm , right).

TEM micrographs are shown in Fig. 4. The characteristic three-dimensional hexagonal array of mesopores can be observed (Fig. 4, top images), confirming the $P6_3/mmc$ space group symmetry of the mesoporous SBA-12.¹² The TEM micrographs

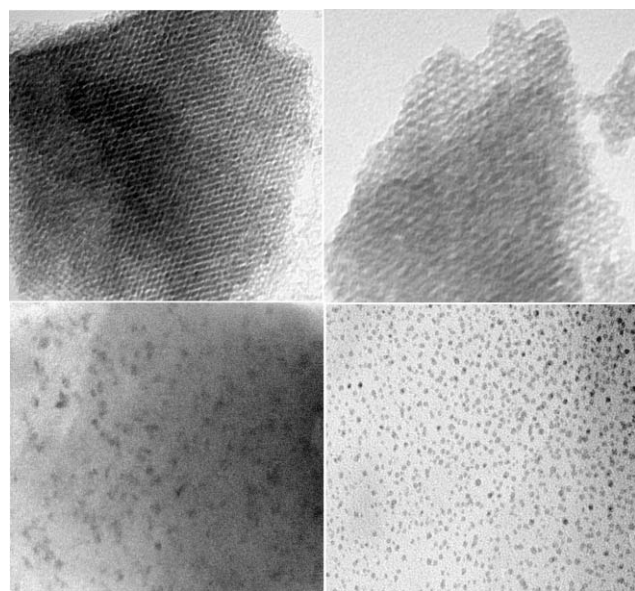


Fig. 4 TEM micrographs of the parent SBA-12 ($\times 160000$, top left) and $\times 300000$ (top right) and Ag (bottom left) and Au nanoparticles on SBA-12 (bottom right) at the same magnification ($\times 300000$, 50 nm scale bar) prepared in a domestic microwave oven.

of the SBA-12 supported MNP (Fig. 4 bottom images) proved the successful preparation of such Au-, Pd- and Ag-SBA-12 materials after 2 minutes of microwave irradiation regardless of the method of preparation. The loading of metal after 2 min was found to be around 1–1.5 wt%.

Microwave irradiation was found to be critical for the preparation of controllable sized, evenly distributed particles. Microwave synthesized supported MNP were compared to those obtained under conventional heating at the same conditions (temperature and time of heating) and the results have been included in Fig. 5. Conventional heating preparation gave an extremely low metal loading with a very poor dispersion of supported MNP (Fig. 5, left) and only higher nanoparticle formation was observed at relatively long times of reaction (over 1 h). An uneven distribution and dispersion of the MNP was also found. The effect of the microwave irradiation is clear. The rapid heating of the reaction mixtures, specially those containing polar solvents (*e.g.* ethanol, water), leads to a rapid and almost simultaneous precipitation of the metal solution of the precursor, which in turn renders materials with small particle sizes and narrow size distributions at very short reaction times (less than 3 min). In addition to that, the solvent (EtOH) reduces the solutions to elemental metal, offering a better control of particle size and morphology, as previously reported.¹³

The average nanoparticle size in the materials was found to be relatively different depending on the metal and the time of microwave irradiation. Au nanoparticles were found to be well dispersed and homogeneously distributed with very small size and reasonably narrow particle size distribution (*ca.* 1.9 nm). Interestingly, Ag- and Pd-SBA-12 materials exhibited less homogeneous nanoparticle dispersion with a bigger nanoparticle size (*ca.* 3.8 and 11.3 nm, respectively). A representative bar plot (inset) of the distribution of the various metal nanoparticle SBA-12 at different times of irradiation are depicted in Fig. 6 and 7.

The particle size distribution shows a very narrow MNP size for each one of the nanoparticles prepared. The particle size was found to increase considerably with an increase in the time of microwave irradiation (Fig. 6 and 7). Longer times of microwave irradiation promoted nanoparticle aggregation and formation of big metal clusters. Of note was the particular case of Pd-SBA-12 prepared after 20 min of mw irradiation (Fig. 7, right) compared to that of the 2 min Pd-SBA-12 (Fig. 7, left). The formation of big palladium clusters (60–70 nm) was exclusively observed in the Pd-SBA-12 after 20 min of microwave irradiation. Such palladium clusters were found to have a 3D structure comprising of smaller nanoparticle agglomerates that can be clearly seen in Fig. 7.

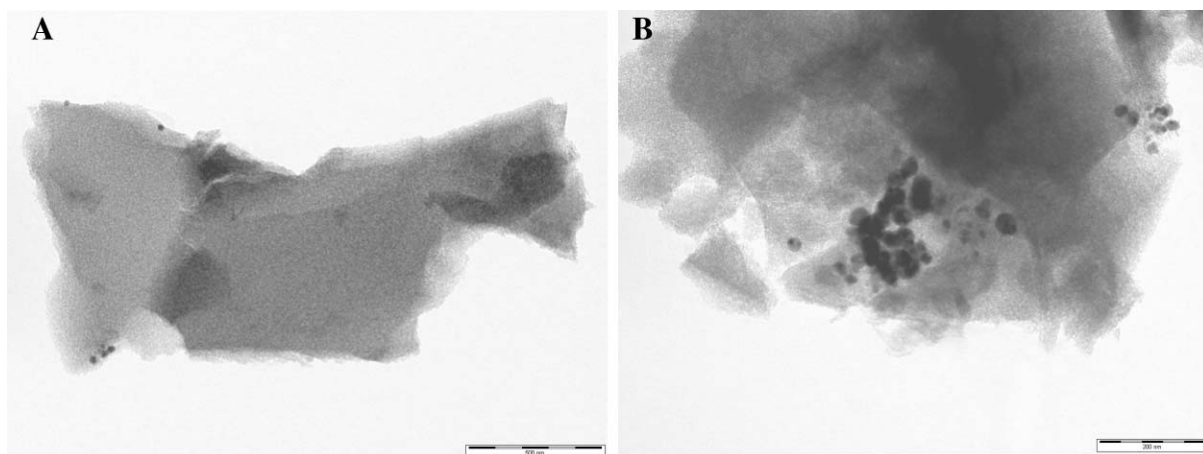


Fig. 5 Au-SBA-12 materials prepared under conventional heating after (A) 15 min (few Au particles can be observed on the top and bottom left of the TEM image) and (B) 1 h (uneven distribution of particles can be observed).

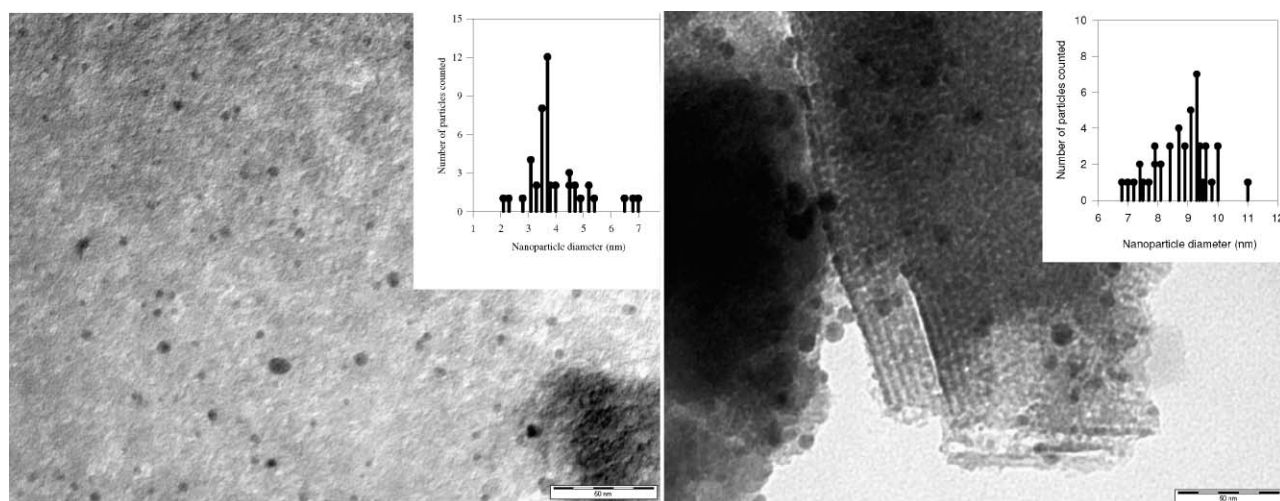


Fig. 6 TEM micrographs and nanoparticle size distribution (inset) of Ag-SBA-12 materials prepared in a domestic microwave oven: Ag-SBA-2 ($\times 300\,000$, 50 nm bar scale) after 2 min (top) and 20 min (bottom) microwave irradiation.

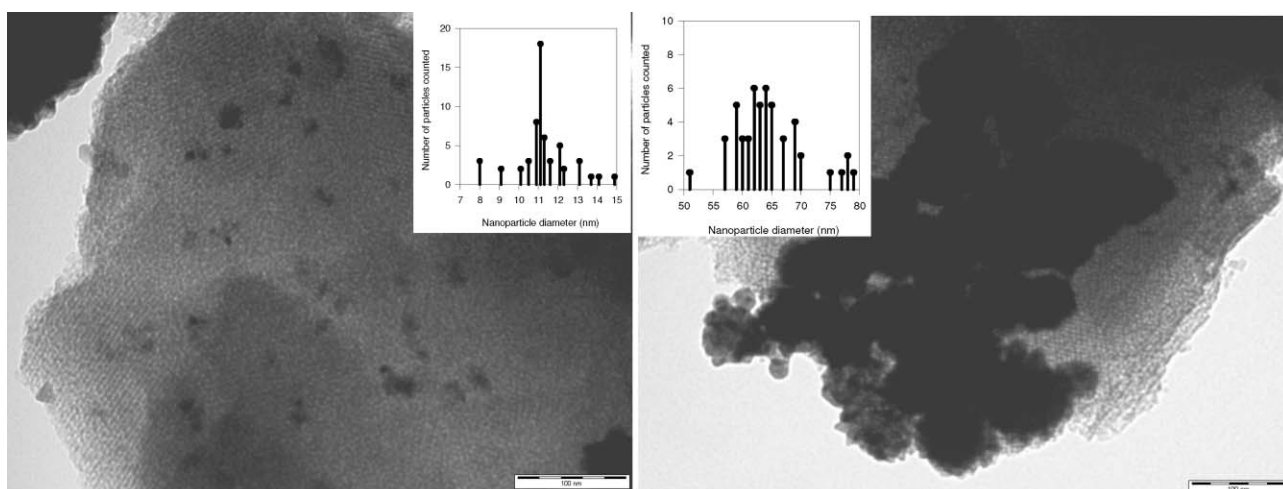


Fig. 7 TEM micrographs and nanoparticle size distribution (inset) of Pd-SBA-12 ($\times 160\,000$, 100 nm bar scale) prepared in a domestic microwave oven after 2 (top) and 20 min (bottom) of microwave irradiation.

Table 2 Catalytic activities [conversion (mol%) and selectivities to the epoxide (S_{epoxide} , mol%), benzaldehyde ($S_{\text{benzaldehyde}}$, mol%) and benzylbenzoate ($S_{\text{benzylbenzoate}}$, mol%)] of metal supported SBA-12 materials in the oxidations of styrene and benzyl alcohol with H_2O_2 under microwave irradiation^a

Material	Oxidation of styrene			Oxidation of benzyl alcohol		
	Conversion (mol%)	S_{epoxide} (mol%)	$S_{\text{benzaldehyde}}$ (mol%)	Conversion (mol%)	$S_{\text{benzaldehyde}}$ (mol%)	$S_{\text{benzylbenzoate}}$ (mol%)
SBA-12	<5	—	—	—	—	—
Au-SBA-12	75	>99	—	50	>95	—
Ag-SBA-12	90	85 ^b	—	<15	>99	—
Pd-SBA-12	>95	—	>95 ^c	68	>95	<5
Pd-SBA-12 ^d	85	—	>99	>99	90	>5

^a 5 mmol starting material, 15 mmol H_2O_2 , 0.1 g catalyst, 300 W (maximum power output), 100–50 °C, 30 min. ^b Phenylacetaldehyde was obtained as major byproduct. ^c Minor quantities of benzoic acid were obtained. ^d 20 min mw irradiation.

Table 3 Reproducibility of the activity of various metal supported SBA-12 materials in the oxidation of styrene with H_2O_2 under microwave irradiation^a

Material	Conversion (mol%)	Selectivity epoxide (mol%)	Selectivity benzaldehyde (mol%)
Au-SBA-12-batch 1	75	>99	—
Au-SBA-12-batch 2	82	>99	—
Au-SBA-12-batch 3	80	>99	—
Au-SBA-12-batch 4	79	>99	—
Ag-SBA-12-batch 1	90	85 ^b	—
Ag-SBA-12-batch 2	87	90 ^b	—
Ag-SBA-12-batch 3	95	83 ^b	—
Pd-SBA-12-batch 1	> 95	—	>95 ^c
Pd-SBA-12-batch 2	> 99	—	>95 ^c
Pd-SBA-12-batch 3	> 99	—	>95 ^c

^a 5 mmol styrene, 15 mmol H_2O_2 , 0.1 g catalyst, 300 W (maximum power output), 100–150 °C, 30 min. ^b Phenylacetaldehyde was obtained as major byproduct. ^c Minor quantities of benzoic acid were obtained.

Judging from the experimental data obtained, it seems that the formation of supported MNP with a narrow size distribution can be achieved under microwave irradiation in a very short period of time (<3 min) using a domestic microwave oven.

MNP with different shapes have different crystallographic faces. It is therefore of interest to study the effect of their shapes and sizes on their catalytic activity in various reactions. The catalytic activity of metal supported SBA-12 materials was investigated in the oxidations of styrene and benzyl alcohol with hydrogen peroxide under microwave irradiation. Results are summarized in Table 2. The oxidation of styrene has been reported to be sensitive to single crystal surfaces in silver.¹⁴

The supported MNP were found to be extremely active and differently selective in the oxidation of styrene. Au- and Ag-SBA-12 promoted the formation of the styrene oxide, and only minor quantities of phenylacetaldehyde were found. Compared to Au and Ag, Pd-SBA-12 materials exhibited great selectivities to benzaldehyde. Au-, Ag- and Pd-SBA-12 materials had different activities in the oxidation of benzyl alcohol. While Ag-SBA-12 was not active, Au- and Pd-SBA-12 exhibited a moderate activity in the oxidation. An increase in metal loading provided quantitative conversion of starting material (Table 2). Almost complete selectivities to benzaldehyde, with minor quantities (<5%) of various by-products, including benzoic acid and benzylbenzoate, were obtained.

The catalytic activity of the materials was also highly reproducible (Table 3). MNP obtained in four different batches exhibited very similar activities and selectivities under identical reaction conditions.

Conclusions

We report a facile and environmentally friendly protocol for the preparation of MNP on SBA-12 using a domestic microwave oven in a very short period of time. Samples were highly active and differently selective depending on the supported metal. The nanoparticle size can be easily controlled for an optimum performance in a particular application (e.g. catalysis) therefore making the supported materials of extreme interest.

References

- (a) C. T. Kresge, M. E. Leonowicz, W. J. Roth, J. C. Vartuli and J. S. Beck, *Nature*, 1992, **359**, 710–12; (b) J. S. Beck, J. C. Vartuli, W. J. Roth, M. E. Leonowicz, C. T. Kresge, K. D. Schmitt, C. T. W. Chu, D. H. Olson, E. W. Sheppard, S. B. McCullen, J. B. Higgins and J. L. Schlenker, *J. Am. Chem. Soc.*, 1992, **114**, 10834–10843; (c) A. Taguchi and F. Schüth, *Microporous Mesoporous Mater.*, 2005, **77**, 1–5; (d) G. E. Fryxell, *Inorg. Chem. Commun.*, 2006, **9**, 1141–1150.
- (a) D. Trong-On, D. Desplandier-Giscard, C. Danumah and S. Kaliaguine, *Appl. Catal., A*, 2003, **253**, 545–553; (b) G. Øye, W. R. Glomm, T. Vrålstad, S. Volden, H. Magnusson, M. Stöcker and J. Sjöblom, *Adv. Colloid Interface Sci.*, 2006, **123–126**, 17–32; (c) J. Y. Ying, C. P. Mehnert and M. S. Wong, *Angew. Chem., Int. Ed.*, 1999, **38**, 56–77.
- (a) J. M. Campelo, D. Luna, R. Luque, J. M. Marinas, A. A. Romero, J. J. Calvino and M. P. Rodriguez-Luque, *J. Catal.*, 2005, **230**, 327–338; (b) R. Luque, J. M. Campelo, D. Luna, J. M. Marinas and A. A. Romero, *Microporous Mesoporous Mater.*, 2005, **84**, 11–0.
- D. Zhao, Q. Huo, J. Feng, B. F. Chmelka and G. D. Stucky, *J. Am. Chem. Soc.*, 1998, **120**, 6024–6036.
- (a) D. Zhao, J. Feng, Q. Huo, N. Melosh, G. H. Fredrickson, B. F. Chmelka and G. D. Stucky, *Science*, 1998, **279**, 548–552; (b) D. Zhao, P. Yang, N. Melosh, J. Feng, B. F. Chmelka and G. D. Stucky, *Adv. Mater.*, 1998, **10**, 1380–1385; (c) B. Karimi, A. Biglari, J. H. Clark and V. Budarin, *Angew. Chem., Int. Ed.*, 2007, **46**, 1–5; (d) G. Du,

- S. Lin, M. Pinault, C. Wang, F. Fang, L. Pfefferle and G. L. Haller, *J. Catal.*, 2008, **253**, 74–90.
- 6 Y. Sakamoto, I. Diaz, O. Terasaki, D. Zhao, J. Perez-Pariente, J. M. Kim and G. D. Stucky, *J. Phys. Chem. B*, 2002, **106**, 3118–3123.
- 7 (a) I. Diaz, F. Mohino, J. Perez-Pariente and E. Sastre, *Stud. Surf. Sci. Catal.*, 2001, **135**, 1383–1390; (b) J. P. Gabaldon, M. Bore and A. K. Datye, *Top. Catal.*, 2007, **44**, 253–62.
- 8 (a) N. Lewis, *Chem. Rev.*, 1993, **93**, 2693–2730; (b) X. Wang, C. E. Egan, M. Zhou, K. Prince, D. R. G. David and R. A. Caruso, *Chem. Commun.*, 2007, 3060–3062; (c) J. K. Edwards, A. Thomas, A. F. Carley, A. A. Herzing, C. J. Kiely and G. J. Hutchings, *Green Chem.*, 2008, **10**, 388–394.
- 9 (a) R. J. Chimentao, I. Kirm, F. Medina, X. Rodriguez, Y. Cesteros, P. Salagre and J. E. Sueiras, *Chem. Commun.*, 2004, 846–847; (b) P. Raveendran, J. Fu and S. L. Wallen, *Green Chem.*, 2006, **8**, 34–38.
- 10 (a) B. Karimi, S. Abedi, J. H. Clark and V. Budarin, *Angew. Chem., Int. Ed.*, 2006, **45**, 4776–4779; (b) V. Budarin, J. H. Clark, R. Luque, D. J. Macquarrie and R. J. White, *Green Chem.*, 2008, **10**, 382–387.
- 11 (a) V. Budarin, J. H. Clark, R. Luque, D. J. Macquarrie, K. Milkowski and R. J. White, *PCT International Patent* WO 2007104798 A2 20070920, 2007; (b) V. Budarin, J. H. Clark, R. Luque, D. J. Macquarrie and R. J. White, *GB Patent Application*, 2007.
- 12 (a) Q. Huo, R. Leon, P. M. Petroff and G. D. Stucky, *Science*, 1995, **268**, 1324–327; (b) Q. Huo, D. I. Margolese and G. D. Stucky, *Chem. Mater.*, 1996, **8**, 1147–160.
- 13 I. Pastoriza-Santos and L. M. Liz-Marzan, *Langmuir*, 2002, **18**, 2888–2894.
- 14 X. Liu, A. Klust, R. J. Madix and C. M. Friend, *J. Phys. Chem. C*, 2007, **111**, 3675–3679.

Green synthesis of silver and palladium nanoparticles at room temperature using coffee and tea extract

Mallikarjuna N. Nadagouda† and Rajender S. Varma*

Received 19th March 2008, Accepted 16th May 2008

First published as an Advance Article on the web 1st July 2008

DOI: 10.1039/b804703k

An extremely simple green approach that generates bulk quantities of nanocrystals of noble metals such as silver (Ag) and palladium (Pd) using coffee and tea extract at room temperature is described. The single-pot method uses no surfactant, capping agent, and/or template. The obtained nanoparticles are in the size range of 20–60 nm and crystallized in face centered cubic symmetry. The method is general and may be extended to other noble metals such as gold (Au) and platinum (Pt).

Introduction

Noble metal nanoparticles have found widespread use in several technological applications,^{1–5} and various wet chemical synthesis methods have been reported.^{6–14} There is a great interest in synthesizing metal and semiconductor nanoparticles due to their extraordinary properties which differ from when they are in bulk. Recently, there is a renewed interest in using green chemistry principles to synthesize metal nanoparticles.^{8,15–25} For example, silver and gold nanoparticles produced from vegetable oil can be used in antibacterial paints.²⁶ Green chemistry is the design, development and implementation of chemical products and processes to reduce or eliminate the use and generation of substances hazardous to human health and the environment.²⁵ Strategies to address mounting environmental concerns with current approaches include the use of environmentally benign solvents, biodegradable polymers and non toxic chemicals. In the synthesis of metal nanoparticles by reduction of the corresponding metal ion salt solutions, there are three areas of opportunity to engage in green chemistry: (i) choice of solvent, (ii) the reducing agent employed, and (iii) the capping agent (or dispersing agent) used. In this area, there has also been increasing interest in identifying environmentally friendly materials that are multifunctional. For example, the caffeine/polyphenols used in this study functions both as a reducing and capping agent for Ag and Pd nanospheres. In addition to its high water solubility, low toxicity, and biodegradability, caffeine is the most widely used behaviourally active drug in the world. In North America, 80–90% of adults report regular use of caffeine. However, there are no reports on preparation of noble metals using caffeine, which also play a crucial role in many medical applications. Hence, this paper reports, for the first time, preparation of noble metals like Ag and Pd using tea/coffee

extract. Caffeine/polyphenols can form complexes with metal ions in solution and reduce them to the corresponding metals. This approach therefore addresses several key requirements from a green chemistry perspective.

Experimental

To prepare the coffee extract, 400 mg of coffee powder (Tata Bru coffee powder 99%) was dissolved in 50 mL of water. Then 2 ml of 0.1 N AgNO₃ (AgNO₃, Aldrich, 99%) was mixed with 10 ml of coffee extract and shaken to ensure thorough mixing. The reaction mixture was allowed to settle at room temperature. For the tea extract, 1 g of tea powder (Red label from Tata, India Ltd. 99%) was boiled in 50 ml of water and filtered through a 25 µm Teflon filter. A similar procedure was repeated for Pd nanoparticles (using 0.1 N PdCl₂, Aldrich, 99%). To evaluate the source (tea and coffee extract) effect on morphology of the Ag and Pd nanoparticles prepared, several experiments were performed employing the above described procedure using the sources as shown in Table 1.

For transmission electron microscopy (TEM), 0.1 mL of the product was dispersed in 5 mL water. TEM grids were prepared by placing a drop of the particle solution on a carbon-coated copper grid and drying at room temperature. The samples for UV-visible measurements were the reaction mixtures that were dispersed in distilled water. TEM was performed with a JEOL-1200 EX II microscope operated at 120 kV. XRD patterns were obtained from Scintag X-ray diffractometer at 2 theta range 2–60° using CuKα radiation. Open-circuit voltage potentials were obtained using 1 M NaCl with reference to a saturated calomel electrode (SCE).

Table 1 Various brands of tea/coffee used to generate nanoparticles

Item	Brand Names
1	Sanka coffee
2	Bigelow tea
3	Luzianne tea
4	Starbucks coffee
5	Folgers coffee
6	Lipton tea

Sustainable Technology Division, US Environmental Protection Agency, National Risk Management Research Laboratory, 26 West Martin Luther King Drive, MS 443, Cincinnati, OH, 45268, USA.
E-mail: varma.rajender@epa.gov; Fax: +1 (513) 569-7677;
Tel: +1 (513) 487-2701

† Present Address: Pegasus Technical Services, 46 E Hollister Street, Cincinnati, Ohio 45219, USA

Results and discussion

TEM results show that Ag and Pd nanoparticles of varying sizes were formed using coffee and tea extract (Fig. 1a–d). At low magnification, a number of highly polydisperse Ag nanoparticles of varying sizes were observed (Fig. 1a,b). It is evident from the TEM image that Ag nanoparticles were well-separated from each other with an apparently uniform inter-particle separation. This indicates that the Ag nanoparticles were capped by organic molecules, namely polyphenols and caffeine. Pd nanoparticles seemed to be smaller than Ag nanoparticles and the inter-particle distance was uniformly separated and well aligned (Fig. 1c,d).

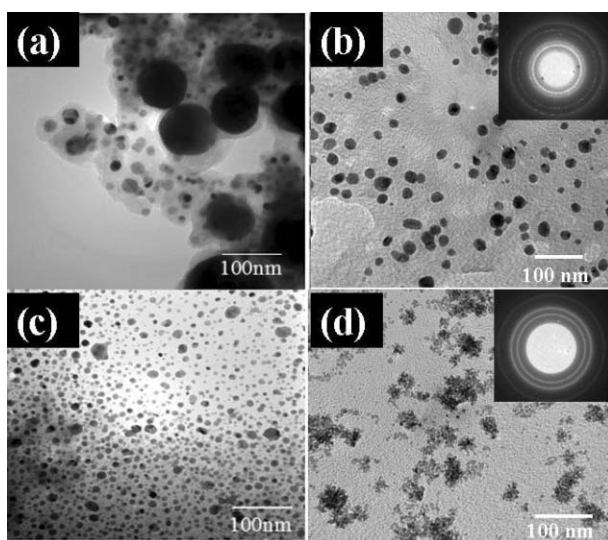


Fig. 1 TEM images of Ag and Pd nanoparticles in aqueous solutions of coffee and tea extract cast on a Cu grid coated with carbon, (a–b) Ag nanoparticles from coffee and tea extract, respectively, and (c–d) Pd nanoparticles from coffee and tea extract, respectively. The inset shows corresponding selected area diffraction patterns.

It is interesting to note that polyphenols acted as a reducing agent as well as a capping agent for the ensuing nanoparticles in the range of 20–60 nm. The control experiments carried out with pure catechin yielded tennis ball-like structures for Au (see Fig. 2) However, pure caffeine yielded wire-like structures for Au (see Fig. 3). The reaction with AgNO_3 was very slow with less yield, and Pd forms a complex without any definite structure. This strategy was extended to different coffee and tea sources (Table 1), and corresponding TEM images are shown in Fig. 4 and 5. The Ag and Pd nanoparticles were found to be mostly spherical with sizes ranging from as low as 5 nm to 100 nm depending upon the source of coffee or tea extract used (see Fig. 4 and 5).

The control experiments carried out with pure catechin yielded spherical structures for Ag and Pd (see Fig. 6).

The formation mechanism of Ag and Pd was studied using UV spectroscopy, which has proved to be a very useful technique for the analysis of nanoparticle formation over time. In order to determine completion of the reaction, 0.1 N AgNO_3 was reacted with tea extract and spectra were recorded every 20 minutes. Initially, no characteristic plasma resonance peak was observed at 1 minute. After 20 minutes of reaction, the plasma resonance

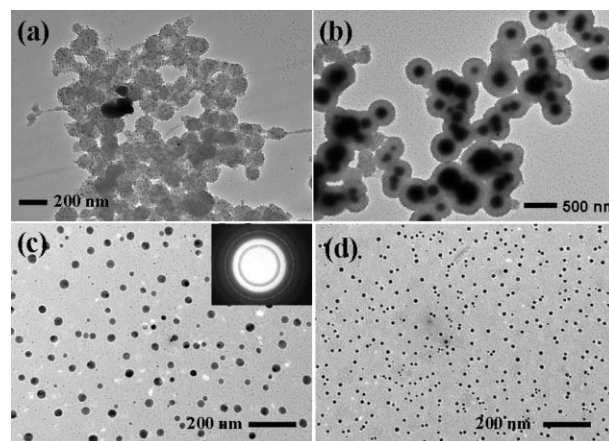


Fig. 2 TEM images of gold nanoparticles (2 mL 0.01 N) reduced with (a) 2 mL (b) 4 mL (c) 6 mL and (d) 8 mL of catechin (0.1 N) aqueous solution. The inset shows corresponding selected area diffraction pattern.

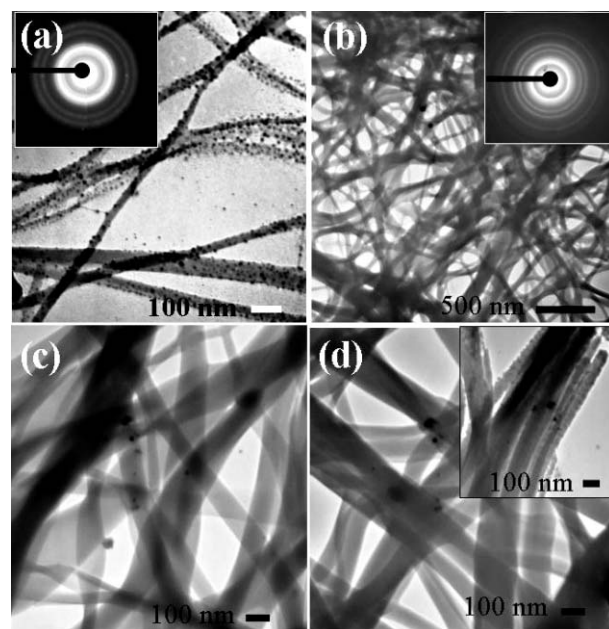


Fig. 3 TEM images of gold nanowires (2 mL of 0.01 N) reduced with (a) with 25 mg (b) 100 mg (c) 200 mg and (d) 300 mg of pure caffeine. The inset in (a–b) shows corresponding selected area diffraction pattern and in (d) shows different magnification image.

peak at ~ 460 nm started appearing and became more prominent at 60 minutes. The reaction was completed after 120 minutes, as there was no increase in intensity of the plasma resonance peak (see Fig. 7a–f). A strong absorption peak was observed at ~ 340 nm corresponding to the absorption of polyphenol compounds present in the tea.

UV spectra of Ag and Pd nanoparticles prepared from coffee and tea extracts are shown in Fig. 8. The broad plasma resonance peak at 460 nm corresponds to Ag nanoparticles prepared from coffee and tea extract (see Fig. 8a,b). The continuous absorption in the UV region was observed for Pd nanoparticles prepared from coffee and tea extract as expected (see Fig. 8c,d). The observation of strong but broad surface plasmon peaks is well

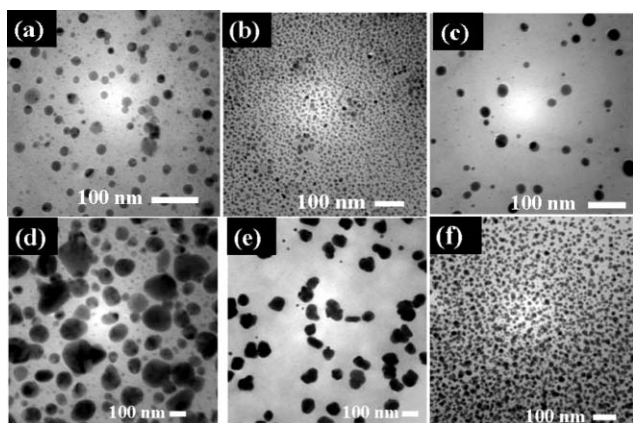


Fig. 4 TEM image of silver nanoparticles synthesized using (a) Bigelow tea, (b) Folgers coffee, (c) Lipton tea, (d) Luzianne tea, (e) Sanka coffee and (f) Starbucks coffee extract at room temperature in one step without using any hazardous reducing chemicals or non-degradable capping agents.

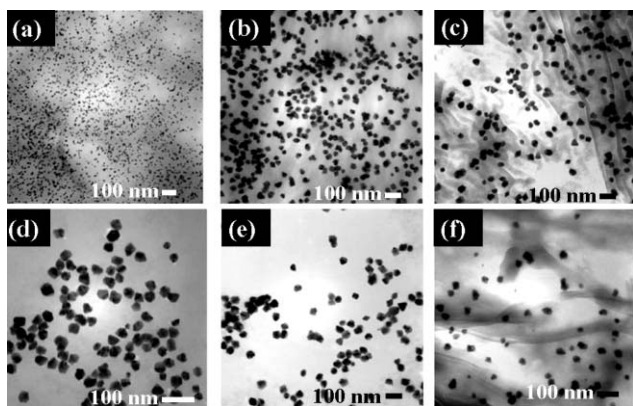


Fig. 5 TEM image of palladium nanoparticles synthesized using (a) Sanka coffee, (b) Bigelow tea, (c) Luzianne tea, (d) Starbucks coffee, (e) Folgers coffee and (f) Lipton tea extract at room temperature in one step without using any hazardous reducing chemicals or non-degradable capping agents.

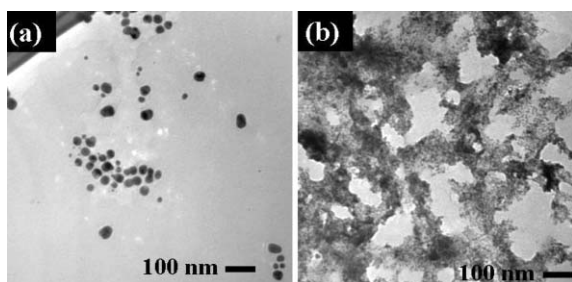


Fig. 6 TEM images of Ag and Pd nanoparticles respectively prepared in aqueous solution using catechin.

known in the case of various metal nanoparticles over a wide range of 200–1200 nm.

The reduction potential of caffeine is ~ 0.3 V vs. SCE (see Fig. 9) which is sufficient to reduce metals *viz.* Pd (reduction potential 0.915 V vs. SCE) and Ag (reduction potential 0.80 V vs. SCE), as well as Au^{+3} to Au^0 (reduction potential is 1.50 V vs. SCE) and Pt (reduction potential 1.20 V vs. SCE). The formation of Ag and Pd nanoparticles with caffeine/polyphenols takes

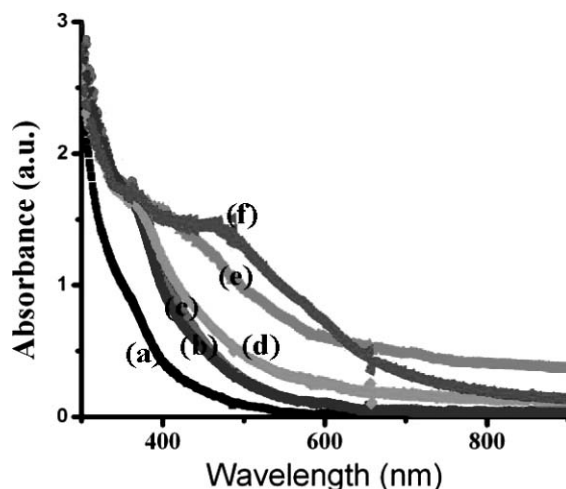


Fig. 7 Reaction profile of tea extract with AgNO_3 over the time; (a) pure tea extract, after (b) 1 min (c) 20 min (d) 40 min (e) 60 min and (f) 2 h.

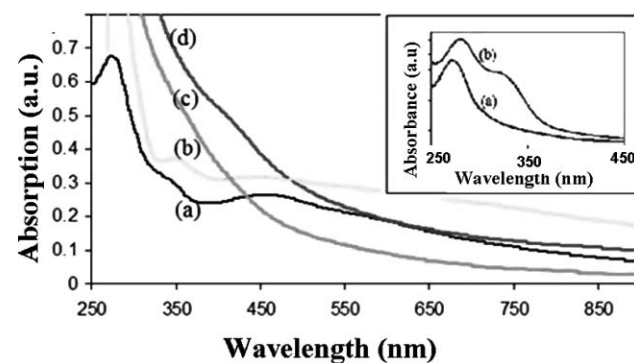


Fig. 8 UV-Vis spectra of Ag and Pd nanoparticles in aqueous solution of coffee and tea leaves extract. (a) Ag nanoparticles from coffee extract, (b) Ag nanoparticles from tea extract, (c) Pd nanoparticles from coffee extract and (d) Pd nanoparticles from tea extract. The inset shows UV-Vis of (a) coffee and (b) tea extract.

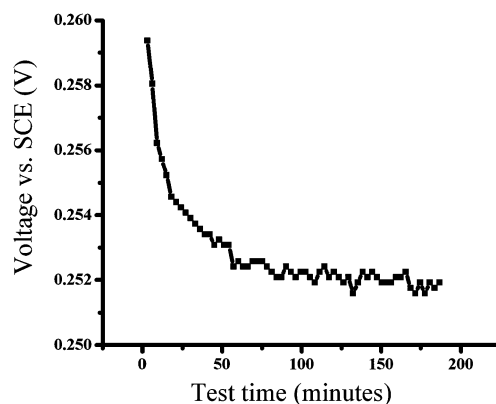


Fig. 9 Open-circuit potential for (V_{oc}) coffee extract in 1 M NaCl.

place *via* the following steps: (1) complexation with Ag and Pd metal salts, (2) simultaneous reduction of Ag and Pd metal, and (3) capping with oxidized polyphenols/caffeine.

Fig. 10a–d shows the XRD patterns of Ag and Pd nanoparticles obtained from coffee and tea extracts, respectively, from

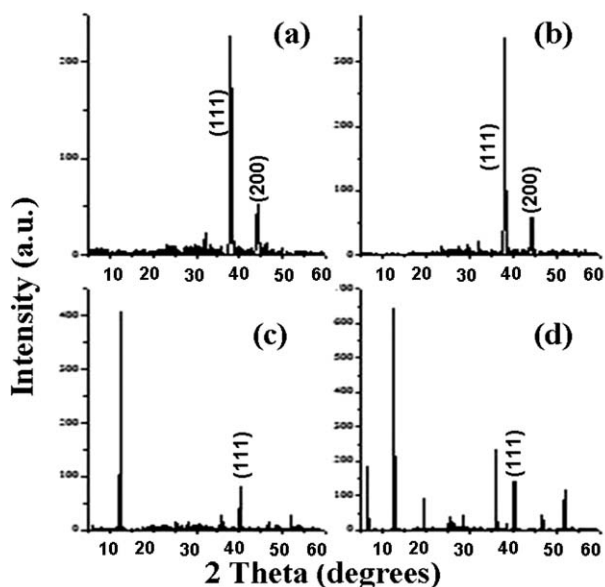


Fig. 10 Representative XRD patterns of nanoparticles in aqueous solution of coffee and tea extract casted on glass plate (a–b) Ag nanoparticles from coffee and tea extract, respectively, and (c–d) Pd nanoparticles from coffee and tea extract, respectively.

an aqueous solution drop-coated film on glass plate. From the XRD patterns, prominent Bragg reflections at 2θ values of 38.3 and 42.6 were observed, which correspond to the (111) and (200) Bragg reflections of face centered cubic (fcc) Ag nanoparticles (Fig. 10a,b).² However, in the case of Pd nanoparticles, layered structures of caffeine²⁷ remained, with a well developed progression of intense reflections, which are successive orders of diffraction with a large d spacing (see Fig. 10c,d). It is clear that diffraction patterns can be interpreted in terms of a crystal structure in which Pd and caffeine molecules occurred in regularly stacked layers with a very large interlayer lattice dimension, and that the interlayer two dimensional lattice possessed relatively small distances. The presence of narrow interlayer reflections indicates that there is crystallographic registry of layers.

Conclusions

In summary, for the first time, we have synthesized Ag and Pd nanoparticles using coffee and tea extracts. Specifically, we describe an environmentally friendly one-step method to synthesize noble nanoparticles, such as Ag and Pd, by reduction of corresponding metal solutions using tea and coffee extract without usage of any special capping agents at room temperature. This green approach may find various medicinal as well as technological applications. The method is general and may be extended to other noble metals such as Au and Pt.

Acknowledgements

Part of the work was initiated and conducted at the University of Texas at Dallas (UT Dallas). We gratefully acknowledge helpful discussions with the late Dr Alan G. MacDiarmid and Dr Sanjeev K. Manohar, and for financial support from UT Dallas. MNN was supported, in part, by the Postgraduate Research Program at the National Risk Management Research Laboratory administered by the Oak Ridge Institute for Science and Education through an interagency agreement between the U.S. Department of Energy and the U.S. Environmental Protection Agency.

References

- X. Wang and Y. Li, *Chem. Commun.*, 2007, 2901.
- Y. Sun and Y. Xia, *Science*, 2002, **298**, 2176.
- J. Chen, J. M. McLellan, A. Siekkinen, Y. Xiong, Z.-Y. Li and Y. Xia, *J. Am. Chem. Soc.*, 2006, **128**, 14776.
- J. W. Stone, P. N. Sisco, E. C. Goldsmith, S. C. Baxter and C. J. Murphy, *Nano Lett.*, 2007, **7**, 116.
- B. Wiley, Y. Sun and Y. Xia, *Acc. Chem. Res.*, 2007, **40**, 1067.
- J. Du, B. Han, Z. Liu and Y. Liu, *Cryst. Growth Design*, 2007, **7**, 900.
- B. Wiley, T. Herricks, Y. Sun and Y. Xia, *Nano Lett.*, 2004, **4**, 2057.
- C. J. Murphy, A. M. Gole, S. E. Hunyadi and C. J. Orendorff, *Inorg. Chem.*, 2006, **45**, 7544.
- B. J. Wiley, Y. Chen, J. M. McLellan, Y. Xiong, Z.-Y. Li, D. Ginger and Y. Xia, *Nanoletters*, 2007, **4**, 1032.
- Y. Xiong, H. Cai, B. J. Wiley, J. Wang, M. J. Kim and Y. Xia, *J. Am. Chem. Soc.*, 2007, **129**, 3665.
- J. Fang, H. You, P. Kong, Y. Yi, X. Song and B. Ding, *Cryst. Growth Design*, 2007, **7**, 864.
- A. Narayan, L. Landstrom and M. Boman, *Appl. Surf. Sci.*, 2003, **137**, 208.
- H. Song, R. M. Rioux, J. D. Hoefelmeyer, R. Komor, K. Niesz, M. Grass, P. Yang and G. A. Somorjai, *J. Am. Chem. Soc.*, 2006, **128**, 3027.
- C. C. Wang, D. H. Chen and T. C. Huang, *Colloids Surf. A*, 2001, **189**, 145.
- M. N. Nadagouda and R. S. Varma, *Green Chem.*, 2006, **8**, 516.
- P. Raveendran, J. Fu and S. L. Wallen, *J. Am. Chem. Soc.*, 2003, **125**, 13940.
- M. N. Nadagouda and R. S. Varma, *Green Chem.*, 2007, **9**, 632.
- R. R. Naik, S. J. Stringer, G. Agarwal, S. E. Jones and M. O. Stone, *Nat. Mater.*, 2002, **1**, 169.
- M. N. Nadagouda and R. S. Varma, *Macromol. Rapid Commun.*, 2007, **28**, 465.
- M. N. Nadagouda and R. S. Varma, *Biomacromolecules*, 2007, **8**, 2762–2767.
- M. N. Nadagouda and R. S. Varma, *Cryst. Growth Design*, 2007, **7**(12), 2582–2587.
- M. N. Nadagouda and R. S. Varma, *Cryst. Growth Design*, 2007, **7**(4), 686–690.
- M. N. Nadagouda and R. S. Varma, *Cryst. Growth Design*, 2008, **8**(1), 291–295.
- J. A. Dahl, L. S. Maddux and J. E. Hutchison, *Chem. Rev.*, 2007, **107**, 2228.
- P. T. Anastas and J. C. Warner, *Green, Chemistry: Theory and Practice*, Oxford University Press, Inc., New York, 1998.
- A. Kumar, P. K. Vemula, P. M. Ajayan and G. John, *Nat. Mater.*, 2008, **7**, 236–241.
- L. M. Juliano and R. R. Griffiths, *Psychopharmacology*, 2004, **176**, 1.

HRP-mediated inverse emulsion polymerisation of acrylamide in supercritical carbon dioxide

Silvia Villarroya,* Kristofer J. Thurecht and Steven M. Howdle*

Received 10th March 2008, Accepted 21st May 2008

First published as an Advance Article on the web 10th July 2008

DOI: 10.1039/b804080j

We report the horseradish peroxidase (HRP)-mediated inverse emulsion polymerisation of water-soluble acrylamide in supercritical carbon dioxide (scCO₂). The enzymatic polymerisation takes place within water droplets formed in scCO₂. These are either stabilised as reversed micelles using perfluoropolyether ammonium carboxylate (PFPE-COO⁻NH₄⁺) or in the absence of stabiliser using very high shear. The viability of water-in-CO₂ (W/C) emulsion as a reaction medium for *in-situ* enzyme-mediated polymerisation has been tested for the first time. There is significant interest in enzymes as they have proven to be powerful and environmentally friendly natural catalysts for the polymerisation of water-soluble monomers that can function under milder reaction conditions than those used in traditional free radical polymerisation techniques. Hence, the combination of scCO₂ and water as reaction medium is a significant advancement in natural polymerisation process.

Introduction

Enzymes have proven to be powerful catalysts for the polymerisation of a wide variety of monomers and macromonomers.¹ Enzyme-mediated polymer synthesis has gained much attention because it offers many advantages in comparison to polymerisation catalysed by traditional catalysts, for instance: (i) high selectivity under mild conditions, (ii) applicability to a very wide range of solvents (*e.g.* water, organic solvents, micelles), (iii) and the potential to synthesise products in high yields. They represent a family of “environmentally-friendly” natural catalysts that might replace potentially toxic catalysts.¹

Horseradish peroxidase (HRP) is well known to catalyse the oxidation of organic substances (phenols and anilines) using hydrogen peroxide (H₂O₂) and/or alkyl peroxide.² The generally accepted mechanism involves the production of free radicals.³ The potential of HRP to catalyse free radical polymerisation of vinyl monomers was first reported by Derango *et al.*⁴ Others have also exploited the enzymatic route, reporting HRP-mediated free radical polymerisation of acrylamide in water^{5,6} and in the presence of surfactants.⁷

Conventionally, the polymerisation is carried out by inverse emulsion using a wide range of surfactants and solvents. Different types of initiation have been used, from oil-soluble AIBN^{8,9} and water-soluble ammonium persulfate^{10,11} to UV initiation.¹² More recently, RAFT inverse miniemulsion polymerisation of acrylamide has been reported.¹³ However, to our knowledge, an enzymatic route to an inverse emulsion has not been reported.

A very promising solvent for polymerisation is supercritical carbon dioxide (scCO₂). Supercritical fluids exhibit liquid-like

densities and gas-like mass transfer, which make them very attractive solvents for polymerisation.¹⁴ ScCO₂ is among the more attractive supercritical solvents because its critical point is easy to reach ($T_c = 31.1\text{ }^\circ\text{C}$, $P_c = 73.8\text{ bar}$), it is inexpensive, non-flammable, non-toxic and environmentally inert. Homogeneous polymerisations in scCO₂ have been reported for the preparation of fluoropolymers which are soluble in the CO₂ phase.¹⁵ However, the majority of polymers are insoluble in scCO₂ and may be dispersed by the addition of surfactant to support successful heterogeneous polymerisation.^{16,17}

Another major limitation to the broader use of scCO₂ is its inability to dissolve a wide range of hydrophilic and ionic compounds. An alternative strategy is the use of CO₂-soluble surfactants to emulsify monomers into the CO₂ phase. Hile *et al.* reported the emulsion copolymerisation of D,L-lactide and glycolide in scCO₂ using a fluorocarbon polymer as the emulsifying agent.^{18,19} More recently, the emulsion polymerisation of water soluble/CO₂ insoluble monomer *N*-ethylacrylamide was effectively emulsified in CO₂ continuous phase using an amphiphilic diblock copolymer consisting of a D-glucose containing glycopolymer and a fluorinated block.²⁰

A different approach is emulsion polymerisation in hybrid CO₂/water mixtures. This is based on the formation of aqueous emulsion droplets in a carbon dioxide-continuous phase with a non-toxic surfactant. The formation of reverse micelles and microemulsions in scCO₂ has been reported by several research groups.^{21,22} The most popular emulsions systems in scCO₂ are those based on ammonium carboxylate perfluoropolyether (PFPE) surfactant.^{23,24} Several research groups have shown that inorganic and organic reactions can be performed in a PFPE/H₂O/CO₂ system. Adamsky and Beckman first examined the emulsion polymerisation of acrylamide in CO₂/water mixtures using an amide-functionalised perfluoropolyether surfactant to stabilise the system: a homogeneous milky white latex emulsion was observed during polymerisation.²⁵

School of Chemistry, University of Nottingham, University Park, Nottingham, UK NG7 2RD. E-mail: steve.howdle@nottingham.ac.uk; Fax: +44 (0)115 9513058; Tel: +44 (0)115 9513486

Several research groups have shown that it is possible to carry out enzymatic reactions directly in supercritical fluids such as CO₂ by using immobilized enzymes or enzyme suspensions.^{26–30} In addition, enzymatic catalysis within the water pool of a reverse micelle formed in scCO₂ has been reported.³¹ The W/C microemulsion have been shown to be able to solubilize enzymes, particularly by using perfluoropolyether type surfactants, providing a unique medium for enzyme-catalysed biotransformations.³²

In this paper, we report the enzymatic emulsion polymerisation of water-soluble acrylamide monomers in water-in-CO₂ emulsion. These monomers generally show limited solubility in pure CO₂. Hydrophilic polymers, in particular poly(acrylamide)s are widely used in industry as flocculants in wastewater treatment applications, as additives in paper making and for drug-delivery systems.

Experimental

Materials

Peroxide from horseradish donor: hydrogen-peroxidase oxidoreductase EC 1.11.1.7. Type II (50 000 units) and Type I, (50–150 units per mg solid) were purchased from Sigma–Aldrich and used as received. Acrylamide (Aldrich), H₂O₂ (30% stabilised aqueous solution), 2,4-pentadione (Aldrich) were used as received. The ammonium carboxylate perfluoropolyether surfactant (PFPE-COO⁻NH₄⁺) was prepared by neutralisation of the commercially available acid (Krytox 157 FSL) with ammonia.

Emulsion polymerisation of acrylamide in scCO₂

Polymerisations in scCO₂ were performed in a 60 mL stainless steel clamp sealed autoclave equipped with a magnetically coupled overhead stirrer and a pressure relief valve.³³ In a typical polymerisation, the reaction vessel was loaded with the desired amount of enzyme dissolved in a specific amount of water, the required amount of surfactant (5 wt% based on the monomer and 0.45 wt% based on total weight of H₂O and CO₂) and acrylamide monomer dissolved in water. The autoclave was purged with a slow flow of CO₂ for 5 min to remove oxygen. Hydrogen peroxide (30% (w/v)) and 2,4-pentadione were added to the water phase. The autoclave was then closed, heated to 35 °C and filled with the desired amount of CO₂ to achieve the reaction pressure. The autoclave was stirred at 600 rpm. After 10 hours the reaction was stopped and the pressure released.

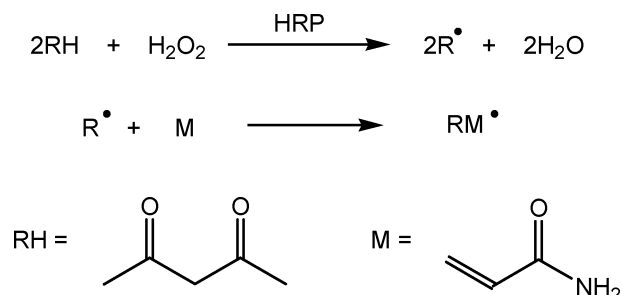
Characterisation

¹H NMR spectra of poly(acrylamide) were obtained in CDCl₃ and were recorded using a Bruker DPX-300 spectrometer (300.14 MHz) referenced to chloroform at 7.28 ppm. Analyses of the spectra was carried out using Mestre-C Software. GPC was performed on a Viscotek “Evolution” instrument provided with PL Aquagel guard plus 2 x mixed bed-OH column, pump and autosampler. 0.2M NaNO₃, 0.01M NaHPO₄ pH 7 was used as the eluent at 30 °C and flow rate of 1 mL min⁻¹. The GPC system was calibrated with poly(ethylene glycol)/poly(ethylene oxide) standards and the results are therefore expressed as “PEG/PEO

equivalent”. The instrument was fitted with an RI detector for molecular weight analysis. A single solution of each sample was prepared by adding 10 mL of eluent to 10 mg of sample and leaving overnight to dissolve. The samples were then warmed for 20 minutes at 40 °C before being cooled, thoroughly mixed and filtered through a 0.45 μm PVDF membrane, with glass-fibre prefilter, prior to chromatography.

Results

The HRP-mediated free radical polymerisation of acrylamide was carried out in an inverse emulsion in water-in-CO₂ mixture. Upon agitation, the enzyme was completely dissolved and the reactor contents adopted a milky appearance similar to that of conventional inverse emulsion polymerisation. The enzyme, hydrogen peroxide and the oxidant 2,4-pentadione need to be present for the polymerization to proceed. No polymer was formed in the absence of enzyme, H₂O₂ or the β-diketone. 2,4-pentadione was selected as reducing agent as it is a good substrate with respect to HRP and it gives radicals able to initiate polymerisation of vinyl monomers. Free radical species are generated along the HRP catalytic cycle and they can be used as primary radicals to initiate vinyl polymerisations according to Scheme 1. Two different commercial peroxidases HRP Type I and HRP type II were evaluated to compare their catalytic activities for acrylamide polymerisation. The yields of poly(acrylamide) when using HRP II and HRP I under the same conditions were 85 and 51% respectively (Table 1, entry 1 and 2). Therefore, HRP Type II was chosen to carry on further studies.



Scheme 1 Enzyme-mediated initiation assuming generation of primary radicals by HRP-catalysed oxidation of a proton donor RH and reaction on vinyl monomer M, where RH is 2,4-pentadione and M is acrylamide.

As previously reported in conventional solvent systems, the optimal ratio of 2,4-pentadione to H₂O₂ was found to be between 1.3–1.5. Initially, 2,4-pentadione and H₂O₂ were used in the ratio 1.58 : 1.00 mol/mol. The ratio of acrylamide to 2,4-pentadione was fixed at 24 : 1 (Table 1, entry 1–4). The effect of varying the concentration of each component was studied. By increasing the concentration of H₂O₂ twofold, the yield decreased from 85 to 65% (Table 1, entry 3). It has been previously shown that high concentration of H₂O₂ causes enzyme degradation, leading in our case to poor monomer conversion.³⁴ It is also shown that the concentration of H₂O₂ does not influence the molecular weight under the conditions of our study (Table 1, entry 3) confirming that chain transfer to H₂O₂ is negligible in our three-component initiating system. The influence of 2,4-pentadione was investigated by increasing the concentration of this compound while keeping the monomer concentration constant

Table 1 HRP-mediated polymerisation of acrylamide in water-in-CO₂ system^a

Entry	Monomer (acrylamide)	Enzyme	Surfactant (PFPE-COO ⁻ NH ₄ ⁺)	H ₂ O ₂	2,4-pentadione	Molar ratio 2,4-pentadione/H ₂ O ₂	Molar ratio acrylamide/2,4-pentadione	Isolated yield (%) ^b	M _n /10 ⁻³ g mol ⁻¹ (GPC) ^c	PDI
1	1 g	33 mg HRP Type II	50 mg	35 µL 0.308 mmol	50 µL 0.488 mmol	1.58	24	85	405	3.0
2	1 g	33 mg HRP Type I	50 mg	35 µL 0.308 mmol	50 µL 0.488 mmol	1.58	24	51	—	—
3	1 g	33 mg HRP Type II	50 mg	70 µL 0.616 mmol	50 µL 0.488 mmol	1.58	24	65	347	3.4
4	1 g	33 mg HRP Type II	50 mg	35 µL 0.308 mmol	100 µL 0.976 mmol	3.15	11.9	87	145	7.4
5	1 g	33 mg HRP Type II	0 mg	35 µL 0.308 mmol	50 µL 0.488 mmol	1.58	24	89	908	2.2

^a Reaction carried out with 1 g of acrylamide (11.63 mmol), 1 mL of water and approx. 10 g of CO₂ at 35 °C and 2500–2700 psi. ^b Yield was obtained gravimetrically after purification from the dried polymer. ^c Molecular weight was determined by aqueous GPC system.

(Table 1, entry 4). We observed lower molecular weight and much higher polydispersity. It is believed that 2,4-pentadione acts as the free radical initiator species for chain growth. Therefore, the higher amount of initiator, the lower molecular weight of polymer that is observed. Furthermore, the increased loading of initiator tends to produce polymers of greater PDI (Fig. 1). In all cases, upon stopping agitation, the material drops to the bottom of the autoclave. The polyacrylamide comes out as a rubbery material from the autoclave. After purification with acetone or methanol the material becomes a brittle solid.

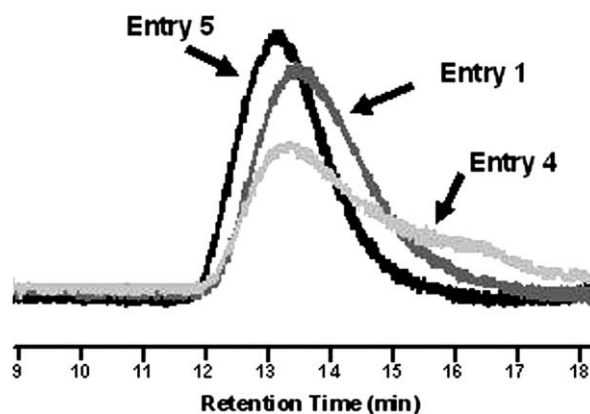


Fig. 1 GPC traces for the HRP-mediated polymerisation of acrylamide in water-in-CO₂ system.

As a result of the formation of carbonic acid, aqueous solutions in contact with CO₂ at elevated pressures are acidic with pH ~ 3.³⁵ However, the pH optimum of HRP is in the range of 6.0 to 6.5.³⁶ It is worth noting that the inherent conditions of low pH of the water droplets in the water-in-CO₂ microemulsion did not inhibit the enzyme activity leading to a very robust method. We also make the point here that we cannot rule out other possible polymerisation mechanisms that might occur due to the very low pH of the water droplets (*e.g.* proton-mediated mechanisms). However, we believe that such processes are probably minimal.

The polymerisation reaction was also performed in the absence of surfactant to yield a very different hard material with high molecular weight (Table 1, entry 5 compared to entry 1). In this experiment, the water was dispersed throughout the scCO₂ phase in small droplets by high shear. DeSimone and coworkers³⁷ reported a similar surfactant-free emulsion polymerisation of methyl methacrylate in a hybrid carbon dioxide/aqueous medium. They showed that poly(methylmethacrylate) latex particles were formed when water-soluble potassium persulfate was used as initiator and a relatively high stirring rate was applied. In our experiment, the inverse emulsion is formed and polymerisation proceeds effectively in the absence of PFPE surfactant. However, the recovery of latex poly(acrylamide) particles at the end of the reaction was impossible because depressurisation results in the agglomeration of poly(acrylamide) due to loss of the dispersive solvent. Although well-defined, spherical particle morphology was not obtained, the polymer still had high monomer conversion leading to high molecular weight.

The kinetics of HRP-mediated polymerization of acrylamide in the water-in-CO₂ system was monitored using ¹H-NMR (Fig. 2). The high-pressure autoclave used for the sampling of the

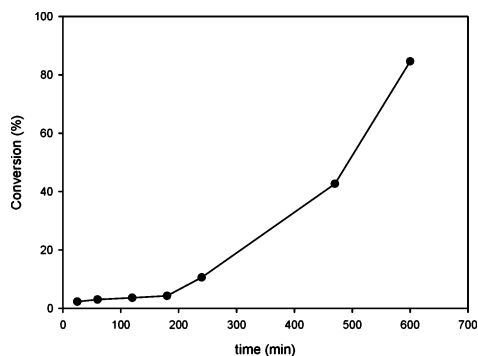


Fig. 2 Free-radical polymerization of acrylamide by HRP-mediated initiation. Conversion–time plot for acrylamide polymerisation in water-in-CO₂ mixture. An inhibition period of 200 minutes was observed. This was caused by traces of oxygen in the mixture.

reaction has been described previously.³⁸ The conversion *versus* time plot showed an initial inhibition period of 200 minutes, after which propagation occurs quite rapidly. This phenomenon was also observed by Lalot³⁹ and Gross⁴⁰ in the HRP-mediated polymerisation of vinyl monomers in water and in aqueous medium with addition of surfactant, respectively. Lalot and Gross reported an inhibition time between 45 and 100 minutes, similar to those observed in our system. They postulated that the inhibition period was caused by traces of residual oxygen in the mixture. In our case, despite exhaustive attempts to remove oxygen from the system, incorporation of some oxygen is inevitable.

A comparison was made of the obtained molecular weight with the results reported by Beckman²⁵ in the inverse emulsion polymerisation of acrylamide in scCO₂ using AIBN as initiator. The molecular weight values reported by Beckman are 4.92×10^6 and 7.09×10^6 for two different surfactant concentration 1% and 2%, respectively. The values obtained for the enzymatic polymerisation of poly(acrylamide) are an order of magnitude lower, with molecular weight ranging from 1.45×10^5 to 4.05×10^5 for different experimental conditions (Table 1), but they are certainly of commercial utility. The difference may be ascribed to the different methodologies used to assess molecular weight, or more likely to the higher initiator loadings (100 times increase in the molar ratio of 2,4-pentadione experiments compared to the AIBN loading²⁵).

Conclusions

We have reported, for the first time, the HRP-mediated inverse emulsion polymerisation of acrylamide in scCO₂ with excellent yields and high molecular weights. Inverse emulsion polymerisation has not been yet thoroughly investigated, but we have shown the potential to produce high-molecular-weight water-soluble polymers. In general, the yields and molecular weights obtained *via* polymerisation in CO₂ are comparable to those generated in a conventional polymerisation in an alkane/water medium. Enzymes have proven to be powerful green catalysts for the polymerisation of a wide variety of monomers and represent an alternative to the heavy metal and/or toxic substances often used in traditional polymerisations. The use of just scCO₂ and water opens up a the possibility of a very green, VOC free system, though of course the challenge now is to identify more

environmentally acceptable surfactant materials that could be used on the commercial scale.

High pressure polymerisations were also carried out in a view cell fitted with sapphire windows in order to visually observe the phase behaviour during the polymerisation and the emulsion formation.

Acknowledgements

This research has been supported by a Marie Curie Intra European Fellow (S.V.; Contract No. MEIF-CT-2005-024092) and the Dutch Polymer Institute (Project 488-K.J.T.). The authors would like to thank Dr Steve Holding from Smithers RAPRA Technology for the aqueous GPC analysis of the poly(acrylamide) samples. S.M.H. is a Royal Society Wolfson Research Merit Award Holder.

Notes and references

- S. Kobayashi, H. Uyama and S. Kimura, *Chem. Rev.*, 2001, **101**, 3793; R. A. Gross, A. Kumar and B. Kalra, *Chem. Rev.*, 2001, **101**, 2097.
- T. E. Barman, *Enzyme Handbook*, Springer-Verlag, New York, 1985, vol. I, p. 234.
- B. C. Saunders, A. G. Holmes-Siedle, B. P. Stark, *Peroxidase*, London, Butterworth, 1994.
- A. R. Derango, L. C. Chiang, R. Dowbenko and J. G. Lasch, *Biotechnol. Technol.*, 1992, **6**, 523.
- O. Emery, T. Lalot, M. Brigodiot and E. Marechal, *J. Polym. Sci., Part A: Polym. Chem.*, 1997, **35**, 3331.
- D. Teixeira, T. Lalot, M. Brigodiot and E. Marechal, *Macromolecules*, 1999, **32**, 70.
- B. Kalra and R. A. Gross, *Green Chem.*, 2002, **4**, 174.
- I. Capek, *Polym. J. (Tokyo, Jpn)*, 2004, **36**, 793.
- A. Thakur, R. K. Wancho, P. Singh and P. Sheoran, *J. Mater. Chem.*, 2006, **23**, 39.
- S. Bi and Z. Lei, *Shanxi Shifan Daxue Xuebao*, 2006, **34**, 63.
- D. Zhang, R. Zhang, M. Zhang, G. Gao, X. Song, D. Wang, F. Liu and Y. Li, *Polym. Prepr. (Am. Chem. Soc., Div. Polym. Chem.)*, 2004, **45**, 1034.
- L. Liu and W. Yang, *Gaofenzi Xuebao*, 2004, **4**, 545.
- G. Qi, C. Jones and F. Schork, *Macromol. Rapid Commun.*, 2007, **28**, 1010.
- J. L. Kendall, D. A. Canelas, J. L. Young and J. M. DeSimone, *Chem. Rev.*, 1999, **99**, 543.
- J. M. DeSimone, Z. Guan and C. S. Elsbernd, *Science*, 1992, **257**, 945.
- A. I. Cooper, *J. Mater. Chem.*, 2000, **10**, 207.
- H. M. Woods, M. M. C. G. Silva, C. Nouvel, K. M. Shakesheff and S. M. Howdle, *J. Mater. Chem.*, 2004, **14**, 1663.
- D. D. Hile and M. V. J. Pishko, *J. Polym. Sci., Part A: Polym. Chem.*, 2001, **39**, 562.
- D. Bratton, M. Brown and S. M. Howdle, *J. Polym. Sci., Part A: Polym. Chem.*, 2005, **43**, 6573.
- W. Ye and J. M. DeSimone, *Macromolecules*, 2005, **38**, 2180.
- K. J. Thurecht, D. J. T. Hill and A. K. Whittaker, *J. Supercrit. Fluids*, 2006, 111.
- R. G. Zienlinski, S. R. Kline, E. W. Kalter and N. Rosov, *Langmuir*, 1997, 3934.
- S. R. P. da Rocha and K. P. Johnston, *Langmuir*, 2000, 3690.
- J. Eastoe, A. Dupont and D. C. Steytler, *Curr. Opin. Colloid Interface Sci.*, 2003, 267.
- F. A. Adamsky and E. J. Beckman, *Macromolecules*, 1994, **27**, 312.
- A. J. Mesiano, E. J. Beckman and A. J. Russell, *Chem. Rev.*, 1999, **99**, 623.
- Z. Knez, M. Habulin and M. Primožic, *Biochem. Eng. J.*, 2005, **27**, 120.
- F. C. Loeker, C. J. Duxbury, R. Kumar, W. Gao, R. A. Gross and S. M. Howdle, *Macromolecules*, 2004, **37**, 2450.

- 29 J. Zhou, S. Villarroya, W. Wang, M. F. Wyatt, C. J. Duxbury, K. J. Thurecht and S. M. Howdle, *Macromolecules*, 2006, **39**, 5352.
- 30 S. Villarroya, K. J. Thurecht, A. Heise and S. M. Howdle, *Chem. Commun.*, 2007, 3805.
- 31 J. D. Holmes, D. C. Steytler, G. D. Rees and B. H. Robinson, *Langmuir*, 1998, **14**, 6371.
- 32 K. P. Johnston, K. L. Harrison, M. J. Clarke, S. M. Howdle, M. P. Heitz, F. V. Bright, C. Carlier and T. W. Randolph, *Science*, 1996, **271**, 624.
- 33 F. Furno, P. Licence, S. M. Howdle and M. Poliakoff, *Acta Chim.*, 2003, 62.
- 34 A. Durand, T. Lalot, M. Brigodiot and E. Marechal, *Polymer*, 2001, 5515.
- 35 S. V. Kamat, E. J. Beckman and A. J. Russell, *Crit. Rev. Biotechnol.*, 1995, **15**, 41.
- 36 D. Schomberg, M. Salzman, D. Stephan, *Enzyme Handbook*, Springer Verlag, Berlin, vol. 7, 1993, EC 1.11.1.7:1–6.
- 37 M. A. Quadir, R. Snook, R. G. Gilbert and J. DeSimone, *Macromolecules*, 1997, **30**, 6015.
- 38 K. J. Thurecht, A. Heise, M. de Geus, S. Villarroya, J. Zhou, M. F. Wyatt and S. M. Howdle, *Macromolecules*, 2006, **39**, 7967.
- 39 T. Lalot, M. Brigodiot and E. Marechal, *Polym. Int.*, 1999, 288.
- 40 B. Kalra and R. A. Gross, *Green Chem.*, 2002, **4**, 174.

Silica-assisted Suzuki–Miyaura reactions of heteroaryl bromides in aqueous media†

Shengyin Shi and Yuhong Zhang*

Received 6th March 2008, Accepted 29th May 2008

First published as an Advance Article on the web 10th July 2008

DOI: 10.1039/b803917h

A new palladium catalysis system has been developed for the Suzuki–Miyaura cross-coupling reactions of heteroaryl bromides in aqueous media. The method allows the preparation of a variety of heterobiaryls in good to excellent yields under mild reaction conditions without the use of phosphine ligands. Silica gel is found to be crucial to the successful performance of the reactions and the catalytic system can be reused eighteen times with high efficiency.

Introduction

Palladium-catalyzed cross-coupling reactions have become powerful tools for carbon–carbon bond formation and have been widely used in the organic synthesis.¹ In particular, the Suzuki–Miyaura reaction has provided a general and applicable method for the preparation of biaryls,² which are the important intermediates and targets of natural products and functional materials.³ The Suzuki–Miyaura reaction involving heterocycles is of interest to the pharmaceutical industry because of the special biological activities displayed by the heterobiaryl compounds.⁴ However, it is reported that heteroaryl halides show a slower reaction rate and are unsuitable coupling partners in the Suzuki–Miyaura reaction, due to the potential binding nature of such substrates to the metal center resulting in the formation of inactive substrate–metal complexes.⁵ Recently, highly active catalysis systems have been pioneered for the Suzuki reaction of heteroaryl halides, and significant improvements are achieved in the presence of phosphine ligands.^{6–10}

Studies in our laboratory demonstrated that the Suzuki–Miyaura reaction can be efficiently performed in the presence of suitable additives, such as PEG and ionic liquids, without the use of phosphine ligands in aqueous media under mild reaction conditions.¹¹ Though the phosphine-free processes in water satisfy the demands of green chemistry,¹² in the case of heteroaryl halides as coupling partners, the reaction has been sluggish and gave very low yields. These limitations prompted us to investigate further new convenient methodology for heteroaryl halides. Herein, we report a new efficient system for the Suzuki–Miyaura reaction of heteroaryl bromides using Pd(OAc)₂ as the catalyst in the presence of PEG 2000 and commercially available silica gel in aqueous media. The cross-coupling reactions of heteroaryl halides with a variety of boronic acids were carried out smoothly with short reaction times at 80 °C to give the

heterobiaryl product in high yields. Notably, the catalysis system can be reused eighteen times with small diminution of activity.

Results and discussion

The Pd(OAc)₂ catalyzed Suzuki reaction between 3-bromopyridine and phenylboronic acid was chosen as a model reaction to evaluate the effects of the various conditions, and the results are summarized in Table 1. It can be seen that the previous efficient reaction conditions for aryl halides, including the mixture of H₂O–acetone, H₂O–PEGs, and H₂O–[BMIM]PF₆,^{11a–c} were not suitable for 3-bromopyridine and only low yields were delivered (Table 1, entries 1–3). It is noteworthy that the addition of silica gel (10–40 μm) significantly improved the Suzuki–Miyaura reaction and a 100% conversion was obtained for 2 h at 80 °C (Table 1, entry 4). The addition of Al₂O₃ and diatomite had a deleterious effect on the process (Table 1, entries 5–6). High conversion was also obtained after the prolongation of reaction time to 6 h when Na₂CO₃ was employed as the base (Table 1, entry 7). The optimized ratio of water and PEG was 3 : 3.5 g (H₂O : PEG).

Table 1 Optimization studies for the Suzuki reaction of heteroaryl halides^a

Entry	Solvent/g	Additive	Yield (%) ^b
1	H ₂ O : [BMIM]PF ₆ (1 : 3)	Null	12
2	H ₂ O : acetone (3.5 : 3)	Null	8
3	H ₂ O : PEG (3 : 3.5)	Null	21
4	H ₂ O : PEG (3 : 3.5)	Silica gel	100
5	H ₂ O : PEG (3 : 3.5)	Al ₂ O ₃	0
6	H ₂ O : PEG (3 : 3.5)	Diatomite	0
7	H ₂ O : PEG (3 : 3.5)	Silica gel	100 ^c

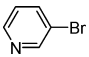
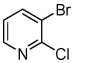
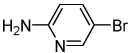
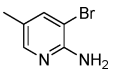
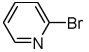
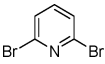
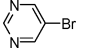
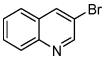
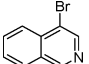
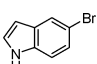
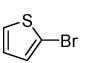
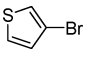
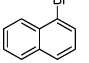
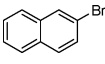
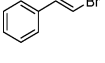
^a Reaction conditions: 3-bromopyridine (1 mmol), phenylboronic acid (1.5 mmol), Pd(OAc)₂ (0.5 mol%), NaOH (2 mmol), additive (0.2 g), PEG 2000, silica gel (10–40 μm), 80 °C, 2 h. ^b GC yields based on 3-bromopyridine. ^c Na₂CO₃ as base, 6 h.

Department of Chemistry, Zhejiang University, Hangzhou, 310027, P. R. China. E-mail: yhzhang@zjuem.zju.edu.cn;

† Electronic supplementary information (ESI) available: The experimental procedure, spectroscopic data (¹H NMR and MS) for the known products, and spectroscopic data (¹H NMR, ¹³C NMR, MS and HRMS) for the new products. For ESI see DOI: 10.1039/b803917h

The scope and limitations of this catalytic system Pd(OAc)₂-H₂O-PEG-silica gel for various heteroaryl bromides were investigated and the results are presented in Table 2. Good selectivity was observed when 2-chloro-3-bromo-pyridine was employed as the substrate, and only 2-chloro-3-phenylpyridine was isolated in 81% yield (Table 2, entry 2). It should be

Table 2 Suzuki-coupling of aryl bromides with phenylboronic acid^a

Entry	Aryl bromide	Base	Time/h	Yield (%) ^b
1		NaOH	2	98
2		NaOH	2	81
3		Na ₂ CO ₃	24	85 ^c
4		Na ₂ CO ₃	24	82
5		Na ₂ CO ₃	24	77 ^d
6		NaOH	24	90 ^e
7		NaOH	2	96
8		NaOH	6	78
9		Na ₂ CO ₃	24	64
10		NaOH	24	82
11		NaOH	24	76
12 ^d		Na ₂ CO ₃	24	35
13		NaOH	4	86
14		NaOH	4	87
15		NaOH	24	95

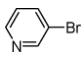
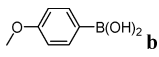
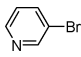
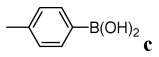
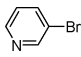
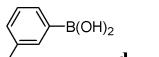
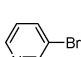
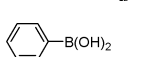
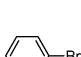
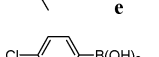
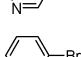
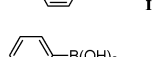
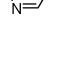

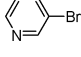
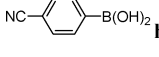
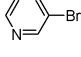
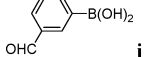
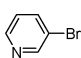
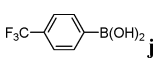
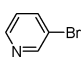
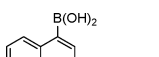
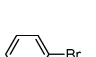
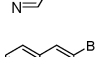
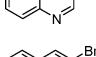
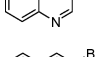
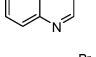
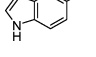
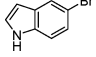
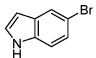
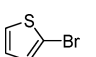
^a Reaction conditions: aryl bromide (1 mmol), phenylboronic acid (1.5 mmol), base (2 mmol), Pd(OAc)₂ (0.5 mol%), H₂O : PEG 2000 = 3 : 3.5 g, silica gel (10–40 μm, 0.2 g), 80 °C. ^b Isolated yields. ^c Pd(OAc)₂ (0.9 mol%). ^d Pd(OAc)₂ (1.8 mol%), 120 °C. ^e Pd(OAc)₂ (0.9 mol%), NaOH (4 mmol).

noted that 2-amino-5-bromopyridine and 2-amino-3-bromo-5-methylpyridine, which are generally protected prior to the cross-coupling reaction due to the retarding effect of the amino group on the organometallic reaction,¹³ smoothly produced the desired biaryls in high yields after 24 h at 80 °C (Table 2, entries 3–4). 5-bromopyridin-2-amine gave the corresponding product in 85% yield (Table 2, entry 3), as good as the results in the previous report using *cis,cis,cis*-1,2,3,4-tetrakis(diphenylphosphinomethyl)cyclopentane as ligand in xylene at 130 °C.^{6d} 2-Bromopyridine was less active and gave comparable yields at 120 °C for 24 h with more catalyst loading (Table 2, entry 5). The bis-coupling product was obtained in 90% yield with 2,6-dibromopyridine (Table 2, entry 6), far more efficient than the silica supported heterogeneous palladium catalyst in *o*-xylene at 120 °C in an N₂ atmosphere.^{5d} 5-Bromopyrimidine afforded 96% yield at the reaction conditions (Table 2, entry 7). The coupling of 3-bromoquinoline with phenylboronic acid produced the desired biaryl in 78% yield at 80 °C for 6 h, while the reaction of 4-bromoisoquinoline gave a lower yield, even after prolongation of the reaction time to 24 h, due to the sterically hindered effect (Table 2, entries 8–9). 5-Bromo-1*H*-indole coupled with phenylboronic acid to give the product in 82% yield (Table 2, entry 10). The sulfur-containing heteroaryl bromides showed the reactivity under the reaction conditions and a 76% yield was obtained using 2-bromothiophene as the coupling partner (Table 2, entry 11). Again, the position of halides on the heteroaromatic ring influenced the efficiency of the reaction, and a low yield was obtained for 3-bromothiophene, even though a higher temperature and more catalyst loading were employed (Table 2, entry 12). 1-Bromonaphthalene and 2-bromonaphthalene, which were inactive in our previous reported reaction conditions^{11a-c}, gave the desired products in high yields (Table 2, entries 13 and 14). In addition, this catalytic process allowed the combination of phenylboronic acid with alkenyl bromides to provide (*E*)-1,2-diphenylethene in excellent yield (Table 2, entry 15).

The coupling reactivity of various aryl boronic acids was examined and the results were summarized in Table 3. The results showed that the catalytic system could tolerate many functional groups, such as OMe, Me, Cl, F, CN, CHO and CF₃, and the electronic property of the substituent group has a poor influence on the reactivity of aryl boronic acid (Table 3, entries 1–9). 3-Formylphenylboronic acid was coupled with 3-bromopyridine to afford the target product in 85% yield in 2 h (Table 3, entry 8), which was comparable with the results using a furancarbothioamide-based palladacycle catalyst in DMA-H₂O at 100 °C for 2 h.^{6j} 2-Methylphenyl boronic acid gave lower yield due to the sterically hindered effect after 24 h (Table 3, entry 4), while naphthalen-1-ylboronic acid afforded the desired product in 84% yield (Table 3, entry 10). Naphthalen-2-ylboronic acid gave the desired product in 97% yield under the standard reaction conditions (Table 3, entry 11). Nitrogen-containing and sulfur-containing heteroaryl bromides also showed high reactivity and delivered good to high yields (Table 3, entries 12–20).

The reusability of the catalyst was investigated because it is very important to industrial and pharmaceutical applications. Our previous studies revealed that the conversion of the fifth cycle was reduced markedly in the Pd(OAc)₂-PEG-H₂O

Table 3 Suzuki-coupling of aryl bromides with various arylboronic acids^a

Entry	Aryl bromide	Boronic acid	Time/h	Yield (%) ^b
1			2	93
2			2	94
3			2	93
4			24	66
5			6	82 ^c
6			6	79
7			6	93
8			2	85
9			2	84
10			24	84
11			2	97
12		b	2	95
13 ^c		j	6	78
14		l	2	82
15 ^c		b	4	89
16		j	24	85
17		l	24	96
18		b	24	89
19 ^c		j	24	90
20		l	24	92

^a Reaction conditions: aryl bromide (1 mmol), arylboronic acid (1.5 mmol), Na₂CO₃ (2 mmol), Pd(OAc)₂ (0.5 mol%), H₂O : PEG 2000 = 3 : 3.5 g, silica gel (10–40 μm, 0.2 g), 80 °C. ^b Isolated yields. ^c NaOH (2 mmol).

catalysis system for the Suzuki reaction.^{11a} The Pd(OAc)₂–PEG–H₂O–silica catalytic system, however, showed much better efficiency of reusability, and could be recycled eighteen times with only a small decrease in activity without the need of addition of catalyst or PEG or silica gel. (Scheme 1). To clarify the role of silica gel, we performed the reaction in Pd(OAc)₂–H₂O–silica and Pd(OAc)₂–PEG–H₂O–silica system. We found that the level of activity of these two catalysis systems for the coupling reaction was almost equal, indicating that the presence of silica gel is essential to the excellent reactivity. However, the palladium catalyst could not be maintained in an aqueous phase and formed a mixture with the product in the organic phase in the absence of PEG for the Pd(OAc)₂–H₂O–silica system (Fig. 1a). The subsequent recycling experiments showed that the activity of the Pd(OAc)₂–H₂O–silica system was drastically decreased in the second run. In contrast, the ICP-AES analysis of the solution obtained by extraction of Pd–PEG–H₂O–silica with diethyl ether established that palladium levels were around 0.2 ppm, indicating the very low leaching of the palladium species into the organic phase. Undoubtedly, PEG played an important role in maintaining the palladium into the aqueous medium and made the separation process quite easy.

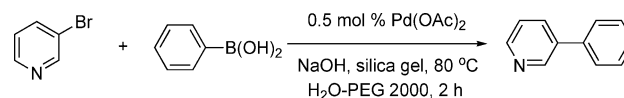
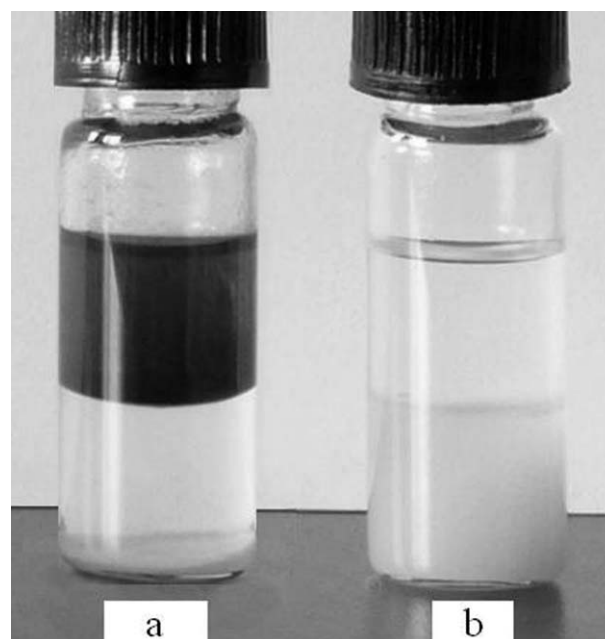
**Scheme 1**

Fig. 1 The upper phase is extraction solution of diethyl ether. (a) Pd(OAc)₂–H₂O–silica gel system. (b) Pd(OAc)₂–H₂O–PEG 2000–silica gel system.

The palladium nanoparticles were widely proved to be active in the coupling reactions,¹⁴ and our previous studies proved that nano-sized palladium was formed in PEGs.¹⁵ Transmission electronic microscopy (TEM) analysis indeed visualized the nicely separated palladium nanoparticles, with an average size of 5 nm, after the fifth run in the Pd(OAc)₂–PEG–H₂O–silica

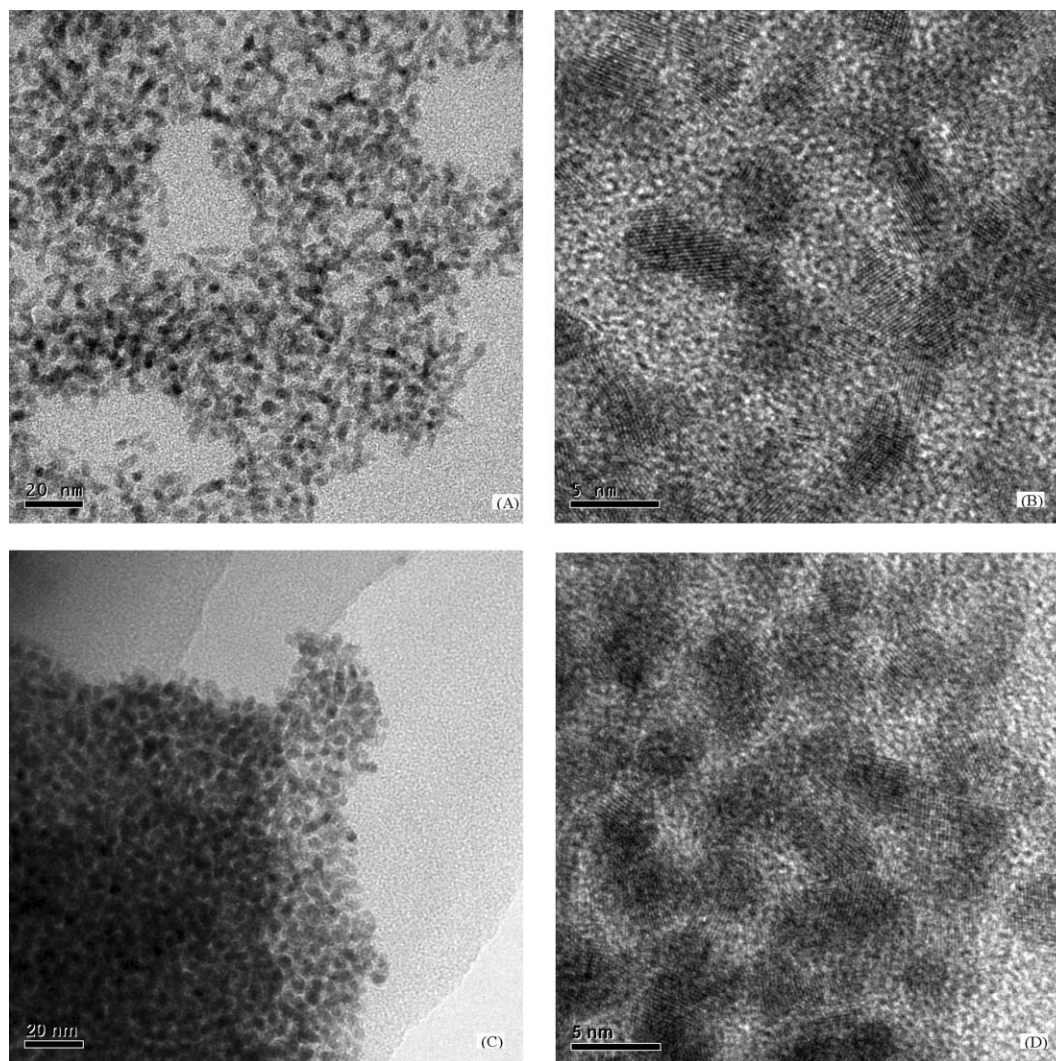


Fig. 2 TEM images in the Pd(OAc)₂-PEG-H₂O-silica gel reaction system. (A) and (B): after the fifth run; (C) and (D): after the fifteenth run.

system (Fig. 2A and B), and surprisingly, the narrow sized palladium nanoparticles were still maintained after the fifteenth run in the Pd(OAc)₂-PEG-H₂O-silica system (Fig. 2C and D), although their dispersion was not as good as that in the system after the fifth run. This result showed that silica played a special role in the stability of nano-palladium. This is the first example of silica being used as an additive in the Suzuki reaction. The stabilized nanostructures of palladium might lead to the excellent recycling properties in the Pd(OAc)₂-PEG-H₂O-silica system.

Conclusions

In summary, we have developed an environmentally benign and recyclable catalytic system for cross-coupling of heteroaryl bromides and arylboronic acids, avoiding the use of phosphine ligands. The simple experimental and product isolation procedures combined with the ease of recovery and reuse of the reaction medium is expected to contribute to the development of a green strategy for the preparation of hetero-aryl compounds. Further research to utilize the catalytic

system in wide synthetic applications is progressing in our laboratory.

Experimental

General procedure for the Suzuki reaction: a mixture of NaOH (0.80 g, 2 mmol) or Na₂CO₃ (0.212 g, 2 mmol), Pd(OAc)₂ (1 mg, 0.5 mol%), silica gel (10–40 μm, 0.2 g), aryl bromide (1 mmol), arylboronic acid (1.5 mmol), distilled water (3 mL) and PEG 2000 (3.5 g) was stirred at 80 °C for the indicated time. Afterward, the reaction solution was cooled to room temperature and extracted four times with diethyl ether (4 × 15 mL). GC and GC-MS was used to analyze the combined organic phase. The further purification of the product was achieved by flash chromatography on a silica gel column.

In the recycling experiment, the residue was subjected to a second run of the Suzuki reaction by charging it with the same substrates (3-bromopyridine, phenylboronic acid, NaOH) without further addition of Pd(OAc)₂ or PEG 2000 or silica gel. In the third, fifth, seventh, ninth and eleventh run, 0.5 ml distilled water was added to the reaction mixture. In the thirteenth,

fifteenth and seventeenth run, 1.0 ml distilled water was added to the reaction mixture.

Acknowledgements

Funding from Natural Science Foundation of China (No. 20571063) and Zhejiang Provincial Natural Science Foundation of China (R407106) is acknowledged.

Notes and references

- (a) F. Diederich and P. J. Stang, *Metal-Catalyzed Cross-Coupling Reactions*, Wiley-VCH, New York, 1998; (b) N. Miyaura, *Cross-Coupling Reactions: A Practical Guide; Topics in Current Chemistry Series 219*, Springer-Verlag, New York, 2002; (c) E.-i. Negishi, *Handbook of Organopalladium Chemistry for Organic Synthesis*, Wiley-Interscience, New York, 2002.
- (a) N. Miyaura and A. Suzuki, *Chem. Rev.*, 1995, **95**, 2457; (b) A. Suzuki, *J. Organomet. Chem.*, 1999, **576**, 147; (c) A. Suzuki, *J. Organomet. Chem.*, 2002, **653**, 83; (d) N. Miyaura, *Top. Curr. Chem.*, 2002, 11; (e) N. Miyaura, *Metal-Catalyzed Cross-Coupling Reactions*, ed. A. de Meijere and F. Diederich, Wiley-VCH, Weinheim, 2nd edn, 2004; Vol. 1, pp 41-124.
- (a) M. Kertesz, C. H. Choi and S. Yang, *Chem. Rev.*, 2005, **105**, 3448; (b) R. Capdeville, E. Buchdunger, J. Zimmermann and A. Matter, *Nat. Rev. Drug Discovery*, 2002, **1**, 493; (c) H. Tomori, J. M. Fox and S. L. Buchwald, *J. Org. Chem.*, 2000, **65**, 5334; (d) S. Lightowler and M. Hird, *Chem. Mater.*, 2005, **17**, 5538.
- (a) V. Bonnet, F. Mongin, F. Trecourt, G. Breton, F. Marsais, P. Knochel and G. Queguiner, *Synlett*, 2002, 1008; (b) A. F. Pozharskii, A. T. Soldatenko and A. Katritzky, *Heterocycles in Life and Society*, Wiley, New York, 1997.
- (a) E. B. Mubofu, J. H. Clark and D. J. Macquarrie, *Green Chem.*, 2001, **3**, 23; (b) C. R. LeBlond, A. T. Andrews, Y. Sun and J. R. Sowa Jr., *Org. Lett.*, 2001, **3**, 1555; (c) C.-J. Li, *Angew. Chem., Int. Ed.*, 2003, **42**, 4856; (d) S. Paul and J. H. Clark, *Green Chem.*, 2003, **5**, 635; (e) N. E. Leadbeater and M. Marco, *Angew. Chem., Int. Ed.*, 2003, **42**, 1407; (f) R. B. DeVasher, L. R. Moore and K. H. Shaughnessy, *J. Org. Chem.*, 2004, **69**, 7919; (g) J.-H. Li, W.-J. Liu and Y.-X. Xie, *J. Org. Chem.*, 2005, **70**, 5409; (h) A. I. Moncada, M. A. Khan and L. M. Slaughter, *Tetrahedron Lett.*, 2005, **46**, 1399; (i) T. Maegawa, Y. Kitamura, S. Sako, T. Udzu, A. Sakurai, A. Tanaka, Y. Kobayashi, K. Endo, U. Bora, T. Kurita, A. Kozaki, Y. Monguchi and H. Sajiki, *Chem.-Eur. J.*, 2007, **13**, 5937; (j) S. Li, Y. Lin, J. Cao and S. Zhang, *J. Org. Chem.*, 2007, **72**, 4067; (k) H. Qiu, S. M. Sarkar, D.-H. Lee and M.-J. Jin, *Green Chem.*, 2008, **10**, 37.
- (a) G. Cooke, H. A. de Creliers, V. M. Rotello, B. Tarbit and P. E. Vanderstraeten, *Tetrahedron*, 2001, **57**, 2787; (b) P. R. Parry, C. Wang, A. S. Batsanov, M. R. Bryce and B. Tarbit, *J. Org. Chem.*, 2002, **67**, 7541; (c) T. Tagata and M. Nishida, *J. Org. Chem.*, 2003, **68**, 9412; (d) M. Feuerstein, H. Doucet and M. Santelli, *J. Organomet. Chem.*, 2003, **687**, 327; (e) A. E. Thompson, G. Hughes, A. S. Batsanov, M. R. Bryce, P. R. Parry and B. Tarbit, *J. Org. Chem.*, 2005, **70**, 388; (f) I. Kondolff, H. Doucet and M. Santelli, *Synlett*, 2005, 2057; (g) O. Navarro, N. Marion, J. Mei and S. P. Nolan, *Chem.-Eur. J.*, 2006, **12**, 5142; (h) Y. Kitamura, S. Sako, T. Udzu, A. Tsutsui, T. Maegawa, Y. Monguchi and H. Sajiki, *Chem. Commun.*, 2007, 5069; (i) C. A. Fleckenstein and H. Plenio, *Green Chem.*, 2007, **9**, 1287; (j) Z. Xiong, N. Wang, M. Dai, A. Li, J. Chen and Z. Yang, *Org. Lett.*, 2004, **6**, 3337.
- (a) T. Itoh and T. Mase, *Tetrahedron Lett.*, 2005, **46**, 3573; (b) A. E. Thompson, G. Hughes, A. S. Batsanov, M. R. Bryce, P. R. Parry and B. Tarbit, *J. Org. Chem.*, 2005, **70**, 388.
- N. Kudo, M. Perseghini and G. C. Fu, *Angew. Chem., Int. Ed.*, 2006, **45**, 1282.
- (a) A. S. Guram, A. O. King, J. G. Allen, X. Wang, L. B. Schenkel, J. Chan, E. E. Bunel, M. M. Faul, R. D. Larsen, M. J. Martinelli and P. J. Reider, *Org. Lett.*, 2006, **8**, 1787; (b) A. S. Guram, X. Wang, E. E. Bunel, M. M. Faul, R. D. Larsen and M. J. Martinelli, *J. Org. Chem.*, 2007, **72**, 5104.
- (a) T. E. Barder, S. D. Walker, J. R. Martinelli and S. L. Buchwald, *J. Am. Chem. Soc.*, 2005, **127**, 4685; (b) K. W. Anderson and S. L. Buchwald, *Angew. Chem., Int. Ed.*, 2005, **44**, 6173; (c) K. L. Billingsley, K. W. Anderson and S. L. Buchwald, *Angew. Chem., Int. Ed.*, 2006, **45**, 3484; (d) K. W. Billingsley and S. L. Buchwald, *J. Am. Chem. Soc.*, 2007, **129**, 3358.
- (a) L. Liu, Y. Zhang and Y. Wang, *J. Org. Chem.*, 2005, **70**, 6122; (b) B. Xin, Y. Zhang, L. Liu and Y. Wang, *Synlett*, 2005, 3083; (c) L. Liu, Y. Zhang and B. Xin, *J. Org. Chem.*, 2006, **71**, 3994; (d) B. Xin, Y. Zhang and K. Cheng, *J. Org. Chem.*, 2006, **71**, 5725; (e) S. Shi and Y. Zhang, *Synlett*, 2007, 1843; (f) S. Shi and Y. Zhang, *J. Org. Chem.*, 2007, **72**, 5927; (g) B. Xin, Y. Zhang and K. Cheng, *Synthesis*, 2007, **13**, 1970; (h) K. Cheng, B. Xin and Y. Zhang, *J. Mol. Catal. A: Chem.*, 2007, **273**, 240.
- (a) C.-J. Li and T.-H. Chan, *Organic Reactions in Aqueous Media*, Wiley, New York, 1997; (b) P. A. Grieco, *Organic Synthesis in Water*, Academic Press, Dordrecht, The Netherlands, 1997; (c) B. Cornils and W. A. Herrmann, *Aqueous-Phase Organometallic Catalysis*, 2nd edn, Wiley-VCH, Weinheim, 2nd edn, 2004; (d) K. H. Shaughnessy and R. B. DeVasher, *Curr. Org. Chem.*, 2005, **9**, 585; (e) N. E. Leadbeater, *Chem. Commun.*, 2005, 2881; (f) C.-J. Li, *Chem. Rev.*, 2005, **105**, 3095.
- (a) J. A. Miller and R. P. Farrell, *Tetrahedron Lett.*, 1998, **39**, 6441; (b) S. Caron, S. S. Massett, D. E. Bogle, M. J. Castaldi and T. F. Braish, *Org. Process Res. Dev.*, 2001, **5**, 254.
- (a) B. M. Choudary, S. Madhi, N. S. Chowdari, M. L. Kantam and B. Sreedha, *J. Am. Chem. Soc.*, 2002, **124**, 14127; (b) M. A. El-Sayed and R. Narayanan, *J. Am. Chem. Soc.*, 2003, **125**, 8340; (c) P. D. Stevens, G. Li, J. Fan, M. Yen and Y. Gao, *Chem. Commun.*, 2005, 4435; (d) R. B. Bedford, U. G. Singh, R. I. Walton, R. T. Williams and S. A. Davis, *Chem. Mater.*, 2005, **17**, 701; (e) J. K. Cho, R. Najman, T. W. Dean, O. Ichihara, C. Muller and M. Bradley, *J. Am. Chem. Soc.*, 2006, **128**, 6276; (f) L. Wu, B.-L. Li, Y.-Y. Huang, H.-F. Zhou, Y.-M. He and Q.-H. Fan, *Org. Lett.*, 2006, **8**, 3605; (g) W. Han, C. Liu and Z. -L. Jin, *Org. Lett.*, 2007, **9**, 4005.
- C. Luo, Y. Zhang and Y. Wang, *J. Mol. Catal. A: Chem.*, 2005, **229**, 7.

The Knoevenagel condensation at room temperature

Ronald Trotzki,^a Markus M. Hoffmann^b and Bernd Ondruschka^{*a}

Received 15th May 2008, Accepted 10th June 2008

First published as an Advance Article on the web 10th July 2008

DOI: 10.1039/b808265k

The Knoevenagel condensation of malononitrile with various arylaldehydes was studied as an uncatalyzed reaction at ambient temperature. This study was prompted after discovering that a reaction mixture left standing for extended times after mechanochemical treatment would continue to react to significantly higher yields. We report that a mixture (solid/solid or solid/liquid) of reactants converts in some cases quantitatively to the target product in the absence of any solvent at room temperature. The yields can be increased if the mixture of reactants is seeded with the target product. It is also possible to carry out the condensation reaction in solution at room temperature without any stirring. Depending on the aldehyde and the polarity of the solvent yields can be quantitative as well.

Introduction

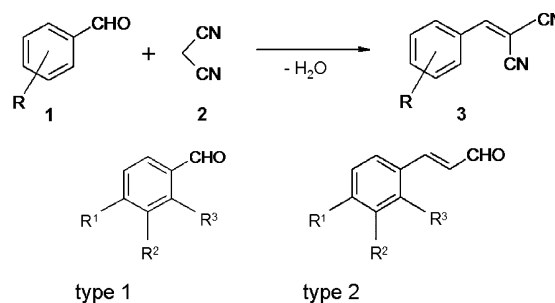
External energy, sometimes in large quantities over extended periods of time, is usually needed for an organic synthetic reaction to proceed. Conventionally, one uses convective heating devices such as heat baths or electric heating mantles. In the 1980's the first microwave-assisted syntheses were reported^{1,2} where reaction times can be considerably shortened through dielectric heating³ with same or even better results. The amount of external energy applied to the reaction mixture is thereby reduced as well. A multitude of reports from microwave-assisted reactions in solutions as well as "solvent-free" were published in the ensuing years. It was not until the 1990's that solvent-free reactions were also carried out mechanochemically, at first only on support materials.⁴⁻⁶ Since 2000 Toda and Tanaka⁷ and Kaupp⁸ have extensively reported on solvent-free syntheses procedures without the use of any support materials or catalysts using stoichiometric amounts of solid reactants which were converted mechanochemically or as a melt under vacuum at elevated temperatures using convective heating. Since no solvent was used and conversions were quantitative, these procedures circumvented any work-up after completion of the reaction. Kaupp's group⁹ has also conducted quantitative stoichiometric Knoevenagel condensation reactions of aldehydes with various methylene components mechanochemically as well as in the melt. As also reviewed by Rodríguez *et al.*,¹⁰ relevant studies by Wada and Suzuki¹¹ and Wang's group,^{12,13} have appeared as well. However, various catalysts were used in these studies. Because Kaupp *et al.* showed only results for a limited number of quantitatively converted aldehydes, we explored in a previous study¹⁴ whether the underlying reaction scheme can be generalized to a wider range of aromatic aldehydes. We found that a

quantitative conversion depends on the chosen aldehyde, and the reaction procedure cannot be generalized. Furthermore, the mechanochemical conversion proved to be advantageous over the microwave-assisted reaction in the melt with respect to handling of the synthesis, product isolation and purity of the product. The electric power consumption of microwave systems is also 300 to 600 times the consumption of milling systems. However, the most unexpected finding of our previous study was the observation that the reaction mixture, both solvent-free and when dissolved in a solvent, continued to react, leading at times to quantitative yields when left standing for extended time periods. This prompted us to further investigate in detail this surprising finding, and we wish to share the results of our investigations in this report.

Experimental

Synthesis details

The Knoevenagel condensation with malononitrile (**2**) shown in Scheme 1 was studied with the same ten substituted aldehydes (solid as well as liquid) of type 1 and type 2 used in our previous investigation.¹⁴



Scheme 1

The stoichiometric reaction mixtures, each containing one of the aldehydes listed in Table 1, were generally converted at room temperature without any catalysts or water absorbing

^aInstitute for Technical Chemistry and Environmental Chemistry, Friedrich-Schiller-University, Lessingstr. 12, Jena, Germany. E-mail: Bernd.Ondruschka@uni-jena.de; Fax: +49 (0) 3641 948402; Tel: +49 (0) 3641 948400

^bDepartment of Chemistry, State University of New York College at Brockport, Brockport, USA

Table 1 Substituents of the aldehydes used

RCHO	R ¹	R ²	R ³	mp/°C ^a
1a	H	H	H	–26
1b	NO ₂	H	H	104–106
1c	(CH ₃) ₂ N	H	H	71–73
1d	OH	OCH ₃	H	82
1e	H	OCH ₃	OCH ₃	48–52
1fb	H	H	H	–9
1g	Cl	H	H	44–47
1h	H	H	Cl	9–11
1i	OH	H	H	112–116
1j	H	H	OH	1–2

^a Melting points were taken from the literature of the chemical supplier (Aldrich). ^b Aldehyde **1f** is of type 2, all others are of type 1.

agents under the same defined reaction conditions. The reactants were directly weighed into sealable reaction vessels. Any coarse-grained or crystalline components were ground with a mortar and pestle prior use. The aldehydes **1a**, **1f**, **1h** and **1j** were freshly distilled. All other aldehydes as well as **2** were used as received (Aldrich, Germany) and were of purity >98%. The reaction mixtures were left standing under nitrogen for defined times expressed in days, where 1 day (1 d) means 24 h. Great care was taken to avoid an inadvertent input of external energy in handling the reaction mixture. To initially mix solid reactants they were stirred briefly for a few seconds with a spatula. Likewise for the experiments in solution, stirring was minimal until the weight-in reactants, each in 10 mmol amounts, were dissolved in 20 ml of solvent. For experiments where reactants were first pre-converted mechanochemically with a mill as described in our previous report,¹⁴ the stoichiometric amounts of reactants were 20 mmol in consideration of the physical size of the mill. The mill used was the planetary mill Pulverisette 7, Fritsch, Germany with 45 mL stainless steel reaction vessels and five balls of 1.5 cm diameter made from the same stainless steel material (Fe87Cr13). After mechanochemical treatment, the reaction mixture was either left standing in the mill itself for pre-determined times upon which the entire contents were dissolved for analysis or, for the continuation experiments in solution, dissolved into 40 ml of the corresponding solvent. The solvents tetrahydrofuran (THF), dimethylformamide (DMF), dimethyl sulfoxide (DMSO), acetone, absolute ethanol (water content < 0.1%), toluene, ethyl acetate and dichloromethane used in this study were of *puriss* purity, and no impurities were indeed detectable with GC.

For the experiments where the effect of exposure to visible and microwave irradiation on the Knoevenagel reaction in solution was tested, a microwave (brand Discover from CEM (USA)) equipped with fiber optic sensors was used. The reaction experiments were carried out for 1 h at 100 W power level and 70 °C under ambient pressure under reflux in a 50 ml glass flask. The UV-light (235 nm) was introduced into the reaction vessel using non-ozone forming, electrode-less lamps which are directly immersed into the reaction vessel and are activated by the microwave light.¹⁵ Thus, the solutions were exposed in these reaction experiments simultaneously to both UV-vis and microwave irradiation.

For the Knoevenagel condensation in ethanol the following typifies the synthesis procedure. 10 mmol of aldehyde **1a**, **1b**,

1g or **1h** and 10 mmol malononitrile are weighed into a 30 ml sealable glass container and dissolved into 20 ml (**1b**: 40 ml) of absolute ethanol and briefly agitated with a magnetic stir bar. The solution is left standing for 1 day and the supernatant is analyzed by GC. If reactant is still found then the solution is left standing and analyzed again after a total of 7 days. The product of the quantitatively converted reaction mixtures is retrieved by vacuum filtration after cooling for 1 h in a refrigerator and subsequently dried at ambient air. The products obtained this way are GC pure, although some traces of impurities are sometimes indicated by slight discoloration.

Measurement and analysis details

The GC examinations were carried out on Hewlett-Packard instruments (FID: series 5890, Mass-selective detector series 5972) using columns HP 5 (30 m, id 0.32 × 0.25 mm). Temperature program: 3 min isotherm at 50 °C, followed by a temperature ramp of 8 K min⁻¹ to 320 °C. The detector temperature was set to 300 °C and the column inlet pressure was entered as 0.7 bar (10 psi), the split-valve setting was 150 : 1. The entire reaction mixture was dissolved in 2 mL solvent per mmol substance, and 1 μL of the obtained solution was injected. The retention times of the target products were between 15–25 min. GC analysis was conducted immediately after the pre-determined reaction times. If products precipitated out of solution the remaining liquid was analyzed for product as well using internal standards. Depending on the respective retention times of reactants and products, hexadecane (**a**, **d**, **e**, **f**, **i**, **j**) or mesitylene (**c**, **g**, **h**) were used as internal standards. It was found after some test measurements with known analyte quantities that measurements of clear solutions do not require a correction to the chromatographic peak areas. All stated % yields are referred to the conversion of aldehyde to the target product. No remaining educt could be detected for yield entries stated as “(100)”. Yields greater than 98% are considered as “quantitative”. Each reaction experiment was repeated, usually with essentially identical results. Additional experiments were conducted if yield deviations were greater than 5%. Other experimental details pertaining to the interpretation and discussion of the results are provided where appropriate in the results and discussion section.

Results and discussion

The first series of experiments was the investigation of continued conversion of the aldehydes **1c**, **1d**, **1e**, **1f**, and **1j** after they were mechanochemically treated as described in our previous report.¹⁴ Yields from aldehydes **1a**, **1b**, **1g**, **1h** and **1i** were already greater than 95% and thus these aldehydes were not included in this series of experiments. The reaction mixtures were completely dissolved after milling in either THF or DMF and immediately analyzed by GC to determine the initial product yield y_0 . These original solutions were left standing at room temperature and were analyzed after 1 day. If yields increased, the reaction mixture was re-analyzed after 7, 14 and 28 days. The results are summarized in Table 2.

Except for **1f**, where apparently y_0 for **3f** was already the maximum obtainable yield, all other aldehydes continued to

Table 2 Yields from continued reaction of the Knoevenagel condensation after initial mechanochemical conversion

RCHO	Solvent	y_0 (%) ^a	Yield 3 (%)			
			1 d	7 d	14 d	28 d
1c	THF	69	69	—	—	—
	DMF	69	72	78	—	81
1d	THF	5	12	28	61	73
	DMF	5	80	92	96	98
1e	THF	94	96	—	—	97
	DMF	94	100	—	—	—
1f	THF	95	95	—	—	—
	DMF	95	95	—	—	—
1j ^b	DMF	63	84	94	97	100

^a The initial product yield y_0 is obtained from GC analysis immediately after initial mechanochemical conversion. ^b For aldehyde **1j** the Knoevenagel product **3j** reacted completely further to benzofuran-2-carbonitrile.

react. The reaction ensued faster and to higher yields in the more polar solvent DMF as can be seen especially for aldehyde **1d**.

In additional experiments we tested how far the reaction mixtures continue to convert after initial mechanochemical treatment when left standing in the mill solvent-free under nitrogen atmosphere to avoid autoxidation. As an additional test to exclude light as a possible source of external energy for the continued conversion, one portion of the reaction mixture was left in the dark. The yields from GC analysis after 1 and 7 days shown in Table 3 were identical regardless of exposure to light or not.

Again all aldehydes continued to react except for **1f** where the y_0 of 95% seems indeed to be the maximum achievable equilibrium yield. The yields were significantly higher compared to the corresponding results in Table 2 for **1c** after 7 days and **1d** after 1 day, where a similar yield for **1d** is only achieved in DMF after 7 days. In the case of **3j**, the stated yields in Tables 2 and 3 are to be understood as conversions of **1j** rather than the yield of **3j**, since **3j** reacted further to form benzo-2-carbonitrile.

The observed continued reactions in the absence of any solvent after initial mechanochemical treatment can be attributed to a direct crystallization process, which is described in the literature¹⁶ but has not yet been observed for the reaction of aldehydes with malononitrile. Direct crystallization processes between solid and liquid reactants, as indicated for the liquid aldehydes in this study, have also not yet been reported. While

Table 3 Yields from solvent-free continued reaction of the Knoevenagel condensation after initial mechanochemical conversion

RCHO	y_0 (%) ^a	Yield 3 (%)	
		1 d	7 d
1c	69	78	96
1d	5	89	93
1e	94	97	99
1f	95	95	—
1j ^b	59	77	87

^a The initial product yield y_0 from GC analysis immediately after initial mechanochemical conversion. ^b For aldehyde **1j** the combined product yields from Knoevenagel condensation and further reaction to benzofuran-2-carbonitrile are stated.

recent reports in the literature show that the Knoevenagel reaction can be pursued at room temperature in ionic liquids,^{17,18} the ionic liquid acted in these cases both as a base and a catalyst and, furthermore, needs to be removed after completion of the reaction.

In a next set of experiments we intended to discern if the Knoevenagel reaction can ensue at room temperature solvent-free even without the presence of an initial amount of target product. Stoichiometric amounts of aldehyde and malononitrile were briefly mixed with a spatula or, in the case of a liquid aldehyde, by brief swirling of the vessel and then left standing under nitrogen at room temperature. A portion of each reaction experiment was also left standing again in darkness. Furthermore, in additional experiments solid aldehydes were also homogeneously mixed with malononitrile by dissolution in THF followed by immediate removal of THF under vacuum at room temperature. Homogenization was not attempted for **1c** and **1e** because these form a eutectic with **2** resulting in a liquid mixture at room temperature. After 1 day each reaction mixture was analyzed with GC and the results are shown in Table 4.

The yields shown in Table 4 were again identical for the runs with and without exposure to light. The experiments with the solid aldehydes **1b** and **1i** resulted in very good yields, but **1g**, which is usually considered as a reactive aldehyde, converted only marginally. The less reactive aldehydes **1c**, **1d**, and **1e** also converted only slightly if at all. The 95% yield for **1i** seems to be a limiting chemical equilibrium value. In comparison to the results in Table 3 this set of experiments shows the significance of the presence of some seed target product for the less reactive aldehydes. For instance, while **1d** reacted only to a yield of 7% in the absence of any initial **3d**, the Knoevenagel reaction proceeded readily at room temperature solvent-free to a yield of 89% within 1 day when 5% of **3d** is initially present. A similar behavior could also hold for **1e** and **1f** but y_0 was already very high in these cases, precluding an unambiguous comparison of the results in Tables 3 and 4.

The results for the liquid aldehydes in Table 4 are overall low. To further investigate the reactivity of the liquid aldehydes, 1 mol% of pure product was added into the obtained liquid reaction mixtures from **1a** and **1h** and left standing for an additional 1 day. Interestingly, the yields as determined by GC increased for **1a** from 13% to 99% as fully crystallized product but the

Table 4 Yields from Knoevenagel reaction by direct crystallization

RCHO	Yield 3 (%) after 1 d	
	Mixture of reactants	Homogenized (THF) ^a
1a	13	—
1b	92	99
1c	0	—
1d	7	7
1e	4	—
1f	13	—
1g	5	6
1h	18	—
1i	95	95
1j	0	—

^a Homogenization in THF was only attempted for reactant mixtures which are solid at room temperature.

reaction mixture remained as a homogenous oil for **3h**, and yields increased only marginally from 18% to 23%. As a further test, a fresh mixture of **1a** with malononitrile was impregnated with 1 mol% **3a** and left standing for 1 day at room temperature. No reaction occurred. Thus, there appears to be a substrate dependent minimum level of impregnation with pure target product which is needed to achieve high, near quantitative yields.

We further investigated more carefully whether light may have an influence on the Knoevenagel reaction in solution. Equimolar amounts of **1a** and **2** were dissolved in 20 ml THF and were irradiated with an electrode-less UV-lamp¹⁵ (235 nm) under concurrent microwave irradiation and solvent reflux for 1 h. No product could be detected. As a representative of an impregnated reaction mixture we also dissolved a portion of the reaction mixture with 23% of **3h** present in 20 ml THF and exposed it for 1 h to the same concurrent UV and microwave irradiation. No further reaction was observed here as well. Therefore, there is strong evidence that light did not serve as an external source of energy for the Knoevenagel reaction.

In the following we describe results from studying the Knoevenagel reaction in solution at room temperature. In a first experiment series, stoichiometric amounts of aldehyde and malononitrile were dissolved in either THF or DMF and let stand at room temperature to be analyzed by GC after 1 day and 7 days. If no products were detected after 1 day further GC inspection was omitted. The results are summarized in Table 5.

As already seen with the reaction experiments in THF and DMF after mechanochemical treatment, the Knoevenagel reaction proceeds significantly better in DMF than in THF. The aldehydes **1c**, **1d**, **1j** do not react in THF. Even after 7 days, only the most reactive aldehyde **1b** converted quantitatively to **3b**. In contrast to THF, **1a**, **1b**, **1e**, **1h** and **1i** reacted to very high yields and no left-over reactants could be detected after 7 days in each case. While for **1d** no reaction occurred in THF a yield of 97% was obtained after 7 days in DMF. **1c** and **1j** reacted to some extent in DMF as well where, as expected, **3j** partially continued to react to benzo-2-carbonitrile. It is somewhat surprising that also in these experiments the usually rather reactive aldehyde **1g** converted in DMF to **3g** only to a yield of 80%. As for **1f**, it only converted partially at room temperature in DMF solution.

Table 5 Knoevenagel reactions of aldehydes with malononitrile in THF and DMF at room temperature

RCHO	Yield 3 (%)			
	THF		DMF	
	1 d	7 d	1 d	7 d
1a	6	15	97	(100)
1b	35	97	99	(100)
1c	0	—	26	49
1d	0	—	75	97
1e	10	12	96	(100)
1f	3	14	41	50
1g	6	16	80	80
1h	21	77	>99	(100)
1i	32	68	93	(100)
1j	0	—	59	81

No remaining reactants could be detected with GC for entries with "(100)".

Table 6 Knoevenagel results with the PM at 400 rpm, 1h

Solvent	Yield 3 (%)	
	1 d	7 d
DMF	99	(100) ^b
DMSO	98	99
THF	35	97
Acetone	23	34
Ethanol (abs.)	>99 ^a	(100) ^b
Toluene	18	40 ^c
Ethyl acetate	10	17
Dichloromethane	10	17

^a Obtained from considering the amount of precipitated product and product remaining in the supernatant solution. ^b No **1b** detected in solution. ^c After 14 d the yield was 42% in solution but some additional product precipitated.

The next series of experiments was conducted with the most reactive aldehyde **1b** to elucidate further the influence of the solvent on the Knoevenagel reaction. Equimolar **1b** and **2** were dissolved in 20 ml of the respective solvent and let stand at room temperature. The yields from GC determination after 1 day and 7 days are shown in Table 6. In the case of ethanol as a solvent, **3b** precipitated out of solution shortly after the start of the reaction, and the yields for **3b** in Table 6 are the combined yields of precipitated **3b** and **3b** left in the supernatant as determined by GC.

There are clearly solvent effects discernable from the yields listed in Table 6. The water liberated from the Knoevenagel condensation can be bound as a hydrate by DMF and DMSO as well as through hydrogen bonding by ethanol. The liberated water is thereby removed from the chemical equilibrium, and the quantitative Knoevenagel reaction is complete within 1 day. The possibility that the reactions were promoted by the liberated heats of hydratization of the reaction water can be disregarded because only a maximum of 0.18 g water is generated and dissolved into the 20 ml of solvent, and the generation of water proceeds only gradually in time. For THF and acetone the liberated water is freely dissolved along with the reactants. While the reaction is nearly quantitative after 7 days in THF, the reaction is surprisingly slow in acetone. **3b** is only poorly soluble in ethanol compared to malononitrile (good) and **1b** (fair), and the rapid precipitation also shifts the equilibrium favorably towards the product side. The nonpolar solvents toluene, ethyl acetate and dichloromethane can barely accept any liberated water and the reaction stops at a low product level. The observed 40% yield after 7 days in toluene appears to be at the solubility limit of **3b**. When left standing for additional time, **3b** begins to precipitate out of solution after 14 days, and after 28 days the yield of **3b** after vacuum filtration was 90%. Unlike for toluene, the in ethyl acetate and dichloromethane generated **3b** at 17% was below the solubility limit in each case, and a precipitation of **3b** was not observed.

Because of the encouraging good yields of **3b** for the Knoevenagel reaction in ethanol at room temperature, the Knoevenagel reaction of malononitrile was also attempted in ethanol at room temperature with all of the ten aldehydes, and the results are summarized in Tables 7 and 8.

Table 7 Knoevenagel reaction in ethanol at room temperature

RCHO	Conversion of 1 (%) ^a	
	1 d	7 d
1a	97	>99
1b	>99	(100)
1c	8	67
1d	64	93
1e	77	82
1f	32	40
1g	72	(100)
1h	98	(100)
1i	87	93
1j	18	37

^a Entries are based on amount of **1** left in solution from GC analysis.

Table 8 Yield budget for the Knoevenagel reaction in ethanol after 7 days at room temperature

RCHO	Isolated yield after 7 days (%)		Unrecovered product (%)	Σ Yield 3 (%)
	<i>m</i> ₁ ^a	<i>m</i> ₂ ^b		
1a	74	20	5.5	>99
1b	94	—	6	(100)
1c	66 ^c	—	1	67
1d	—	—	—	93 ^e
1e	79	9	10	98
1f	—	—	—	40 ^e
1g	89	2	9	(100)
1h	63	5	32	(100)
1i	—	—	—	93 ^e
1j	32 ^d	—	5	37

^a *m*₁ is the yield from the directly precipitated product. ^b *m*₂ is the additional yield obtained from isolating the product left in the supernatant. ^c The precipitate also contained an additional 13% of unconverted malononitrile. ^d The precipitate also contained unconverted **1j**. ^e No precipitation of product observed, isolation of **3** not attempted.

Solid product precipitated within 1 day from solution in the cases of **1a**, **1c**, **1e**, **1g**, **1h**, and **1j**, but the reaction solution stayed clear for **1d**, **1f**, and **1i** even after 7 days. The yield analysis is somewhat more complicated for reactions where precipitation occurred since the amount of precipitated product was only determined after 7 days when the product was isolated by vacuum filtration. Thus, we report in Table 7 the conversion of **1** based on how much aldehyde remains in solution as per GC analysis using internal standards as described in the Experimental section. In Table 8 is shown an itemized yield budget which includes the yield contributions from the precipitated product, *m*₁, and further product isolation from the supernatant, *m*₂, by adding twice the volume of water to induce additional product precipitation. Since **3d**, **3f**, and **3i** did not precipitate out of solution, product isolation after 7 days was not attempted for these reaction solutions. Further product isolation from the supernatant was also not attempted for **3b** because 94% precipitated already out of solution and for **3c** and **3j** because these were contaminated with reactant. Although product isolation from the reaction solution was not quantitative, overall, the results in Tables 7 and 8 show that the Knoevenagel reaction proceeded well in ethanol at room

temperature with quantitative conversions for **1a**, **1b**, **1e**, **1g**, and **1h**. The conversions after 7 days are similar to the results in Table 5 for using DMF as the solvent. Since **3i** did not precipitate from ethanol, this explains the 93% yield compared to the 100% yield in DMF. In turn, **3g** precipitated from ethanol but not from DMF, and the yield in DMF was only 80%. Yields were similar for **1d** and **1f** which precipitated neither from ethanol nor from DMF. If the reaction proceeds slowly then not only the product may precipitate but also the aldehyde, as was the case for **3c**, or the malononitrile, as was the case for **3j**. From the GC analysis of the reaction solutions the lowest solubility in ethanol was observed for **3c** with about 8% and thus precipitation occurred already at very low concentrations, similar to what was observed during the solvent dependent reaction studies (Table 6) for **3b** in ethanol as well as in toluene. The product recovery is therefore also facilitated when product solubility is low. For products which were more soluble in ethanol, a quantitative isolation became difficult. Even when twice the volume of water was added to the separated supernatant to induce further precipitation the theoretical yields could not be obtained and some of the product remained in solution. This was the case for **3a**, **3e**, **3g** and **3h** where respectively 94%, 88%, 91% and 68% of the product could be obtained even though conversion was in each case greater than 97%.

According to GC analysis, the products **3a**, **3b**, **3e**, **3g**, and **3h** from both, the precipitate from reaction solution and the precipitate from the supernatant mother liquor induced by the addition of water, were 100% pure, although some slight discoloration was noticed in some cases. Interestingly, in the case of **1j** nearly pure **3j** was obtained. The GC analysis, where a small sample of the white, crystalline solid was dissolved in THF and immediately analyzed, showed only slight traces of benzo-2-carbonitrile. The difference in reactivity of **3j** towards the continued reaction to benzo-2-carbonitrile can also be confirmed by visual observation. When the dissolved **3j** is left standing in THF, an orange precipitate of benzo-2-carbonitrile over a dark orange-red solution is observed within 1 day. In contrast, the precipitating product **3j**, which forms in a solution of **1j** and **2**, turns only slightly yellow within the first two days and yellow orange after 7 days at which point the supernatant solution has turned into a red-orange color. Most likely, intermolecular interactions of **3j** with the hydroxyl group of ethanol as well as perhaps of salicylic aldehyde makes the liberation of HCN and thus the ring closure to benzo-2-carbonitrile more difficult.

Since the solubility of the product in ethanol is a key factor in obtaining quantitative results, some exemplary reaction experiments with more concentrated solutions were attempted. Instead of dissolving 10 mmol of each reactant in 20 ml of solvent, only 10 ml of alcohol was used. As before, the solution was left standing at room temperature and GC samples were taken after 1 day and 7 days. If precipitation of the product occurred then it was isolated and the amount was included in evaluating the total yield. While **3d** and **3i** still did not precipitate out of solution, **3f** did precipitate and 52% of the product could be isolated. The combined conversion from precipitate and product remaining in solution increased from 40% (Table 7) to 77%. In the case of **1a**, the same results as in Table 7 were obtained.

Finally, another reaction experiment was performed dissolving **1b** in 40 ml ethanol, that is, twice the amount of solvent. The clear solution becomes cloudy after 10 min and after 1 h solution is completely filled with the voluminous reaction product **3b**. No reactant could be found by GC analysis in the supernatant after 1 day indicating quantitative conversion. The final yield of the isolated product was 94%, and no impurities could be detected by GC analysis.

Conclusions

It was shown that the Knoevenagel reaction of stoichiometric amounts of aldehyde and malononitrile in the absence of catalysts can be achieved at room temperature with quantitative conversions. In confirmation to our previous findings, the conversions are highly dependent on the reactivity of the chosen aldehyde. In the absence of any solvent only the reactive aldehydes **1b** and **1i** converted as a mixture of reactants with malononitrile to yields >90%. Homogenization of the solid mixture through dissolution in THF and subsequent immediate removal of THF improved the yields only for **1b**. While high conversions can be achieved with some aldehydes if the solid reaction mixture is left standing at room temperature after initial mechanochemical treatment, the direct solvent-free conversion without impregnation leads at best to only marginal results. For reactions in solution at room temperature, quantitative conversions could be achieved in DMF and ethanol for a number of aldehydes, where ethanol is an attractive solvent because it is inexpensive, toxicologically benign and biodegradable. A study of the solvent dependence of the Knoevenagel reaction at room temperature allowed for the interpretation of some of the solvent effects. DMF and DMSO (hydratization) and ethanol (hydrogen bonding) can bind water liberated from the reaction and thereby shift the chemical equilibrium towards the product side. The reaction proceeds less effective in polar solvents where the water is dissolved but not bound. In addition, the chemical equilibrium is further shifted to the product side when the product precipitates out of solution because of low solubility.

Overall, the findings of the study show that the Knoevenagel condensation can principally proceed on its own at room

temperature in solution and, albeit less effective, solvent-free as a mixture of reactants. It is conceivable that a number of other organic synthesis reactions could proceed quantitatively as well at room temperature. Our findings also explain why yields stated in the literature can oftentimes not be reproduced because the reaction may continue to proceed in the samples from the reaction mixture prepared for yield analysis.

Acknowledgements

This study was supported by the Fonds der chemischen Industrie. MMH acknowledges support from the American Chemical Society (PRF 46578-UFS) and SUNY Brockport for a sabbatical leave at FSU Jena, Germany.

Notes and references

- 1 R. Geyde, F. Smith, K. Westaway, H. Ali, L. Baldisera, L. Laberge and J. Rousell, *Tetrahedron Lett.*, 1986, **27**, 279–282.
- 2 R. J. Giguere, T. L. Bray, S. M. Duncan and G. Majetich, *Tetrahedron Lett.*, 1986, **27**, 4945–4948.
- 3 D. M. Mingos and D. R. Baghurst, *Chem. Soc. Rev.*, 1991, **20**, 1–47.
- 4 L. D. Field, S. Sternhell and H. V. Wilton, *Tetrahedron*, 1997, **53**, 4051–4062.
- 5 H. Sohmiya, T. Kimura, M. Fujita and T. Ando, *Tetrahedron*, 1998, **54**, 13737–13750.
- 6 M. Nüchter, B. Ondruschka and R. Trotzki, *J. Prakt. Chem.*, 2000, **342**(No. 7), 720–724.
- 7 K. Tanaka and F. Toda, *Chem. Rev.*, 2000, **100**, 1025–1074.
- 8 G. Kaupp, *Top. Curr. Chem.*, 2005, **254**, 95–183.
- 9 G. Kaupp, M. R. Naimi-Jamal and J. Schmeyers, *Tetrahedron*, 2003, **59**, 3753–3760.
- 10 B. Rodríguez, A. Bruckmann, T. Rantanen and C. Bolm, *Adv. Synth. Catal.*, 2007, **349**, 2213.
- 11 S. Wada and H. Suzuki, *Tetrahedron Lett.*, 2003, **44**, 399–401.
- 12 G.-W. Wang and B. Cheng, *ARKIVOC*, 2004, 4–8.
- 13 Z. Zhang, J. Gao, J.-J. Xia and G.-W. Wang, *Org. Biomol. Chem.*, 2005, **3**, 1617–1619.
- 14 R. Trotzki, M. M. Hoffmann and B. Ondruschka, *Green Chem.*, 2008, **10**, 767–772.
- 15 M. Nüchter, B. Ondruschka, A. Jungnickel and U. Müller, *J. Phys. Org. Chem.*, 2000, **13**, 579–586.
- 16 G. Kaupp, *CrystEngComm*, 2006, **8**, 794–804.
- 17 C. Yue, A. Mao, Y. Wei and M. Lü, *Catal. Commun.*, 2008, **9**, 1571–1574.
- 18 F. Santamarta, P. Verdía and E. Tojo, *Catal. Commun.*, 2008, **9**, 1779–1781.

Absorption of CO₂ by ionic liquid/polyethylene glycol mixture and the thermodynamic parameters†

Xiaoyong Li,^{a,b} Minqiang Hou,^b Zhaofu Zhang,^b Buxing Han,^{*b} Guanying Yang,^b Xiaoling Wang^a and Lizhuang Zou^{*a}

Received 4th February 2008, Accepted 6th June 2008

First published as an Advance Article on the web 10th July 2008

DOI: 10.1039/b801948g

Absorption/desorption of CO₂ by ionic liquid (IL) where both cation and anion are from renewable materials, (2-hydroxyethyl)-trimethyl-ammonium (*S*)-2-pyrrolidine-carboxylic acid salt [Choline][Pro], and [Choline][Pro]/polyethylene glycol 200 (PEG200) mixture, were studied in the 308.15 K to 353.15 K range at ambient pressure. It was demonstrated that both the neat ionic liquid (IL) and the IL/PEG200 mixture could capture CO₂ effectively and could be easily regenerated under vacuum or by bubbling nitrogen through the solution, and the molar ratio of CO₂ to the IL could exceed 0.5 slightly, which is the theoretical maximum for absorption of CO₂ chemically, indicating that both chemical and physical absorption existed. Addition of PEG200 in the IL could enhance the rates of absorption and desorption of CO₂ significantly. The solubility of CO₂ in [Choline][Pro]/PEG200 at different pressures from 0 to 1.1 bar was also measured, and the enthalpy and entropy of solution of CO₂ were calculated from the solubility data. At all the conditions, the enthalpy and entropy of solution were large negative values, indicating that the absorption process is exothermic.

1 Introduction

The increasing accumulation of CO₂ in the atmosphere has resulted in the global warming effect and serious environmental problems. The development of efficient methods to capture CO₂ from industrial flue gases has become an important issue in recent years. Various technologies for CO₂ capture can be used, including absorption, adsorption, membranes, and hybrid applications of these three. Currently, capture with aqueous amines seems to be the leading candidate in industrial processes.^{1,2} Although these aqueous amine solutions are effective, there are some serious drawbacks inherently connected to them. For example, the concurrent loss of the volatile amines and the uptake of water into the gas stream causes intensive energy consumption, cost increase, and corrosion problems. Therefore, it is desirable to seek new agents with favorable characteristics such as a negligible vapor pressure and high stability, without additional water.^{2,3}

It is known that ionic liquids (ILs) have some unusual properties, such as extremely low vapor pressure, wide liquid temperature range, high thermal and chemical stability, and ability to dissolve a variety of chemical compounds.⁴⁻⁶ Application of supercritical CO₂/IL biphasic system has a promising

future in separation^{7,8} and chemical reactions,^{9,10} which can avoid cross-contamination at suitable conditions. Therefore, much research on the solubility of CO₂ in ILs has been studied at elevated pressure.¹¹⁻¹⁸ Absorption of acidic gases, such as H₂S,¹⁹ SO₂,^{20,21} and CO₂,^{2,22,23} at ambient pressure using basic ILs have attracted much attention in recent years. Davis and coworkers studied the capture of CO₂ using an ionic liquid consisting of an imidazolium cation with a primary amine moiety and tetrafluoroborate anion. They found that the IL was very effective for absorption of CO₂ and molar uptake of CO₂ per mole of IL could approach 0.5, which is the theoretical maximum for CO₂ sequestration as an ammonium carbamate salt.² Zhang *et al.*²² studied the absorption of CO₂ by tetrabutylphosphonium amino acids supported on porous silica gel, and they found that fast and reversible CO₂ absorption could be achieved when compared with bubbling CO₂ into the bulk of the ionic liquids. Sanchez *et al.*²³ studied the solubility of CO₂ in different imidazolium-based ILs with and without basic groups. The results showed that the efficiency of CO₂ absorption could be enhanced significantly by the attached functional groups. Xie *et al.* reported that chitin and chitosan dissolved in 1-butyl-3-methyl-imidazolium chloride could capture CO₂ effectively.²⁴

Some ILs have been proven to be toxic, and the toxicology of most ILs is unclear and needs to be evaluated.²⁵⁻²⁷ In recent years, synthesis of ILs using renewable raw materials has become attractive.^{23,28-31} In previous work, we synthesized IL (2-hydroxyethyl)-trimethyl-ammonium (*S*)-2-pyrrolidinecarboxylic acid salt ([Choline][Pro]),³² and it was used to catalyze direct aldol reactions. The feature of this IL is that both cation and anion are from renewable materials.

^aSchool of Chemical & Environmental Engineering, China University of Mining & Technology, Beijing, 100083, China

^bBeijing National Laboratory for Molecular Sciences, Institute of Chemistry, Chinese Academy of Sciences, Beijing, 100080, China. E-mail: hanbx@iccas.ac.cn

† Electronic supplementary information (ESI) available: Data for absorption and desorption cycles and plots of $\ln P_1$ vs. $1/T$ and $\ln P_1$ vs. $\ln T$. See DOI: 10.1039/b801948g

Polyethylene glycol (PEG), which has the molecular formula $\text{HO}-(\text{CH}_2\text{CH}_2\text{O})_n-\text{H}$, has been used widely in pharmaceutical, cosmetics and food industries. PEGs have some unusual properties, such as nonvolatile, nontoxic, biodegradable, inexpensive, widely available, and their properties can be tuned by changing molecular weight. Recently, PEGs have also been used as environmentally benign solvents to replace volatile organic solvents in different processes.^{33,34}

In this work, we studied the ability of [Choline][Pro] and [Choline][Pro]/PEG200 (PEG with an average molecular weight of 200 g mol^{-1}) to capture CO_2 . It was found that both the neat IL and the IL/PEG200 mixture were very effective for capturing CO_2 , and the absorbent could be easily regenerated under vacuum or bubbling nitrogen through the solution. Addition of PEG200 in the IL could enhance the absorption and desorption rates of CO_2 significantly. We believe that this green and nonvolatile adsorbent has potential application. The solubility CO_2 in [Choline][Pro]/PEG200 at equilibrium condition was also measured, and the enthalpy and entropy of solution of CO_2 were calculated from the solubility data and thermodynamics theory. The solubility and thermodynamic data are of importance from both fundamental and practical points of view.

2 Experimental

Materials

CO_2 with a purity of 99.995% was supplied by Beijing Analytical Instrument Factory. N_2 with a purity of 99.99% was supplied by Beijing Tailong Electro-technology Corporation Ltd. Choline hydroxide solution (~45% in methanol) was supplied by ALDRICH. L-proline (99%) was produced by Chinese National Medicine Corporation Ltd. PEG200, which had average molecular weights of 200 g mol^{-1} , was analytical grade produced by Beijing Chemical Reagent Plant. The chemicals were used as received. The procedure to synthesize the IL [Choline][Pro] (Scheme 1) was similar to that described previously.³² The IL was obtained by neutralization of choline hydroxide and L-proline. The IL and PEG200 were dried under vacuum at 353 K for 48 h before use.

Apparatus and procedures to study the absorption of CO_2

The apparatus and procedures were similar to that reported previously.²⁰ In the experiment CO_2 of ambient pressure was bubbled through about 3.0 g of the IL or [Choline][Pro]/PEG200 solution in a glass tube with an inner diameter of 12 mm, and the flow rate was about 60 mL min^{-1} . The glass tube was partly immersed in a water bath of desired temperature. The weight of the IL solution was determined at regular intervals

by the electronic balance (OHAUS Corp. AR2140, USA) with a resolution of 0.1 mg. Nitrogen was bubbled through the solution to regenerate the absorbent.

Apparatus and procedures to determine the solubility of CO_2

The schematic diagram of the apparatus is shown in Fig. 1. It consisted mainly of a stainless steel cell (6 mL) with a magnetic stirrer, a constant temperature air bath, a Heise pressure gauge which could be accurate to 0.002 bar in the pressure range of 0–2 bar. The temperature of the air bath was controlled to $\pm 0.1 \text{ K}$ of the experimental temperature. In a typical experiment, a suitable amount of IL/PEG200 mixture was charged into the stainless steel cell and degassed at 40°C under vacuum for 2 h. The mass of the liquid in the stainless steel cell was determined by an electronic balance (OHAUS Corp. AR2140, USA). CO_2 was then charged into the cell after thermal equilibrium had been reached. The stirrer in the cell was started to enhance the dissolution of CO_2 in the liquid. It was assumed that equilibrium was reached after the pressure of the system had been constant for 5 h. The valve of the equilibrium cell was closed and the mass of the cell was determined. The total amount of the CO_2 in the cell was known easily from masses of the cell with and without CO_2 . Most of the CO_2 in the cell was dissolved in the IL, and a small portion existed in the vapor phase. In this work, the amount of the CO_2 in the vapor phase was calculated accurately using the Peng–Robinson equation of state,³⁶ and the amount of CO_2 in the liquid phase was known from the total amount of CO_2 and that in the vapor phase. The solubility of CO_2 in the liquid was calculated from the masses of CO_2 and the liquid in the liquid phase.

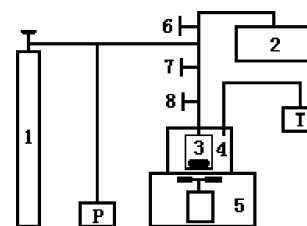
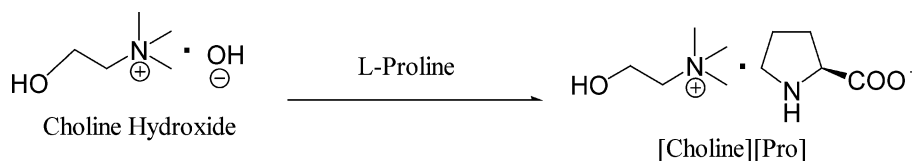


Fig. 1 Experimental apparatus to determine the solubility of CO_2 in liquid 1. CO₂ cylinder; 2. Vacuum pump; 3. Stainless steel cell; 4. Constant temperature air bath 5. Magnetic stirrer; 6, 7, 8. Valves; T. Temperature controller and temperature display; P. Pressure gauge.

In this work, we determined the solubility of CO_2 in the liquid at equilibrium condition, which was confirmed by the fact that the solubility was independent of equilibration time at fixed temperature and pressure.



Scheme 1 Schematic illustration to synthesize the IL [Choline][Pro]

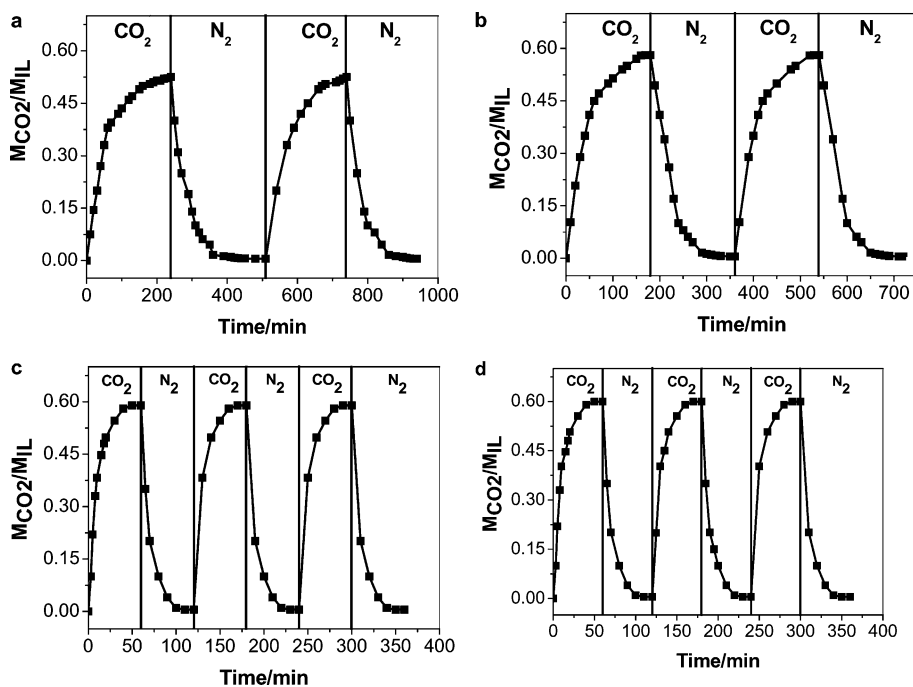


Fig. 2 Cycles of CO₂ absorption by [Choline][Pro] and [Choline][Pro]/PEG200 mixtures. (a) $W_{[\text{Choline}][\text{Pro}]} / W_{\text{PEG200}} = 1:0$, 323.15 K; (b) $W_{[\text{Choline}][\text{Pro}]} / W_{\text{PEG200}} = 2:1$, 308.15 K; (c) $W_{[\text{Choline}][\text{Pro}]} / W_{\text{PEG200}} = 1:1$, 308.15 K; (d) $W_{[\text{Choline}][\text{Pro}]} / W_{\text{PEG200}} = 1:3$, 308.15 K.

3. Results and discussion

Absorption of CO₂

In this work we studied the absorption and desorption of CO₂ in [Choline][Pro] and [Choline][Pro]/PEG200 mixtures

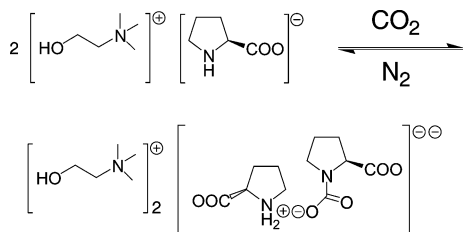
with [Choline][Pro] to PEG200 weight ratios of 1 : 0, 2 : 1, 1 : 1, and 1 : 3. For the [Choline][Pro]/PEG200 mixtures, the absorption and desorption at 308.15 K were investigated. For the neat IL, the experiments were conducted at 323.15 K because the IL became very viscous after absorbing enough

Table 1 The solubility of CO₂ (x_1 , mole fraction) in [Choline][Pro]/PEG200 and the molar ratio of CO₂ to the IL ($M_{\text{CO}_2} / M_{\text{IL}}$)

T/K	$W_{\text{IL}} / W_{\text{PEG}} = 1:1$			$W_{\text{IL}} / W_{\text{PEG}} = 1:2$			$W_{\text{IL}} / W_{\text{PEG}} = 1:3$		
	P/bar	x_1	$M_{\text{CO}_2} / M_{\text{IL}}$	P/bar	x_1	$M_{\text{CO}_2} / M_{\text{IL}}$	P/bar	x_1	$M_{\text{CO}_2} / M_{\text{IL}}$
308.15	0.051	0.108	0.253	0.050	0.074	0.253	0.041	0.055	0.243
	0.089	0.125	0.297	0.102	0.090	0.313	0.120	0.073	0.334
	0.262	0.176	0.446	0.251	0.122	0.441	0.301	0.099	0.469
	0.503	0.206	0.540	0.501	0.145	0.540	0.509	0.114	0.548
	0.601	0.217	0.580	0.652	0.154	0.580	0.598	0.118	0.573
	0.736	0.223	0.600	0.724	0.157	0.592	0.749	0.123	0.601
	0.802	0.226	0.609	0.848	0.162	0.613	0.832	0.125	0.611
	0.049	0.082	0.188	0.055	0.056	0.188	0.051	0.042	0.188
323.15	0.095	0.106	0.248	0.105	0.076	0.263	0.089	0.053	0.241
	0.252	0.150	0.367	0.211	0.097	0.340	0.225	0.075	0.346
	0.365	0.171	0.431	0.404	0.124	0.451	0.351	0.091	0.427
	0.650	0.202	0.530	0.636	0.142	0.525	0.648	0.110	0.530
	0.877	0.216	0.575	0.809	0.151	0.566	0.795	0.116	0.558
	1.042	0.220	0.590	1.050	0.156	0.590	1.046	0.121	0.590
	0.099	0.080	0.183	0.089	0.053	0.179	0.101	0.041	0.183
	0.265	0.128	0.307	0.255	0.088	0.305	0.250	0.066	0.302
338.15	0.439	0.159	0.396	0.405	0.105	0.373	0.446	0.085	0.396
	0.591	0.174	0.441	0.597	0.123	0.444	0.654	0.098	0.462
	0.698	0.184	0.472	0.748	0.132	0.483	0.801	0.103	0.491
	0.865	0.195	0.505	0.853	0.137	0.504	0.947	0.106	0.508
	1.072	0.199	0.520	1.078	0.141	0.522	1.074	0.109	0.520
	0.101	0.052	0.114	0.080	0.030	0.099	0.052	0.013	0.054
	0.249	0.098	0.228	0.209	0.060	0.203	0.201	0.043	0.191
	0.425	0.134	0.322	0.472	0.097	0.342	0.399	0.067	0.308
353.15	0.699	0.159	0.396	0.753	0.112	0.400	0.588	0.080	0.374
	0.852	0.168	0.421	0.850	0.117	0.421	0.812	0.089	0.417
	1.001	0.171	0.431	0.952	0.119	0.428	1.013	0.092	0.431
	1.052	0.173	0.436	1.060	0.122	0.436	1.054	0.093	0.436

CO₂ at lower temperature. All the results are presented in Fig. 2.

Fig. 2 shows that the CO₂ absorbed by the IL could be released by bubbling N₂ through the solution. The recovered ionic liquid has been repeatedly recycled for CO₂ absorption without observed loss of efficiency, indicating that the process of CO₂ uptake is reversible. On the basis of the reaction for the ILs with amine to absorb CO₂ reported by other authors,^{2,22} we can propose the reaction of CO₂ absorption by the IL in this work, which is shown in Scheme 2. Our experiment showed that the CO₂ absorbed could also be removed under vacuum at 313.15 K.



Scheme 2 Proposed reaction for absorption of CO₂ by [Choline][Pro].

The data in Fig. 2 indicate that the time required for the absorption to approach equilibrium depended strongly on the composition of the absorbent. For the neat IL, the times required for absorption and desorption to approach equilibrium 323.15 K were longer than 240 min and 260 min, respectively. The absorption and desorption rates increased significantly with increasing content of PEG200 in the absorbent even at lower temperature. For example, for the mixture with [Choline][Pro] to PEG200 weight ratio of 1 : 1, the absorption and desorption could approach equilibrium in about 50 min at 308.15 K. This demonstrates that addition of a suitable amount of PEG200 is kinetically favorable to the absorption and desorption.

The effect of PEG200 content on the molar ratio of CO₂ to IL was not considerable, as shown in Fig. 2. This indicates that the contribution of PEG 200 to the uptake of CO₂ is very limited. This is easy to understand because the solubility of CO₂ in PEG200 at ambient pressure is very small.³⁵ In other words, PEG200 acted as the solvent for the IL and could enhance the absorption rate dramatically.

Chemically, one mole IL can absorb half a mole of CO₂.² Fig. 2 illustrates that the molar ratio of CO₂ to the IL could exceed 0.5 slightly. This suggests that physical absorption also contributes to the uptake of CO₂. It is known from the molecular weights of CO₂ and the IL that the mass ratio of CO₂ to the IL was 0.12 as the molar ratio was 0.6.

Solubility of CO₂ in [Choline][Pro] + PEG200

The study of absorption at equilibrium condition is of importance both fundamentally and practically. In this work we determined the solubility of CO₂ in [Choline][Pro]/PEG200 at 308.15 K, 323.15 K, 338.15 K and 353.15 K at pressures up to 1.1 bar. The weight ratios of [Choline][Pro] to PEG200 selected were 1 : 1, 1 : 2, 1 : 3, respectively. Table 1 lists the solubility data at different conditions determined in this work. In the table, x_1 stands for the mole fraction of CO₂ in the liquid phase. It is estimated that the uncertainty of x_1 values in the table is

$\pm 1.0\%$. Fig. 3 demonstrates the dependence of the solubility on temperature and pressure. The solubility of CO₂ in the mixtures increased with increasing pressure, and the solubility is more sensitive to pressure in the low-pressure range. It can also be seen that the solubility of CO₂ in the mixtures decreased with increasing temperature at all the pressures.

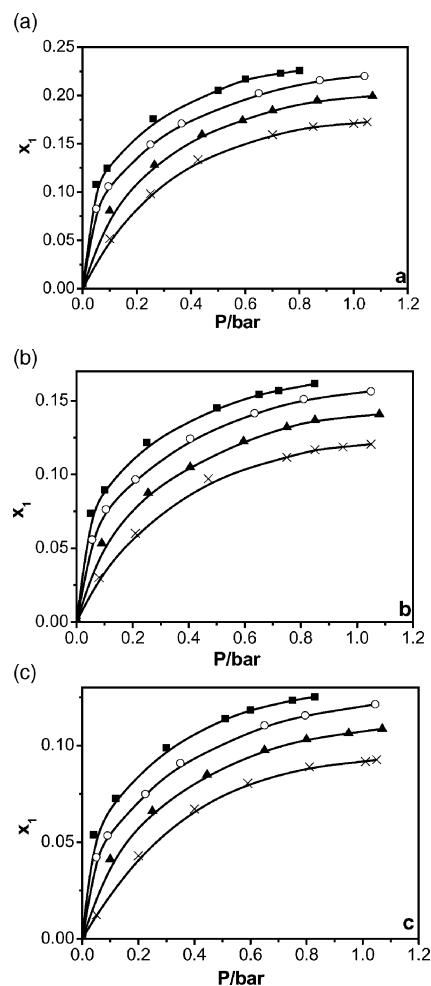


Fig. 3 Dependence of solubility of CO₂ in [Choline][Pro]/PEG200 mixture on temperature and pressure; (a) $W_{IL}/W_{PEG} = 1 : 1$, (b) $W_{IL}/W_{PEG} = 1 : 2$, (c) $W_{IL}/W_{PEG} = 1 : 3$; ■ 308.15 K, ○ 323.15 K, ▲ 338.15 K, × 353.15 K.

It is known from the data in Fig. 3 that at the same temperature and pressure the solubility of CO₂ in [Choline][Pro]/PEG200 mixture decreased with increasing PEG200 content. The reason is that, as discussed above, the solubility of CO₂ in PEG200 is very low. In order to show the role of the IL and PEG200 in the dissolution of the gas clearly, Fig. 4 illustrates the molar ratio of CO₂ to the IL (M_{CO_2}/M_{IL}) in the system at different [Choline][Pro] to PEG200 weight ratios. Clearly, the effect of the weight ratio of [Choline][Pro] to PEG200 on the M_{CO_2}/M_{IL} is very limited. In other words, the gas is mainly absorbed by the IL. The reason is that the interaction between the basic group in [Choline][Pro] and CO₂ is very strong.

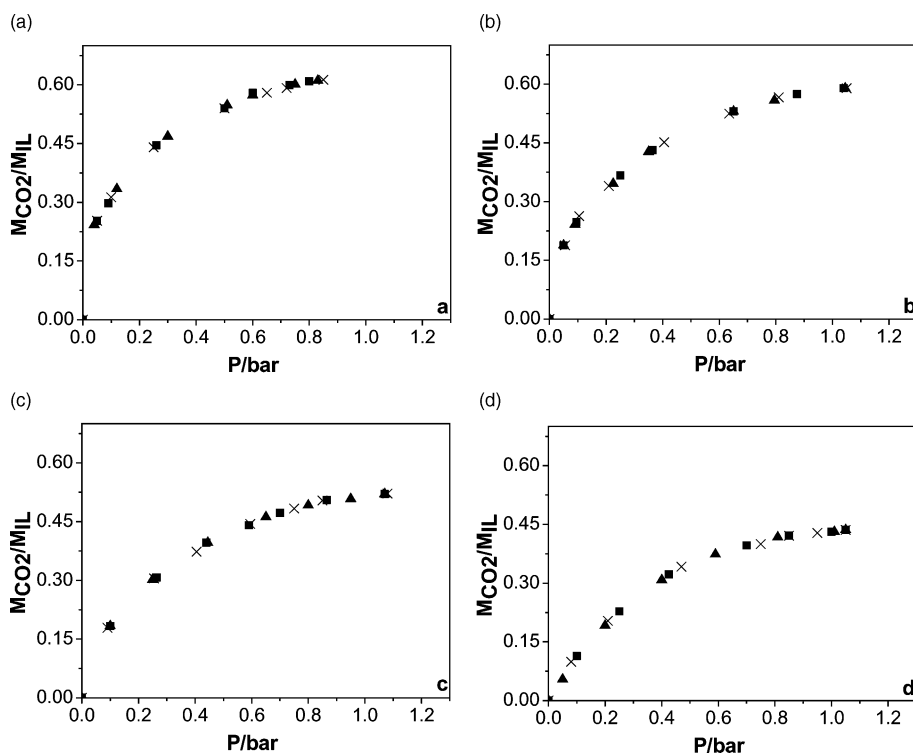


Fig. 4 The effect of temperature and pressure on the molar ratio of CO₂ to the IL ($M_{\text{CO}_2}/M_{\text{IL}}$); (a) 308.15 K, (b) 323.15 K, (c) 338.15 K, (d) 353.15 K; ■ $W_{\text{IL}}/W_{\text{PEG}} = 1 : 1$, × $W_{\text{IL}}/W_{\text{PEG}} = 1 : 2$, ▲ $W_{\text{IL}}/W_{\text{PEG}} = 1 : 3$.

Enthalpy and entropy of solution

The enthalpy ΔH_{sol} and entropy ΔS_{sol} of solution are important parameters of the system because they are related to strength of interaction between the liquid and the gas. ΔH_{sol} and ΔS_{sol} can be evaluated from the dependence of the solubility of CO₂ on temperature using the following well-known equations.¹¹

$$\frac{\Delta H_{\text{sol}}}{R} = \left(\frac{\partial \ln P_1}{\partial (1/T)} \right)_{x_1} \quad (1)$$

$$\frac{\Delta S_{\text{sol}}}{R} = - \left(\frac{\partial \ln P_1}{\partial \ln T} \right)_{x_1} \quad (2)$$

where x_1 is the mole fraction of CO₂ in the liquid phase. For the system studied in this work, $\ln P_1$ is a linear function of $1/T$ and $\ln T$ at fixed x_1 within experimental error. As an example, Fig. 5 shows the dependence of $\ln P_1$ on $1/T$ at $x_1 = 0.108$ and $W_{\text{IL}}/W_{\text{PEG}} = 1 : 1$. All other plots of $\ln P_1$ vs. $1/T$ and $\ln P_1$ vs. $\ln T$ are given in the ESI.† Therefore, the ΔH_{sol} and ΔS_{sol} values at different compositions are listed in Table 2. Under all the conditions, the enthalpy of solution is a large negative value, *i.e.*, a large amount of heat is released during the absorption process, which should be considered in the process design. This also indicates that the interaction between the IL and CO₂ is very strong. The entropy of solution is also negative, indicating a higher ordering degree when CO₂ is dissolved in liquid.

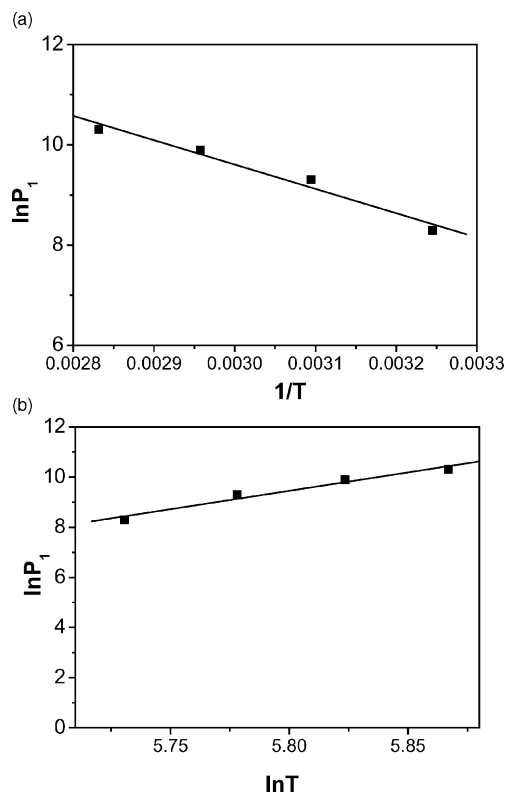


Fig. 5 Dependence of $\ln P_1$ on $1/T$ and $\ln T$ at $x_1 = 0.108$ and $W_{\text{IL}}/W_{\text{PEG}} = 1 : 1$.

Table 2 Enthalpy (kJ mol⁻¹) and entropy (J K⁻¹ mol⁻¹) of solution of CO₂ in [Choline][Pro]/PEG200 mixtures ($T = 308\text{--}353\text{K}$; x_1 stands for mole fraction of CO₂ in the liquid phase)

$W_{\text{IL}}/W_{\text{PEG}} = 1 : 1$			$W_{\text{IL}}/W_{\text{PEG}} = 1 : 2$			$W_{\text{IL}}/W_{\text{PEG}} = 1 : 3$		
x_1	$-\Delta H_{\text{sol}}$	$-\Delta S_{\text{sol}}$	x_1	$-\Delta H_{\text{sol}}$	$-\Delta S_{\text{sol}}$	x_1	$-\Delta H_{\text{sol}}$	$-\Delta S_{\text{sol}}$
0.108	40.3	121.9	0.073	40.3	122.0	0.053	34.8	105.4
0.125	31.7	96.1	0.085	30.4	92.2	0.065	29.3	88.7
0.150	24.8	75.2	0.100	26.2	79.6	0.080	25.3	76.7
0.170	25.5	77.4	0.115	25.3	76.7	0.090	25.5	77.4

4. Conclusion

The IL synthesized from renewable materials [Choline][Pro] and the [Choline][Pro]/PEG200 mixture could absorb CO₂ effectively and the molar ratio of CO₂ and the IL can reach 0.6. The CO₂ can be released under vacuum or bubbling nitrogen through the solution, and can be reused. Both chemical and physical absorption exist in the system. PEG200 in the system IL enhances kinetics of the absorption and desorption of CO₂ significantly. The solubility CO₂ in [Choline][Pro]/PEG200 increase with increasing pressure of CO₂ and is more sensitive to pressure at lower pressures. The absorption is an exothermic process.

Acknowledgements

This work was supported by National Natural Science Foundation of China (20533010)

References

- R. Idem and P. Tontiwachwuthikul, *Ind. Eng. Chem. Res.*, 2006, **45**, 2413–2413.
- E. D. Bates, R. D. Mayton, I. Ntai and J. H. Davis, *J. Am. Chem. Soc.*, 2002, **124**, 926–927.
- G. R. Yu, S. J. Zhang, X. Q. Yao, J. M. Zhang, K. Dong, W. B. Dai and R. Mori, *Ind. Eng. Chem. Res.*, 2006, **45**, 2875–2880.
- P. Wasserscheid, T. Welton, *Ionic Liquids in Synthesis*, Wiley-VCH, Weinheim, 2003.
- V. I. Parvulescu and C. Hardacre, *Chem. Rev.*, 2007, **107**, 2615–2665.
- R. D. Rogers and K. R. Seddon, *Science*, 2003, **302**, 792–793.
- L. A. Blanchard, D. Hancu, E. J. Bechman and J. F. Brennecke, *Nature*, 1999, **399**, 28–29.
- M. C. Kroon, S. J. van, C. J. Peters, R. A. Sheldon and G. J. Witkamp, *Green Chem.*, 2006, **8**, 246–249.
- D. J. Cole-Hamilton, *Science*, 2003, **299**, 1702–1706.
- R. A. Brown, P. Pollet, E. McKoon, C. A. Eckert, C. L. Liotta and P. G. Jessop, *J. Am. Chem. Soc.*, 2001, **123**, 1254–1255.
- J. L. Anthony, E. J. Maginn and J. F. Brennecke, *J. Phys. Chem. B*, 2002, **106**, 7315–7320.
- J. L. Anderson, J. K. Dixon and J. F. Brennecke, *Acc. Chem. Res.*, 2007, **40**, 1208–1216.
- B. Breure, S. B. Bottini, G. J. Witkamp and C. J. Peters, *J. Phys. Chem. B*, 2007, **111**, 14265–14270.
- E. Kuhne, C. J. Peters, S. J. van and G. J. Witkamp, *Green Chem.*, 2006, **8**, 287–291.
- X. L. Yuan, S. J. Zhang, J. Liu and X. M. Lu, *Fluid Phase Equilib.*, 2007, **257**, 195–200.
- M. B. Shiflett and A. Yokozeki, *J. Phys. Chem. B*, 2007, **111**, 2070–2074.
- Y. S. Kim, J. H. Jang, B. D. Lim, J. W. Kang and C. S. Lee, *Fluid Phase Equilib.*, 2007, **256**, 70–74.
- G. Hong, J. Jacquemin, M. Deetlefs, C. Hardacre, P. Husson and M. F. Costa Gomes, *Fluid Phase Equilib.*, 2007, **257**, 27–34.
- J. H. Davis, Jr., in *Green Industrial Applications of Ionic Liquids*, NATO Science Series, Volume 92, Ed: R. D. Rogers, K. R. Seddon, S. Volkov, Kluwer Academic Publishers, Dordrecht, 2000.
- W. Z. Wu, B. X. Han, H. X. Gao, Z. M. Liu, T. Jiang and J. Huang, *Angew. Chem., Int. Ed.*, 2004, **43**, 2415–2417.
- J. Huang, A. Riisager, P. Wasserscheid and R. Fehrmann, *Chem. Commun.*, 2006, **38**, 4027–4029.
- J. M. Zhang, S. J. Zhang, K. Dong, Y. Q. Zhang, Y. Q. Shen and X. M. Lv, *Chem.–Eur. J.*, 2006, **12**, 4021–4026.
- L. M. Galan Sanchez, G. W. Meindersma and A. B. de Haan, *Chem. Eng. Res. Des.*, 2007, **85**, 31–39.
- H. B. Xie, S. B. Zhang and S. H. Li, *Green Chem.*, 2006, **8**, 630–633.
- R. P. Swatloski, J. D. Holbrey and R. D. Rogers, *Green Chem.*, 2003, **5**, 361–363.
- M. T. Garcia, N. Gathergood and P. J. Scammells, *Green Chem.*, 2005, **7**, 9–14.
- C. Pretti, C. Chiappe, D. Pieraccini, M. Gregori, F. Abramo, G. Monni and L. Intorre, *Green Chem.*, 2006, **8**, 238–240.
- M. Avalos, R. Babiano, P. Cintas, J. L. Jimenez and J. C. Palacios, *Angew. Chem., Int. Ed.*, 2006, **45**, 3904–3908.
- K. Fukumoto, M. Yoshizawa and H. Ohno, *J. Am. Chem. Soc.*, 2005, **127**, 2398–2399.
- G. H. Tao, L. He, N. Sun and Y. Kou, *Chem. Commun.*, 2005, **28**, 3562–3564.
- A. P. Abbott, G. Capper, D. L. Davies, R. K. Rasheed and V. Tambyrajah, *Chem. Commun.*, 2003, **1**, 70–71.
- S. Q. Hu, T. Jiang, Z. F. Zhang, A. L. Zhu, B. X. Han, J. L. Song, Y. Xie and W. J. Li, *Tetrahedron Lett.*, 2007, **48**, 5613–5617.
- J. Chen, S. K. Spear, J. G. Huddleston and R. D. Rogers, *Green Chem.*, 2005, **7**, 64–82.
- Z. S. Hou, N. Theyssen, A. Brindmann and W. Leitner, *Angew. Chem., Int. Ed.*, 2005, **44**, 1346–1349.
- M. Q. Hou, S. G. Liang, Z. F. Zhang, J. Y. Song, T. Jiang and B. X. Han, *Fluid Phase Equilib.*, 2007, **258**, 108–114.
- D. Y. Peng and D. B. Robindon, *Ind. Eng. Chem. Fundam.*, 1976, **15**, 59–64.

Non-occurrence of a Zincke-like process upon treatment of 1-(2,4-dinitrophenyl)-3-methylimidazolium chloride with a chiral primary amine†

Julio Cezar Pastre,^a Carlos Roque D. Correia^a and Yves Génisson^{*b}

Received 18th March 2008, Accepted 9th June 2008

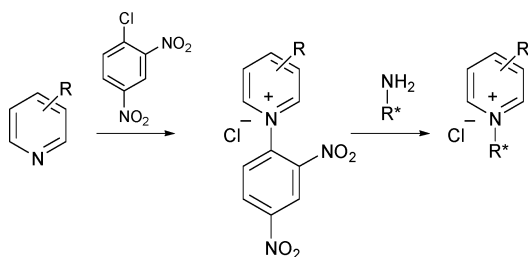
First published as an Advance Article on the web 14th July 2008

DOI: 10.1039/b804650f

Huang's preparation of chiral imidazolium salts by means of a Zincke-like process was re-investigated. It was shown that treatment of 1-(2,4-dinitrophenyl)-3-methylimidazolium chloride with L-alaninol gives rise to complete decomposition of the starting salt *via* an S_NAr reaction and that the material described by Huang was not the claimed chiral imidazolium salt, thus questioning the occurrence of the ionic liquids reported in the original work.

Introduction

In the 90's, Marazano and ourselves demonstrated that the Zincke's reaction was a unique and versatile synthetic tool for the preparation of chiral pyridinium salts bearing an asymmetric centre directly attached to the heterocyclic nitrogen (Scheme 1).¹



Scheme 1

This route basically relies on the reaction of a highly activated (2,4-dinitrophenyl)pyridinium chloride with various chiral primary amines. From a mechanistic standpoint, the overall process involves nucleophilic attack onto the C-2 of the pyridinium nucleus by the primary amine, ring opening/electrocyclisation and finally re-aromatization driven by the elimination of 2,4-dinitroaniline. This approach has found widespread application in the field of asymmetric synthesis in Marazano's group.² It was also recently used for the preparation of the first pyridinium type chiral ionic liquids by Lauth-de Viguierie and ourselves.³ Lately we further exploited this route for the preparation of a phenyl glycinol-derived chiral ionic liquid. Access to salt 3

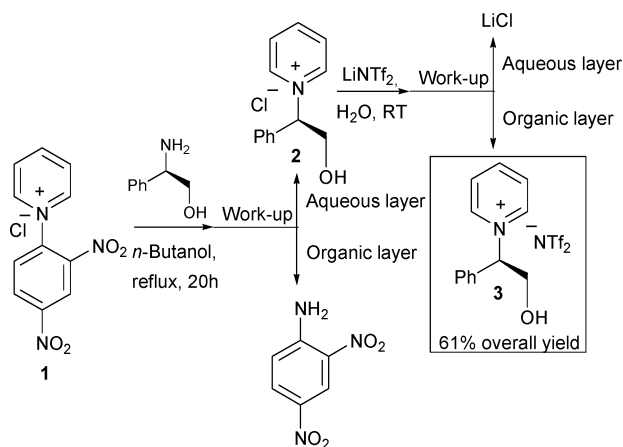
^aInstituto de Química, Universidade Estadual de Campinas, UNICAMP, C.P. 6154, CEP. 13084-971, Campinas, São Paulo, Brasil

^bLaboratoire de Synthèse et Physicochimie de Molécules d'Intérêt Biologique UMR-CNRS 5068, Université Paul Sabatier, 118 route de Narbonne, 31062, Toulouse, France.

E-mail: genisson@chimie.ups-tlse.fr; Fax: +33(0)561556011; Tel: +33(0)561556299

† Electronic supplementary information (ESI) available: ¹H and ¹³C NMR spectra for all compounds. ¹H NMR spectra of **4** in DMSO-d₆/D₂O. 2D NMR (COSY/HSQC) experiments and MS/HRMS for **10**. For ESI see DOI: 10.1039/b804650f

was secured in a practical two-step sequence avoiding the use of any column chromatography thanks to the solubility of the pyridinium salt in water for the chloride **2** and in CH₂Cl₂ for the bistrifluoromethanesulfonimide **3** (Scheme 2).



Scheme 2

In 2006, Huang and Ou reported the use of a Zincke-like process for the synthesis of three chiral aminoalcohol-derived imidazolium salts, their transformation into the corresponding chiral ionic liquids through counter-anion metathesis and the use of these salts as phase-transfer catalysts.⁴ The discrepancy between these results and our own attempts to develop a Zincke-like reaction in the imidazolium series prompted us to re-investigate this chemistry. We wish to report here the results of this study.

Results and discussion

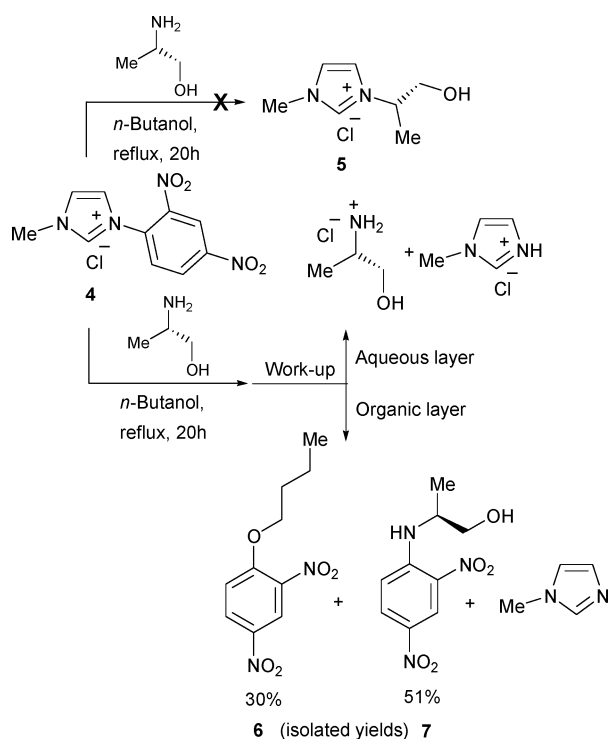
Background

In 2005, we reported a synthetic route to chiral imidazolinic entities, their transformation into chiral ionic liquids and preliminary attempts to use these salts in asymmetric phase-transfer catalysis.⁵ In line with this work, we had also naturally

tried to apply Marazano's approach to the imidazolium series. Indeed, one might expect an initial nucleophilic attack onto the C-2 position of the imidazolium nucleus which could trigger a Zincke-like process. However, preliminary experiments with 1-(2,4-dinitrophenyl)-3-methylimidazolium chloride and α -methylbenzylamine soon indicated that the process was not directly transposable. The reaction was run under Marazano's standard conditions (1.1 eq of amine, 20 h in refluxing *n*-butanol) and the crude mixture partitioned between CH_2Cl_2 and water. The material resulting from the concentration to dryness of the aqueous phase could, at first glance, be confused with the expected imidazolium salt on the basis of its ^1H NMR analysis. However we had already prepared the corresponding iodide salt using our own route and it was noticed that the proton carried by the stereogenic centre (typically around 5.90 ppm) was far too shielded (observed below 4.50 ppm). We thus concluded that the aqueous phase was composed of an equimolar mixture of α -methylbenzylamine hydrochloride and 1-methylimidazole hydrochloride. The formation of these products was attributed to the decomposition of the starting imidazolium chloride (*vide infra*) which was further confirmed by mass spectroscopy analysis.

Re-investigating Huang's results

In 2006, Huang and Ou reported the reaction between three aminoalcohols and 1-(2,4-dinitrophenyl)-3-methylimidazolium chloride in refluxing *n*-butanol to give the corresponding chiral imidazolium salts, according to a Zincke-like process (Scheme 3).



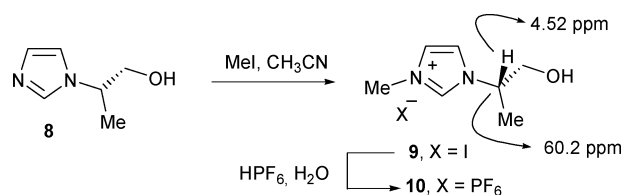
We were intrigued by the fact that only poorly sterically demanding amino alcohols were used, the classical phenyl

glycinol, for example, being omitted. Wondering if this might not be a key parameter, we re-investigated the reported results. We selected *L*-alaninol as a representative reactant, being the least bulky starting aminoalcohol. However, the claimed formation of a chiral imidazolium salt was not observed upon reproducing the published procedure with this substrate. Careful analysis of the crude reaction mixture by means of LC-MS did not allow detection of the cation corresponding to the expected imidazolium (m/z 141). On the contrary, complete degradation of the 1-(2,4-dinitrophenyl)-3-methylimidazolium chloride through an $\text{S}_{\text{N}}\text{Ar}$ process involving either a molecule of *n*-butanol or a molecule of the starting aminoalcohol was observed (Scheme 3). Column chromatography allowed isolation of the known aromatic ether **6** and the aniline **7** in 30% and 51% yields respectively (81% combined yield).⁶ A more complete analysis of the crude reaction mixture was carried out by partition between CH_2Cl_2 and water. ^1H NMR analysis of the organic phase clearly showed the presence of the aromatic ether **6** and the aniline **7** (in a 37 : 63 ratio) along with a small amount of 1-methylimidazole. Consistently, the aqueous phase contained only *L*-alaninol hydrochloride and 1-methylimidazole hydrochloride. It thus appeared that, in our hands, the Zincke-type starting imidazolium salt exclusively underwent the so-called exocyclic attack, in opposition to the expected endocyclic pathway, the imidazolium moiety thus acting as an efficient nucleofuge. In the pyridinium series, this side reaction was only observed when the heterocyclic nucleus was substituted with electron-donating alkyl groups. However, 1-(2,4-dinitrophenyl)-3-methylimidazolium chloride appeared so susceptible to such an $\text{S}_{\text{N}}\text{Ar}$ reaction that *L*-alaninol smoothly attacked the highly activated phenyl ring at RT in CH_2Cl_2 . In this case, a gummy material accumulated after 48 h of reaction. ^1H NMR analysis of the bright yellow supernatant revealed the major presence of the 2,4-dinitroaniline **7** and the 1-methylimidazole. The solid precipitate was essentially composed of the remaining 1-(2,4-dinitrophenyl)-3-methylimidazolium chloride and the generated *L*-alaninol hydrochloride. Column chromatography of the whole crude reaction mixture gave a 38% yield of the aniline **7** (for a maximum of *ca.* 50% yield owing to the *in situ* protonation of the primary amine by the generated HCl). Interestingly, we observed in ^1H NMR that the H-2 of 1-(2,4-dinitrophenyl)-3-methylimidazolium chloride is highly exchangeable, and, contrary to what has been mistakenly described by Huang, cannot be observed in CD_3OD but appears at 10.2 ppm in $\text{DMSO}-d_6$. Progressive disappearance of this signal was observed after addition of D_2O and gentle warming of the sample (see ESI[†]). This further indicated the powerful electron-withdrawing effect exerted by the 2,4-dinitrophenyl nucleus.

Preparation of the imidazolium hexafluorophosphate and comparison of the spectral data

Thus, to unequivocally show that the compounds described by Huang were not the claimed chiral imidazolium salts, we independently prepared the imidazolium hexafluorophosphate **10** as a representative example (Scheme 4).

The sequence reported by Bao *et al.* was used to synthesise the required imidazole intermediate.⁷ From there, quaternarisation with methyl iodide followed by anion metathesis gave the desired



Scheme 4

chiral ionic liquid. This unusually hydrophilic hexafluorophosphate salt was fully characterised: 1D and 2D ¹H and ¹³C NMR, IR, [α]_D, MS and HRMS. The NMR spectral data obtained for our sample were in contradiction with that reported by Huang. Noteworthy is the NMR chemical shift of 4.52 ppm for the proton carried by the stereogenic centre, the carbon itself appearing at 60.2 ppm in ¹³C NMR. These characteristic signals were absent from Huang's description of compound **10** (*vide infra*). As a matter of fact, none of the nine similar imidazolium derivatives described in Huang's article displayed a ¹H signal between 4–5 ppm.

So, if the sample described by Huang was not the claimed imidazolium salt, what could it be? The NMR data reported for the proposed L-alanine-derived imidazolium chloride showed the proton carried by the center of chirality notably up-field (*ca.* 3.35 ppm). In fact, the whole set of ¹H signals corresponding to the chiral appendage was highly reminiscent of that of the alaninol hydrochloride. However, the signals associated with the 1-methylimidazolium moiety did not correspond to that of the free base or to that of the hydrochloride. Reasoning that the reaction was producing a mixture of 1-methylimidazole and 1-methylimidazole hydrochloride (*vide supra*) we analysed a *ca.* 50 : 25 : 25 mixture of L-alanine hydrochloride, 1-methylimidazole and 1-methylimidazole hydrochloride. The resulting ¹H and ¹³C NMR spectra were surprisingly consistent with the one reported by Huang for the L-alanine-derived imidazolium chloride (Fig. 1 and Fig. 2). In particular, the proton around 3.35 ppm and the carbon at 49.5 ppm associated to the center of chirality were present. Such a mixture (possibly obtained upon washing of the chromatography column with MeOH) might therefore have been, *in the absence of mass spectroscopy analysis*, erroneously taken for the desired imidazolium salt. ‡

Conclusions

It was thus shown that, contrary to what had been reported by Huang and Ou, the treatment of 1-(2,4-dinitrophenyl)-3-methylimidazolium chloride with a chiral primary amine did not lead to a Zincke-like process but only to the decomposition of the starting material *via* an S_NAr reaction due to the strong nucleofugal behaviour of the imidazolium nucleus. Spectral data reported herein for the representative L-alanine-derived ionic liquid **9** further demonstrate that Huang did not describe this chiral imidazolium salt and therefore casts doubt on all the imidazolium-based ionic liquids reported in the original article.

‡ Eluting the silica gel chromatography column with wet MeOH at the end of the purification gave us a similar mixture.

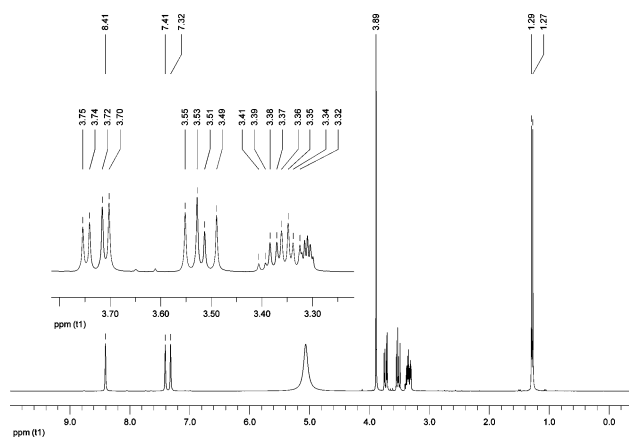


Fig. 1 ¹H NMR spectra (300 MHz, CD₃OD) of a mixture of L-alanine hydrochloride, 1-methylimidazole hydrochloride and 1-methylimidazole.

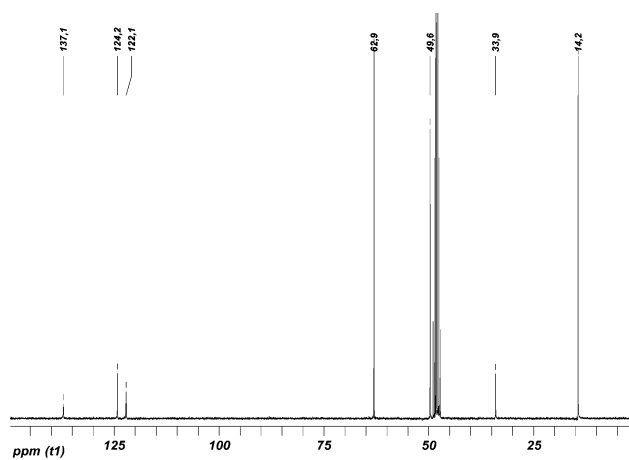


Fig. 2 ¹³C NMR spectra (75 MHz, CD₃OD) of a mixture of L-alanine hydrochloride, 1-methylimidazole hydrochloride and 1-methylimidazole.

Experimental

1-[(2*R*)-1-hydroxy-2-phenyl-2-ethanyl]pyridinium bistrifluoromethanesulfonimide (**3**)

To a suspension of 1-(2,4-dinitrophenyl)pyridinium chloride (2.25 g, 8.00 mmol) in *n*-butanol (80 cm³) was added (–)-(*R*)-2-phenylglycinol (1.10 g, 8.00 mmol) and the resulting mixture was refluxed for 20 h. After cooling to room temperature, the solvent was removed under reduced pressure and to the residue obtained was added water (60 cm³). The aqueous solution was washed with dichloromethane (3 × 80 cm³) and concentrated to dryness *in vacuo* to give a light brown oil, which was used in the following step without further purification. Then, this residue was dissolved in water (50 cm³) and lithium bistrifluoromethanesulfonimide (2.53 g, 8.80 mmol) was added at once. The resulting suspension was heated at 70 °C for 2 h and allowed to stand at room temperature overnight. The insoluble oily material was extracted with dichloromethane (3 × 80 cm³) and the combined organic layers were washed with water (6 × 50 cm³), dried over anhydrous Na₂SO₄, filtered and concentrated to dryness to give the expected bistrifluoromethanesulfonimide salt **3** (2.34 g, 61% for the 2 steps) as a light brown liquid.

$[\alpha]_{\text{D}}^{20} -34.0$ (c 1.70 in CH_3OH); ν_{max} (film)/ cm^{-1} 3521, 3136, 3093, 1633, 1486, 1352, 1196, 1138, 1058, 791 and 741; δ_{H} (300 MHz, CD_3OD) 9.05 (2 H, dd, J 1.3 and 6.8, arom. H), 8.63 (1 H, tt, J 1.3 and 7.9), 8.13 (2 H, t, J 7.0, arom. H), 7.56–7.47 (5 H, m, Ph), 6.04 (1 H, dd, J 4.1 and 8.6, CHCH_2OH) and 4.46 (2 H, AB of an ABX, $\Delta\delta$ 0.15, J 12.4, 8.6 and 4.1, CH_2OH); δ_{C} (75 MHz, CD_3OD) 147.8, 145.6, 135.2, 131.5, 130.9, 129.6, 129.5, 121.4 (q, J 320.5, SO_2CF_3), 77.8 and 63.6; m/z (ESI^+) 200 (M^+ , 100%); (ESI^-) 280 (TF_3N^- , 100%); HRMS (ESI^+) 200.1096 (M^+ , $\text{C}_{13}\text{H}_{14}\text{NO}$ requires 200.1075).

1-(2,4-dinitrophenyl)-3-methylimidazolium chloride (4)

To a solution of 1-methylimidazole (2.50 g, 30.50 mmol) in acetone (20 cm^3) was added 1-chloro-2,4-dinitrobenzene (6.20 g, 30.60 mmol) and the resulting mixture was refluxed for 6 h. After cooling to room temperature, the precipitate was filtered, washed with acetone and dried under reduced pressure to give the Zincke-type salt **4** (7.04 g, 81%) as an off-white powder. Mp 235 °C (dec.); ν_{max} (KBr)/ cm^{-1} 3076, 2927, 1607, 1583, 1536, 1356, 1221, 1089, 954, 859 and 770; δ_{H} (300 MHz, $\text{DMSO}-d_6$) 9.90 (1 H, s, 2-H), 9.03 (1 H, d, J 2.5, arom. H), 8.87 (1 H, dd, J 2.6 and 8.7, arom. H), 8.28 (1 H, d, J 8.7, arom. H), 8.19 (1 H, t, J 1.8, 4-H or 5-H), 8.06 (1 H, t, J 1.8, 4-H or 5-H) and 4.04 (3 H, s, 3- CH_3); δ_{C} (75 MHz, $\text{DMSO}-d_6$) 148.4, 143.8, 138.5, 132.5, 131.8, 129.6, 124.1, 123.8, 121.5 and 36.3; m/z (ESI^+) 249 (M^+ , 100%), HRMS (ESI^+) 249.0614 (M^+ , $\text{C}_{10}\text{H}_9\text{N}_4\text{O}_4$ requires 249.0624).

1-butoxy-2,4-dinitrobenzene (6) and (S)-2-(2,4-dinitrophenylamino)propan-1-ol (7)

L-Alaninol (145 mg, 1.93 mmol) in solution in *n*-butanol (0.50 cm^3) was added to a stirred suspension of imidazolium chloride **4** (500 mg, 1.76 mg) in *n*-butanol (5 cm^3) at room temperature. A rapid yellow color of the supernatant ensued. The reaction mixture was then gradually heated and was maintained under reflux for 20 h. Upon heating, the reaction mixture turned to a black homogenous solution. After cooling to room temperature, the solvent was evaporated off under vacuum and the resulting residue was purified by flash chromatography over silica gel ($\text{CH}_2\text{Cl}_2/\text{EtOAc}$, 100 : 0, 90 : 10 and 80 : 20) to give the aromatic ether **6** as a colourless liquid (125 mg, 30%) and the aniline **7** (218 mg, 51%) as a yellow-orange solid.

1-butoxy-2,4-dinitrobenzene (6)

ν_{max} (film)/ cm^{-1} 3117, 2962, 2875, 1608, 1526, 1343, 1287, 1152, 1069, 962, 833 and 744; δ_{H} (300 MHz, CDCl_3) 8.69 (1 H, d, J 2.8, arom. H), 8.40 (1 H, dd, J 9.3 and 2.8, arom. H), 7.21 (1 H, d, J 9.3, arom. H), 4.24 (2 H, t, J 6.3, OCH_2), 1.91–1.81 (2 H, m, CH_2CH_2), 1.59–1.46 (2 H, m, CH_2CH_2) and 0.97 (3 H, d, J 7.3, CH_3); δ_{C} (75 MHz, CDCl_3) 156.9, 139.7, 138.8, 129.0, 121.7, 114.2, 70.5, 30.6, 18.9 and 13.5; m/z (ESI^+) 503 (2M + Na^+ , 79%) and 263 (M + Na^+ , 100%).

(S)-2-(2,4-dinitrophenylamino)propan-1-ol (7)

Mp 69–70 °C; $[\alpha]_{\text{D}}^{20} + 16.0$ (c 1.20 in CHCl_3); ν_{max} (KBr)/ cm^{-1} 3350, 3089, 2939, 1625, 1585, 1504, 1422, 1342, 1274, 1124, 1082, 995, 827 and 743; δ_{H} (300 MHz, CDCl_3) 9.06 (1 H, d, J

2.7, arom. H), 8.72 (1 H, br d, J 7.1, NH), 8.21 (1 H, ddd, J 9.6, 2.7 and 0.6, arom. H), 7.02 (1 H, d, J 9.6, arom. H), 4.04–3.92 (1 H, m, CHCH_2OH), 3.82 (2 H, AB of an ABX, $\Delta\delta$ 0.10, J 11.0, 5.4 and 4.1, CH_2OH), 2.35 (1 H, br s, OH) and 1.38 (3 H, d, J 6.5, CH_3); δ_{C} (75 MHz, CDCl_3) 148.1, 135.7, 130.2, 124.4, 114.6, 65.6, 50.5 and 16.9; m/z (ESI^+) 505 (2M + Na^+ , 46%), 264 (M + Na^+ , 100%), 242 (M + H^+ , 26%); HRMS (ESI^+) 505.1295 (2M + Na^+ , $\text{C}_{18}\text{H}_{22}\text{N}_6\text{O}_{10}\text{Na}$ requires 505.1306).

1-Methyl-3-[(2S)-1-hydroxy-2-propanyl]imidazolium iodide (9)

To a solution of the imidazole **8** (0.52 g, 4.10 mmol) in acetonitrile (9 cm^3) was added iodomethane (0.28 cm^3 , 4.51 mmol) and the resulting mixture was stirred for 20 h at room temperature. The solvent was removed under reduced pressure giving the desired imidazolium iodide **9** in quantitative yield (1.10 g) as a light yellow powder. Mp 71–72 °C; $[\alpha]_{\text{D}}^{20} + 5.81$ (c 0.86 in CH_3OH); ν_{max} (KBr)/ cm^{-1} 3331, 3140, 3105, 3074, 2969, 1572, 1560, 1341, 1171, 1047, 827, 753 and 651; δ_{H} (300 MHz, CD_3OD) 9.09 (1 H, s, 2-H), 7.75 (1 H, t, J 1.8, 4-H or 5-H), 7.63 (1 H, t, J 1.8, 4-H or 5-H), 4.62 (1 H, dq, J 3.7 and 7.0, CHCH_2OH), 3.98 (3H, s, CH_3), 3.81 (2 H, AB of an ABX, $\Delta\delta$ 0.11, J 12.0, 7.0 and 3.7, CH_2OH) and 1.59 (3 H, d, J 7.0, CHCH_3); δ_{C} (75 MHz, CD_3OD) 137.5, 124.8, 122.4, 65.5, 60.1, 36.9 and 16.9; m/z (ESI^+) 141 (M^+ , 100%); (ESI^-) 127 (I^- , 100%); HRMS (ESI^+) 141.1053 (M^+ , $\text{C}_7\text{H}_{13}\text{N}_2\text{O}$ requires 141.1028).

1-Methyl-3-[(2S)-1-hydroxy-2-propanyl]imidazolium hexafluorophosphate (10)

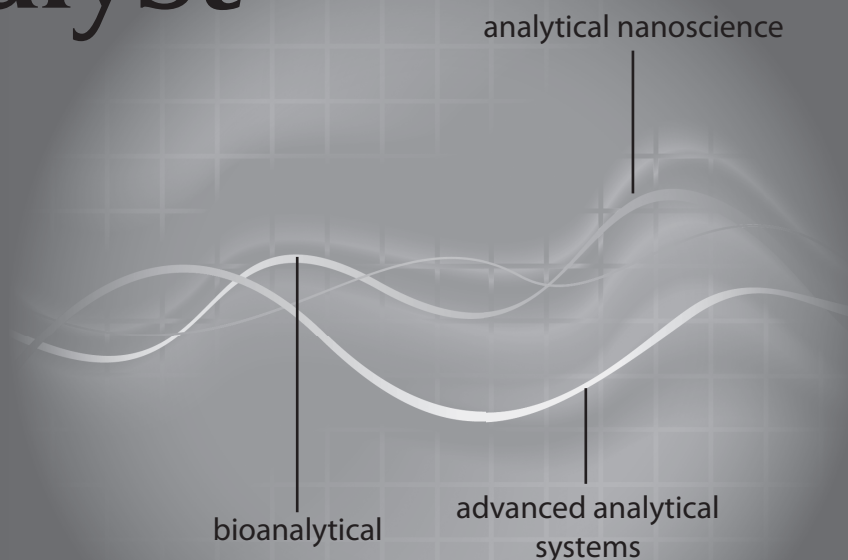
To a solution of the imidazolium iodide **9** (175 mg, 0.65 mmol) in water at 0 °C (5 cm^3) was added hexafluorophosphoric acid (0.2 cm^3 of a 60% aqueous solution, 1.31 mmol) and the mixture was stirred in the dark at room temperature for 24 h. The resulting yellow solution was then concentrated *in vacuo*. The residue was taken up in water and the mixture was concentrated *in vacuo*. This operation was repeated until a colourless crude mixture was obtained. The residue was then dissolved in water and the acidic solution was neutralized by addition of solid NaHCO_3 . The residue was then filtered over C18 silica gel eluting with water to give the desired imidazolium hexafluorophosphate **10** (145 mg, 78%) as a colourless material. $[\alpha]_{\text{D}}^{20} + 0.62$ (c 1.94 in CH_3CN); ν_{max} (film)/ cm^{-1} 3399, 3152, 2950, 1573, 1543, 1461, 1171, 1052, 839 and 558; δ_{H} (300 MHz, CD_3OD) 8.83 (1 H, s, 2-H), 7.64 (1 H, t, J 1.8, 4-H or 5-H), 7.52 (1 H, t, J 1.8, 4-H or 5-H), 4.52 (1 H, dq, J 3.7 and 7.0, CHCH_2OH), 3.92 (3H, s, CH_3), 3.77 (2 H, AB of an ABX, $\Delta\delta$ 0.11, J 12.0, 7.0 and 3.7, CH_2OH) and 1.55 (3 H, d, J 7.0, CHCH_3); δ_{C} (75 MHz, CD_3OD) 137.2, 124.7, 122.2, 65.5, 60.2, 36.4 and 16.6; m/z (ESI^+) 141 (M^+ , 100%); (ESI^-) 145 (PF_6^- , 100%); HRMS (ESI^+) 141.1026 (M^+ , $\text{C}_7\text{H}_{13}\text{N}_2\text{O}$ requires 141.1028).

References

- Y. Génisson, C. Marazano, M. Mehmandoust, D. Gnecco and B. C. Das, *Synlett*, 1992, **46**, 431–434. See also: G. H. R. Viana, I. C. Santos, R. B. Alves, L. Gil, C. Marazano and R. P. F. Gil, *Tetrahedron Lett.*, 2005, **46**, 7773–7776; T. M. Nguyen, M. del Rayo Sanchez-Salvadori, J.-C. Wypych and C. Marazano, *J. Org. Chem.*, 2007, **72**, 5916–5919.

- 2 Selected references: Y. Génisson, C. Marazano and B. C. Das, *J. Org. Chem.*, 1993, **58**, 2052–2057; Y.-S. Wong, C. Marazano, D. Gnecco, Y. Génisson, A. Chiaroni and B. C. Das, *J. Org. Chem.*, 1997, **62**, 729–733; D. Compere, C. Marazano and B. C. Das, *J. Org. Chem.*, 1999, **64**, 4528–4532; L. Gil, D. Compere, B. Guilloteau-Bertin, A. Chiaroni and C. Marazano, *Synthesis*, 2000, 2117–2126; B. Guilloteau-Bertin, D. Compere, L. Gil, C. Marazano and B. C. Das, *Eur. J. Org. Chem.*, 2000, 1391–1399.
- 3 C. Patrascu, C. Sugisaki, C. Mingotaud, J.-D. Marty, Y. Génisson and N. Lauth-de Viguierie, *Heterocycles*, 2004, **63**, 2033–2041.
- 4 W.-H. Ou and Z.-Z. Huang, *Green Chem.*, 2006, **8**, 731–734.
- 5 Y. Génisson, N. Lauth-de Viguierie, C. André, M. Baltas and L. Gorrichon, *Tetrahedron: Asymmetry*, 2005, **16**, 1017–1023.
- 6 Y. Ogata and M. Okano, *J. Am. Chem. Soc.*, 1949, **71**, 3211–3212.
- 7 W. Bao, Z. Wang and Y. Li, *J. Org. Chem.*, 2003, **68**, 591–593.

The Analyst



Advanced analytical systems

050830

Examples of recent articles include:

Diamond microelectrodes for in vitro electroanalytical measurements: current status and remaining challenges

Jinwoo Park, Veronika Quaiserová-Mocko, Bhavik Anil Patel, Martin Novotný, Aihua Liu, Xiaochun Bian, James J. Galligan and Greg M. Swain
Analyst, 2008, **133**, 17 - 24, DOI: 10.1039/b710236b

Photoelectrochemical ruler: measurement at the micron scale

Nicole Fietkau, Javier del Campo, Roser Mas, Francesc Xavier Muñoz and Richard G. Compton
Analyst, 2007, **132**, 983 - 985, DOI: 10.1039/b711828g

Rapid analysis of metabolites and drugs of abuse from urine samples by desorption electrospray ionization-mass spectrometry

Tiina J. Kauppila, Nari Talaty, Tiia Kuuranne, Tapio Kotiaho, Risto Kostiainen and R. Graham Cooks
Analyst, 2007, **132**, 868 - 875, DOI: 10.1039/b703524a

Forensic analysis of inks by imaging desorption electrospray ionization (DESI) mass spectrometry

D. R. Ifa, L. M. Gumaelius, L. S. Eberlin, N. E. Manicke and R. Graham Cooks
Analyst, 2007, **132**, 461 - 467, DOI: 10.1039/b700236j

Electrophoretic method for assessment of substrate promiscuity of a heterogeneous biocatalyst using an area imaging ultraviolet detector

Pawel L. Urban, Edmund T. Bergström, David M. Goodall, Sreedevi Narayanaswamy and Neil C. Bruce
Analyst, 2007, **132**, 979 - 982, DOI: 10.1039/b710495b

Submit your work today!

RSC Publishing

www.rsc.org/analyst

Registered Charity Number 207890



42nd IUPAC CONGRESS Chemistry Solutions

2–7 August 2009 | SECC | Glasgow | Scotland | UK

On behalf of IUPAC, the RSC is delighted to host the 42nd Congress (IUPAC 2009), the history of which goes back to 1894. RSC and IUPAC members, groups and networks have contributed a wealth of ideas to make this the biggest UK chemistry conference for several years.

As well as a programme including more than 50 symposia, a large poster session and a scientific exhibition, we are planning a series of social and satellite events to enhance networking and discussion opportunities.

Sponsored by  Schering-Plough

Call for abstracts

This is your chance to take part in IUPAC 2009. Contributions are invited for oral presentation by 16 January 2009 and poster abstracts are welcome until 5 June 2009.

Themes

- Analysis & Detection
- Chemistry for Health
- Communication & Education
- Energy & Environment
- Industry & Innovation
- Materials
- Synthesis & Mechanisms

Plenary speakers

Peter G Bruce, University of St Andrews
 Chris Dobson, University of Cambridge
 Ben L Feringa, University of Groningen
 Sir Harold Kroto, Florida State University
 Klaus Müllen, Max-Planck Institute for Polymer Research
 Sir J Fraser Stoddart, Northwestern University
 Vivian W W Yam, The University of Hong Kong
 Richard N Zare, Stanford University

For a detailed list of symposia, keynote speakers and to submit an abstract visit our website.



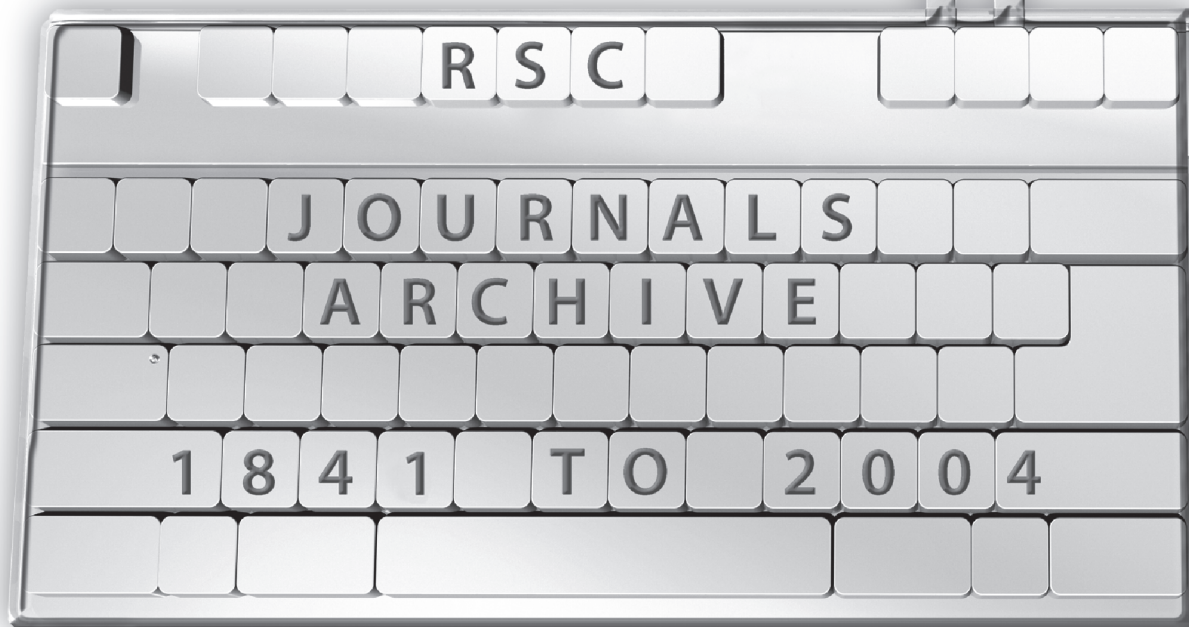
RSC | Advancing the
Chemical Sciences



www.iupac2009.org

Registered Charity Number 207890

Chemical science research at your fingertips!



Featuring almost 1.4 million pages of ground-breaking chemical science in a single archive, the **RSC Journals Archive** gives you instant access to **over 238,000 original articles** published by the Royal Society of Chemistry (and its forerunner Societies) between 1840-2004.

The RSC Journals Archive gives a supreme history of top title journals including: *Chemical Communications, Dalton Transactions, Organic & Biomolecular Chemistry* and *Physical Chemistry Chemical Physics*.

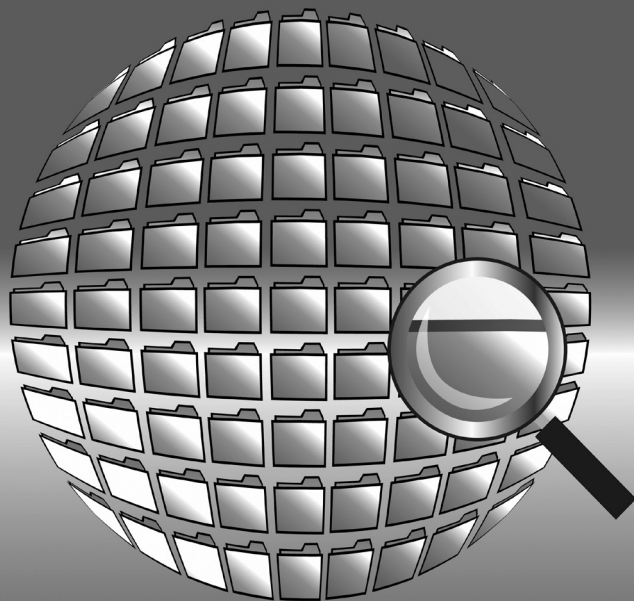
As well as a complete set of journals with multi-access availability, the RSC Journals Archive comes in a variety of purchase options and available discounts.

For more information please contact sales@rsc.org

RSC Publishing

www.rsc.org/archive

RSC Database and Current Awareness Products



- Abstracted from high quality sources
- Easy to use search functions
- Clearly displayed results
- Spanning the chemical sciences

for quick and easy searching

Graphical Databases

present search results in both text and graphical form. Titles include *Catalysts & Catalysed Reactions*, *Methods in Organic Synthesis* and *Natural Product Updates*.

Specialist Databases

review both academic and industrial literature on a wide range of hard to reach and unique information. Titles include *Chemical Hazards in Industry* and *Laboratory Hazards Bulletin*.

Analytical Abstracts

is the first stop for analytical scientists. Offering coverage on all areas of analytical and bioanalytical science. With a fresh new look, including improved search and results features, *Analytical Abstracts* offers an excellent online service.

Find out more at

RSC Publishing

www.rsc.org/databases

Registered Charity Number 207890

'I wish the others were as easy to use.'



'ReSource is the best online submission system of any publisher.'

'It leads the way for online submission and refereeing.'



ReSource



A selection of comments received from just a few of the thousands of satisfied RSC authors and referees who have used ReSource to submit and referee manuscripts. The online portal provides a host of services, to help you through every step of the publication process.

authors benefit from a user-friendly electronic submission process, manuscript tracking facilities, online proof collection, free pdf reprints, and can review all aspects of their publishing history

referees can download articles, submit reports, monitor the outcome of reviewed manuscripts, and check and update their personal profile

NEW!! We have added a number of enhancements to ReSource, to improve your publishing experience even further. New features include:

- the facility for authors to save manuscript submissions at key stages in the process (handy for those juggling a hectic research schedule)
- checklists and support notes (with useful hints, tips and reminders)
- and a fresh new look (so that you can more easily see what you have done and need to do next)

A class-leading submission and refereeing service, top quality high impact journals, all from a not-for-profit society publisher ... is it any wonder that more and more researchers are supporting RSC Publishing? Go online today and find out more.

Registered Charity No. 207890

RSC Publishing

www.rsc.org/resource

New journals from RSC Publishing in 2009!



Metallomics

Integrated biometal science

A journal covering the research fields related to biometals. It is expected to be the core journal for the emerging metallomics community. 6 issues in 2009, monthly from 2010.

Editorial Board chair is Professor Joe Caruso, University of Cincinnati/Agilent Technologies Metallomics Center of the Americas.

Contact the Editor, Niamh O'Connor, metallomics@rsc.org

www.rsc.org/metallomics

Integrative Biology

Quantitative biosciences from nano to macro

A unique, highly interdisciplinary journal focused on quantitative multi-scale biology using enabling technologies and tools to exploit the convergence of biology with physics, chemistry, engineering, imaging and informatics. Monthly from 2009.

Editorial Board chair is Distinguished Scientist Dr Mina J Bissell, Lawrence Berkeley National Laboratory.

Contact the Editor, Harp Minhas, ibiology@rsc.org

www.rsc.org/ibiology



From launch, the latest issue of *Metallomics* and *Integrative Biology* will be made freely available to all readers *via* the website. Free institutional access to 2009 and 2010 content is available following a simple registration process.

RSC eBook Collection

Access and download existing and new books from the RSC

- **Comprehensive:** covering all areas of the chemical sciences
- **Fully searchable:** advance search and filter options
- **Wide ranging:** from research level monograph to popular science book

See for yourself –
go online to search
the collection and
read selected
chapters
for free!



RSC Publishing

www.rsc.org/ebooks

Registered Charity Number 207890